NDT-BASED SERVICE LIFE PREDICTION OF DETERIORATING WATER MAINS

by

Tadeusz Ciszkiewicz
Department of Civil Engineering

Submitted in partial fulfilment
of the requirements for the degree of
Master of Engineering Science

Faculty of Graduate Studies
The University of Western Ontario
London, Ontario
June 1998

Abstract

The accelerating deterioration of water mains and the escalating cost of maintaining existing infrastructure has led to the development of the Hydroscope tool for non-destructive evaluation of cast and ductile iron pipes.

A computer program, PIPEXSC.EXE, was developed to simulate the distribution of the section modulus of corroded pipe cross-sections using the recorded average and the minimum wall thicknesses measured at specific location along the line by the Hydroscope tool. The sensitivity of the probability distribution of the section modulus to the uncertainty in the non-destructive tool and to the mathematical modelling of the cross-section was investigated.

A method of forecasting the remaining service life of a pipeline, which considers flexural failures and perforations of a pipe wall due to corrosion, was incorporated into a computer program called PIPEREL.EXE. The historical failure records and the results of simulations using PIPEXSC.EXE are used as input for the analysis of a pipeline. The sensitivity of the estimated remaining service life of cast and ductile iron pipelines to corrosion rates, wall thickness measurement errors, and other failure mode specific parameters was investigated using the program.

Acknowledgments

The author would like to express his sincere appreciation to his advisor, Dr. F.M. Bartlett, for his continual guidance, advice and encouragement throughout the M.E.Sc. program, and his tremendous help in creating the final form of this thesis.

The author would like to thank Mr. Larry Staples and the staff of Hydroscope Canada Inc. in Edmonton, Alberta, for providing invaluable information and suggestions. The author would also like to thank the staff of Hydroscope Canada Inc. for their hospitality during his three visits to the company.

Financial support from Natural Science and Engineering Research Council, Hydroscope Canada Inc., and the University of Western Ontario is gratefully acknowledged.

Last, but not the least, the author would like to thank his best friend, Aleksandra, for her support and understanding. It is to her that this work is dedicated.

Table of Contents

List of Tables

List of Figures

Nomenclature

a lower bound of Beta distribution; lower bound of S/S_o distribution; designation for outside corrosion of pipe cross-section

b upper bound of Beta distribution; upper bound of S/S_o distribution; designation for inside corrosion of pipe cross-section

c designation for a cross-section with inside and outside corrosion; desigantion of a cross-section with pits centered within quadrants

c_1 depth of outside corrosion

c_2 depth of inside corrosion

c_{CL} present cost of installation of one clamp

c_J present cost of joint replacement

c_L present cost of the replacement of the whole line

d distance from the neutral axis of bending to the extreme tension fibre

f scaling factor of the standard deviation of the minimum wall thickness

f_t maximum tensile stress

$f_Y(y)$ Beta probability density function of random variable y

$f_R(r)$ probability density function of the applied load effect.

$f\left(S/S_o\right)$ probability distribution of the normalized section modulus S/S_o

k total number of simulations of pipe cross-section; corrosion rate constant for average thickness loss in mm/year

m considered number of variable orientations of applied bending moment

m_y mean value of random variable y

n time exponent n in corrosion rate equation

$\bar{n}$ mean value of the time exponent n in corrosion rate equation

n_r discretized distribution of time exponent n.

$n[l]$ number of elements from Group[l]

$n_o[t_{min}]$ minimum number of elements to form a pit

$n_o[t_{min(i)}]$ minimum number of elements to form a pit in the ith quadrant

p_{ij} weighting factor for a pair of wall thicknesses t_{aj}, t_{mi}

p_f probability of failure of pipe cross-section

$p_{f_{ij}}$ probability of failure for a pair of wall thicknesses, t_{aj}, t_{mi}

$p_f(l.m)$ probability of failure of the m^{th} cross-section within the l^{th} joint

r parameter of the Beta distribution; designation for random order of element or random placement of pits within quadrants

r_1 radius of a pit measured for unfolded section of a pipe

r_i radial distance from the origin of reference axes (x_r, y_r) to the c.g. of ith element

r_n radius of the hole assumed as failure

r_r depth of the pit causing the failure of the pipe

rd relative demand

$rd(l.m)$ relative demand for the m^{th} cross-section of the l^{th} joint

t thickness of sound material: parameter of the Beta distribution

$\bar{t}$ calculated average wall thickness of pipe cross-section

t_f minimum wall thickness assumed as corrosion failure criterion

t_o nominal wall thickness of the undeteriorated pipe

t_{mk} discretized minimum wall thicknesses approximating distribution of t_{min}

t_{ak} discretized average wall thicknesses approximating distribution of t_{avg}

t_{min} minimum wall thickness of pipe cross-section

$t_{min(i)}$ minimum wall thickness in i[th] quadrant

t_{avg} average wall thickness of pipe cross-section

t_{rem} uniform wall thickness of pipe cross-section

$\overline{t_{min}}$ measured minimum wall thickness

$\overline{t_{avg}}$ measured average wall thickness

$\overline{t_{min(i)}}$ measured minimum wall thickness in i[th] quadrant

t_{min} minimum wall thickness of a cross-section at time T_c

t_{avg} average wall thickness of a cross-section at time T_c

t_{ai} discretized average wall thickness of a cross-section, t_{ai}, at time T_c

t_{mi} discretized minimum wall thickness of a cross-section, t_{mi}, at time T_c

$t_{min}(T)$ minimum wall thickness of a cross-section at time T

$t_{avg}(T)$ average wall thickness of a cross-section at time T

$\overline{t_{min}}(l,m)$ measured minimum wall thickness for the m^{th} cross-section of the l^{th} joint

$\overline{t_{avg}}(l,m)$ measured average wall thickness for the m^{th} cross-section of the l^{th} joint

u time exponent in the experimental corrosion rate equation for average weight loss

w weighting factor

x angular extent of a pit

x_i angular extent of a pit in i[th] quadrant

x_{min} minimum angular extent of a pit

x_{max} maximum angular extent of a pit

x_{min_i} minimum angular extent of a pit in i[th] quadrant

x_{max_i} maximum angular extent of a pit in i[th] quadrant

$x_r^{L_i}$ x_r coordinate of point L_i

x_{CG} x_r coordinate of the center of gravity (C.G.[d])

x_{ri} x_r coordinate of the c.g. of the i[th] element with respect to reference axis x_r

y random variable

y_{ri} y_r coordinate of the c.g. of the i[th] element with respect to reference axis y_r

$y_r^{L_i}$ y_r coordinate of point L_i

y_{CG} y_r coordinate of the center of gravity (C.G.[d])

z_k normal variate dividing standard normal distribution into a number of intervals

Upper case notation

A total area of the pipe cross-section

A_i area of sound material of the i[th] element

A_n area of the hole assumed as the failure criterion for corrosion failure mode

B beta function, normalized constant

C.G.^{u} center of gravity of the undeteriorated initial pipe cross-section

C.G.^{d} center of gravity of the deteriorated pipe cross-section

C factor validating pairs of discretized wall thicknesses, t_{aj}, t_{mi}

D outside diameter of undeteriorated pipe

D_f flexural demand

$D_f(l.m)$ flexural demand for the m^{th} cross-section of the l^{th} joint

D_r reference demand

D_o inside diameter of undeteriorated pipe

$\{EL\}$ array of elements chosen to construct a pipe cross-section

$\{El\}$ array of elements chosen to construct a quadrant of a pipe cross-section

$F_r(r)$ cumulative distribution function of the resistance

Group[t] group of elements with the thickness of sound material t in mm

H designation of high corrosion rate

Ix_p principal second moment of area of a cross-section about principal axis x_p

Iy_p principal second moment of area of a cross-section about principal axis y_p

Ix_r second moment of area of a cross-section about reference axis x_r

Iy_r second moment of area of a cross-section about reference axis y_r

Ix_r' second moment of area of a cross-section about axis x_r'

Iy_r' second moment of area of a cross-section about axis y_r'

Ix_{pi} second moment of area of the ith element about its principal axis x_{pi}

Iy_{pi} second moment of area of the ith element about its principal axis y_{pi}

$Ix_r y_r$ product of inertia of a cross-section about x_r and y_r axes

$Ix_r' y_r'$ product of inertia of a cross-section about x_r' and y_r' axes

IR interest rate on the basis of time ΔT

K corrosion rate constant for pitting in mm/year

L_i characteristic point of the i^{th} element describing the outer surface of cross-section

L_k a point on the outer surface of the pipe cross-section experiencing maximum tensile stress due to bending moment M

L designation of low corrosion rate

M bending moment

M designation of medium corrosion rate

Mx_p component of the bending moment vector M parallel to the principal axis x_p

My_p component of the bending moment vector M parallel to the principal axis y_p

N number of elements or points around the outer surface of a cross-section

N_j number of joint within the line

N_s number of sampled cross-section within the joint

N_e number of points for approximation of a continuous distribution

N_{JF} number of joint failures or the number of replaced joints

N_{SF} number of section failures or the number of installed clamps

$N_{\Delta t}$ number of time intervals

P_s probability of no failure for a pipe joint

P_f probability of failure for a pipe joint

PW(LRC) present worth cost of line replacement

PW(MC) present worth cost of repairs

PW(LRC+MC) present worth total cost

R_o initial inside radius of the pipe

R_{avg} average radius of the pipe

RC approximate ratio of depths of outside and inside corrosion

RC' input ratio of outside and inside corrosion

T time over which a pipe remains in the soil

T_e elapsed time from the line inspection

T_o time of the line inspection

T estimated remaining service life of a pipeline

Type 1(or *2*, or *3*, or *4*) type of cross-section model

V_{min} minimum volume of detectable pit

VL designation of very low corrosion rate

S section modulus of deteriorated pipe cross-section

S_o section modulus of undeteriorated pipe cross-section

S_α section modulus for the moment vector inclined with angle α with respect to the principal axis x_p

S_k first moment of area of k^{th} interval of discretized normal distribution

Sx_i first moment of area of the i^{th} element about x_r

Sy_i first moment of area of the i^{th} element about y_r

Sx_r first moment of area about x_r

Sy_r first moment of area about y_r

$S.S_o$ normalized tension section modulus of a cross-section

Z_k center of gravity of the k^{th} interval of the discretized standard normal distribution

W sum of elements in the weight matrix corresponding to the matrix of pairs of discretized distributions of minimum and average wall thicknesses, weighting factor

Greek notations

α angle between the moment vector M and the principal axis x_p

β one half of the angular dimension of an element

μ mean value of means of S/S_o distribution

ν_{crit} critical failure frequency

ν_p predicted failure frequency

ν_o failure frequency observed or extrapolated from historic failure records

π constant 3.14

σ_a standard deviation of the average wall thickness distribution

σ_m standard deviation of the minimum wall thickness distribution

σ_u standard deviation of the time exponent u for experimental equation for average weight loss

σ_z standard deviation of the standard normal distribution, equals 1.0

σ_n standard deviation of the distribution of the corrosion rate exponent n

σ_1 the maximum tensile stress

σ_2 standard deviation of S/S_o for a single cross-section due to variable orientations of applied bending moment vector

σ_3 square root of variance of mean values of S/S_o for a number of simulations

σ_4 square root of mean of variances of S/S_o

σ_5 square root of variance of standard deviation of S/S_o for a number of simulations

σ_o overall standard deviation of S/S_o distribution

σ_y^2 variance of y

ΔT time interval for reliability analysis

Γ gamma function

Φ angle of inclination of the principal axis x_p with respect to the reference axis x_r

Subscripts

i

j

k

r

Indeces

i

j

l

m

Chapter 1 Background and thesis outline

1.1 Introduction

Chapter 1 provides the necessary background on deteriorating water mains, the scale of the water main failure problem, and the most recently emerging non-destructive method for the assessment of pipeline condition. The objective of this thesis is also presented in this chapter, followed by the detailed outline of all parts of this study.

1.2 Background

The problem of accelerating deterioration of water mains and escalating cost of maintaining the serviceability of existing infrastructure is a serious problem in many North American municipalities. The estimated cost of water mains replacement in the United States over the next twenty years is about $13.5 billion (Wagner, 1997). Water main networks constructed using gray and ductile cast iron pipes contribute the most to the severity of the problem. There is a need for a new non-destructive method to provide fairly inexpensive, accurate, and quick assessment of the condition of water mains. The Hydroscope tool, developed by Hydroscope Canada Inc. for the evaluation of cast and ductile iron pipelines using state-of-the-art technology, offers an efficient and reliable means to assess the pipeline condition.

1.2.1 Failures of cast and ductile iron water mains

Gray and ductile cast iron are the most prevalent water main pipe materials for both Canadian and American water distribution networks. Table 1.1 (Staples, 1996) shows the detailed material composition of Canadian and American water supply networks.

Table 1.1 Material composition of American and Canadian waterline assets

Pipe material	American waterline assets	Canadian waterline assets
Cast Iron	48%	44%
Ductile Iron	19%	29%
Steel	4%	2%
Conc&AC	17%	15%
PVC	9%	11%
Other	2%	

Although the use of gray cast iron pipes was completely discontinued in Canada between the late 1960's and the late 1970's, they still constitute 44% of the water distribution infrastructure. The average age of gray cast iron pipes in Canada is between 40-50 years (Rajani *et al*, 1995), and many of those pipes were installed without proper corrosion protection (Jakobs and Hewes, 1987). The deterioration over time due to corrosion is the primary cause of the existing maintenance problem.

Ductile cast iron pipes, which were installed extensively in the period after gray cast iron pipe installation was abandoned, are the second major component of Canadian water

distribution infrastructure. Although some type of protective coating has been used for ductile cast iron pipes from the beginning, the corrosion protection methods used in the past have been ineffective, and the currently observed failure rate is steadily increasing (Jakobs and Hewes, 1987).

The majority of cast and ductile iron pipes fail by a transverse break or by perforation of the pipe wall. Table 1.2 summarizes recent break data for 21 Canadian cities (Rajani *et al*, 1995), categorized according to five distinct failure modes, which are shown in Figure 1.1 (based on Clarke, 1968). The longitudinal break, where four cracks (which are spaced approximately every 90° about the circumference of the pipe) propagate along the pipe joint, occurs due to excessive vertical load or inadequate bedding. The transverse break, which is a bending failure of the pipe cross-section, is mainly caused by soil movement or differential settlement. Local loss of pipe wall thickness, which can even include perforation of pipe wall, is caused by underground corrosion. The bell-spigot failure, which is a failure of the connection between two pipe joints, may be caused by a leverage fracture involving excessive angular displacement between pipe joints or by restraint of thermal expansion of the pipe. There are many other incidental types of failure including, for example, a bearing fracture due to a hard spot in the pipe bed.

In 1992, 85% of all failures of cast iron pipes were due to the transverse break or pitting. Similarly 95% of all failures of ductile cast iron pipes were attributed to these causes. These high percentages were observed again in 1993 as shown in Table 1.2.

Table 1.2 Summary of the number of failures for different failure modes for 21 cities across Canada

Pipe material	Year	Total # of breaks	# of breaks for a particular failure mode				
			longitudinal breaks	transverse breaks	hole/pit	bell-spigot	other
Cast Iron	1992	3075	202 (7%)	1965 (64%)	655 (21%)	179 (6%)	74 (2%)
	1993	3216	233 (7%)	2069 (64%)	595 (19%)	197 (6%)	122 (4%)
Ductile Cast Iron	1992	392	2 (0.5%)	75 (19%)	297 (76%)	15 (4%)	3 (0.8%)
	1993	414	9 (2%)	60 (14%)	321 (78%)	7 (2%)	17 (4%)

It is conventional to characterize the condition of the water distribution networks as the frequency of failures per length of pipe. Table 1.3 shows the average frequency of failures of cast and ductile iron pipes for the 21 cities surveyed in 1992 and 1993 (Rajani *et al.*, 1995). The frequency of failure for cast iron mains is approximately four times greater than that for ductile iron pipes, perhaps because cast iron pipes are much older.

Table 1.3 Frequency of failures for cast and ductile iron waterlines

Pipe material	Year	Length of pipe (km)	# of breaks per 100 km
Cast Iron	1992	8769.9	35.1
	1993	8769.9	36.7
Ductile Cast Iron	1992	4237.5	9.3
	1993	4237.5	9.8

The frequency of failures for individual cities are shown in Figures 1.2 and 1.3. For example, the failure frequency of cast iron pipes in Regina was over 200 failures per 100 km in 1993, while the failure frequency of ductile iron pipes in Moose Jaw was close to 80 failures per 100 km in 1992. Those relatively high failure rates clearly show that deterioration of the water distribution infrastructure is becoming a serious problem in some of Canadian cities.

Managing an aging network with limited resources requires a good assessment of the condition of the water mains. The cost of failure is often much higher than the cost of the repairs necessary to restore serviceability of the line (Shamir, 1979). Resources would be more efficiently managed if the maintenance schedule could be prioritized by targeting sections of the network that are highly susceptible to failure. The Hydroscope tool described in the next section was developed in response to these needs to provide a detailed profile of the pipeline wall thickness.

1.2.2 Non-Destructive Evaluation (NDE) using the Hydroscope tool

The Hydroscope tool (Staples. 1996) is an example of the recent generation of intelligent "pigs", that conduct measurements and collect data during the inspection of a pipeline. A variety of intelligent "pigs" have been used by the gas and oil industry for a long time to inspect large diameter pipelines. The application of this technology to water line inspection is a fairly new concept because waterline networks are composed of small

diameter pipes and so require miniaturized tools. The first generation prototype of the tool was tested in 1994 (Staples, 1996). The second generation tool with the enhanced digital technology was used commercially in 1995.

Figure 1.4 shows a typical setup of the Hydroscope tool for field inspection of a water main. The tool is launched and retrieved through fire hydrants. It is propelled through the section of main to be assessed either by the water flow or by winching. In Figure 1.4, the water supplied to the left hydrant would propel the tool from left to right, or an external winch at the end of the wire line would pull the tool back from right to left.

The Hydroscope tool consists of a number of sealed modules that house exciter and detector coils, and data processing and transmission electronics. The design of the tool is based on remote field technology, shown schematically in Figure 1.5. The magnetic field created by the exciter coil propagates through the pipe wall and the material surrounding the pipe, and it is picked up by the detector coil after passing again through the pipe wall. Measurements of the phase shift and the amplitude of the signal arriving at the detector coil are correlated with wall loss of the pipe cross-section.

Figure 1.6 shows an example of the recorded phase shift and amplitude for two pipe joints of a pipeline inspected using the Hydroscope tool. Proprietary software converts the phase and the amplitude records into the pipe wall thickness profile for the pipeline. Figure 1.7 shows an example of the output for a pipeline consisting of 51 pipe joints,

where each pipe joint is approximately 5 to 6 m long. In this case, only the average wall thickness and the minimum wall thickness have been plotted for each joint as the percentages of the original wall thickness. However, the tool can sample the pipe wall thickness on an almost continues basis, providing a large quantity of data for each pipe joint.

The most significant capabilities of the Hydroscope tool (Staples, 1996) are:

- ability to penetrate thick-walled inhomogeneous pipe;
- ability to measure pipe wall thickness regardless of lining or internal scale;
- sensitivity to both the external and internal local thickness losses - that is corrosion losses at the outside of the pipe or the inside of the pipe or both;
- ability to negotiate bends up to 90°;
- ability to operate at a variable speed between 1-10 m/min; and
- ability to register hardware such as line valves, sleeves, tees and joints. For example bell and spigot locations are readily identified from the signal, as shown in Figure 1.6.

1.3 Objective of the thesis

The objective of this thesis is to develop procedures for the reliability analysis of a water line that accommodate data collected by the Hydroscope tool. Particular consideration will be given to the two most prevalent failure modes of gray and ductile cast iron water

mains, namely the perforation and the flexural failure. The objective set for this study is accomplished through:

- development of a method for obtaining the probabilistic description of the flexural capacity of a corroded pipe cross-section using simulations based on the measured average and minimum pipe wall thicknesses
- review of the literature on underground corrosion of ferrous material
- development of a method for calculating the probability of failure of a sampled pipe cross-section
- development of a simplified method to forecast the future frequency of failures for a pipeline that has been assessed using one pass of the Hydroscope tool

The calculation methods developed for detailed investigation will also be used to assess the sensitivity of the results to various parameters involved.

1.4 Outline of the thesis

The following subsections present the outline of this thesis. Chapters 2&3 discuss the method and results of simulations of the deteriorated pipe cross-section with average and minimum thicknesses as defined by the results of the assessment using the Hydroscope tool. Chapter 4 provides brief literature review concerning underground corrosion of ferrous materials. The simplified reliability analysis of a pipeline and the results of such

analysis are covered by Chapters 5 and 6. The summary of this thesis is presented in Chapter 7. Figure 1.8 presents schematically the form in which this thesis is organized.

1.4.1 Chapter 2

Chapter 2 presents all basic assumptions and procedures incorporated in the program PIPEXSC.EXE. The program generates simulated cross-sections of deteriorated pipe using the data provided by the Hydroscope tool as input. For each simulated cross-section, the section modulus is calculated for a number of different orientations of the applied bending moment and analyzed statistically. For the set of all simulated pipe cross-sections, with common average and minimum wall thicknesses, statistical analyses are again performed providing the final and complete description of the section modulus distribution. The program PIPEXSC.EXE can analyze ten different models of deteriorated pipe cross-sections, which reflect current capabilities of the tool and possible future enhancements. The basic differences between those models and their application for the analysis is also discussed.

1.4.2 Chapter 3

Chapter 3 discusses application of the program PIPEXSC.EXE and presents sensitivity analysis of simulated results. The first part of Chapter 3 presents the results generated by the program for deteriorated 6" diameter pipe. The results include plots of the magnitude and variation of the section modulus due to variable orientation of the bending moment,

figures showing the simulated cross-sections, and plots of the statistical parameters describing the probability distribution of section modulus obtained for specified minimum and average wall thickness values. The second part of Chapter 3 is devoted to sensitivity analyses and parametric studies. The parameters affecting the results generated by the program can be characterized as the tool-related and the simulation-related. Some of the simulation-related parameters investigated are the number of simulations and various parameters defining the pipe cross-section models. The tool-related parameters investigated include the measurement errors of the average and the minimum wall thicknesses, and the effect of the variable orientation of the bending moment the pipe cross-section is subjected to. The effect of the possible future tool enhancements allowing collection of more data is also analyzed in Chapter 3.

1.4.3 Chapter 4

Chapter 4 reviews the literature concerning the underground corrosion of water pipelines, focusing on the influence of a number of different environmental conditions on the rate of corrosion of both gray and ductile cast iron pipe. The experimental studies and theoretical investigations published on this subject are used to establish corrosion models for the reliability analysis program described in Chapter 5.

1.4.4 Chapter 5

Chapter 5 presents all basic assumptions and procedures incorporated in the program PIPEREL.EXE . The program performs simplified reliability analyses of a pipeline, and forecasts the frequency of future failures. The reliability analysis is based on data collected by the Hydroscope tool during the field inspection of a pipeline, and on user defined parameters defining the rate of corrosion. The program considers the two most common failure modes for cast iron pipes, namely the corrosion failure which is characteristic for ductile iron and the flexural failure which is common for gray cast iron. For flexural failure, the program PIPEREL.EXE presents the practical application of the results obtained from the simulation of deteriorated pipe cross-section determined in Chapter 2. Two optional features of the program allow different repairs scenarios and present worth cost associated with chosen repair options to be considered.

1.4.5 Chapter 6

Chapter 6 presents the analytical results from the program PIPEREL.EXE for a typical deteriorated pipeline. A file containing simulated field measurements collected by the Hydroscope tool during the line inspection is the basis for all analyses. The two predominant failure modes are investigated by the program, and the effects of the adopted calculation procedures, the measurements errors associated with the data from the field inspection, and other parameters affecting the real pipeline performance such as the corrosion rates or the maintenance strategy are investigated.

1.4.6 Chapter 7

Chapter 7 presents the summary and conclusions of the work covered by Chapters 2 through 6.

1.4.7 Appendix A

Appendix A is a users guide for the program PIPEXSC.EXE, that facilitates the use of the program and presents all output files created. The first part of Appendix A presents examples of the user interface for entering all data required for the simulation of a deteriorated pipe cross-section. The format and purpose of all output files are described in the second part. Output can be used as input for the statistical analysis software C-fit (CFER, 1996) or can be analyzed using MS Excel. In either case, the output file must be processed before it can be use as a data file, and this necessary step is also discussed. Finally, Appendix A presents example plots obtained from simulations of pipe cross-section using all ten models, with some model-specific options.

1.4.8 Appendix B

Appendix B is a users guide for the program PIPEREL.EXE. There are two types of input data required for the reliability analysis: the user-specified keyboard input and the data supplied in form of a number of data files. Appendix B presents in detail the user interface for entering data and the necessary format and content of data files required for analysis. Examples output files are also presented and discussed.

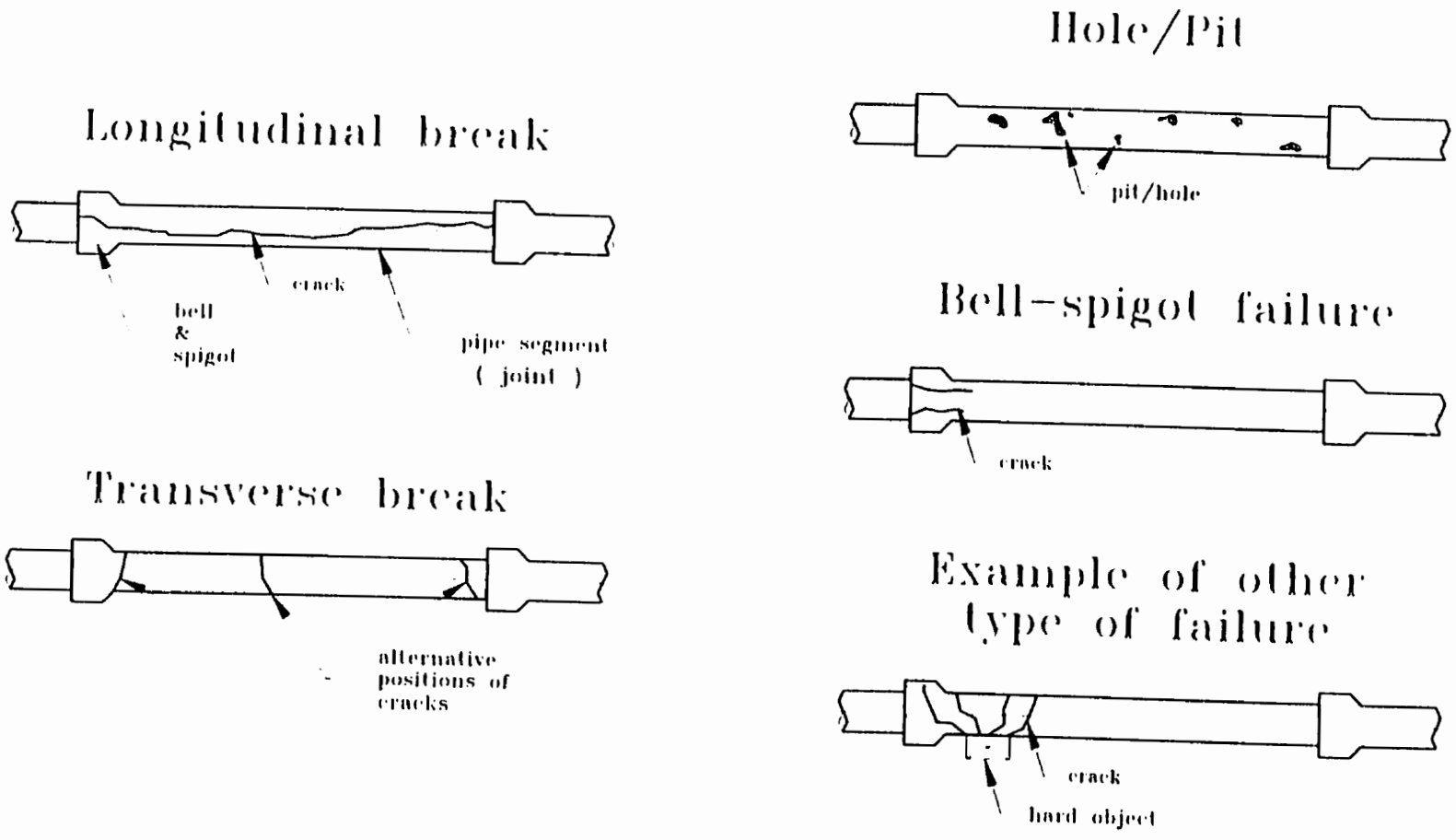

Figure 1.1 Typical failure modes of rigid pipes (based on Clarke, 1968)

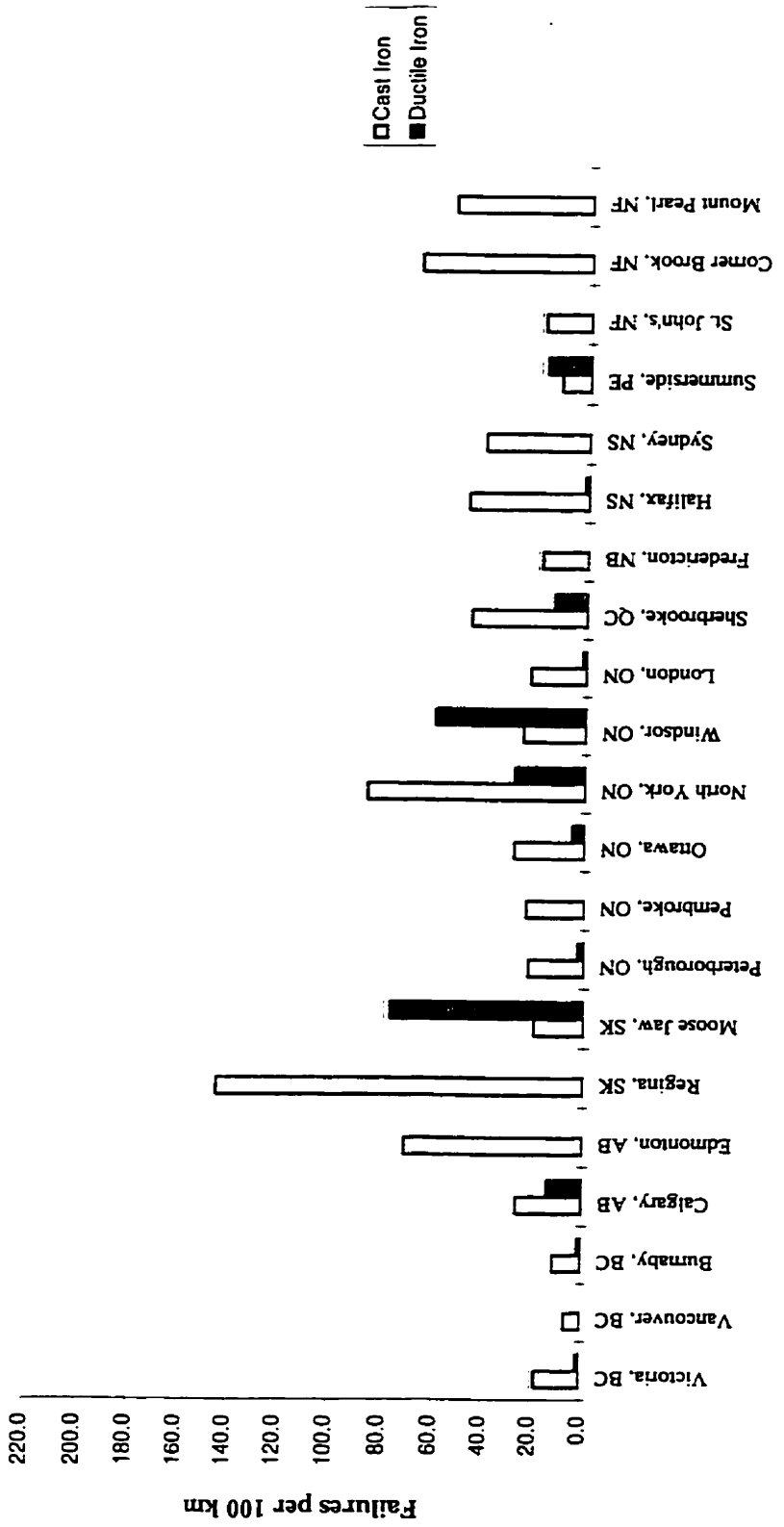

Figure 1.2 Frequency of water main breaks for various Canadian cities, 1992 (data based on Rajani *et al*, 1995)

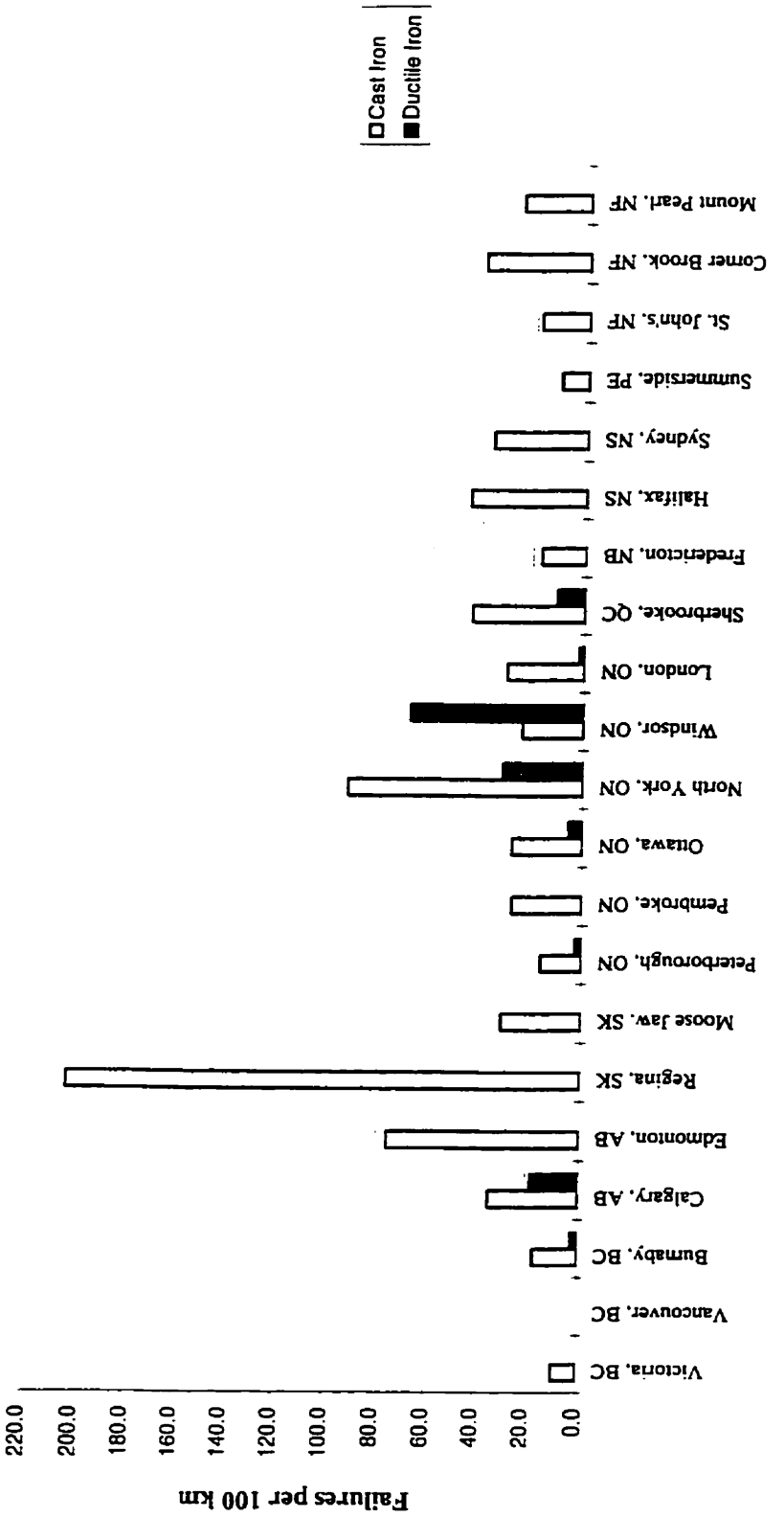

Figure 1.3 Frequency of water main breaks for various Canadian cities, 1993 (data based on Rajani *et al*, 1995)

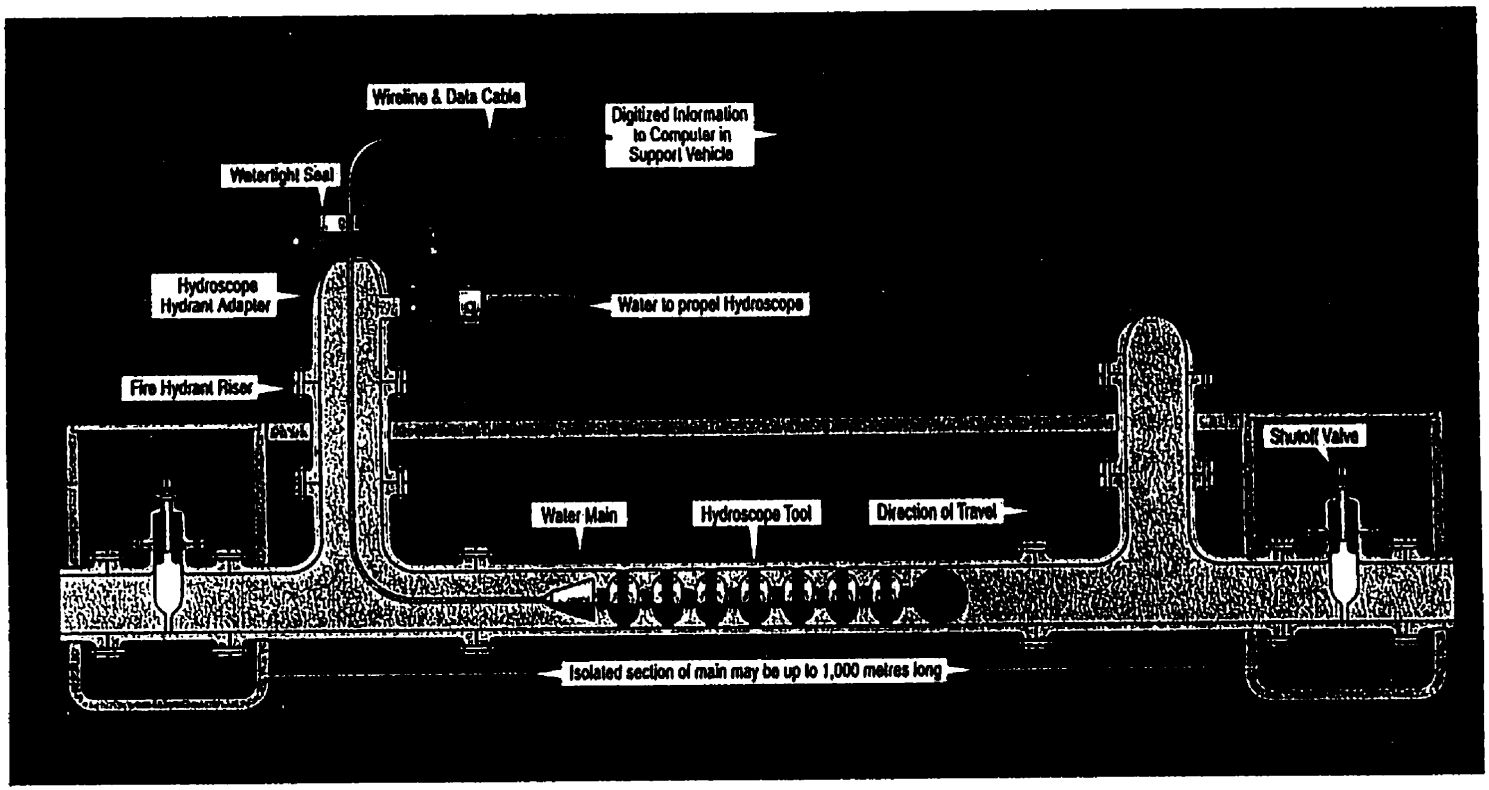

Figure 1.4 General setup of the Hydroscope tool for field inspection (courtesy of Hydroscope Inc.)

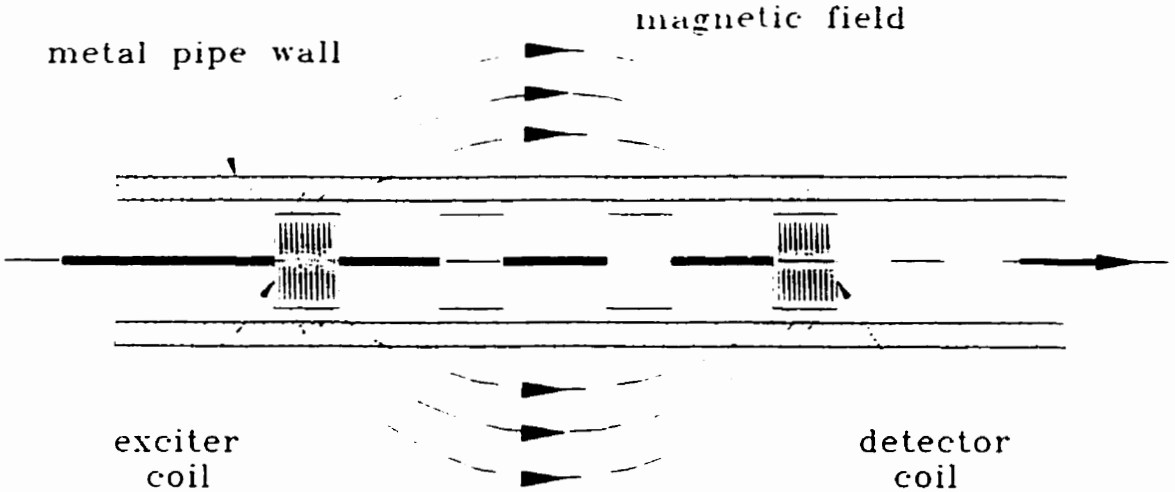

Figure 1.5 Wall thickness measuring system of exciter-detector coils (after Staples, 1996)

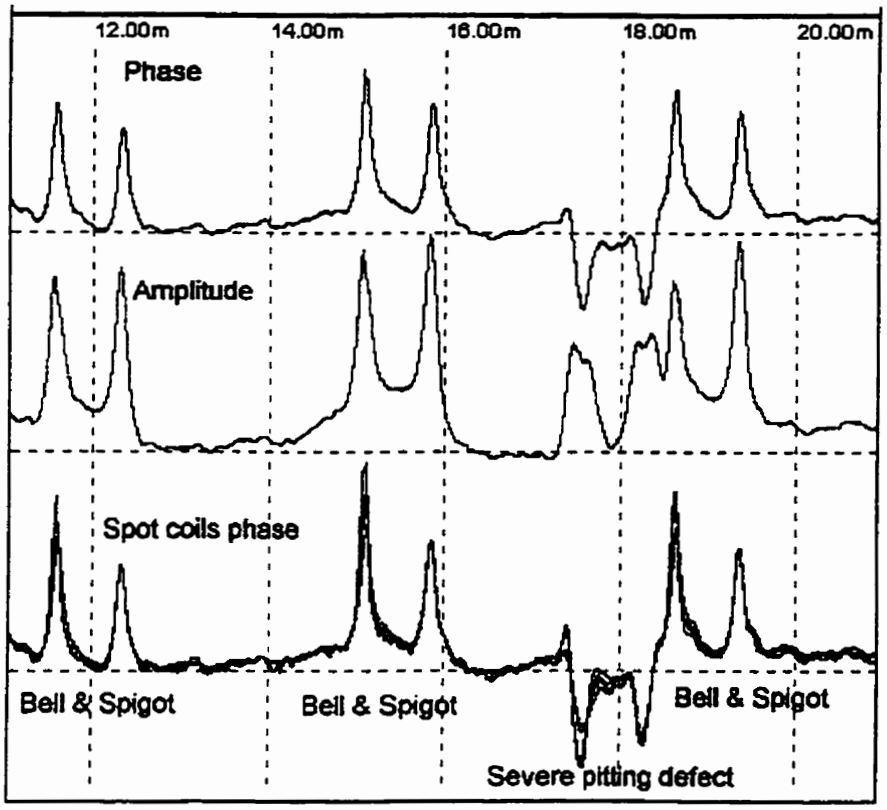

Figure 1.6 Diagram of recorded phase and amplitude (courtesy of Hydroscope Inc.)

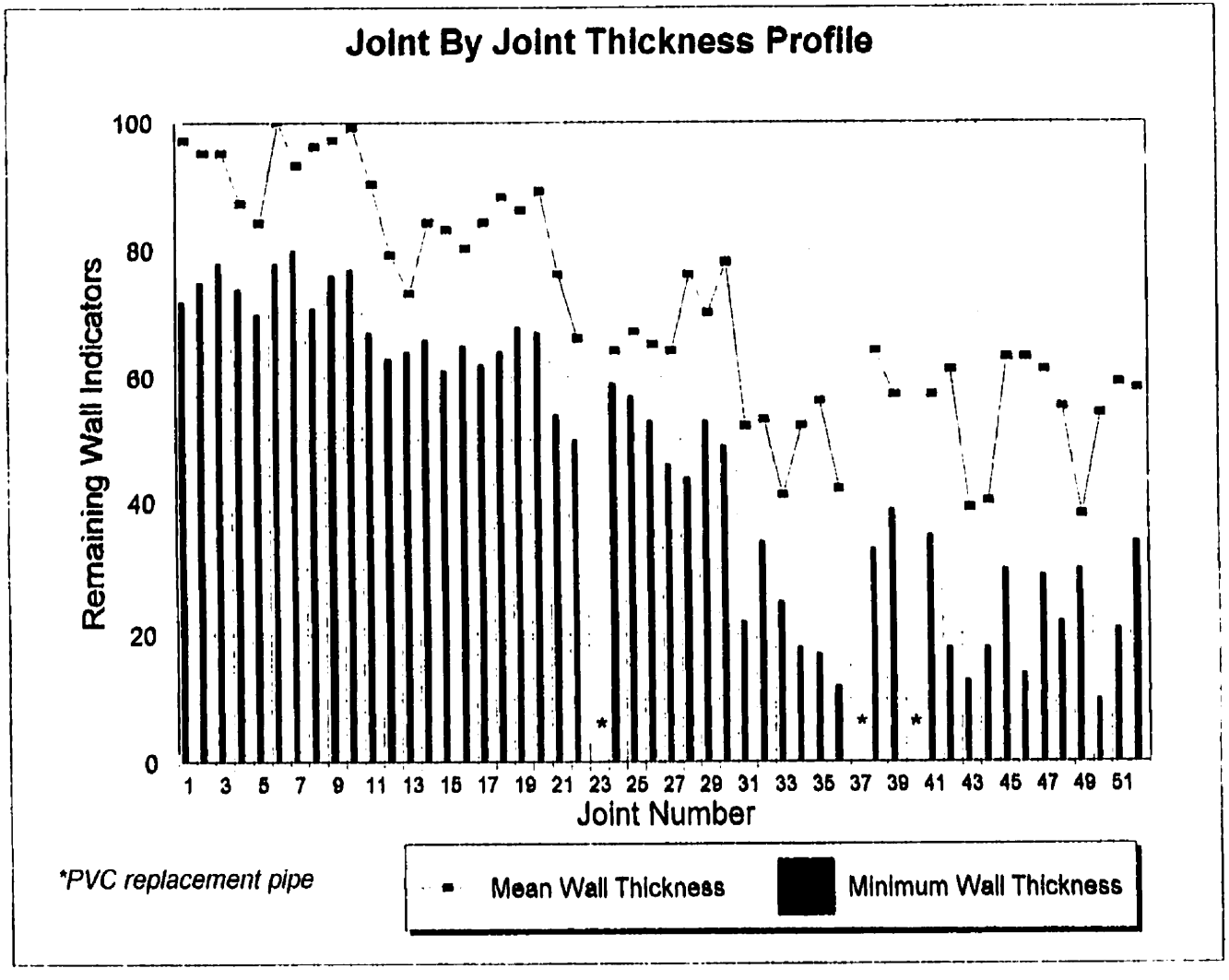

Figure 1.7 Example of the wall thickness profile obtained using data analysis software (courtesy of Hydroscope Inc.)

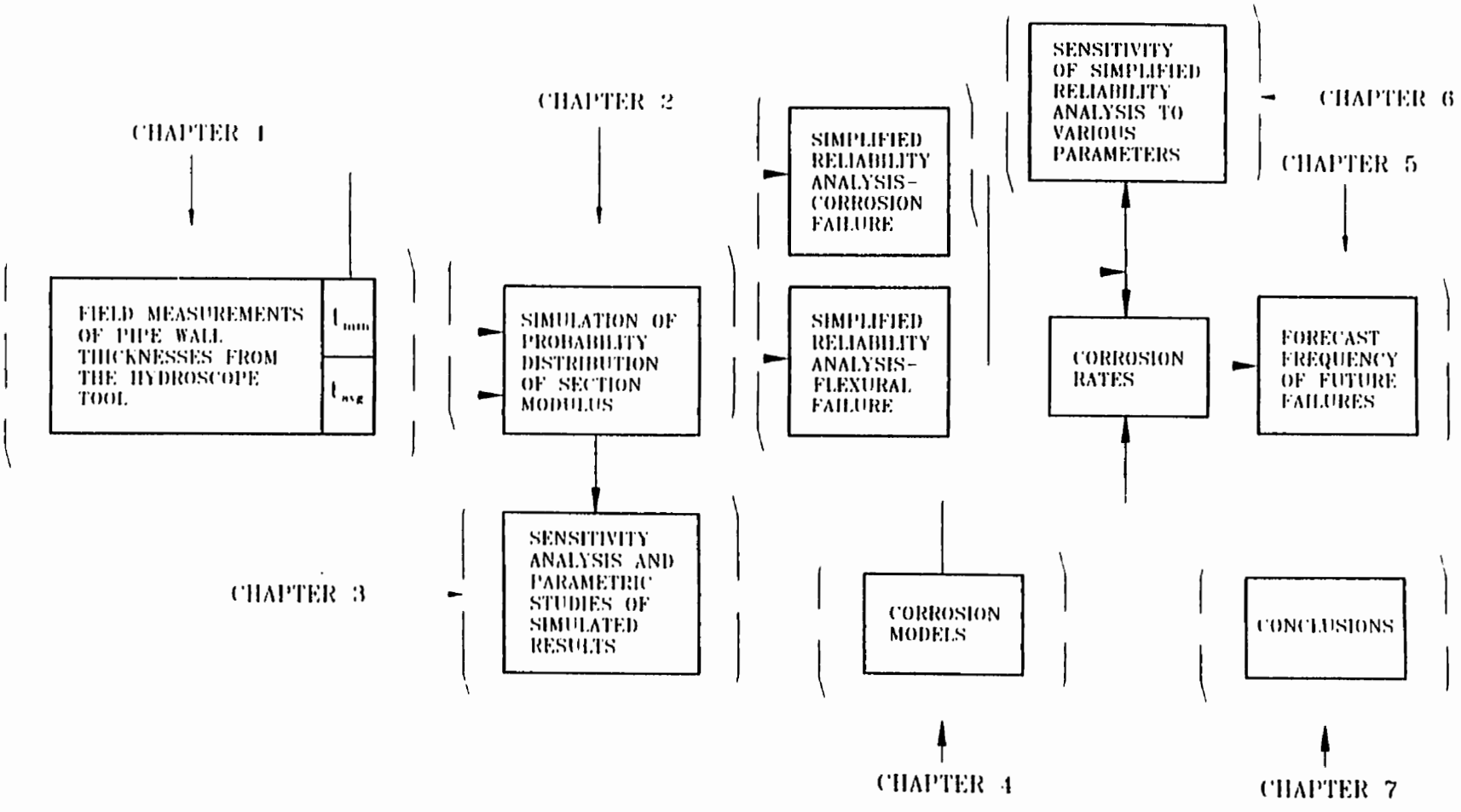

Figure 1.8 Schematic outline of the thesis

Chapter 2 Modelling of corroded pipe cross-section

2.1 Introduction

The objective of this chapter is to present the mathematical basis for the algorithms in the computer program PIPEXSC.EXE which assesses the normalized section modulus, S/S_o, of a deteriorated pipe. The normalized section modulus is defined as the section modulus at the time of the Hydroscope run, S, divided by the section modulus of an undeteriorated pipe S_o.

The program generates the cross-section of a corroded pipe, and considers a number of different positions of the neutral axis of bending for calculations of S/S_o. Subsequently the statistical analysis of a number of simulated results is performed. The final results reported by the program include a number of statistical measures allowing the complete description of the S/S_o distribution.

The program PIPEXSC.EXE allows analysis of a number of models of pipe cross-section, which are consistent with the information from the Hydroscope tool. The basic difference among those models lies in their applicability and complexity. The applicability of a model for simulation of a cross-section of deteriorating pipe depends only on the quantity of data collected by the pig at each sampling point along a pipe joint, and the character of assumed corrosion pattern (only internal, only external, or both). On the other hand, the level of sophistication of the model will manifest itself firstly by the

time required to complete calculations, and secondly by the degree of realism in the resulting simulated cross-section.

The number of random variables involved in this problem, their relevance to the data provided by the Hydroscope tool, as well as their treatment implemented in the program, are also discussed in this chapter.

2.2 Deterministic analysis of deteriorating pipe cross-section

In this section, the basis of the numerical algorithms used in the program PIPEXSC.EXE will be presented, first for the deterministic case where the actual geometry of the pipe cross-section is known, and subsequently for the real case where the cross-section geometry is random. The deterministic analysis transforms the pipe geometry to equivalent cross-section properties, defined for the principal axes of the pipe.

2.2.1 Analysis of cross-section properties

Figure 2.1 shows the cross-section of a deteriorated pipe with non-uniform wall thickness, where hatched areas symbolize corroded pipe material. This is an example of a pipe with some degree of inside and outside corrosion. The following dimensions of the pipe cross-section are known:

- D_o - the initial inside diameter of the pipe
- t_o - the nominal wall thickness of the undeteriorated pipe

- c_2 and c_1 - the depths of the inside and outside corrosion, respectively, in any radial direction from the center of gravity (C.G.^{u}) of the undeteriorated initial pipe cross-section. The thickness of sound material equals t_n - ($c_1 + c_2$).
- t_{min} , t_{avg} - the minimum and the average thicknesses of the pipe wall, respectively.

The analysis of the cross-section will be performed in two stages:

1. Calculate properties of the cross-section for an arbitrary reference axis system
2. Locate principal axes and transform the cross-section properties to the principal axes

Before proceeding with the calculations involved in the first stage of the analysis, the cross-section shown in Figure 2.1 is "discretized" into N elements having the same angular dimension 2β , as shown in Figure 2.2. The angle β , defined as

$$\beta = \frac{\pi}{N} \qquad [2.1]$$

is sufficiently small that uniform thickness of inside and outside corrosion within the element can be assumed. The origin of an adopted reference axis system (x_r , y_r) is placed in the centre of gravity (C.G.^{u}) of the original, undeteriorated pipe cross-section. The minimum thickness, t_{min} , of the pipe cross-section shown in Figure 2.1 is the smallest element thickness t_i from all N elements forming the discretized cross-section shown in Figure 2.2. The average thickness of the cross-section, t_{avg}, is equal to:

$$t_{avg} = \frac{1}{N}\sum_{i=1}^{N} t_i \qquad [2.2]$$

Some formulae for an angular element of the cross-section are necessary for subsequent calculations. Figure 2.3 shows the i[th] element of the pipe cross-section, which principal axis x_{pi} and y_{pi}, are inclined with some angle φ_i to the reference axis x_r. The equations for the various geometric properties of this arc about its principal axes are (CISC, 1989):

$$A_i = \beta \cdot t_i \cdot (2 \cdot R_o + 2 \cdot c_{2i} + t_i) \qquad [2.3]$$

$$Ix_{pi} = (\beta + \sin\beta \cdot \cos\beta - \frac{\sin^2\beta}{0.5 \cdot \beta}) \cdot (R_o + c_{2i} + 0.5 \cdot t_i)^3 \cdot t_i \qquad [2.4]$$

$$Iy_{pi} = (\beta - \sin\beta \cdot \cos\beta) \cdot (R_o + c_{2i} + t_i)^3 \cdot t_i \qquad [2.5]$$

$$r_i = \frac{\sin\beta}{\beta} \cdot (R_o + c_{2i} + 0.5 \cdot t_i) \qquad [2.6]$$

where: A_i is the area of sound material of the i[th] element: Ix_{pi} is the second moment of area of the i[th] element about its principal axis x_{pi}: Iy_{pi} is the second moment of area of the i[th] element about its principal axis y_{pi}: and, r_i is the radial distance from the origin of (x_r, y_r) to the c.g. of i[th] element.

The following equations locate the centre of gravity and extreme fibre of the element, shown as c.g. and L_i respectively in Figure 2.3, with respect to the reference axes:

$$x_{ri} = r_i \cdot \cos\varphi_i \qquad [2.7]$$

$$y_{ri} = r_i \cdot \sin\varphi_i \qquad [2.8]$$

$$x_r^L = (R_o + c_{2i} + t_i) \cdot \cos\varphi_i \qquad [2.9]$$

$$y_r^L = (R_o + c_{2i} + t_i) \cdot \sin\varphi_i \qquad [2.10]$$

where: R_o is the inside radius of the undeteriorated pipe: $x_r^{L_i}$ is the x_r coordinate of point L_i; $y_r^{L_i}$ is the y_r coordinate of point L_i; x_{ri} is the x_r coordinate of the c.g. of the ith element with respect to reference axis x_r: and, y_{ri} is the y_r coordinate of the c.g. of the ith element with respect to reference axis y_r.

First moments of area of the ith element about the reference axes are calculated as:

$$Sx_{ri} = A_i \cdot y_{ri} \qquad [2.11]$$

$$Sy_{ri} = A_i \cdot x_{ri} \qquad [2.12]$$

where Sx_{ri} and Sy_{ri} are the first moments of area of the ith element about x_r and y_r axes. respectively.

It is also necessary to transform the second moments of area from the principal axes of each element to a new local coordinate system (x_i, y_i) that is parallel to the reference axes system (x_r, y_r). This step is necessary to use the parallel axis theorem (Beer. 1972) to determine the properties of the overall section from the summation of the properties of all N elements. The transformation is achieved using Mohr's circle for second moment of area (Beer. 1972)

$$Ix_i = 0.5 \cdot (Ix_{pi} + Iy_{pi}) - 0.5 \cdot (Iy_{pi} - Ix_{pi}) \cdot \cos(\varphi_i - 0.5 \cdot \pi) \qquad [2.13]$$

$$Iy_i = 0.5 \cdot (Ix_{pi} + Iy_{pi}) + 0.5 \cdot (Iy_{pi} - Ix_{pi}) \cdot \cos(\varphi_i - 0.5 \cdot \pi) \qquad [2.14]$$

$$Ix_i y_i = 0.5 \cdot (Iy_{pi} - Ix_{pi}) \cdot \sin(2 \cdot \varphi_i - \pi) \qquad [2.15]$$

where: Ix_i is the second moment of area of the i[th] element about its principal axis x_i: Iy_i is the second moment of area of the i[th] element about its principal axis y_i; and, Ix_iy_i is the product of inertia about x_i and y_i axes.

The geometric properties of the overall cross-section can now be calculated as a simple summation over all constitutive elements of the cross-section.

$$A = \sum_{i=1}^{N} A_i \qquad [2.16]$$

$$Ix_r = \sum_{i=1}^{N} (Ix_i + A_i \cdot y_n^{\,2}) \qquad [2.17]$$

$$Iy_r = \sum_{i=1}^{N} (Iy_i + A_i \cdot x_n^{\,2}) \qquad [2.18]$$

$$Ix_ry_r = \sum_{i=1}^{N} (Ix_iy_i + A_i \cdot x_n \cdot y_n) \qquad [2.19]$$

$$Sx_r = \sum_{i=1}^{N} Sx_n \qquad [2.20]$$

$$Sy_r = \sum_{i=1}^{N} Sy_n \qquad [2.21]$$

$$x_{CG} = Sy_r / A \qquad [2.22]$$

$$y_{CG} = Sx_r / A \qquad [2.23]$$

In Eqs.[2.16] to [2.23]: A is the total area of the pipe cross-section; Ix_r is the second moment of area about x_r; Iy_r is the second moment of area about y_r; Ix_ry_r is the product of inertia about x_r and y_r; Sx_r is the first moment of area about x_r; Sy_r is the first moment of area about y_r; x_{CG} is the x_r coordinate of the centre of gravity (C.G.^{d}): and, y_{CG} is the y_r coordinate of the centre of gravity (C.G.^{d}):

In the second stage of the calculations, the properties about the arbitrary axes (x_r, y_r) are transformed to properties about the principal axes (x_p, y_p). Knowing the location of the centre of gravity of the deteriorated cross-section, and second moments of area about the reference axis (x_r, y_r), the principal moments of area are calculated through simple transformations.

The section properties are determined for axes (x_r', y_r'), which are parallel to the reference axes (x_r, y_r) but pass through the centre of gravity of the deteriorated cross-section C.G.^{d}, as shown in Figure 2.4. The transformation is a second application of the parallel axis theorem:

$$Ix_r' = Ix_r - A \cdot y_{CG}^2 \qquad [2.24]$$

$$Iy_r' = Iy_r - A \cdot x_{CG}^2 \qquad [2.25]$$

$$Ix_r'y_r' = Ix_ry_r - A \cdot x_{CG} \cdot y_{CG} \qquad [2.26]$$

where: Ix_r is the second moment of area about x_r axis; Iy_r is the second moment of area about y_r axis; and, $Ix_r y_r$ is the product of inertia about x_r and y_r axes.

The angle of inclination, Φ, of the principal axis x_p with respect to the reference axis x_r, as shown in Figure 2.4, can be calculated using Mohr's circle for principal axes:

$$\Phi = 0.5 \cdot a\tan\left(\frac{2 \cdot Ix_r y_r}{Iy_r - Ix_r}\right) \qquad [2.27]$$

and the principal second moments of area can now be obtained as:

$$Ix_p = 0.5 \cdot (Ix_r + Iy_r) + 0.5 \cdot (Ix_r - Iy_r) \cdot \cos(2\Phi) - Ix_r y_r \cdot \sin(2\Phi) \qquad [2.28]$$

$$Iy_p = 0.5 \cdot (Ix_r + Iy_r) - 0.5 \cdot (Ix_r - Iy_r) \cdot \cos(2\Phi) + Ix_r y_r \cdot \sin(2\Phi) \qquad [2.29]$$

where: Ix_p is the principal moment of inertia about x_p axis; and, Iy_p is the principal moment of inertia about y_p axis.

The coordinates of all points L_i, lying on the outer surface of the cross-section, are transformed to the principal axis system, using the following equations:

$$x_p^{L_i} = (x_r^{L_i} - x_{CG}) \cdot \cos\Phi + (y_r^{L_i} - y_{CG}) \cdot \sin\Phi \qquad [2.30]$$

$$y_p^{L_i} = (x_{CG} - x_r^{L_i}) \cdot \sin\Phi + (y_r^{L_i} - y_{CG}) \cdot \cos\Phi \qquad [2.31]$$

where, $x_p^{L_i}$ and $y_p^{L_i}$ are coordinates of point L_i in the principal axis system.

Thus, when the calculations presented in this section are completed, the principal moments of inertia of the overall deteriorated pipe cross-section are known, and the outer surface is defined by N points (L_i) with respect to the principal axis system. This is sufficient information for the calculation of the approximated section modulus for bending moment applied about any arbitrary axis.

2.2.2 Section modulus for tension due to bending

Figure 2.5 shows the idealized cross-section subjected to some bending moment M, applied along an axis that is inclined at an angle α to the principal axis x_p. The maximum tensile stress due to this moment occurs at the point L_k, which is readily found as the point that is farthest from the neutral axis of all points (L_i) on the outer surface. This is accomplished numerically by transformation of coordinates (x_p , y_p) of all L_i points to the new temporary coordinate system (x_{temp} , y_{temp}), which is created by rotating the principal axis system by the angle α. The point L_k will have the largest positive y_{temp} coordinate, which is denoted as d. The coordinates of point L_k in the principal axis system are ($x_p^{L_k}$, $y_p^{L_k}$). The bending moment M is resolved as two components parallel to the principal axis, Mx_p and My_p, where:

$$Mx_p = M \cdot \cos\alpha \qquad [2.32]$$

$$My_p = M \cdot \sin\alpha \qquad [2.33]$$

The tensile stress, σ_T, at point L_k is the sum of stresses due to the two components of the bending moment:

$$\sigma_T = \frac{M \cdot \cos\alpha}{Ix_p} y_p^{L_k} - \frac{M \cdot \sin\alpha}{Iy_p} x_p^{L_k} \qquad [2.34]$$

The section modulus for tension, S_α, can be expressed as:

$$S_\alpha = \frac{M}{\sigma_T} \qquad [2.35]$$

and, rearranging Eq.[2.34], S_α is calculated from Eq.[2.37] as:

$$S_\alpha = \frac{Ix_p \cdot Iy_p}{Iy_p \cdot y_p^{L_k} \cdot \cos\alpha - Ix_p \cdot x_p^{L_k} \cdot \sin\alpha} \qquad [2.37]$$

For deteriorating pipe, it is convenient to normalize the section modulus as the fraction of the section modulus of the original pipe cross section

$$\left(S/S_o\right)_\alpha = \frac{Ix_p \cdot Iy_p}{S_o\left(Iy_p \cdot y_p^{L_k} \cdot \cos\alpha - Ix_p \cdot x_p^{L_k} \cdot \sin\alpha\right)} \qquad [2.38]$$

where S_o is defined as:

$$S_o = \frac{\pi}{4} \cdot \frac{(R_o + t_o)^4 - R_o^4}{R_o + t_o} \qquad [2.39]$$

2.3 Analysis of random pipe cross-sections by simulation using program PIPEXSC.EXE

The analysis of a random pipe cross-section by simulation using the program PIPEXSC.EXE will be presented in this section. Various models of a corroded pipe cross-section which are based on the Hydroscope measurements were developed. The method of generation of a random cross-section using only one specific model will be presented in detail. However, the modifications to the procedure for generation of a random pipe cross-section using other models will also be discussed. The simulation of a number of pipe cross-sections will allow the statistical analysis of simulated results.

2.3.1 Data provided by the Hydroscope tool

The data provided by the Hydroscope tool, at the current stage of development, consists of average and minimum thicknesses for each pipe joint. The average thickness reported can be either a local average, which corresponds to the location where the reported minimum thickness occurs, or it can be the overall average for the pipe joint. The tool has the capability to obtain a very large data sample, based on $\overline{t_{min}}$ and $\overline{t_{avg}}$ measurements for each 50 mm segment of pipe length. However this quantity of data is hard to store, and it is envisaged that typically measurements will be retained for the 4 or 5 sections per joint with the least minimum thicknesses.

It is necessary to account for the resolution of the data reported by the pig in any analytical simulation. The smallest pit that can be detected by the tool is limited to some

volume V_{min}. The reported wall thicknesses $\overline{t_{min}}$ and $\overline{t_{avg}}$ are measurements with associated errors that are conventionally expressed as fractions of the nominal wall thickness t_o. Thus the analytical simulation must be programmed to permit the user to define values of V_{min} and measurement errors of $\overline{t_{min}}$ and $\overline{t_{avg}}$. As development of the tool continues, it is envisaged that the magnitude of these quantities will be reduced.

Future enhancement of the tool will allow measurement of the minimum thickness to be reported for each quadrant of each sampled section. The simulation should be able to accommodate this development.

2.3.2 Models to simulate different types of pipe deterioration

Figure 2.6 shows 10 models that simulate pipe cross-sections with different types of deterioration, which are available for the analysis of cross-section properties using the program PIPEXSC.EXE. The first five models, denoted as *Type 1(a, b)* and *2(a, b, c)*, are applicable if the set of measurements coming from the Hydroscope tool consists only of the average thickness of pipe cross-section, $\overline{t_{avg}}$, and the minimum thickness of pipe cross-section, $\overline{t_{min}}$, at each sampling point along the pipeline.

The *Type 3* and *4* models, which may also be considered as refined *Type 1* and *2* respectively, address the case where the minimum thickness of the pipe wall is measured in each quadrant of a cross-section ($\overline{t_{min(1)}}$ to $\overline{t_{min(4)}}$). For all models shown in Figure

2.6, minimum volume of a detectable pit, which reflects the resolution of the tool, is defined by the user and accounted for in the analysis.

Most of the analyses presented in this thesis are based on *Type 1* and *Type 2* models. The *Type 1(a, b)* models consider the formation of a single pit having an angular extent x and uniform depth $t_o - t_{min}$. The thickness of sound material (t_{rem}) on the remaining part of the cross-section is also assumed to be uniform. For model *Type 1a*, it is assumed that corrosion takes place on the outside of the pipe, whereas for model *Type 1b* corrosion takes place only on the inside of the pipe. The models denoted as *Type 2(a, b, c)* permit more sophisticated analysis, because the wall thicknesses are non-uniform and consider corrosion on the outside only (*2a*), the inside only (*2b*), or both the outside and inside (*2c*). Although the *Type 2* models generally provide better quality results, the time required for analysis is substantially longer than that needed for analysis using one of the corresponding *Type 1* alternatives.

The remaining models shown in the Figure 2.6 are denoted as *Type 3(a, b)* and *Type 4(a, b, c)*, and are not entirely different from *Types 1* and *2*. The *Type 3* and *4* models are developed in anticipation of the enhancements of the pig in the near future. Using two different models (e.g. *Type 2* and *Type 4*), the effectiveness of the tool enhancement can be assessed.

The refinement of the two basic models (*Type 1* and *2*) can be carried on even further if,

for example, more measurements of local defects (pits) become available.

In the following section a detailed description of the method for analyzing *Type 2* models is presented. The analysis of *Type 1*, *3* and *4* models is presented in Section 2.3.6.

2.3.3 Random pipe cross-section - *Type 2 (a, b, c)* models

The program PIPESXC.EXE, used for the analysis of a random pipe cross-section, incorporates almost entirely the procedure presented for the deterministic case in Section 2.2. There are, however, some significant enhancements. Many deterministic variables such as t_{avg}, t_{min}, or the angle α of inclination of the applied bending moment with respect to the principal axis x_p, now have to be treated as random variables. The geometry of the cross-section is also random, with the constraint that the average and minimum thicknesses must be consistent with the values reported by the tool. Thus there are three necessary steps involving simulations of random variables prior to the construction of a random cross-section:

1. simulation of random values of t_{avg} and t_{min}, corresponding to the measured $\overline{t_{avg}}$ and $\overline{t_{min}}$, with measurement errors being considered;
2. generation of N elements with random thicknesses to represent the overall pipe cross-section; and,
3. construction of some ordering system that governs the arrangement of the individual wall elements around the circumference of the pipe cross-section.

The orientation of the applied moment vector is also a random variable that is independent of the geometry of the section. Once the random cross-section is assembled, a number of different orientations of the applied moment vector must be considered.

2.3.4 Simulation of random variables

2.3.4.1 Measurement errors of reported average and minimum wall thickness values

Both measurements provided by the pig for each sampled section, $\overline{t_{avg}}$ and $\overline{t_{min}}$, are treated as independent normally-distributed random variables, t_{avg} and t_{min}, with variabilities defined by user specified measurement tolerances. The measurement errors are independent identically distributed. The mean value of t_{avg} or t_{min} is assumed equal to the reported value. The standard deviation of t_{avg} or t_{min} is assumed equal to half the user-defined tolerance. For example, if the tolerance is specified to be $0.20t_o$, the standard deviation is assumed equal to $0.10t_o$, and it is assumed that roughly 95% of the distribution lies within the range $\pm 0.20t_o$. Randomly generated values of t_{avg} and t_{min} are used for calculation of the section modulus of a pipe cross-section, unless the user defines measurement error equal to 0. The randomly generated wall thicknesses must satisfy the following:

- $t_{avg} \leq t_o$
- $t_{min} \leq t_{avg}$
- both t_{min} and $t_{avg} \geq 0$

These three conditions imply that either the distribution of t_{min} or t_{avg} may be bounded on one or sometimes both sides of the mean value, by a value different than two standard deviation. Because t_{avg} may function as an upper bound for random t_{min}, t_{avg} value is generated first. All possible cases for the distributions of t_{avg} and t_{min} are illustrated in Figures 2.7(a) to (f).

2.3.4.2 Unknown elements of a random pipe cross-section

The previous example considered a deterministic cross-section, where dimensions of all elements were known. For a randomly-generated cross-section, both the number and thickness of the elements have to be assumed. There is no unique solution to this problem, and many different methods can be developed to generate a suitable set of elements, which then can be assembled to form a random pipe cross-section. However, there are three characteristics of a random pipe cross-section which should be considered by the procedure: the average wall thickness t_{avg}; the minimum wall thickness t_{min}; and, the minimum pit volume V_{min}.

It is expedient to define a discrete set of wall elements that will serve as the pool from which the cross-section is randomly generated. The general analysis for the deterministic case presented in the previous section did not required constraints concerning the number of elements or the corrosion depth for a single element. For the random cross-section, it is convenient to define a pool of distinct elements for analysis, where only incremental

changes to the wall thickness and corrosion depth of an element are considered. The pool of elements considered in the program PIPEXSC.EXE, evolves logically from assumptions that the nominal thickness, t_o, and minimum thickness, t_{min}, of the pipe cross-section are both integer values. The procedure incorporated in the program generates a suitable set of elements to simulate a deteriorated pipe cross-section using a number of distinct *Groups* of elements. All elements belonging to a particular Group have the same thickness of sound material, which is also the designation number for the Group. Elements within a particular Group may have different thicknesses of inside and outside corrosion. For a pipe with the nominal wall thickness t_o, there are t_o+1 distinct possible Groups of elements. It is assumed that the depths of corrosion outside and inside the pipe, c_1 and c_2 respectively, are integer values hence the thickness of remaining sound material, t, is also an integer.

To illustrate the concept of Groups, and the elements contained in each group, consider for example a pipe with the nominal thickness of t_o equal to 10 mm. The total number of Groups equals (10 + 1 =) 11. Group[0] represents the case of complete perforation, where thickness of remaining sound material is 0 mm. Group[10] represents the case of no corrosion, where the thickness of sound material is 10 mm. There are nine intermediate groups designated as Group[t], where t is the thickness of remaining sound material. For example Group[4] has a total depth of inside and outside corrosion equal to 6 mm, and the thickness of remaining sound material is 4 mm.

A number of different elements defined within each group depends on how much of the corrosion occurs at the inside of the wall and how much occurs at the outside. For the example pipe with t_o = 10 mm, Figure 2.8 shows all possible configurations of inside and outside corrosion for the Group[7], and the depths of inside and outside corrosion in millimeters are shown. The numbering system for all elements is:

$$element\ \# = t \cdot t_o + c_2 \qquad [2.40]$$

This system is particularly convenient because information about an element is stored in its designation number.

Similarly, Figure 2.9 shows an example of the Group[2] elements, which for the nominal thickness of the pipe wall t_o = 10 mm contains nine elements. Although the elements shown are not rectangular, they were depicted as such in Figures 2.8 and 2.9 for simplicity.

The number of Groups, and the associated number of elements belonging to each group, depends only on the nominal thickness of the pipe and the corrosion pattern, i.e. inside corrosion only, outside corrosion only, or both. For the cases of only inside corrosion or only outside corrosion, each group consists of a single element only. Once the various possible elements of all appropriate Groups are defined, elements can be selected randomly to build a pipe cross-section. The total number of elements located about the circumference of the cross-section, N, can be expressed as:

$$N = \sum_{t=0}^{t_o} n[t] \qquad [2.41]$$

where $n[t]$ is a number of elements to be selected from Group[t]. To simulate the deteriorated pipe cross-section, the $n[t]$ values must be generated randomly while achieving the desired minimum and average thicknesses, and minimum pit volume.

The minimum thickness value can be achieved using the condition that the thickness of sound material t of an element used for the cross-section can not be smaller than t_{min}. This condition defines the lower bound of the groups that can be considered for a given simulation, and thus the total number of elements, N, can be expressed as:

$$N = \sum_{t=t_{min}}^{t_o} n[t] \qquad [2.42]$$

The minimum pit volume condition can be expressed as a minimum number of elements having thickness t_{min}. Figure 2.10 shows an unfolded length ΔL of a pipe containing a circular pit. The mean radius of the pipe, r, is

$$r = R_o + 0.5 \cdot t_o \qquad [2.43]$$

where R_o is the inside radius of the pipe and t_o is the original wall thickness. Assuming a circular pit with radius r_1 and uniform depth equal to $(t_o - t_{min})$, the volume of the pit is:

$$V = \pi \cdot r_1^2 \cdot (t_o - t_{min}) \qquad [2.44]$$

Thus to satisfy the minimum pit volume condition $V \geq V_{min}$,

$$r_1 \geq \sqrt{\frac{V_{min}}{\pi \cdot (t_o - t_{min})}} \qquad [2.45]$$

Thus along section A-A the total width of the pit is $2r_1$ and the mean pipe circumference is $2\pi \cdot r$. The associated minimum number of elements having thickness t_{min}, $n_o[t_{min}]$, is therefore:

$$n_o[t_{min}] = N \cdot \frac{r_1}{\pi \cdot r} \qquad [2.46]$$

Recalling Eq.[2.1], and using Eqs.[2.43] and [2.45] to eliminate r and r_1 respectively, from Eq.[2.46]

$$n_o[t_{min}] = \frac{1}{\beta \cdot (R_o + 0.5 \cdot t_o)} \sqrt{\frac{V_{min}}{\pi \cdot (t_o - t_{min})}} \qquad [2.47]$$

Thus according to the minimum wall thickness and minimum pit volume, the total number of elements N can be now expressed as:

$$N = n_o[t_{min}] + \sum_{t=t_{min}}^{t_o} n[t] \qquad [2.48]$$

The remaining objective of the element selection process is to randomly generate $N - n_o[t_{min}]$ element thicknesses such that the average thickness of all elements selected

equals the target value. This can be achieved by calculating the average value, $\bar{t}$, after each element is selected using the equation

$$\bar{t} = \frac{n_o[t_{min}] \cdot t_{min} + \sum_{t=t_{min}}^{t_o} (n[t] \cdot t)}{n_o[t_{min}] + \sum_{t=t_{min}}^{t_o} n[t]} \qquad [2.49]$$

If the average value $\bar{t}$ is less than the target value, then the next element is randomly selected from the subset $t_{avg} \le t \le t_o$, and the associated number of elements selected from that group, $n[\,t\,]$ is incremented by one. If the average value $\bar{t}$ is greater than the target value, than the next element is randomly selected from the subset $t_{min} \le t \le t_{avg}$. The random choice of a Group[t] on either side of the average thickness t_{avg} is based on the uniform distribution. If more data regarding the distribution of the wall thickness of a cross-section of corroded pipe is available in the future, the type of the distribution for Group selection can be easily adjusted to account for the new information. The Group selection continues until the total number of elements selected, given by Eq.[2.48], equals N.

To illustrate this process, consider an example cross-section with t_o = 10 mm, t_{avg} = 7.5 mm, t_{min} = 3.0 mm and N = 90 elements. If the pipe radius R_o is 66 mm and V_{min} = 3000 mm^2, the minimum number of elements with the minimum thickness of 3 mm is, from Eq.[2.47], 5. The current average thickness of these 5 elements selected is

3.0 mm, and to bring this average closer to the target value of 7.5 mm, the next thickness must be randomly selected from one of groups [8], [9], or [10]. The new average will be determined for the $n_o[\ t_{min}\ ] + 1$ elements and will be again compared to the target value of 7.5 mm. If the actual average exceeds 7.5 mm, the next thickness must be randomly selected from groups [3], [4], [5], [6] or [7]. The process is repeated until all 90 elements are selected. Figure 2.11 shows graphically the process of selection of elements for this particular example. The running average approaches very quickly the target value, and after that $\bar{t}$ oscillates very closely around t_{avg} with each subsequent selection of a new element.

The next step of the procedure is to randomly generate numbers of elements within each group, accounting for the extent of external or internal corrosion. It is expedient to simultaneously assemble an array, $\{\ EL\ \}$, that contains all elements of the randomly generated pipe cross-section. Following the number of elements $n[\ t\ ]$ to be drawn from a particular Group[t] (for $t = t_{min}, t_o$), selection of elements of the array $\{\ EL\ \}$ begins from the Group[t_{min}]. In the cases when only inside or only outside corrosion is considered, each Group has only one element, and this step is trivialized. If, however, the corrosion is considered to occur on both the inside and the outside, program PIPEXSC.EXE allows the elements within each group to be assigned randomly, or chosen to match a user-defined ration of the depth of outside and inside corrosion.

The random choice of elements is based on the uniform distribution, and the resulting distributions of elements selected for each Group are approximately uniform. The degree of approximation to the uniform distribution will depend on the magnitude of the individual $n[\,t\,]$ value. The ratio of the depth of the outside corrosion to the depth of the inside corrosion, RC, can be simply approximated as:

$$RC = \frac{1 + \sum_{i=1}^{N} c_{1i}}{1 + \sum_{i=1}^{N} c_{2i}} \qquad [2.50]$$

If the elements in a Group are selected randomly, the generated cross-section will have approximately the same degree of inside and outside corrosion. This is a direct consequence of the uniform distribution of elements selected from one Group, and the definition the elements in a Group itself.

If the choice of elements is governed by the ratio RC' specified by the user, then a selection process based on the running value of the RC is used. Prior to the selection of an element, the current ratio RC is evaluated from Eq.[2.50], then the element which minimizes the difference between the target RC' and the one calculated from Eq.[2.50] is selected.

After all N elements are chosen, elements are ordered in array $\{ EL \}$ in accordance with the increasing thickness of sound material. The array of elements for the previous example for the *Type 2c* model, may look like

$$\{ EL \} = \{ \underbrace{34, 35, 37, \ldots\ldots, 36}_{n_o[3]+n[3]}, \underbrace{43, 45, 46, 43}_{n[4]}, \underbrace{\ldots\ldots, 90, 91, \ldots\ldots, \ldots\ldots 100}_{n[5], n[6], \ldots, n[10]} \} \qquad [2.51]$$

2.3.4.3 Location of elements forming a pipe cross-section

The assembly of a pipe cross-section requires a routine to govern the placement of elements of the array $\{ EL \}$ around the circumference of a cross-section. To assure creation of a pit having a volume of at least V_{min}, $n_o[t_{min}]$ elements must be placed in adjacent positions. The program PIPEXSC.EXE allows for the placement of the remaining ($N - n_o[t_{min}]$) elements of the array $\{EL\}$ in random order or in order of increasing thickness. For random order, elements are randomly placed around the circumference of a cross-section. For placement in the order of increasing thickness, the order of the placement follows the one already incorporated in the array $\{ EL \}$, starting at each side of the pit and placing consecutive elements of the array on alternating sides.

This step completes the generation of a random cross-section with mean thickness, minimum thickness, and minimum pit volume corresponding to typical readings from the Hydroscope tool. The procedure for calculation of the cross-section properties is exactly the same as the one outlined for the deterministic cross-section.

2.3.4.4 Uncertain location of the neutral axis of bending

The orientation of the neutral axis of bending is another important random variable which has to be addressed in the analysis. The inclination of the neutral axis with respect to any of the principal axis of the cross-section is unknown, making it necessary to consider a number, m, of possible orientations. The angle of inclination of the neutral axis, α_j, with respect to the principal axis x_p, that are considered are

$$\alpha_j = \frac{2\pi}{m} \cdot j \qquad [2.52]$$

where $j = 1...m$. This leads to m different normalized values of the section modulus $(S/S_o)_j$ for each set of randomly generated elements, corresponding to a single pipe cross-section.

2.3.5 Statistical parameters of the S/S_o distribution reported by the program

Statistics calculated by the program consider k simulated random cross-sections for a single set of t_{avg}, t_{min} , and V_{min} values. The calculations of the statistical measures describing the distribution of S/S_o are performed in two steps. For the simulation of the i^{th} cross-section, with $j = 1...m$ positions of the neutral axis of bending, five statistical parameters are calculated. The mean value of the normalized section modulus, $\left(\overline{S/S_o}\right)_i$, is:

$$\left(\overline{S/S_o}\right)_i = \frac{1}{m}\sum_{j=1}^{m}\left(S/S_o\right)_{ij} \qquad [2.53]$$

The variance, $\sigma^2_{\bar{z}_i}$ is:

$$\sigma^2_{\bar{z}_i} = \sigma^2_{\left(S/S_o\right)_i} = \frac{1}{m-1}\sum_{j=1}^{m}\left[\left(S/S_o\right)_{ij} - \left(\overline{S/S_o}\right)_i\right]^2 \qquad [2.54]$$

and the standard deviation of $\left(S/S_o\right)_i$ is:

$$\sigma_{\bar{z}_i} = \sigma_{\left(S/S_o\right)_i} = \sqrt{\frac{1}{m-1}\sum_{j=1}^{m}\left[\left(S/S_o\right)_{ij} - \left(\overline{S/S_o}\right)_i\right]^2} \qquad [2.55]$$

The minimum and maximum recorded values of S/S_o encountered during the simulation of the i^{th} cross-section are:

$$MIN\left(S/S_o\right)_i = \min\left\{\left(S/S_o\right)_{ij}\right\} \qquad [2.56]$$

$$MAX\left(S/S_o\right)_i = \max\left\{\left(S/S_o\right)_{ij}\right\} \qquad [2.57]$$

For the data corresponding to the set of k simulated cross-sections, six statistical parameters are calculated. The mean value of means, μ, is:

$$\mu = \frac{1}{k}\sum_{i=1}^{k}\left(\overline{S/S_o}\right)_i \qquad [2.58]$$

The mean value of means represents the expected value of S/S_o for a section with a given $\overline{t_{avg}}$ and $\overline{t_{min}}$, based on k simulations.

$$\sigma_3^2 = \sigma^2_{\left(\overline{S/S_o}\right)} = \frac{1}{k-1}\sum_{i=1}^{k}\left[\left(\overline{S/S_o}\right)_i - \mu\right]^2 \qquad [2.59]$$

The mean variance, σ_4^2, for k simulated cross-section is:

$$\sigma_4^2 = \frac{1}{k}\sum_{i=1}^{k}\sigma_{2_i}^2 \qquad [2.60]$$

and the variance of the standard deviation of the normalized section modulus is:

$$\sigma_5^2 = \frac{1}{k-1}\sum_{i=1}^{k}\left[\sigma_{2_i} - \sigma_4\right]^2 \qquad [2.61]$$

The minimum and maximum recorded values of S/S_o . a and b respectively, recorded for k simulated cross-sections are:

$$a = \min\left\{MIN\left(S/S_o\right)_i\right\} \qquad [2.62]$$

$$b = \max\left\{MAX\left(S/S_o\right)_i\right\} \qquad [2.63]$$

In the case of a single simulation, parameters of the S/S_o distribution expressed by Eqs.[2.53], and [2.55] to [2.57] describe the effect of the unknown orientation of the neutral axis of bending. If a number of simulations is carried out. Eqs.[2.58] and [2.61] to [2.63] are applicable and account for the effect of the unknown deterioration profile around the pipe circumference.

To thoroughly describe the characteristics of S/S_o distributions for a particular type of pipe defined by D_o and t_o a number of different combinations of t_{min} and t_{avg} can be considered, with the requirement that $t_{avg} \geq t_{min}$. Thus for $0 \leq t_{min} \leq t_o$ and $t_{min} \leq t_{avg} \leq t_o$, statistical results of the simulations can be reported as a set of triangular matrices, where each matrix describes fully one parameter of the S/S_o distribution, as defined by one of Eqs.[2.58] to [2.63] above. This is the presentation format used for output of the program PIPEXSC.EXE, as described in Appendix A.

2.3.6 Modifications to the basic procedure for *Type 1, 3* and *4* models

The basic analysis of the deterministic cross-section and the random generation of *Type 2 (a, b, c)* deteriorated cross-sections was presented in the previous section. In this section modifications to this basic procedure will be presented for the *Type 1*, *Type 3* and *Type 4* cross-sections. The treatment of the minimum volume of a detectable pit, V_{min}, and the generation of random wall thicknesses based on measured values and the measurement errors, are common for all types of models. Similarly, the solution to the problem of unknown orientation of the neutral axis of bending and the statistical analysis of simulated results are independent of the type of model used.

2.3.6.1 Models *Type 1(a, b)*

There are three random variables involved in the generation of a pipe cross-section using *Type 1* models: the average wall thickness, t_{avg}; the minimum wall thickness, t_{min}; and the

angular extent of the single pit x. The average and the minimum random wall thickness are generated in the same manner as for the *Type 2* models. The angular extent of the pit is randomly selected from a range of acceptable values. The requirement that the volume of the pit equals or exceeds V_{min} gives the minimum value. from Figure 2.6 and Eq.[2.44] is:

$$x_{min} = \frac{2}{(R_o + 0.5 \cdot t_o)} \sqrt{\frac{V_{min}}{\pi \cdot (t_o - t_{min})}} \qquad [2.64]$$

The requirement that the remaining thickness of the pipe wall, t_{rem}, must be less than the original wall thickness, t_o, gives the maximum value x_{max}. The average wall thickness t_{avg} for the *Type 1* cross-section models can be expressed as:

$$t_{avg} = \frac{t_{rem} \cdot (2\pi - x) + t_{min} \cdot x}{2\pi} \qquad [2.65]$$

Substituting t_{rem} with t_o in Eq.[2.65], x_{max} can be calculated as:

$$x_{max} = 2\pi \cdot \frac{t_o - t_{avg}}{t_o - t_{min}} \qquad [2.66]$$

Once the range of acceptable values of the angular extent of the pit is established, x is randomly drawn from the range (x_{min} , x_{max}) assuming a uniform distribution, and the t_{rem} is calculated from Eq.[2.65] as:

$$t_{rem} = \frac{2\pi \cdot t_{avg} - x \cdot t_{min}}{2\pi - x} \qquad [2.67]$$

At this point, all dimensions of the cross-section have been randomly generated. Assuming the reference axis system (x_r , y_r) as shown in Figure 2.6, the calculations of the cross-section properties follow the steps for a deterministic cross-section outlined in Section 2.2. There are only two elements of the pipe cross-section which have to be considered in the summation leading to the cross-section properties - the ring and the arc element constituting the pit. Although a continuous description of the outer surface of the cross-section is possible in this case, the description in the form of N points is used in the program PIPEXSC.EXE, to allow the use of one subroutine for computation of the S/S_o for all models.

2.3.6.2 Models *Type 3(a, b)*

The analysis of the cross-section properties using models *Type 3(a, b)* is very similar to the one describe for the *Type 1* models. *Type 3(a, b)* models, shown in Figure 2.6, have single pits located in each quadrant of the cross-section. There are number of random variables involved in the generation of a random pipe cross-section: the overall average thickness, t_{avg}; the minimum thicknesses for each quadrant, $t_{min(1)}$, $t_{min(2)}$, $t_{min(3)}$ and $t_{min(4)}$; the angular extent of pit for each quadrant, x_1, x_2, x_3, x_4; and the locations of pits within the quadrants. The overall average wall thickness and the minimum wall thicknesses in each quadrant are randomly generated in the same manner as for the *Type 2* models. The

angular extent of the pits are randomly selected from a range of acceptable values. The requirement that the volume of the i[th] pit equals or exceeds V_{min} gives the minimum value, $x_{min(i)}$, calculated from Eq.[2.64] as:

$$x_{min(i)} = \frac{2}{(R_o + 0.5 \cdot t_o)} \sqrt{\frac{V_{min}}{\pi \cdot (t_o - t_{min(i)})}} \qquad [2.68]$$

where i = 1,2,3 and 4, is the designation for the quadrant. Similar to *Type 1* models, the requirement that the remaining thickness of the pipe wall, t_{rem}, must be less than the original wall thickness, t_o, gives the maximum value $x_{max(i)}$. The average wall thickness, t_{avg}, for the *Type 3* cross-section models can be expressed modifying Eq.[2.65] as:

$$t_{avg} = \frac{1}{2 \cdot \pi} \left[t_{rem} \left(2\pi - \sum_{i=1}^{4} x_i \right) + \sum_{i=1}^{4} x_i \cdot t_{min(i)} \right] \qquad [2.69]$$

Substituting t_{rem} with t_o in Eq.[2.69], and considering that each pit is generated within a quadrant, $x_{max(i)}$ is calculated as:

$$x_{max(i)} = \frac{1}{t_o - t_{min(i)}} \left[2\pi \cdot (t_o - t_{avg}) - \sum_{j=1, j \neq i}^{4} x_j (t_o - t_{min(j)}) \right], \text{ and } x_{max(i)} \leq \frac{\pi}{2} \qquad [2.70]$$

Eq.[2.70] implies that the $x_{max(i)}$ for any quadrant can be established only if the extents of the pits in the remaining three quadrants are known.

Prior to randomly selectioning a pit extent for each quadrant, the quadrants are randomly ordered for each simulation of a pipe cross-section (e.g. i = 2,3,1 and 4). The initial extent of each pit, x_i, is set to its minimum value, which is obtained using Eq.[2.68]. Following the order of quadrants, the maximum value $x_{max(i)}$, for first quadrant considered is determined from Eq.[2.70], and x_i is randomly selected from the range $(x_{min(i)}, x_{max(i)})$. The consecutive random selections of remaining pit extents use constantly updated values of x_i to determine the applicable range.

Once the random selections of x_i are completed, the remaining uniform wall thickness, t_{rem}, is obtained from the modified Eq.[2.67] as:

$$t_{rem} = \frac{2\pi \cdot t_{avg} - \sum_{i=1}^{4} \left(x_i \cdot t_{min(i)}\right)}{2\pi - \sum_{i=1}^{4} x_i} \qquad [2.71]$$

The random selection of shifts of all pits within their respective quadrants, where for the i[th] quadrant the shift is generated from the range $\left(0, \frac{\pi}{2} - x_i\right)$, completes the procedure leading to the assessment of the geometry of randomly generated pipe cross-section. The calculations of the cross-section properties are performed following the procedure outlined in Section 2.2. There are only five distinct elements of the pipe cross-section in the case of *Type 3* models: the ring and the four arc elements constituting pits in each

quadrant. The description of the outer surface of the cross-section, in the form of N points, is used to calculated the normalized section modulus S/S_o.

2.3.6.3 Models *Type 4(a, b, c)*

The analysis of the cross-section properties using models *Type 4(a, b, c)* is very similar to the one described in Section 2.3.3 for the *Type 2* models, except that most operations leading to the construction of the pipe cross-section are done on a quadrant basis. There are six random variables involved in the generation of a random pipe cross-section: the overall average thickness, t_{avg}; the minimum thicknesses for each quadrant, $t_{min(1)}$, $t_{min(2)}$, $t_{min(3)}$ and $t_{min(4)}$; and the location of a pit within the quadrant. Specification of the minimum wall thicknesses in each quadrant makes no difference for the generation of random wall thicknesses, and the routine for the *Type 2* models applies entirely. The procedure which generates a number of elements $n[\ t\ ]$ from each appropriate Group[t] , outlined in detail for the *Type 2*, is no different except for two small modifications. The first modification is that the smallest minimum thickness out of $t_{min(1)}$ to $t_{min(4)}$ defines the lower end of the range of applicable Groups considered in the simulation. The second modification is that the minimum pit volume (V_{min}) translates into four preset numbers of elements ($n_o[t_{min(1)}]$, $n_o[t_{min(2)}]$, $n_o[t_{min(3)}]$ and $n_o[t_{min(4)}]$), associated with the formation of a minimum pit in each quadrant. These modifications require minor changes in Eqs.[2.48] and [2.49], to include $n_o[t_{min(1)}]$ to $n_o[t_{min(4)}]$, before proceeding with generation of $n[\ t\ ]$. Once $n[\ t\ ]$ are determined for the cross-section, numbers of elements for each

quadrant, denoted as $n_1[t] - n_4[t]$, are randomly selected from $n[t]$. It is necessary to select elements for the quadrant with the least value of the minimum thickness last to avoid possible problems with the last quadrant, which is already determined by the selection made for the preceding ones.

The total number of elements in each quadrant is:

$$\frac{N}{4} = n_o\left[t_{min(i)}\right] + \sum_{t=t_{min(i)}}^{t_o} n_i[t] \qquad [2.72]$$

where $i = 1,2,3,4$, is the designation for the quadrant. The process of random selection of $n_i[t]$ for the ith quadrant is performed in following steps:

1. $n_i[t]$ are set to 0, for $t = t_{min(i)} \ldots t_o$
2. number of elements to be drawn N^*, is evaluated based on the right side of Eq.[2.72]
3. t is randomly selected from the range ($t_{min(i)}$, t_o)
4. $n_i[t]$ is incremented by a number randomly selected from the range of 0 and the smaller of $n[t]$ or $N/4 - N^*$
5. steps 2-4 are repeated until all elements for the quadrant are selected

Once the $n_i[t]$ for each quadrant are determined, the selection of specific elements with a simultaneous assembly of an array $\{ El_t \}$ for each quadrant is performed in the same manner as for the *Type 2* models. The intermediate assembly of the ith quadrant is done by placing $n_o[t_{min(i)}]$ elements in the centre of the quadrant to form a pit, then the remaining

elements are placed using one of the routines describe for the *Type 2* models. The possible random shift of the pit within a quadrant can be expressed in terms of a number of single elements as:

$$\pm 0.5 \cdot \left(\frac{N}{4} - n_o \left[t_{min(i)} \right] \right) \qquad [2.73]$$

where a positive value represents a counterclockwise direction along the quadrant, and a negative value represents a clockwise direction. The shift of the pit, in terms of the number of elements, is randomly selected from the applicable range, and then the selected number of elements is displaced to the other end of the quadrant. If the ordered arrangement was assumed for elements, sorting of elements based on their thickness of sound material is required after random placement of the pit is completed. Sorting of elements is not required if elements are arranged randomly.

Once the random pipe cross-section is assembled, the analysis leading to the principal moments of inertia is identical as outlined for the *Type 2* cross-sections.

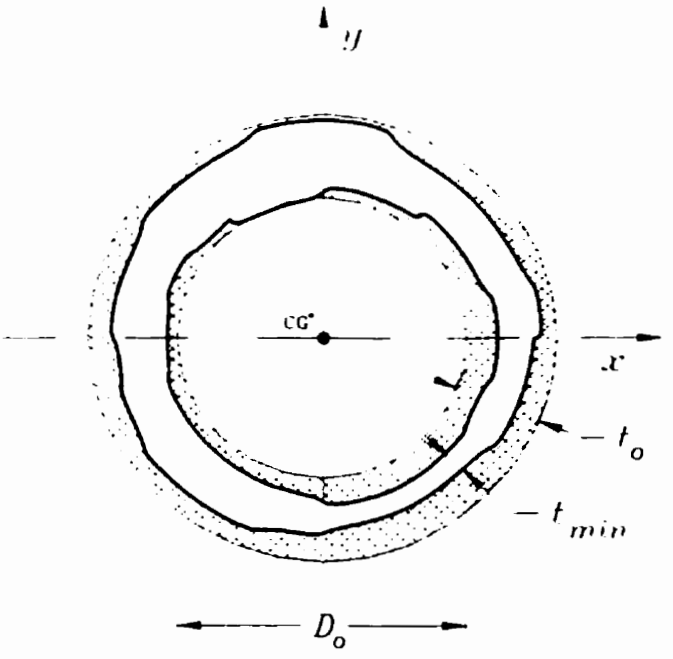

Figure 2.1 Example of deteriorated pipe cross-section

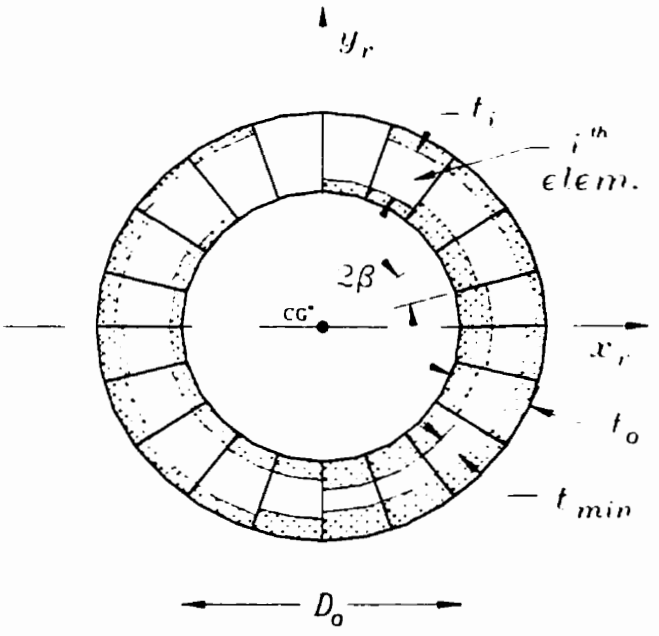

Figure 2.2 Discretized cross-section of deteriorated pipe and the assumed reference axis system

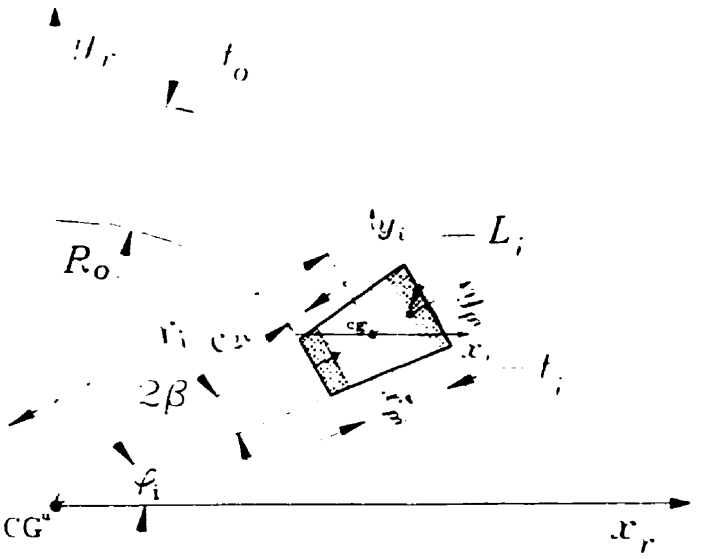

Figure 2.3 Single element of a pipe cross-section

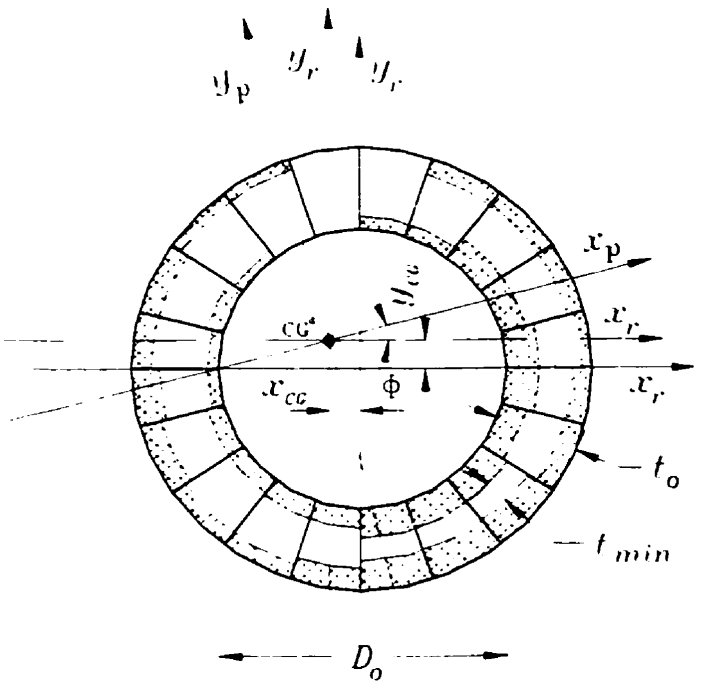

Figure 2.4 Principal axis of the cross-section

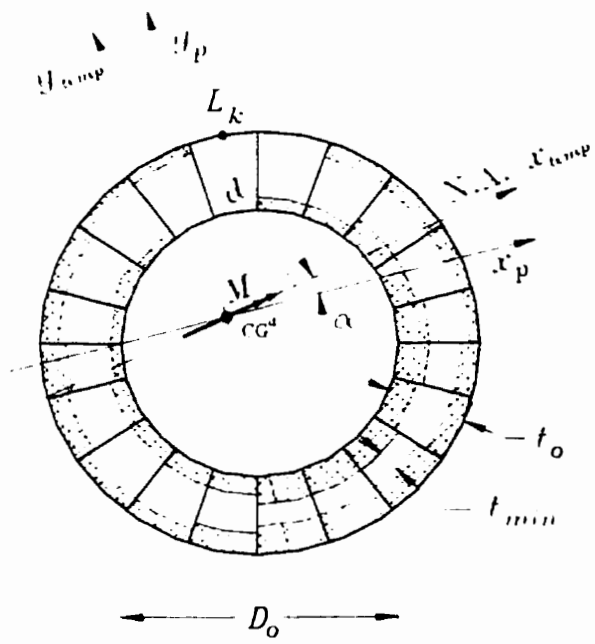

Figure 2.5 Pipe cross-section subjected to the bending moment *M*

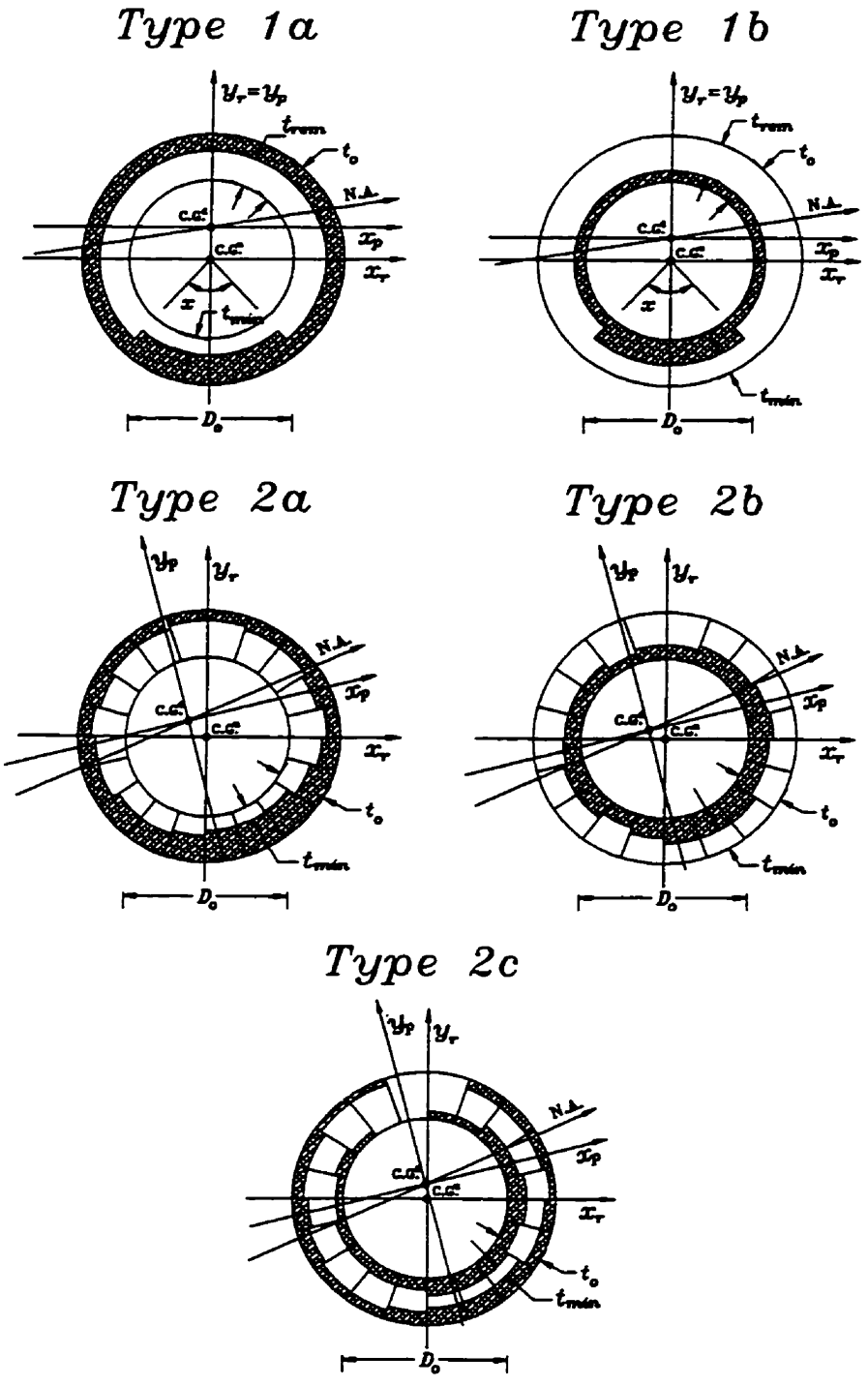

Figure 2.6 Types of models used for simulation of a cross-section of deteriorated pipe

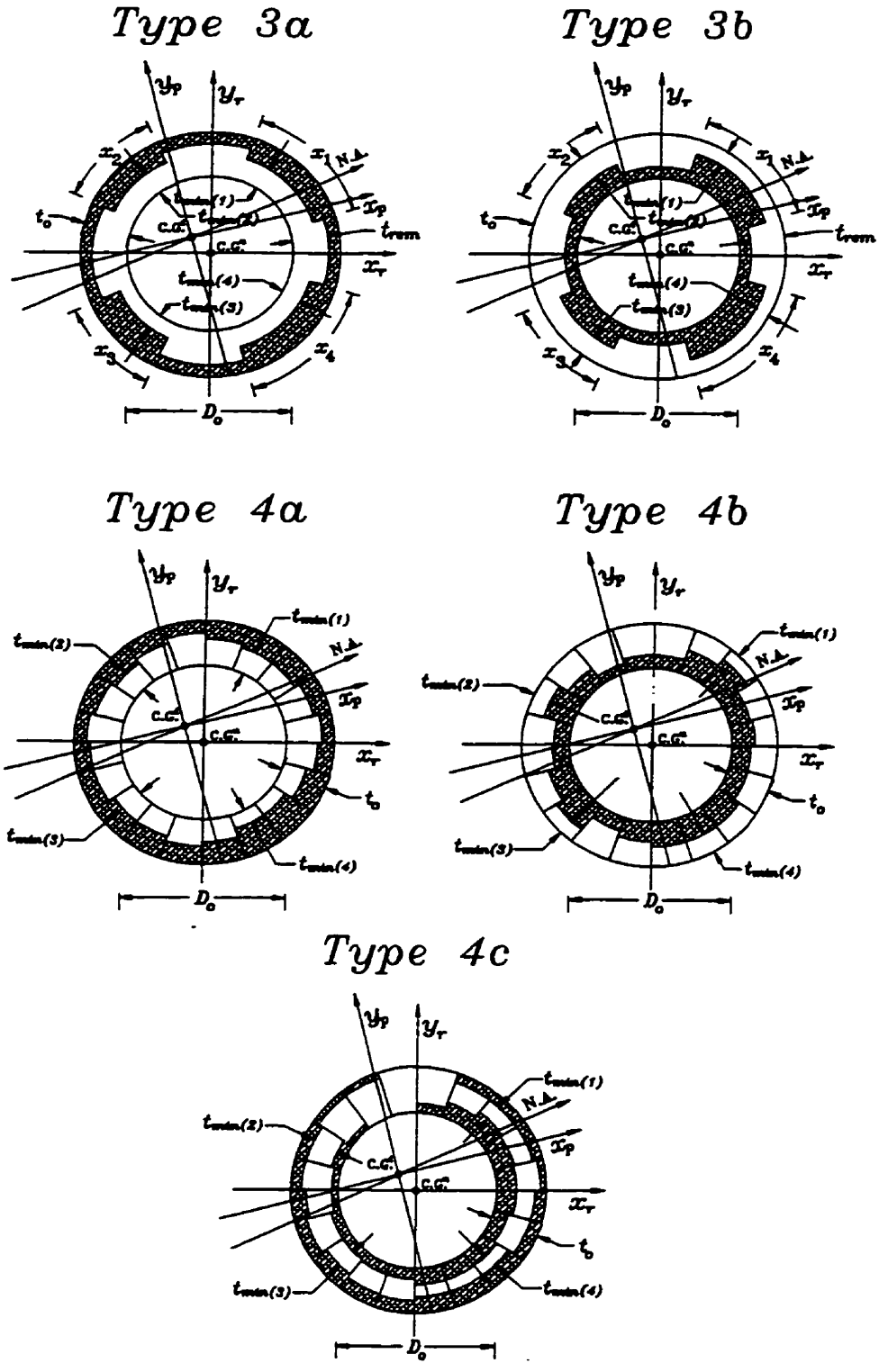

Figure 2.6(contd) Types of models used for simulation of a cross-section of deteriorated pipe

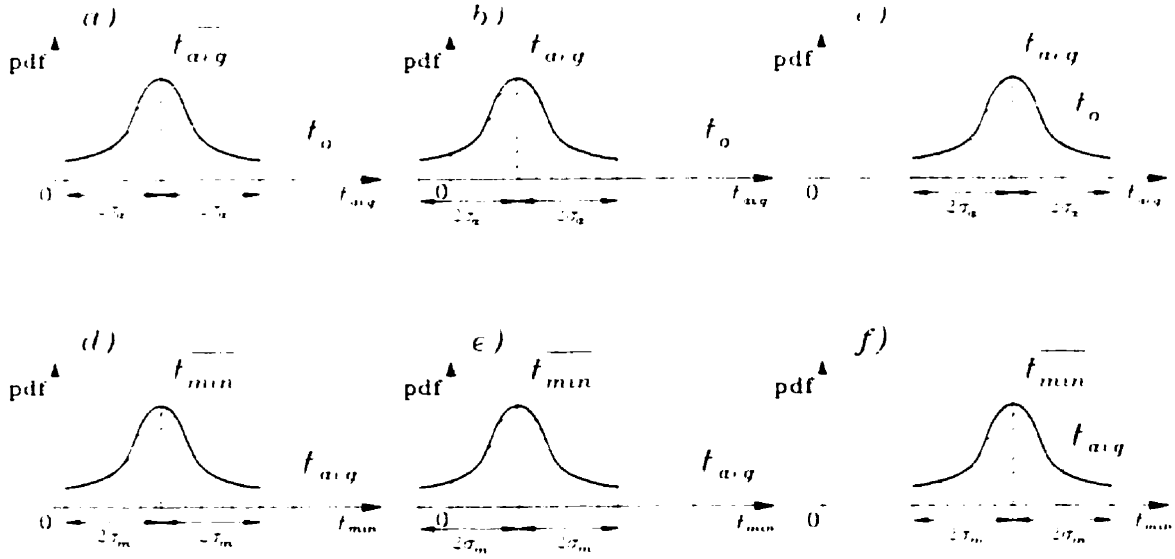

Figure 2.7 Assumed distributions of the minimum and the average thickness of pipe wall

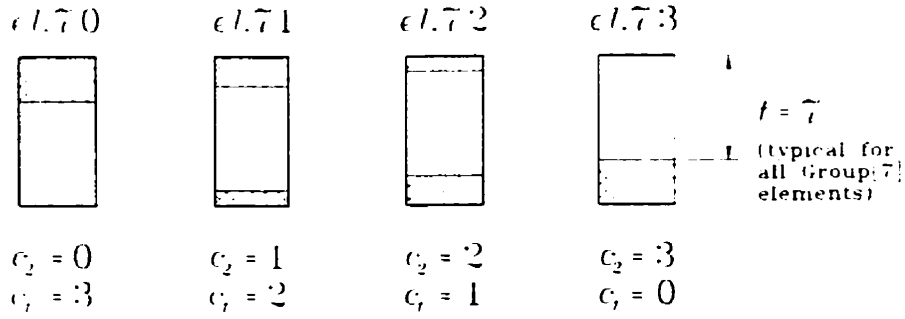

Figure 2.8 Group[7] - elements for t_o = 10 mm

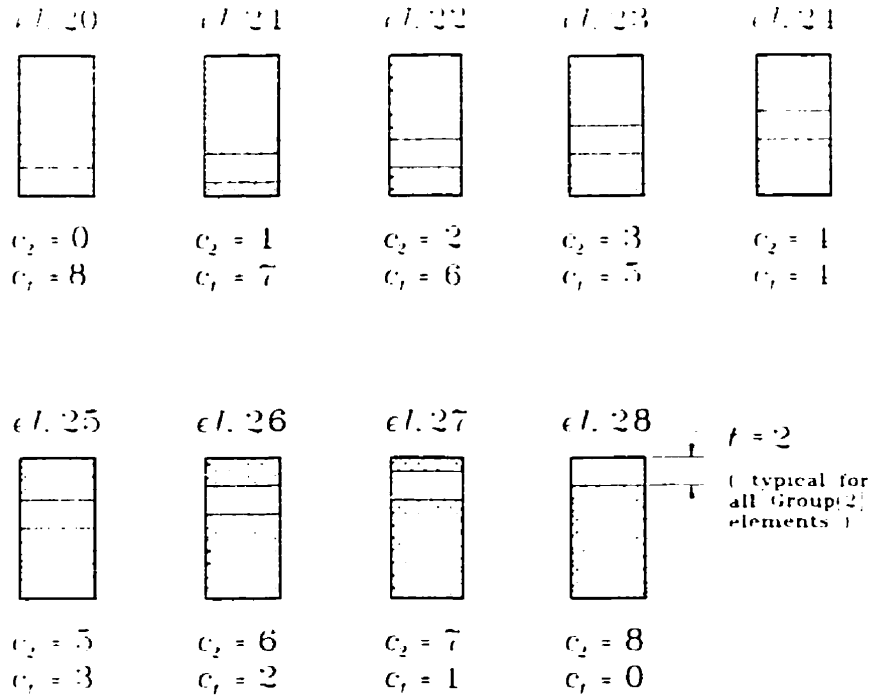

Figure 2.9 Group[2] - elements for t_o = 10 mm

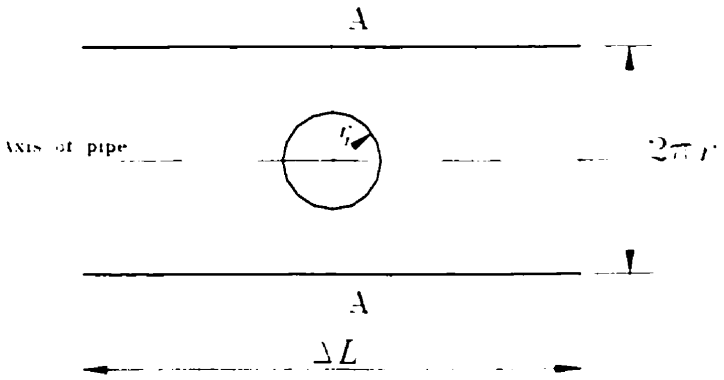

Figure 2.10 Unfolded pipe section with a circular pit

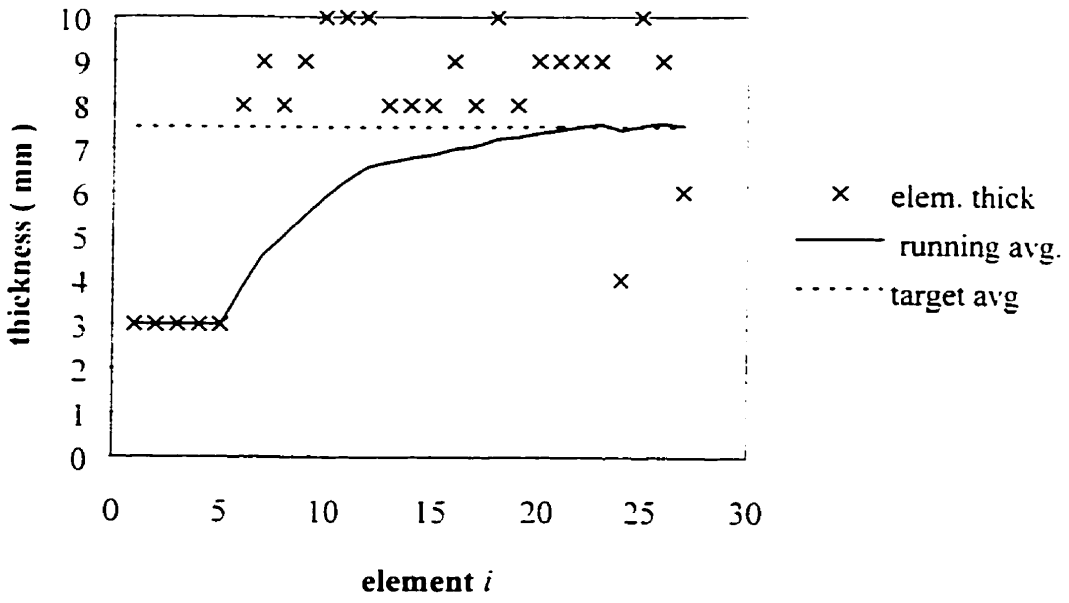

Figure 2.11 Choice of individual elements to match the target average wall thickness

Chapter 3 Pipe cross-section simulation results

3.1 Introduction

Chapter 3 presents sensitivity analysis and parametric studies using the program PIPEXSC.EXE. The objective of these analyses is to determine a probability distribution that represents the section modulus of a pipe cross-section with values of minimum and average wall thickness as measured by the Hydroscope tool.

The first part of Chapter 3 presents an investigation of the type of probability distribution that should be fit to the simulated S/S_o data. The investigation considers two variations of the *Type 2a* model, with elements arranged either randomly or according to the increasing thickness of sound material as discussed in Chapter 2. Graphs of the variation of the normalized section modulus due to the variable orientation of the bending moment are also presented.

The second part of Chapter 3 presents the results of simulations obtained for 152 mm (6") diameter pipe with nominal wall thickness t_o = 10 mm. and various combinations of the measured average and minimum wall thicknesses. $\overline{t_{avg}}$ and $\overline{t_{min}}$. Consideration of various combinations of $\overline{t_{avg}}$ and $\overline{t_{min}}$ address the problem of the flexural strength of corroded pipe in different stages of deterioration. The statistical parameters describing the

probability distribution of the normalized section modulus obtained for *Type 2a* model are also discussed.

The third part of Chapter 3 presents sensitivity analyses and parametric studies of the parameters of the S/S_o distribution as obtained by simulation. The parameters affecting the results generated by the program can be characterized as either tool-related or simulation-related. Tool-related parameters are associated with the nature and accuracy of the data reported by the tool. The tool-related parameters investigated include the measurement errors of the average and the minimum wall thicknesses, and different pipe cross-section models which correspond to possible tool enhancements. Simulation-related parameters are associated with the specifics of the pipe cross-section model and the simulation of the pipe cross-section. The simulation-related parameters investigated are the number of simulations and the number of elements used to generate a random pipe cross-section. Although the unknown orientation of applied bending moment is a tool-related parameter, the number of orientations of the moment vector considered in simulation of a pipe cross-section is treated as a simulation-related parameter.

3.2 Type of the probability distribution for S/S_o

The objective of this part of the investigation is to determine a suitable type of probability distribution to represent the ratio S/S_o for a cross-section with mean and minimum wall thicknesses as recorded by the Hydroscope tool. The *Type 2a* section, shown in Figure

2.6, was investigated because this type of the pipe cross-section model is currently of interest at the present stage of the tool development. Two possible arrangements of the elements in the cross-section were considered: a random arrangement; and an arrangement where the element thicknesses vary from a minimum at one point in the section to a maximum at the opposite point.

The analysis for a single set of data containing the average and the minimum pipe wall thicknesses is the most basic analysis allowed by the program PIPEXSC.EXE. The optional supplementary files SROT.DAT and ROTS.DAT, which can be obtained from analysis of a single cross-section, allow the results generated by PIPEXSC.EXE to be presented graphically and analyzed as described in Appendix A. The file SROT.DAT summarizes the results for up to 50 randomly-chosen simulations of pipe cross-section in a format that allows the type of distribution to be investigated using statistical analysis software, C-fit (CFER, 1996). The file ROTS.DAT summarizes the results for a single simulation. A complete description of these files and their content is presented in Appendix A.

3.2.1 Results for ordered arrangement of elements

The results presented in this section are for simulations of pipe cross-sections with an ordered arrangement of elements, denoted as *Type 2ac*, as shown in Figure 3.1. Due to the method of choosing elements and the ordering system assumed for the assembly of

elements, both described in Chapter 2, any simulated pipe cross-section is almost symmetrical about one of its principal axes. The investigation of a suitable type of probability distribution to represent the ratio S/S_o will first consider the results of simulations for the case where errors of the wall thickness measurements reported by the Hydroscope tool are assumed to be negligible. Then results for cases considering non-zero wall thickness measurement errors will be considered.

3.2.1.1 Simulations with no measurement errors

Figure 3.2 shows an example of the variation of the normalized section modulus S/S_o with respect to the angle, α, between the applied bending moment vector and the principal axes x_p. The values shown by the solid line with filled squares are for pipe with $\overline{t_{avg}}$ = 6 mm, $\overline{t_{min}}$ = 4 mm and no measurement errors. The range of the S/S_o values is from 0.475 to 0.675. The variation of S/S_o with α is consistent with the previous statement that *Type 2ac* model tends to be almost symmetrical about one principal axis.

The difference between the maximum and the minimum values of S/S_o depends on the magnitude of the shift of the position of the centre of gravity of simulated cross-section, as shown in Figure 2.4. For this particular pipe cross-section model, the translation of the centre of gravity from its initial position C.G.^{u} to its position C.G.^{d} due to deterioration of the pipe may be quite significant. The magnitude will depend on the variation of the wall thickness around the perimeter of the cross-section. For example, if the $\overline{t_{avg}}$ is close to

either $\overline{t_{min}}$ or t_o the shift of the C.G.[d] from its original position will be small. The line marked with open boxes in Figure 3.2 shows the results for $\overline{t_{avg}}$ = 6 mm and $\overline{t_{min}}$ = 2 mm. The range of S/S_o values is from 0.390 to 0.669, and it is larger than in the case of $\overline{t_{min}}$ = 4 mm.

Figure 3.3 shows a histogram of 4500 simulated values of S/S_o, for 50 cross-sections of pipe with $\overline{t_{avg}}$ = 6 mm and $\overline{t_{min}}$ = 4 mm, obtained using C-fit (CFER, 1996). The shape of the histogram varies with the wall measurements and the model used for simulations, but the simulated data are always in the range from 0 to 1.0. The dashed line shown in the figure marked as "LS Beta" represents the Beta distribution with parameters obtained from the simulated data using the least squares method. Different types of distribution, including the normal, the lognormal and Weibull, were fit to the data using C-fit, and in all cases the Beta distribution gave the best fit for the generated data.

Figures 3.4 and 3.5 show examples of the sample cumulative distribution, 4500 data points in each case, plotted on Beta probability paper. As in the case of the histogram shown in Figure 3.3 the least squares method was used to determine parameters of the fitted distribution.

3.2.1.2 Simulations with measurement errors

Figures 3.6 and 3.7 show the graphs of the sample cumulative distribution of S/S_o for the cross-section with the $\overline{t_{avg}}$ = 7.5 mm and $\overline{t_{min}}$ = 3 mm, and varying wall thickness measurement errors. In both figures, the error of the minimum thickness measurement is assumed to be $\pm 0.10 t_o$ which, as described in Chapter 2, represents a standard deviation of $0.05 t_o$. In Figure 3.6, the error of the average thickness is assumed to be $\pm 0.10 t_o$, and in Figure 3.7 it is $\pm 0.20 t_o$. These simulation results can be compared with the results for "no measurement error" case shown in Figure 3.5, which also has $\overline{t_{avg}}$ = 7.5 mm and $\overline{t_{min}}$ = 3 mm. The fit of the Beta distribution to the data improves markedly if the measurement errors are considered in the analysis.

When measurement errors are accounted for in the analysis, the range of simulated values of S/S_o increases. The variation of the range with the measurement error for a pipe with $\overline{t_{avg}}$ = 7.5 mm and $\overline{t_{min}}$ = 3 mm can be determined for Figures 3.5, 3.6 and 3.7. From Figure 3.5, for the case of "no measurement errors" S/S_o ranges from 0.528 to 0.837. From Figure 3.6, for the case of $\overline{t_{avg}}$ error $\pm 0.10\ t_o$ and $\overline{t_{min}}$ error $\pm 0.10\ t_o$, the range is from 0.447 to 0.926. From Figure 3.7, for the case of $\overline{t_{avg}}$ error $\pm 0.20\ t_o$ and $\overline{t_{min}}$ error $\pm 0.10\ t_o$, the range is from 0.334 to 1.0. It can be noted that the variation of range with the measurement error of $\overline{t_{avg}}$ is almost linear.

Section 3.5.2 will discuss the effect of measurement errors in more detail.

3.2.2 Results for random order of elements

In this section, simulated results obtained using the *Type 2a* model with elements distributed randomly around the pipe cross-section are presented. An example of the simulated cross-section, denoted as *Type 2ar*, is shown in Figure 3.8. In this case, the position of the centre of gravity of the deteriorated cross-section will be close to the initial centre of gravity C.G.^{u} of undeteriorated pipe cross-section. Thus, it is to be expected that the range of simulated values of S/S_o for a particular set of $\overline{t_{avg}}$ and $\overline{t_{min}}$ will be much smaller than for the case where the element arrangement is ordered, as considered in the previous section. The investigation of a suitable type of probability distribution to represent the ratio S/S_o will first consider the results of simulations for wall thickness measurements assumed to be exact, then the analysis of the results of simulations for wall thickness measurements subjected to some errors will follow.

3.2.2.1 Simulations with no measurement errors

Figure 3.9 shows the variation of the normalized section modulus S/S_o with respect to the angle, α, between the applied bending moment vector and the principal axis x_p. The variation of S/S_o shown for two simulated cross-section with $\overline{t_{avg}}$ = 6.0 mm and $\overline{t_{min}}$ equal to 4 mm and 2 mm, is erratic, with local peaks, and is quite different from the smooth curves shown in Figure 3.2. The range of S/S_o values obtained for $\overline{t_{min}}$ = 4 mm is from 0.532 to 0.594, while for $\overline{t_{min}}$ = 2 mm it is from 0.527 to 0.605. These ranges are much smaller than the ranges of sections with identical minimum and average wall

thicknesses, shown in Figure 3.2, where the elements are arranged in order of their thicknesses. Thus, this seemingly small difference in modelling of these two cross-sections may have a significant effect on their calculated probabilities of flexural failure.

Figure 3.10 shows a histogram of 4500 simulated values of S/S_o, for 50 cross-sections of pipe with $\overline{t_{avg}}$ = 6.0 mm and $\overline{t_{min}}$ = 4 mm, obtained using C-fit (CFER, 1996). The dashed line represents the Beta distribution, which parameters were obtained using the least squares method. The data are concentrated around the mean value, where in case of the ordered arrangement of elements, shown in Figure 3.3, the data are more concentrated in the tails.

Figures 3.11 and 3.12 show the graphs of the sample cumulative distribution of S/S_o for cross-sections with the same $\overline{t_{avg}}$ and $\overline{t_{min}}$ as shown in Figures 3.4 and 3.5 and discussed in Section 3.2.1. The fit of the Beta distribution to the data is improved in every case if the elements are randomly assembled to form the simulated pipe cross-section.

3.2.2.2 Simulations with measurement errors

Figures 3.13 and 3.14 show the graphs of the sample cumulative distribution of S/S_o for the cross-section with the $\overline{t_{avg}}$ = 7.5 mm and $\overline{t_{min}}$ = 3 mm, and varying wall thickness measurement errors. In both figures, the error of the minimum thickness measurement is assumed to be $\pm 0.10 t_o$ which, as described in Chapter 2, represents a standard deviation

of $0.05t_o$. In Figure 3.13, the error of the average thickness is assumed to be $\pm 0.10t_o$ and in Figure 3.14 it is $\pm 0.20t_o$. These simulation results can be compared with the results for "no measurement error" case shown in Figure 3.12, which also has $\overline{t_{avg}}$ = 7.5 mm and $\overline{t_{min}}$ = 3 mm. The fit of the Beta distribution to the data for randomly-arranged elements improves if the measurement errors are considered in the analysis, as was noted for the cross-section with ordered arrangements of elements.

When measurement errors are accounted for in the analysis, the range of simulated values of S/S_o increases. The variation of the range with the measurement error for a pipe with $\overline{t_{avg}}$ = 7.5 mm and $\overline{t_{min}}$ = 3 mm can be determined for Figures 3.12, 3.14 and 3.14. From Figure 3.12, for the case of "no measurement errors" S/S_o ranges from 0.657 to 0.772. From Figure 3.13, for the case of $\overline{t_{avg}}$ error $\pm 0.10\ t_o$ and $\overline{t_{min}}$ error $\pm 0.10\ t_o$ the range is from 0.586 to 0.865. From Figure 3.14, for the case of $\overline{t_{avg}}$ error $\pm 0.20\ t_o$ and $\overline{t_{min}}$ error $\pm 0.10\ t_o$ the range is from 0.500 to 0.981. It can be noted that the variation of range with the measurement error of $\overline{t_{avg}}$ is not as close to linear as in the case of the *Type 2ac* model discussed in Section 3.2.1.2.

3.2.3 Summary of the investigation of the type of distribution of S/S_o

The results presented in Sections 3.2.1 and 3.2.2 are typical of results obtained for other cross-section models, and for wide variations of $\overline{t_{avg}}$ and $\overline{t_{min}}$. In all cases the Beta

distribution provided the best fit to the simulated S/S_o distribution, regardless of the model type or the specified $\overline{t_{avg}}$ and $\overline{t_{min}}$ values. Thus the Beta distribution of the normalized section modulus will be used in the reliability analysis of a pipeline presented in Chapter 5 and 6.

3.3 Generation of statistical parameters for 6" (152 mm) diameter pipe using

Type 2ac model

In this section, statistical parameters are presented for the S/S_o distribution of a pipe with nominal outside diameter D and nominal wall thickness t_o, and various average and minimum measured wall thicknesses. This parameters are generated using the analysis method derived in Chapter 2 for unique values of average and minimum wall thickness, as implemented in the program PIPEXSC.EXE described in Appendix A. Considering various combinations of $\overline{t_{avg}}$ and $\overline{t_{min}}$, the complete statistical description of the remaining strength of deteriorated pipe is provided in terms of the normalized section modulus S/S_o.

Equations used to calculate the various parameters of the S/S_o distribution were discussed in Chapter 2. The mean value μ is the mean value of the mean S/S_o given by Eq.[2.58]. The standard deviation σ_3 is the standard deviation of the mean S/S_o values given by Eq.[2.59]. The standard deviation σ_4 is the square root of the mean value of variances of

S/S_o given by Eq.[2.60]. The maximum and minimum values, a and b, are the smallest and the largest values of S/S_o given by Eqs.[2.62] and [2.63].

The statistical parameters for a pipe with an outside diameter of 6" (152 mm) and a nominal wall thickness of 10 mm is presented in this section. Each set of statistical parameters for a given ($\overline{t_{avg}}$, $\overline{t_{min}}$) pair is based on 1000 simulated pipe cross-sections. For each simulated cross-section, 360 wall elements were generated and 90 orientations of the applied bending moment vector were considered. Measurement errors were not considered.

These results will be used as the reference for the sensitivity analyses and parametric studies presented later in this chapter.

3.3.1 Mean values of S/S_o - μ

Figures 3.15 and 3.16 are graphs of the overall mean value of the normalized section modulus, μ, for various sets of the average and the minimum wall thicknesses. In Figure 3.15, the variation μ with the measured average wall thickness $\overline{t_{avg}}$ is almost linear, and the effect of the minimum wall thickness $\overline{t_{min}}$ is slight. This is corroborated in Figure 3.16 where, for a given average thickness, the lines showing the variation of μ with $\overline{t_{min}}$ are almost horizontal. An approximate equation for the normalized section modulus S/S_o can be obtained from either Eq.[2.4] or [2.5], which define the second moment of area for

an arc element shown in Figure 2.3. Substituting $\beta = \pi$ and $t_i = t_{avg}$ in Eq.[2.4], the second moment of area for the pipe cross-section can be estimated as:

$$Ix = \pi \cdot \left(R_o + c_2 + 0.5 \cdot t_{avg}\right)^3 \cdot t_{avg} \qquad [3.1]$$

Neglecting c_2 as a very small value comparing to R_o, and denoting the term $R_o + 0.5 \cdot t_{avg}$ as the average radius of the pipe. R_{avg}, Eq.[3.1] can be expressed as:

$$Ix = \pi \cdot R_{avg}^3 \cdot t_{avg} \qquad [3.1a]$$

The approximate section modulus S is:

$$S = \frac{Ix}{R_{avg} + 0.5 \cdot t_{avg}} \qquad [3.2]$$

Substituting Eq.[3.1] into Eq.[3.2] and noting that $R_{avg} >> t_{avg}$, the section modulus S can be expressed as:

$$S = \pi \cdot R_{avg}^2 \cdot t_{avg} \qquad [3.2a]$$

Thus the normalized section modulus S/S_o is approximated as:

$$S/S_o = \frac{\pi \cdot R_{avg}^2}{S_o} \cdot t_{avg} \qquad [3.3]$$

The effect of variable t_{avg} value on the average radius, R_{avg} , is very small, therefore S/S_o is almost a linear function of t_{avg} , and the mean value μ can be approximated as:

$$\mu = \frac{\pi \cdot R_{avg}^2}{S_o} \cdot \overline{t_{avg}} \qquad [3.3a]$$

Thus it can be concluded that the effect of the minimum wall thickness is much less significant, especially for greater values of the average wall thicknesses as shown in Figure 3.16.

3.3.2 Standard deviations σ_4 and σ_3

The standard deviation σ_3 is the standard deviation of the mean S/S_o values given by Eq.[2.59], and the standard deviation σ_4 is the square root of the mean value of the variance of S/S_o given by Eq.[2.60].

Figure 3.17 shows the variation of the mean standard deviation of S/S_o for an individual pipe, σ_4, with the average wall thickness $\overline{t_{avg}}$ for various $\overline{t_{min}}$ values. The standard deviation σ_4 is affected by the minimum wall thickness, and as $\overline{t_{min}}$ decreases, the standard deviation increases. However, if the average wall thickness approaches the minimum wall thickness or the nominal wall thickness t_o, the mean standard deviation

approaches 0.0. In either case, the simulated cross-section has almost uniform wall thickness, and so the strength of the cross-section is the same for any orientation of the applied bending moment. By inspection of Figure 3.17, the largest value of σ_4 occurs for the cross-section with the average wall thickness equal to the average value between $\overline{t_{min}}$ and t_o. This combination of $\overline{t_{avg}}$ and $\overline{t_{min}}$ corresponds to the pipe cross-section with the most unbalanced cross-section, if the elements are not randomly ordered, and so causes the largest σ_4 value.

Figure 3.18 shows the variation of σ_3, the standard deviation of the mean S/S_o, with the average wall thickness. The plotted values of σ_3 exhibit similar characteristics to the σ_4 values. Firstly, as $\overline{t_{min}}$ decreases, the standard deviation increases, and secondly, the largest value of σ_3 occurs for the cross-section with the average wall thickness equal to the average value between $\overline{t_{min}}$ and t_o. However, the magnitudes of calculated values of σ_3 are very small. The scale of the vertical axis of Figure 3.17 is 35 times larger than the vertical axis in Figure 3.18. Theoretically the ratio of σ_4/σ_3 should be equal to $\sqrt{1000} = 31.6$, where 1000 is the number of simulations, so the magnitude of the difference of the vertical scales is corroborated.

3.3.3 Minimum and maximum values of S/S_o - *a* and *b*

Figure 3.19 shows the variation of the maximum and the minimum values of S/S_o

with the average wall thickness. For each unique pair of minimum and average wall thicknesses, the plotted quantity represents the smallest or the largest value from 90000 simulated values of S/S_o, representing 1000 simulated cross-sections, each with 90 orientations of applied bending moment. The range of the S/S_o for a particular average wall thickness, which represents the vertical distance b-a on Figure 3.19, exhibits characteristics which are similar to those of standard deviations σ_4 and σ_3. Firstly, the range of the S/S_o reflects the difference between $\overline{t_{min}}$ and $\overline{t_{avg}}$, or $\overline{t_{avg}}$ and t_o. As either difference reduces, the range of S/S_o also reduces. Secondly, for a specified $\overline{t_{min}}$ value, the maximum range of S/S_o will occur when $\overline{t_{avg}}$ is the average of $\overline{t_{min}}$ and t_o. This combination of $\overline{t_{avg}}$ and $\overline{t_{min}}$ corresponds to the pipe cross-section with the most unbalanced cross-section, if the elements are not randomly ordered, and so causes the largest range of S/S_o.

3.3.4 Summary

The results presented in Sections 3.3.1 to 3.3.3 illustrate the generation of statistical parameters defining the distribution of the normalized section modulus S/S_o, μ , σ_3, σ_4, a and b, for a specific type of a pipe, the specific type of the cross-section model, and different stage of deterioration defined by the combination of the measured average and minimum wall thicknesses, $\overline{t_{avg}}$ and $\overline{t_{min}}$. The tabulated parameters of the S/S_o distribution, obtained from simulations using the program PIPEXSC.EXE will be

subsequently used for the reliability analysis of flexural failures a pipeline presented in Chapter 5 and 6.

3.4 Sensitivity analysis for simulation-related parameters

In this section, the sensitivity of the statistical parameters to various simulation-related parameters is investigated for the *Type 2ac* model. In the input to the simulation program, the user defines the number of simulations, the number of elements used to form a pipe cross-section and the number of variable orientations of the applied bending moment. Investigation of the sensitivity of the results to those input values is warranted because, as either number is reduced, the computation time is also dramatically reduced.

The investigation of the effect of a particular simulation-related input parameter on the quality of results produced by the program and its overall performance is presented in the next three subsections. It is envisaged that the effect of the number of simulations will be consistent for the four types of models shown in Figure 2.6. The effect of the number of elements applies only to *Type 2* and *4* models, but is believed to be similar to the effect of the number of circumferential points considered in *Type 1* and *3* models.

3.4.1 Number of simulations

Figure 3.20 shows the results of the sensitivity analysis conducted to investigate the effect of the number of simulations on each of the parameters of distribution of S/S_o. The analysis considered values $\overline{t_{min}}$ varying between 1.0 and 9.0 mm, but for brevity, only

the results for the case of $\overline{t_{min}}$ = 2.0 mm, which are representative of all results obtained, will be presented. The values of μ, a and b obtained using 300, 500 and 1000 simulated cross-sections are shown in Figure 3.20a. The curves for each different number of simulations fall on top of each other, indicating that the effect of the number of simulations is not significant. Similarly, the values of σ_3 and σ_4 are shown in Figure 3.20b and indicate no significant difference for the cases of 300, 500 and 1000 simulations. Similar findings were observed for other values of $\overline{t_{min}}$.

3.4.2 Number of elements used to create a pipe cross-section

Figures 3.21 presents the results of analysis for the number of elements used to create pipe cross-section equal to 360, 180, 120, and 60. Again the analysis considered values $\overline{t_{min}}$ varying between 1.0 and 9.0 mm, but only the results for the case of $\overline{t_{min}}$ = 2.0 mm are shown. In all of the investigated cases, μ, σ_3 and σ_4 of the S/S_o, are not affected by the number of elements. However, this is not true for the maximum and the minimum values of S/S_o, a and b. It can be seen in Figure 3.21b that, if the number of elements decreases the minimum value of S/S_o decreases and the maximum value of S/S_o increases. Thus the range of S/S_o may increase slightly if a smaller number of elements is used for analysis. Similar findings were observed for all other values of $\overline{t_{min}}$.

3.4.3 Number of variable orientations of applied bending moment

Figures 3.22 presents the result of analysis obtained for 90, 60, 30, and 10 orientations of the applied bending moment. The analysis considered values $\overline{t_{min}}$ varying between 1.0 and 9.0 mm, and a similar effect of variable orientations of applied bending moment was observed in all cases. Thus, only the results for the $\overline{t_{min}}$ = 2.0 mm are shown in Figure 3.22 . For this particular cross-section model, the number of orientations of the applied bending moment vector can be reduced from 90 to 10 without significantly affecting the results. If only 10 variable orientations are considered, the angle between the applied moment vector and the principal axis, defined by Eq.[2.52], is increased in 36° increments. The greatest sensitivity occurs only for the mean variance of S/S_o, $\sigma_{\downarrow}^2$. However, as shown in Figure 3.22b, the value of $\sigma_{\downarrow}$ based on 10 orientations is only at most 5.5% greater than the value of $\sigma_{\downarrow}$ based on 90 orientations. In this case, it is conservative and efficient to use only 10 orientations of the applied moment vector.

In the case of the *Type 2ar* cross-section model consideration of a small number of variable positions of the applied bending moment vector will have more significant effect on the errors in calculations of parameters of S/S_o distribution. This conclusion can be reached by considering the different variations of S/S_o with the orientation of the neutral axis shown in Figures 3.9 and 3.2. The random order of elements, Figure 3.9, results in a much more erratic plot of S/S_o values. To capture this erratic variation, a large number of neutral axis orientations must be considered. However, the range of simulated values is

much smaller than that shown in Figure 3.2, therefore even larger errors of parameters of S/S_o distribution due to a limited number of orientations of the moment vector may still be acceptable.

3.4.4 Summary

The sensitivity analyses of simulation-related parameters for the *Type 2a* cross-section model with the ordered arrangement of elements presented in previous sections suggest that the numbers of simulations, variable orientations of the applied bending moment vector and elements forming pipe cross-section can all be reduced while maintaining reasonable results. Although the combined effect of reduced numbers of simulations, variable orientations of the applied bending moment vector and elements forming pipe cross-section was not presented, the optimal values were determined based on additional simulations. It is suggested for this particular model that 300 simulations be used with 120 elements and 10 orientations of variable neutral axis.

3.5 Sensitivity analysis for tool-related parameters

In this section, the sensitivity of the statistical parameters of S/S_o distribution to various tool-related parameters is investigated. In the input to the simulation program, the user defines the measurement errors of $\overline{t_{avg}}$ and $\overline{t_{min}}$ and the type of cross-section model. The relation of the measurements errors to the tool is obvious. Each pipe cross-section model, shown in Figure 2.6, corresponds to a specific number of pipe wall thickness

measurements collected at a sampled cross-section, hence, the pipe cross-section model can be considered as a tool-related parameter. In the current stage of the tool development, the models *Type 1* and *2* are applicable. However, imminent future enhancements will allow the tool to measure the minimum wall thickness in each quadrant of a pipe cross-section, which would make models *Type 3* and *4* applicable.

The following subsections present the effects of measurement errors of $\overline{t_{avg}}$ and $\overline{t_{min}}$, and the effect of using more refined pipe cross-section model for the analysis. Investigation of the sensitivity of the results to these input values is warranted because it allows the assessment of the benefits of possible tool enhancements.

3.5.1 Measurement errors

The measurement errors are tool-related parameters that significantly affect the statistical parameters for the simulated results. The measurement errors of the average wall thickness $\overline{t_{avg}}$ considered were ± 0.05, 0.10 , 0.15 and 0.20 of the nominal wall thickness t_o. Similarly, the measurement errors of the minimum wall thickness $\overline{t_{min}}$ considered were ± 0.10 and 0.20 of the nominal wall thickness t_o. A smaller range of error was considered for the minimum wall thickness because, as noted in Section 3.3, the statistical parameters are sensitive to the average wall thickness and the difference between the average and minimum wall thicknesses.

The first sets of simulations considered an error of $\overline{t_{min}}$ of ±0.10 of t_o, and errors of $\overline{t_{avg}}$ of ± 0.05, 0.10, 0.15 and 0.20 of t_o. Typical results, for the case of $\overline{t_{min}}$ equal to 2.0 mm, and $\overline{t_{avg}}$ ranging between $\overline{t_{min}}$ and 9.0 mm, are presented in Figures 3.23 and 3.24. In Figure 3.23, the variation of μ, a and b with $\overline{t_{avg}}$ is shown. The results for the case of "no measurement error" are shown as a solid line for μ, dotted line for a, and a dashed line for b. The results for the cases where measurement errors are present are shown as symbols. It can be seen from the figure that measurement errors do not affect the overall mean value, μ, of the S/S_o distribution. However, as the measurement error of $\overline{t_{avg}}$ increases, the lower limit, a, of the S/S_o distribution reduces and the upper limit, b, increases. Thus the domain of the S/S_o distribution, b-a, increases markedly as the measurement error of $\overline{t_{avg}}$ increases. For example, for $\overline{t_{min}}$ = 2.0 mm and $\overline{t_{avg}}$ = 4.0 mm, the range for "no measurement error" is 0.504-0.260= 0.244. If the measurement error for $\overline{t_{avg}}$ = ±0.20 t_o, the range increases by 129% to 0.687-0.127= 0.560. This substantial increase can also be approximated using Eq.[3.3] to estimate the lower limit and upper limit of the average S/S_o values. For the measurement error of $\overline{t_{avg}}$ equal to ±0.20 t_o, which for t_o = 10 mm is equal to ±2 mm, the lower limit, a, will occur for t_{avg} = 4-2 = 2.0 mm which is 50% of t_{avg} for the "no measurement error" case. Similarly, the upper limit, b, will occur for t_{avg} = 4+2 = 6.0 mm which is 150% of t_{avg} for the "no measurement error" case. Using Eq.[3.3], the range for the measurement error case can be estimated from the range obtained for the "no measurement error case" as

$1.5 \cdot 0.504 - 0.5 \cdot 0.260 = 0.756 - 0.130 = 0.626$. This estimated range is 156% greater than the range for the "no measurement error" case, and confirms the magnitude of the increase observed in the simulation results.

In Figure 3.24, the variation of σ_3 and σ_4 with $\overline{t_{avg}}$ is shown. The results for the case of "no measurement error" are shown as solid lines for σ_4 and σ_3. The effect of measurement error of $\overline{t_{avg}}$ on σ_4 is slight for the cases where σ_4 is largest, and increases when the average wall thickness approaches the minimum wall thickness or the original wall thickness. This observation can be verified by considering the shape of the graph of σ_4 for "no measurement error" case. For an average wall thickness $\overline{t_{avg}} = 5$ mm and the measurement error $\pm 0.10\, t_o$, where $t_o = 10$ mm, the domain of simulated values of t_{avg} is bounded by $t_{avg} = 4$ mm and $t_{avg} = 6$ mm as described in Section 2.3.4.1. Thus the σ_4 value for this case of measurement error can be estimated as the average of all σ_4 value for the "no measurement error" case contained in the interval from $\overline{t_{avg}} = 4$ mm to $\overline{t_{avg}} = 6$ mm. It can be seen from Figure 3.24 that, because the "no measurement error" line is reasonably linear over this interval, the estimated value of σ_4 would be close to that for "no measurement error" case. If the measurement error of $\overline{t_{avg}}$ increases, for example to $\pm 0.20\, t_o$, the average value of σ_4 from the interval $\overline{t_{avg}} = 3$ mm to $\overline{t_{avg}} = 7$ mm would be again quite close to the value obtained for $\overline{t_{avg}} = 5$ mm and "no measurement error". When the average wall thickness approaches the minimum wall thickness or the original

wall thickness truncation of the distribution of t_{avg}, as shown in Figure 2.7(b) and (c), increases the calculated value of σ_4 when measurements errors are considered.

For the case of the standard deviation of mean of S/S_o, σ_3, shown in Figure 3.24, the effect of the measurement error of $\overline{t_{avg}}$ is very significant. The standard deviation σ_3 increases as the measurement error increases, and the relationship between σ_3 and the standard deviation of the average wall thickness, σ_a, is almost linear for all measurements of $\overline{t_{avg}}$ varying between 2 mm and 9 mm. Considering the approximation for the normalized section modulus defined by Eq.[3.3]

$$S/S_o = \left(\frac{\pi \cdot R_{avg}^2}{S_o} \right) \cdot t_{avg} \qquad [3.3]$$

and recalling that the expression in the brackets varies very little with the average wall thickness, the variance of the mean value of S/S_o can be calculated as:

$$\sigma_3^2 = \left(\frac{\pi \cdot R_{avg}^2}{S_o} \right)^2 \cdot \sigma_a^2 \qquad [3.4]$$

therefore, the standard deviation σ_3 is :

$$\sigma_3 = \left(\frac{\pi \cdot R_{avg}^2}{S_o} \right) \cdot \sigma_a \qquad [3.4a]$$

Thus, a roughly linear relationship between the measurement error of the average wall thickness, or the standard deviation of the average wall thickness distribution, and the standard deviation of mean values of S/S_o should be expected.

The second sets of simulations considered an error of $\overline{t_{min}}$ of ±0.20 of t_o, and the errors of $\overline{t_{avg}}$ again varying between ±0.05 and 0.20 of t_o. The results, presented in Figures 3.25 and 3.26, exhibit very similar characteristics to those identified already for the $\overline{t_{min}}$ error of ±0.10 of t_o. The effect of the error of $\overline{t_{avg}}$ on the variation of parameter of the S/S_o distribution, μ, a, b, σ_3 and σ_4, is the same as for case shown in Figures 3.23 and 3.24. The effect of larger error of $\overline{t_{min}}$ can be assessed by comparing the results for the error of ±0.10 and ±0.20 of t_o for the same error of $\overline{t_{avg}}$. By inspection of Figures 3.23 and 3.25, no difference can be observed for the mean value μ and the upper bound of S/S_o, b. However, the lower bound of S/S_o, a, reduces as the error of the minimum wall thickness increases. Similarly, comparing the results shown in Figures 3.24 and 3.26, in the case of $\overline{t_{min}}$ error of ±0.20 t_o, σ_4 is larger for $\overline{t_{avg}}$ close to either $\overline{t_{min}}$ or t_o, and σ_3 is slightly larger or practically the same as for the error of $\overline{t_{min}}$ of ±0.10 t_o.

From these simulations it can be concluded that the statistical parameters for the flexural strength of a pipe cross-section are more significantly affected by measurement errors of $\overline{t_{avg}}$ than measurement errors of $\overline{t_{min}}$. However, for the analysis of corrosion failures due

to perforations of the pipe, the effect of the error of $\overline{t_{min}}$ becomes much more significant as will be discussed in Chapter 5.

3.5.2 Overall variance of the S/S_o distribution - *Type 2ac/2ar* models

In previous section the effect of measurement errors of the average and the minimum wall thickness on the standard deviation of the mean S/S_o, σ_3, and the mean variance of S/S_o, σ_4^2, was analyzed. In this section the expression for total variance and the total standard deviation of the S/S_o distribution will be presented, and the effect of measurement errors on the total standard deviation of the S/S_o distribution will be investigated. The results of this investigation will allow assessment of the effectiveness of the tool enhancement that result in lower measurement errors.

3.5.2.1 Overall standard deviation of S/S_o distribution

From ASTM E691, the overall variance of the S/S_o distribution, σ_6^2, can be calculated using the following equation:

$$\sigma_6^2 = \sigma_3^2 + \left(\frac{k}{k-1}\right)\sigma_4^2 \qquad [3.5]$$

where σ_3 is the standard deviation of the mean S/S_o defined by Eq.[2.59], σ_4^2 is the mean variance of S/S_o defined by Eq.[2.60], and k is the number of simulations of pipe cross-sections.

The overall standard deviation of the S/S_o can therefore be calculated as the square root of the variance:

$$\sigma_6 = \sqrt{\sigma_3^2 + \left(\frac{k}{k-1}\right)\sigma_4^2} \qquad [3.5a]$$

3.5.2.2 Sensitivity analysis of the total standard deviation

Figure 3.27 shows graphs of σ_3, σ_4, and σ_6 versus error in $\overline{t_{avg}}$ for six pipe cross-sections ("a" to "f") analyzed using *2ac* model, which is the *Type 2a* model with the ordered arrangement of elements. Various combinations of minimum and average wall thicknesses were considered, as shown on the figures. The measurements error of $\overline{t_{min}}$ was ±0.10 of t_o, and the measurement error of $\overline{t_{avg}}$ was 0.0, ±0.05, ±0.10, ±0.15 and ±0.20 of t_o. For all six cases, the total standard deviation σ_6 increases as either σ_3 or σ_4 increases as suggested by Eq.[3.5a]. However, in most cases the magnitude of σ_4 exceeds that of σ_3 and so dominates the overall standard deviation when the measurement error of $\overline{t_{avg}}$ is less than ±0.15 of t_o. The exception is for case "c" which is

somewhat unrealistic because the average and minimum wall thicknesses are small and equal. Even in this case, σ_4 exceeds σ_3 when the measurement error of $\overline{t_{avg}}$ is less than ±0.10 of t_o. Therefore the effectiveness of a tool enhancement that reduces the error of the reported average thickness measurement is slight.

The figures also shown that the mean standard deviation σ_4 in all cases does not vary much with the measurement error of $\overline{t_{avg}}$. This is because the *2ac* model has a large variation of S/S_o depending of the unknown orientation of the applied moment vector as shown in Figure 3.2. Figure 3.27 can be used to assess the impact of improvements to the Hydroscope tool that would reduce the measurement error of the average wall thickness. Although more accurate measurements will markedly reduce the standard deviation of mean S/S_o, as shown in Figures 3.24 and 3.26, they will not reduced the overall standard deviation of S/S_o distribution as effectively, as shown in Figure 3.27. For example, if the measurement of $\overline{t_{avg}}$ is reduced from ±0.20 to ±0.10 of t_o, the overall standard deviation decreases by only 18.7% for the case shown in Figure 3.27(a), 16.0% for the case shown in Figure 3.27(b), 31.4% for the case shown in Figure 3.27(c), 21.5% for the case shown in Figure 3.27(d), 21.1% for the case shown in Figure 3.27(e) and 20.7% for the case shown in Figure 3.27(f).

A similar analysis was conducted with an error of $\overline{t_{min}}$ set to ±0.20 of t_o. The results, shown for one cross-section only in Figure 3.28(a), were virtually no different from those

shown in Figure 3.27(b). This confirms that the error of the $\overline{t_{min}}$ measurement is not a significant factor in the analysis of the flexural strength of corroded pipe cross-section with the elements arranged in order from greatest to least thickness across the depth of the section.

The benefit of more precise measurements, in the form of smaller overall standard deviations of the S/S_o distribution, is more apparent for *Type 2ar* cross-section model, shown in Figure 3.8. Figure 3.28(b) shows a comparison of the total standard deviation σ_6, σ_4 and σ_3, obtained for a pipe with cross-section modeled using *Type 2ar* and *2ac* models. In this case, the random arrangement of elements around the perimeter of the pipe creates a fairly balanced pipe cross-section model, with a very small mean standard deviation σ_4. The overall standard deviation σ_6 for a *Type 2ar* model is largely due to the standard deviation of the mean S/S_o values, σ_3, which is roughly proportional to the measurement error of $\overline{t_{avg}}$.

Based on the analysis presented in this section it can be concluded that the enhancement of the tool resulting in reduced measurement errors will be very effective for the analysis using a pipe cross-section model with elements arranged randomly, and much less effective if the model with ordered arrangement of elements is used.

3.5.3 The effect of enhanced tool capabilities - model *Type 2ac/2ar* vs. *Type 4ac*

A potential future enhancement of the tool will allow the minimum wall thicknesses taken in each quadrant of a sampled cross-section to be measured. In this case, where five recorded wall thicknesses are available, the *Type 3* and *4* cross-section models described in Chapter 2 can be used for simulations to obtain the probability distribution of the S/S_o. Examples of simulated *Type 3* and *Type 4* cross-sections are shown in Appendix A.

To investigate the effect of this enhancement on the S/S_o distribution a number of *Type 4a* simulated cross-sections, with ordered arrangements of elements and pits randomly placed within each quadrant, were investigated. An example of the cross-section investigated, denoted as *Type 4acr*, is shown in Figure 3.29. The Beta distribution was again found to provide very good fit to the simulated data. Figure 3.30 shows an example of fitting the simulated data to Beta distribution for the *Type 4acr* cross-section model with $\overline{t_{avg}}$ = 7.0 mm, $\overline{t_{min(1)}}$ = 3.0 mm, $\overline{t_{min(2)}}$ = 6.0 mm, $\overline{t_{min(3)}}$ = 7.0 mm, and $\overline{t_{min(4)}}$ = 6.0 mm. However, the results of these simulations can not be easily presented in the form of tables summarizing the statistical parameters of the S/S_o distribution. In this case a set of five dimensional matrices would be required, where four matrix dimensions would correspond to the minimum wall thicknesses appropriate for each particular quadrant and one dimension would be reserved for the average wall thickness.

The comparison of three models, *Type 4acr*, *Type 2ac* and *Type 2ar*, for a wide range of wall thicknesses is an easy but laborious task. In the present investigation, these three

models will be compared on the basis of only a few randomly-chosen wall thicknesses $\overline{t_{avg}}$ and $\overline{t_{min}}$.

To assess the impact of this potential tool enhancement, the single case of a 6" (152 mm) pipe with $\overline{t_{avg}}$ = 7.0 mm and $\overline{t_{min}}$ = 3.0 mm with no measurement errors was investigated. The results for the current version of the tool can be determined by analysis of a *2ac* or *2ar* model, yielding all five calculated parameters of the S/S_o distribution, $\mu, \sigma_4, \sigma_3, a$ and b.

If the same cross-section is inspected with the new enhanced tool, four measurements of the minimum wall thicknesses will be collected instead of one. However, the minimum thickness recorded for at least one quadrant will still be equal to 3.0 mm, while the average wall thickness will remain equal to 7.0 mm. The minimum thicknesses in the other quadrants are unknown, but examples of permissible values are shown in Table 3.1. Section No 1 has only one measurement specified, $\overline{t_{min}}$ corresponding to the data provided by the tool currently. Sections No 2 through No 10 have measurements of the minimum wall thickness specified for each quadrant, corresponding to data provided by the enhanced tool. Cross-sections No 2 through No 10 would be recognized by the current tool as having $\overline{t_{avg}}$ = 7.0 mm and $\overline{t_{min}}$ = 3.0 mm.

Table 3.1 Minimum wall thickness measurements at each quadrant of pipe cross-section

Section No	(t_{min}) $\overline{t_{min(1)}}$	$\overline{t_{min(2)}}$	$\overline{t_{min(3)}}$	$\overline{t_{min(4)}}$
1	3	-	-	-
2	3	6	6	6
3	3	5	7	7
4	3	5	7	6
5	3	6	7	6
6	3	5	5	5
7	3	4	4	4
8	3	4	5	4
9	3	5	7	5
10	3	5	7	4

Each set of $\overline{t_{min(1)}}$ to $\overline{t_{min(4)}}$ measurements shown in Table 3.1 was used to obtain parameters of the S/S_o distribution shown in Table 3.2. The results were obtained using the *Type 2ac* model for Section No 1a, the *Type 2ar* for Section No 1b, and the *Type 4acr* model for the remaining sections.

The parameters shown indicate that the overall mean, μ, of the S/S_o distribution is slightly higher for the enhanced, *Type 4acr*, model. The standard deviation of mean S/S_o, σ_3, is a very small value in all cases. The mean standard deviation of S/S_o, σ_4, for the enhanced model is approximately equal to the average value of σ_4 obtain for two current models, *Type 2ac* and *Type 2ar*. The minimum values of S/S_o, a, are roughly the same except for the *Type 2ar* model, while the maximum values of S/S_o, b, are in all cases

higher for the enhanced model. The shape of the probability density function of S/S_o derived using data reported by the enhanced tool resembles closely the bell-shaped probability density function obtained for *Type 2ar* model shown in Figure 3.10.

Table 3.2 Parameters of the S/S_o probability distribution

Section No	μ	σ_3	σ_4	a	b
1a	0.660	0.002	0.093	0.492	0.769
1b	0.669	0.001	0.021	0.587	0.734
2	0.673	0.003	0.062	0.509	0.847
3	0.673	0.003	0.062	0.495	0.837
4	0.674	0.003	0.059	0.501	0.842
5	0.673	0.003	0.064	0.509	0.832
6	0.675	0.003	0.054	0.508	0.855
7	0.676	0.003	0.050	0.503	0.857
8	0.676	0.003	0.051	0.498	0.855
9	0.674	0.003	0.057	0.503	0.850
10	0.675	0.003	0.056	0.492	0.839

Based on the results of this very limited analysis, it is concluded that the use of data from the enhanced tool in a reliability analysis could result in smaller calculated probabilities of failure. Figure 3.31 shows schematically graphs of the cumulative distributions for the two current models and the enhanced model. A deterministic flexural demand, D_f, is also shown to illustrate the effect of the shape of the cumulative distribution on the probability of failure of a specific cross-section. CDF for *Type 2ac* model exceeds CDF for *Type 4ac* model for all values less than the mean value μ. Thus the probability of failure determined using the enhanced tool would be less than that for the *Type 2ac* model

if the demand is less than the mean resistance μ. The cumulative distribution of S/S_o for *Type 2ar* model, derived using data from the current tool, would result in the lowest probability of failure if the specific demand is lower than the mean resistance value. However, the use of the *Type 2ar* for the reliability analysis requires the assumption that the distribution of wall thicknesses around the pipe perimeter is random which may be. The calculations of the probability of flexural failure of a pipe cross-section are discussed in more detail in Chapter 5.

3.5.4 Summary

In this section, the effect of a number of tool enhancements on the S/S_o distribution have been considered. Improving the accuracy of the minimum wall thickness measurement does not affect the S/S_o distribution significantly. The effectiveness of increasing the accuracy of the average wall thickness measurement depends on the pipe cross-section model considered. For the *Type 2ac* model of pipe cross-section, the reduced error of measured wall thicknesses will have little effect on the mean μ, will reduce the range of the S/S_o distribution, and will reduce the overall standard deviation of the S/S_o distribution. For the *Type 2ar* model, effect are similar except that the overall standard deviation is much more markedly reduced when the error of $\overline{t_{avg}}$ reduces. This is due to the relatively small effect of the variable orientation of the applied bending moment in the case of the *Type 2ar* model, which is reflected by the very small standard deviation of mean S/S_o, σ_3.

The second possible enhancement of the tool allowing collection of minimum thicknesses in each quadrant of each sampled cross-section was investigated using the *Type 4acr* cross-section model. There seems to be a real benefit associated with this tool enhancement, because it allows more refined modelling of the pipe cross-section. The enhanced tool would minimize the effect of the assumed arrangement of elements, which is otherwise significant.

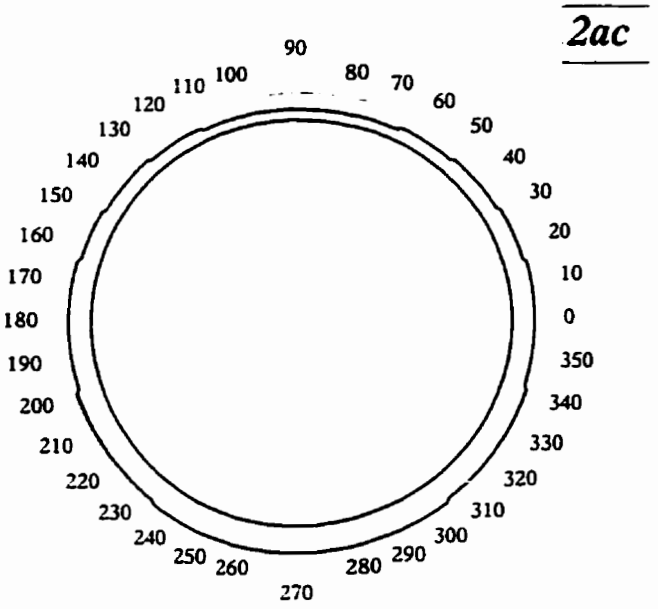

Figure 3.1 Simulated *Type 2a* section with ordered arrangement of elements

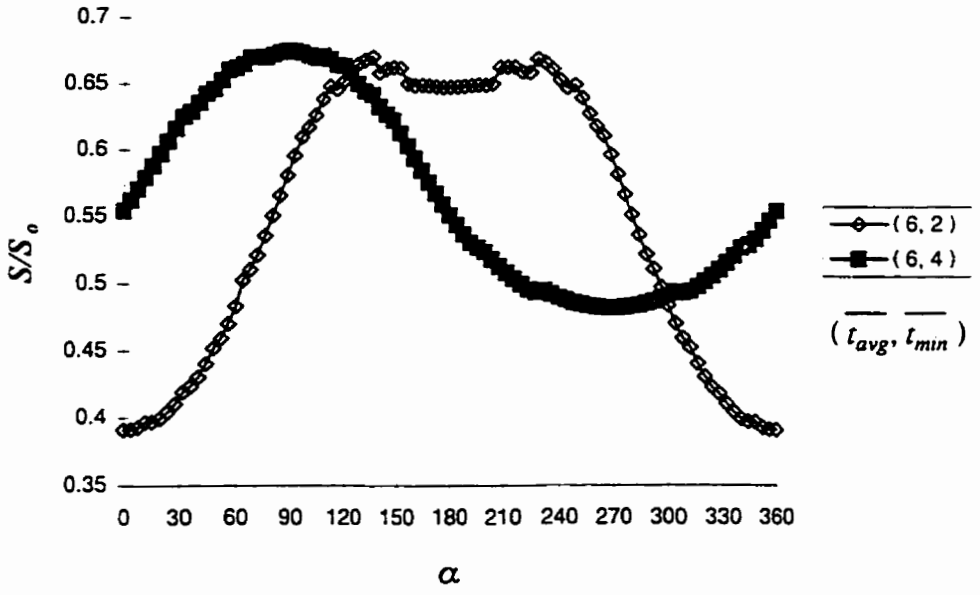

Figure 3.2 Variation of S/S_o due to orientation of the bending moment vector (cross-section *2ac*, $\overline{t_{avg}}$ = 6.0 mm, $\overline{t_{min}}$ = 4.0 mm and 2.0 mm, no measurement errors)

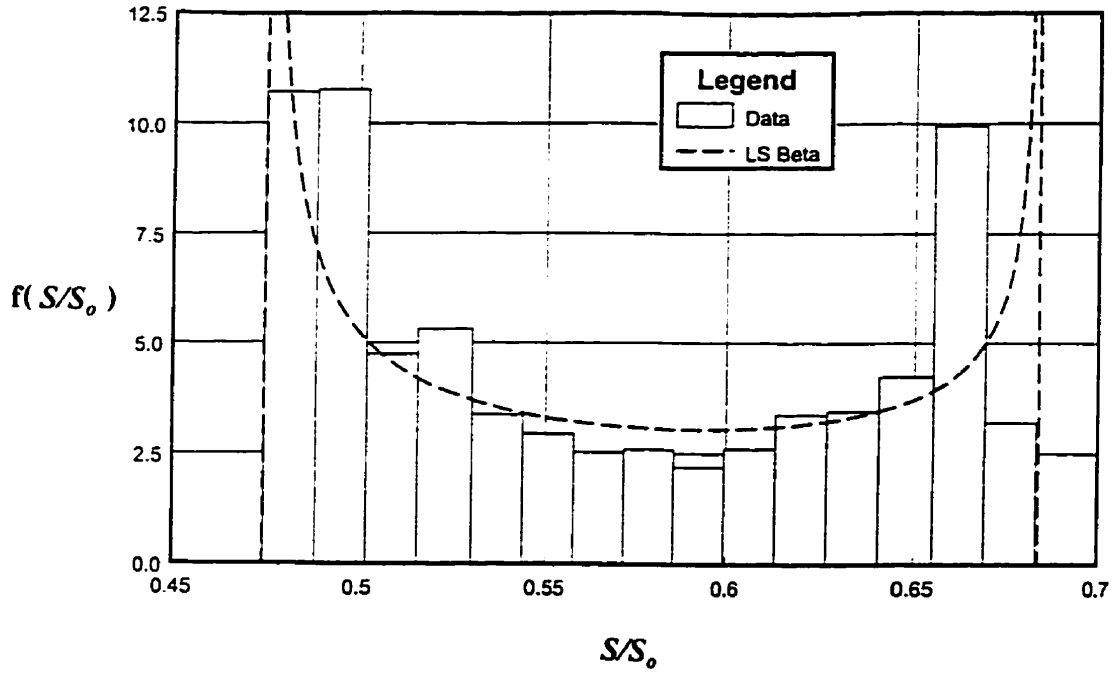

Figure 3.3 Probability density function of S/S_o
(cross-section *2ac*, $\overline{t_{avg}}$ = 6.0 mm, $\overline{t_{min}}$ = 4.0 mm, no measurement errors)

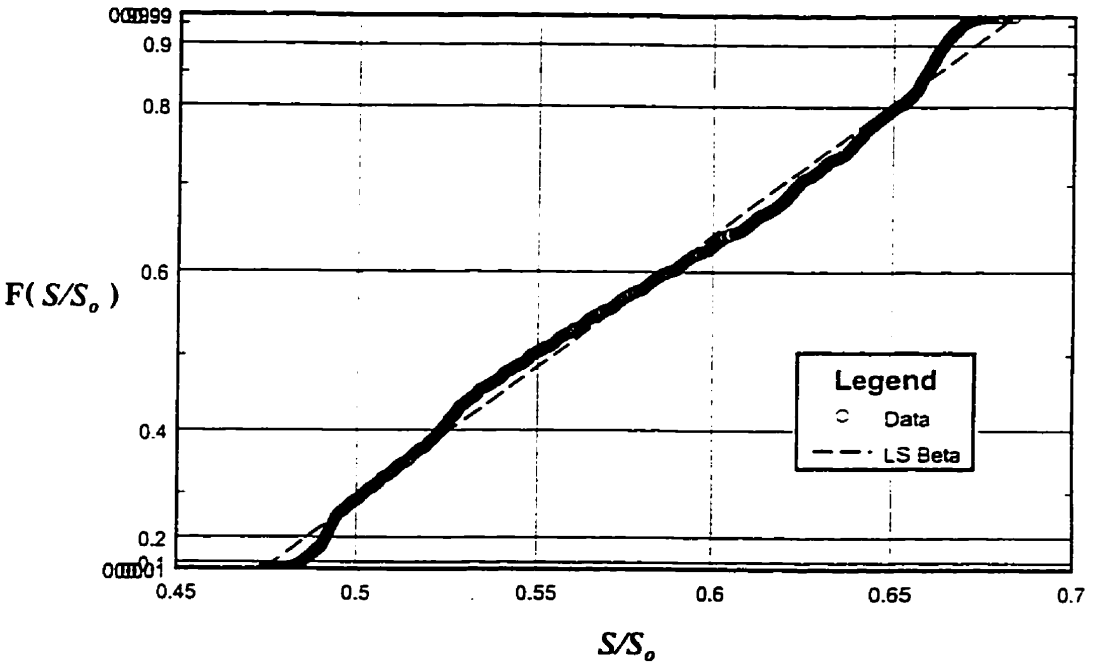

Figure 3.4 S/S_o distribution plotted on Beta probability paper
(cross-section *2ac*, $\overline{t_{avg}}$ = 6.0 mm, $\overline{t_{min}}$ = 4.0 mm, no measurement errors)

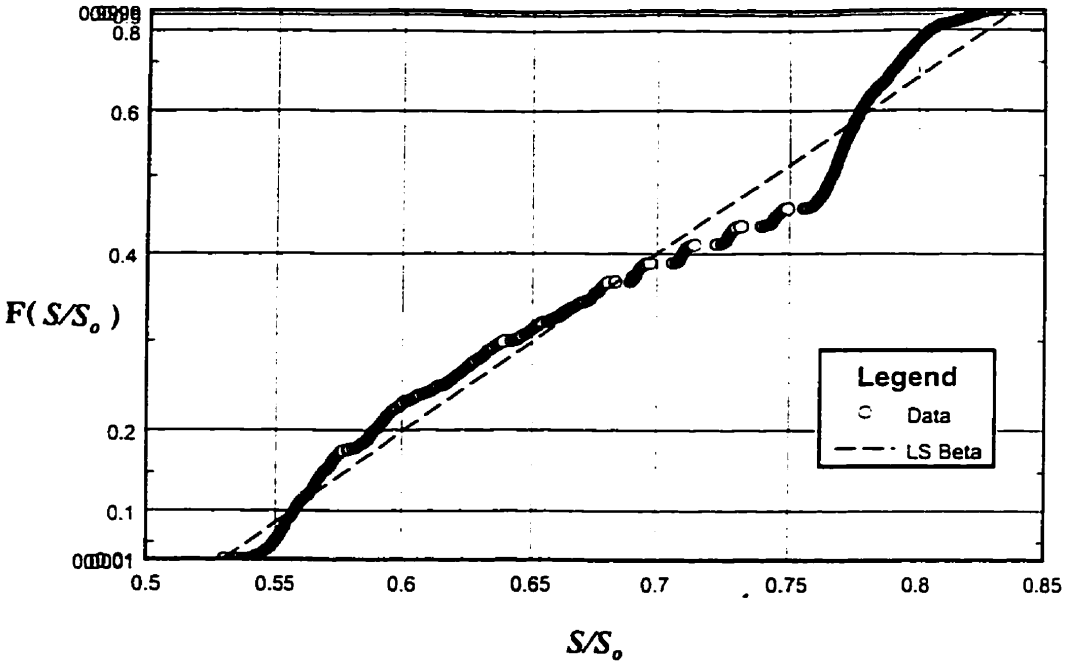

Figure 3.5 S/S_o **distribution plotted on Beta probability paper**
(cross-section *2ac*, $\overline{t_{avg}}$ = 7.5 mm, $\overline{t_{min}}$ = 3.0 mm, **no measurement errors)**

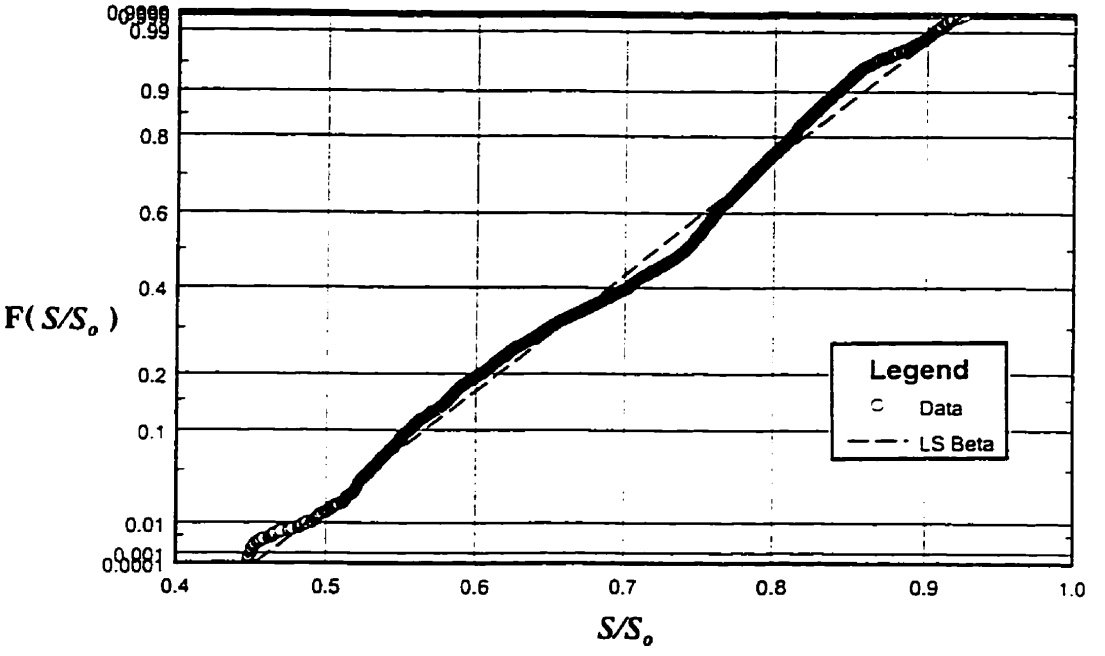

Figure 3.6 S/S_o **distribution plotted on Beta probability paper**
(cross-section *2ac*, $\overline{t_{avg}}$ = 7.5 mm, $\overline{t_{min}}$ = 3.0 mm,
error of $\overline{t_{avg}}$ $=\pm 0.1t_o$, **error of** $\overline{t_{min}}$ $=\pm 0.1t_o$)

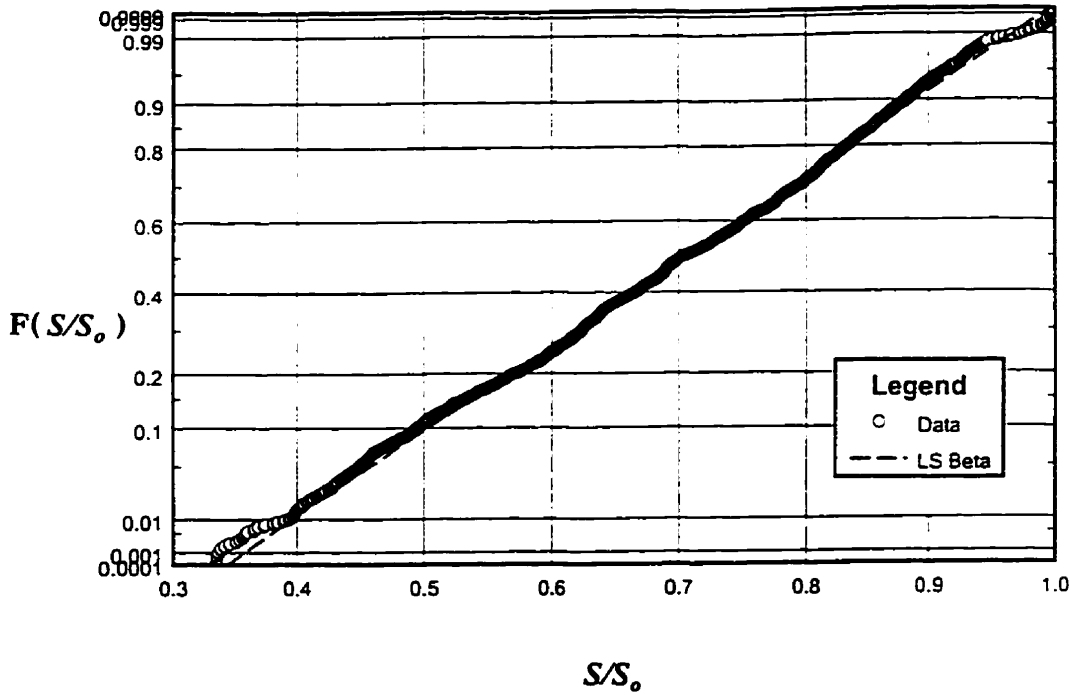

Figure 3.7 S/S_o distribution plotted on Beta probability paper (cross-section *2ac*, $\overline{t_{avg}}$ = 7.5 mm, $\overline{t_{min}}$ = 3.0 mm, error of $\overline{t_{avg}}$ =±0.2t_o , error of $\overline{t_{min}}$ =±0.1t_o)

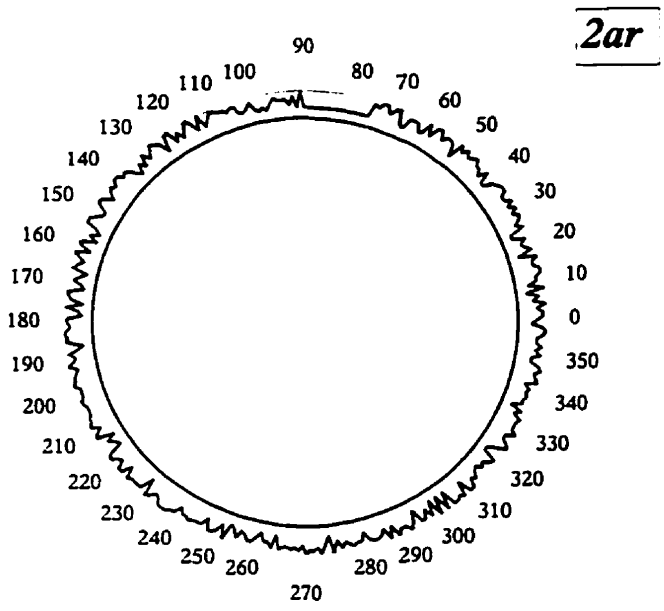

Figure 3.8 Simulated *Type 2a* section with random ordered of elements

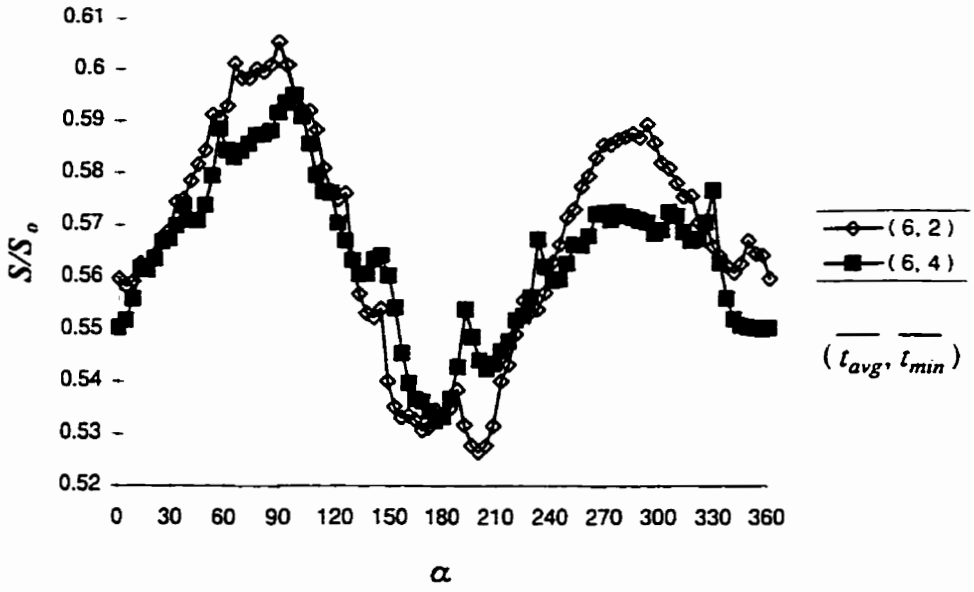

Figure 3.9 Variation of S/S_o due to orientation of the bending moment vector (cross-section *2ar*, $\overline{t_{avg}}$ = 6.0 mm, $\overline{t_{min}}$ = 4.0 mm and 2.0 mm, no measurement errors)

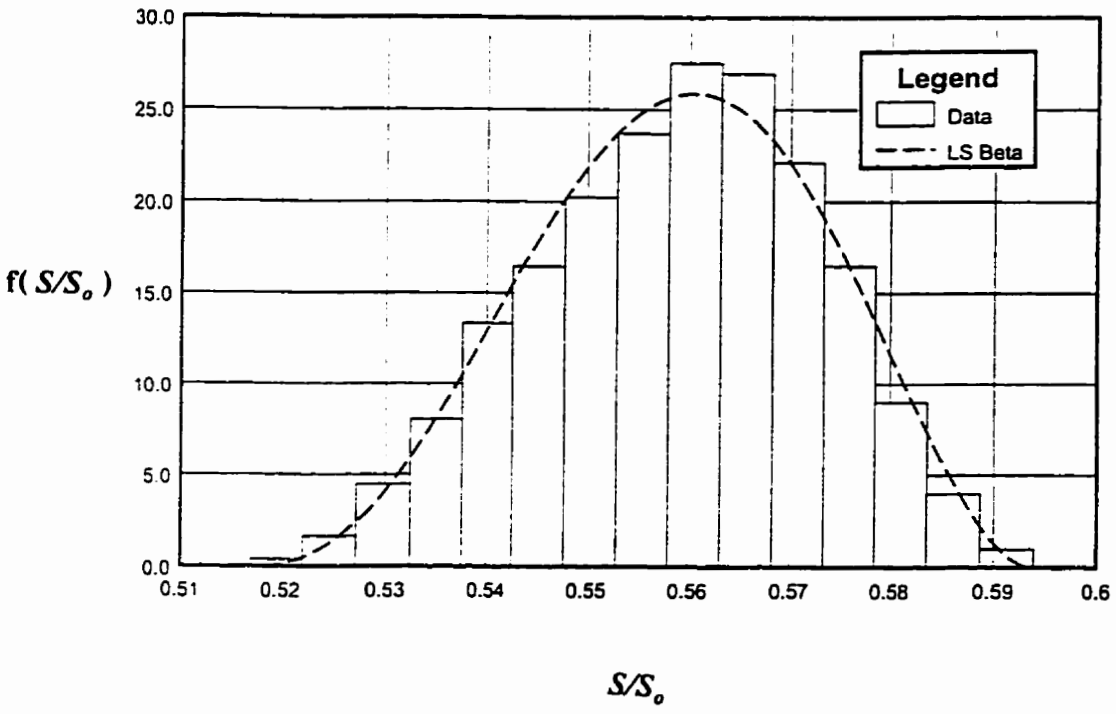

Figure 3.10 Probability density function of S/S_o (cross-section *2ar*, $\overline{t_{avg}}$ = 6.0 mm, $\overline{t_{min}}$ = 4.0 mm, no measurement errors)

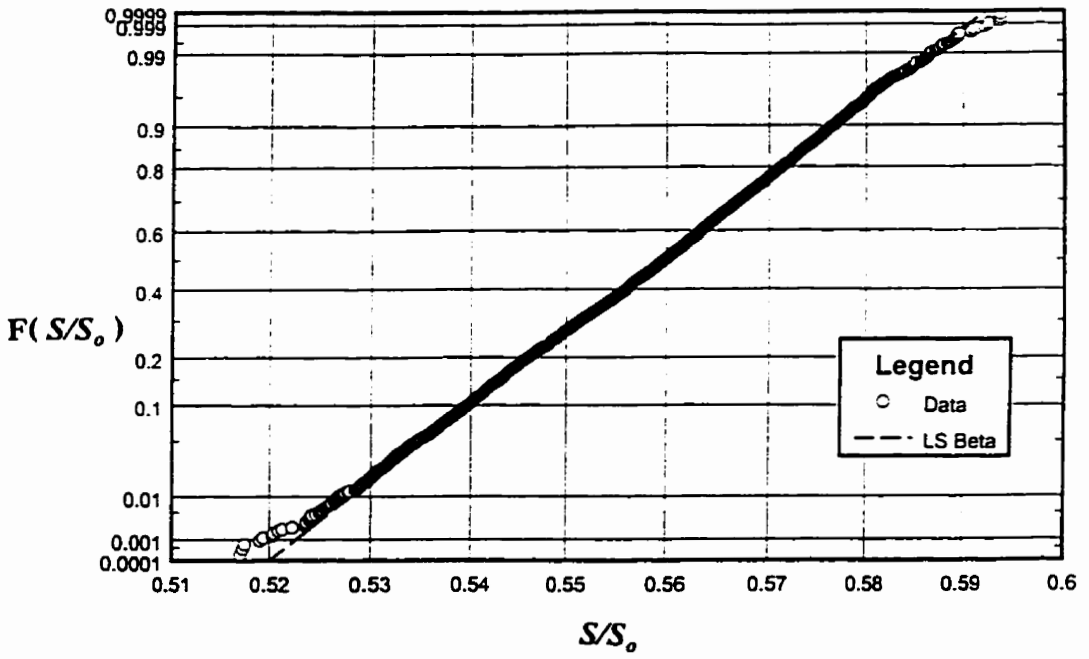

Figure 3.11 S/S_o **distribution plotted on Beta probability paper**
(cross-section *2ar*, $\overline{t_{avg}}$ **= 6.0 mm,** $\overline{t_{min}}$ **= 4.0 mm, no measurement errors)**

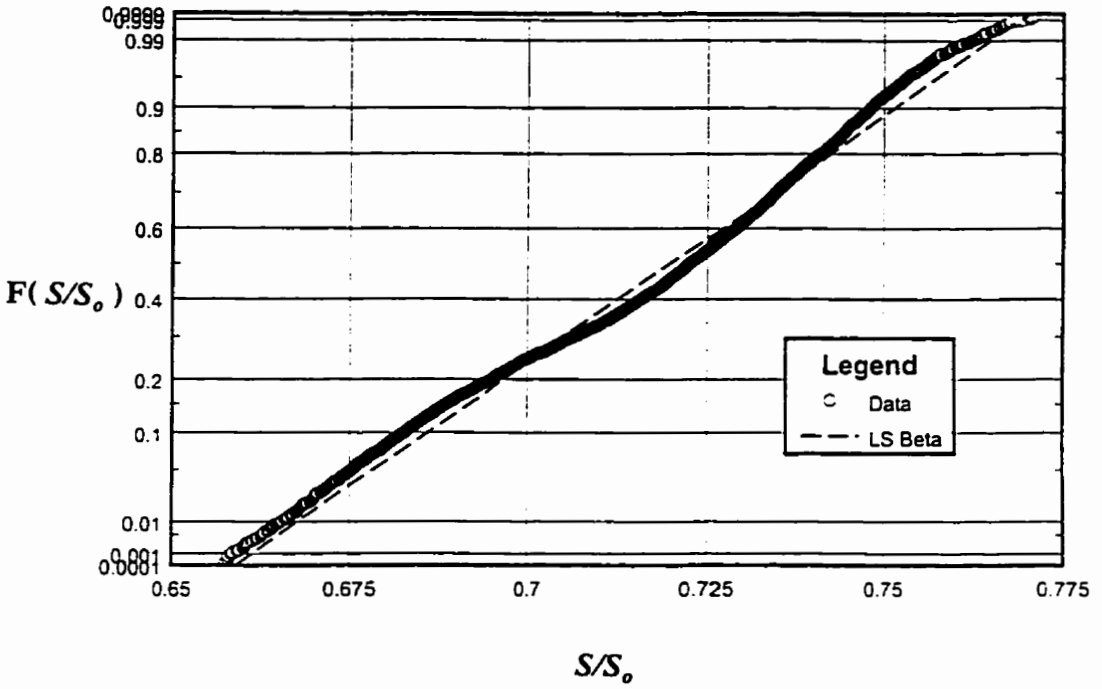

Figure 3.12 S/S_o **distribution plotted on Beta probability paper**
(cross-section *2ar*, $\overline{t_{avg}}$ **= 7.5 mm,** $\overline{t_{min}}$ **= 3.0 mm, no measurement errors)**

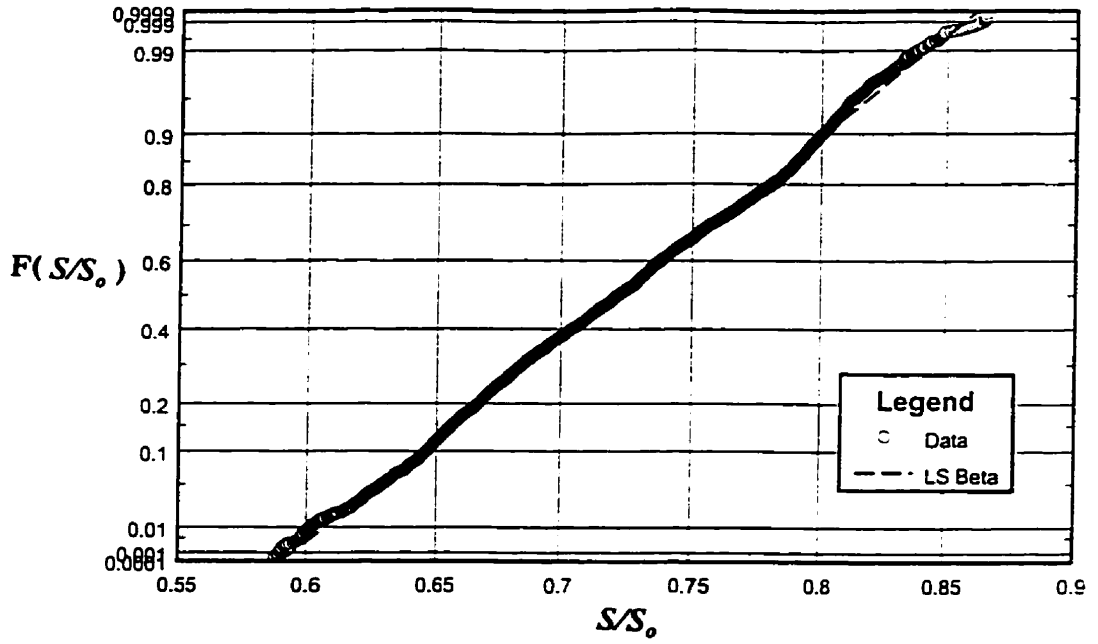

Figure 3.13 S/S_o **distribution plotted on Beta probability paper**
(cross-section *2ar*, $\overline{t_{avg}}$ **= 7.5 mm,** $\overline{t_{min}}$ **= 3.0 mm,**
error of $\overline{t_{avg}}$ $=\pm 0.1t_o$ **, error of** $\overline{t_{min}}$ $=\pm 0.1t_o$**)**

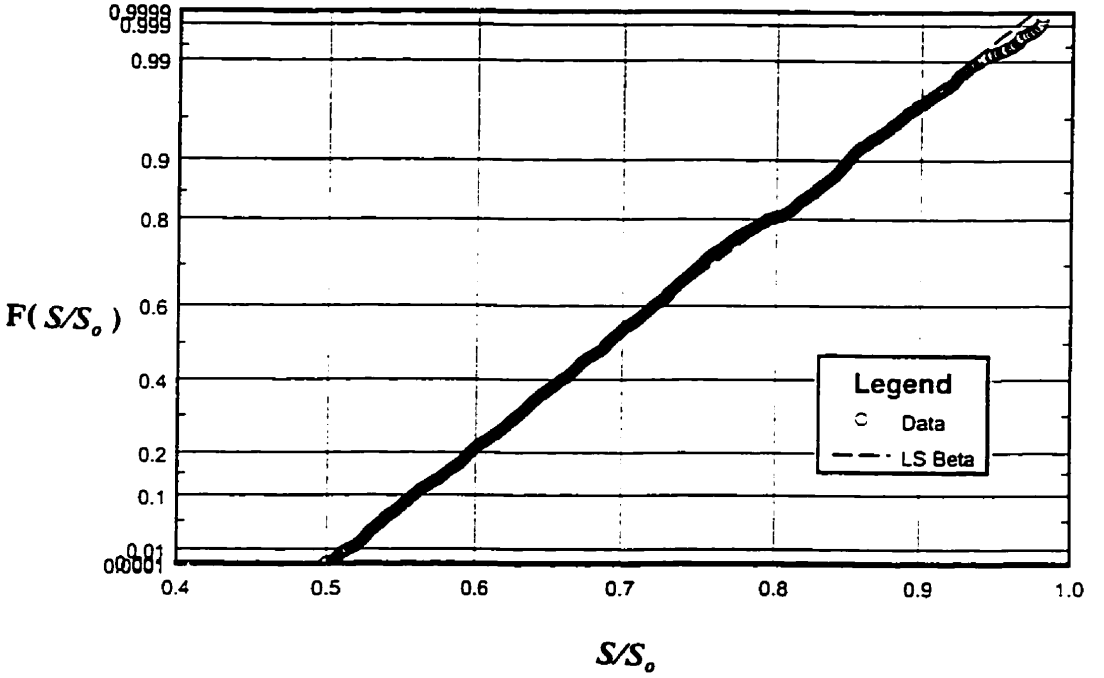

Figure 3.14 S/S_o **distribution plotted on Beta probability paper**
(cross-section *2ar*, $\overline{t_{avg}}$ **= 7.5 mm,** $\overline{t_{min}}$ **= 3.0 mm,**
error of $\overline{t_{avg}}$ $=\pm 0.2t_o$ **, error of** $\overline{t_{min}}$ $=\pm 0.1t_o$**)**

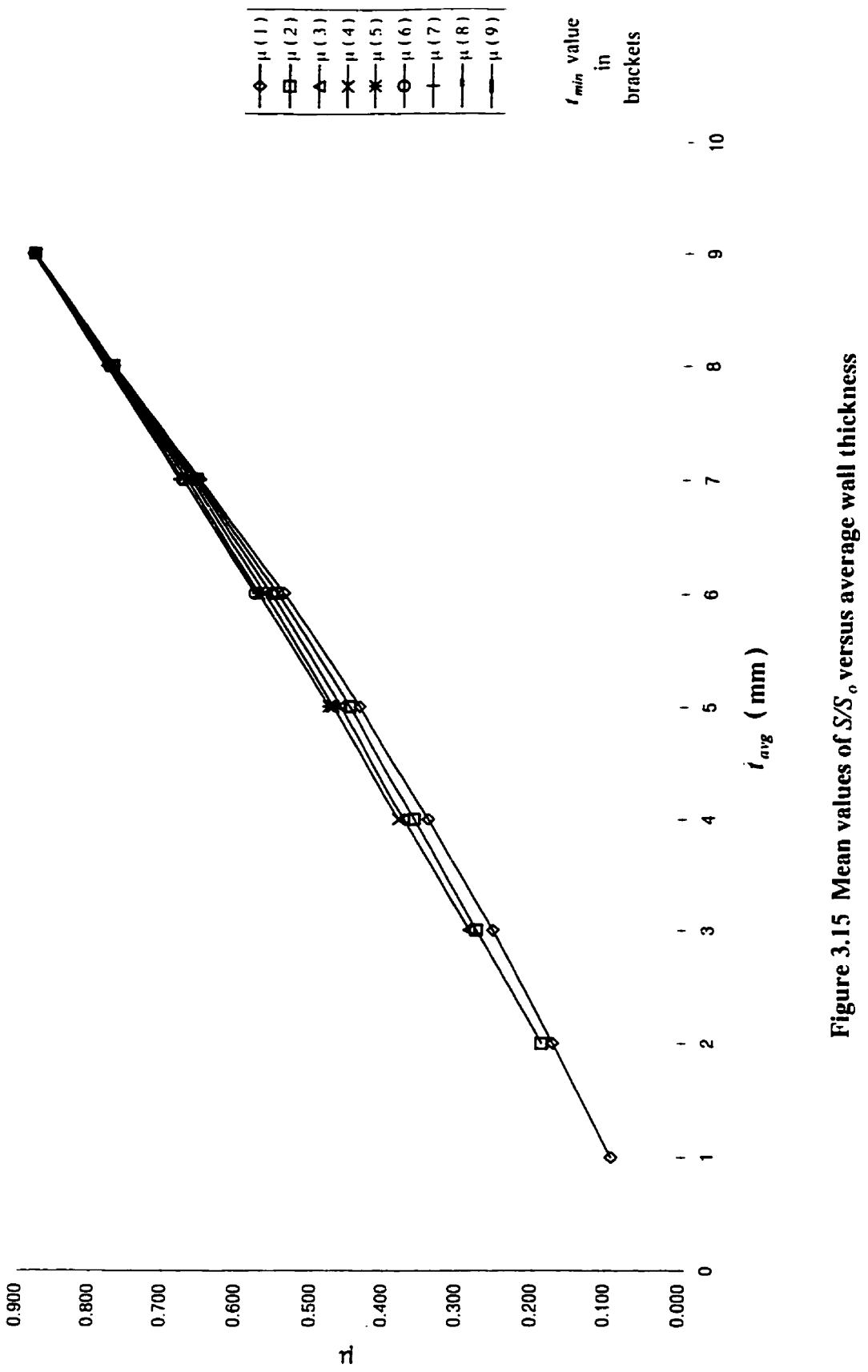

Figure 3.15 Mean values of S/S_o versus average wall thickness

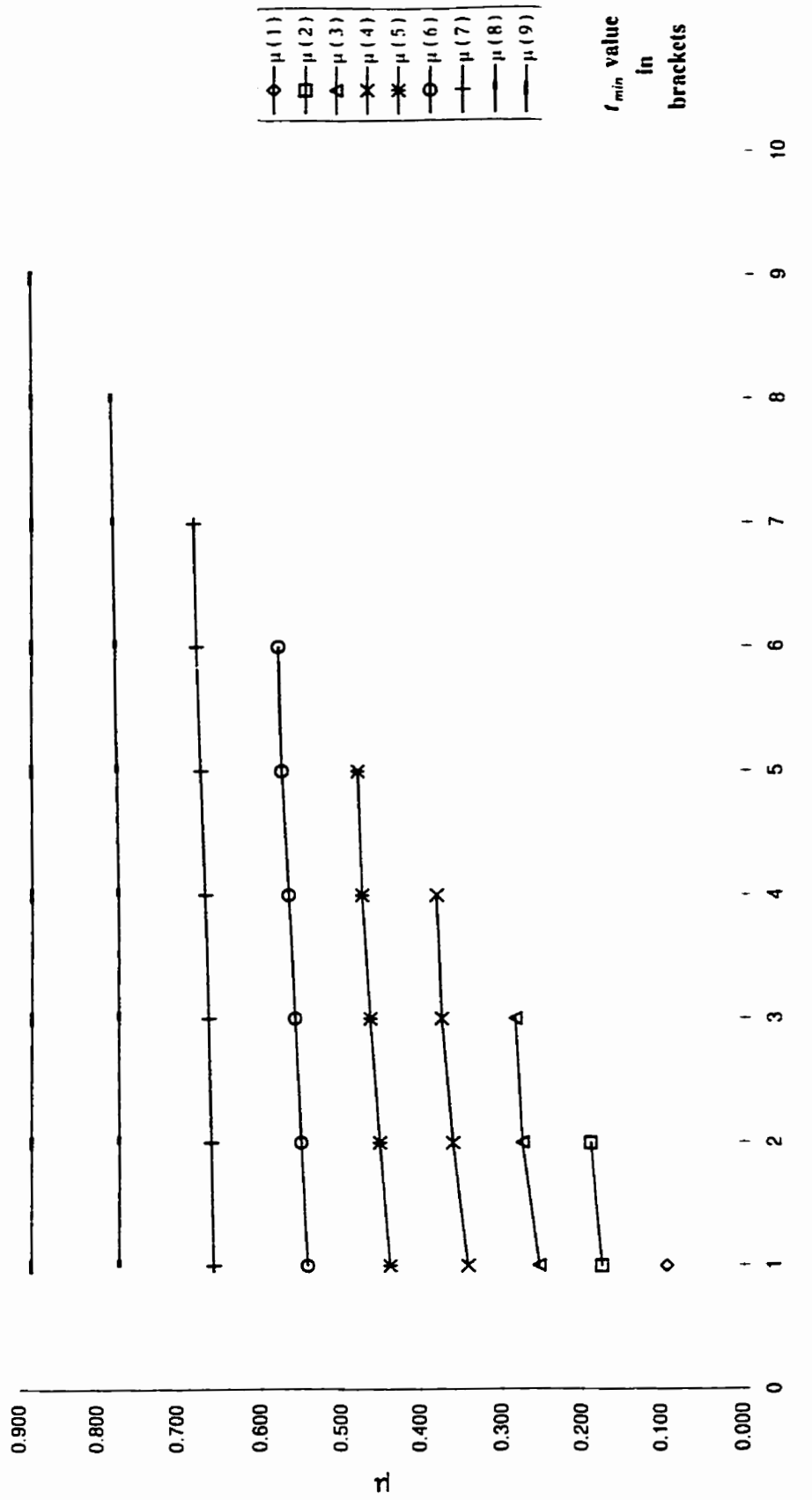

Figure 3.16 Mean value of the S/S_o versus minimum wall thickness

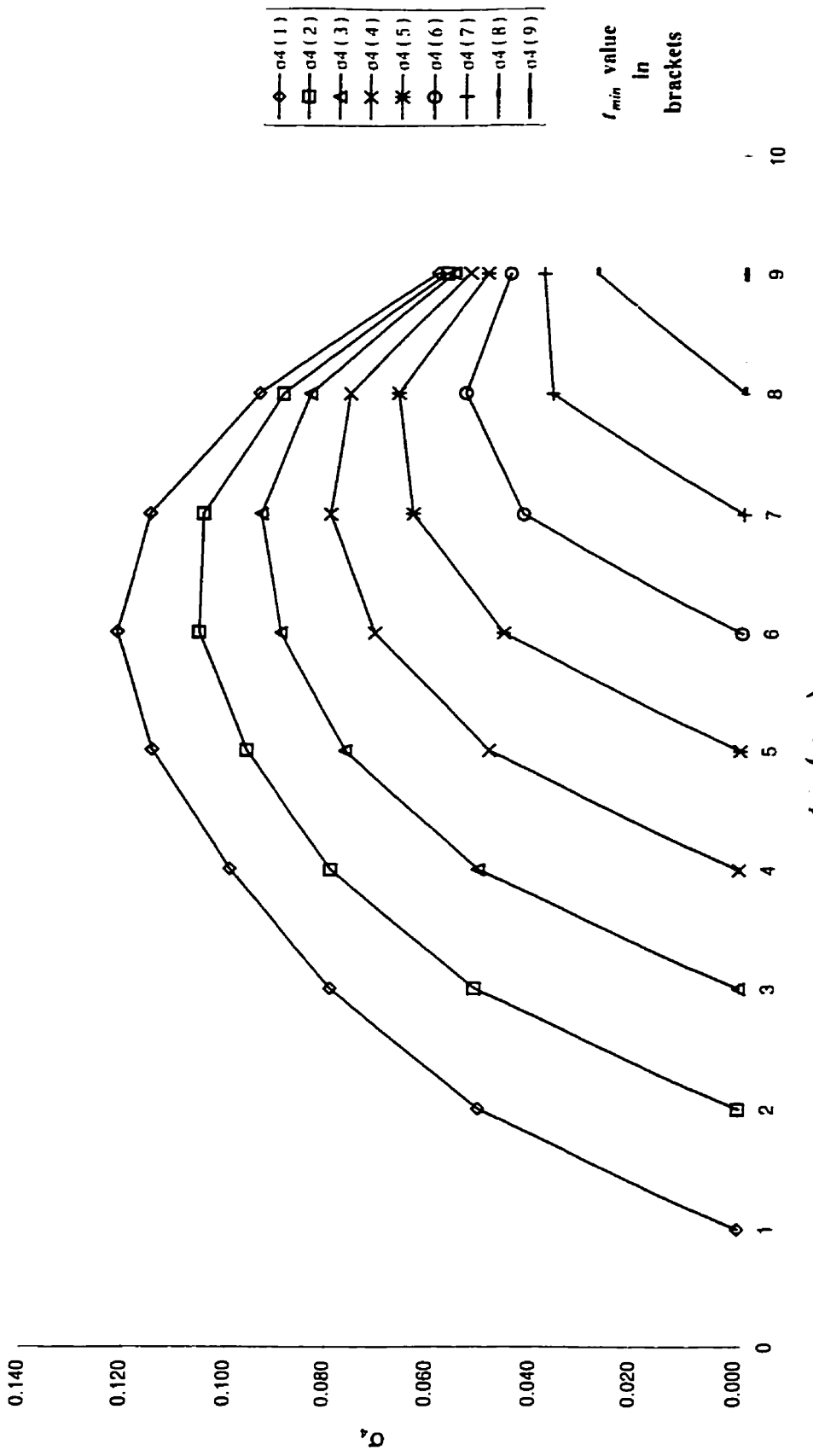

Figure 3.17 Standard deviation, σ_4, of S/S_o versus average wall thickness

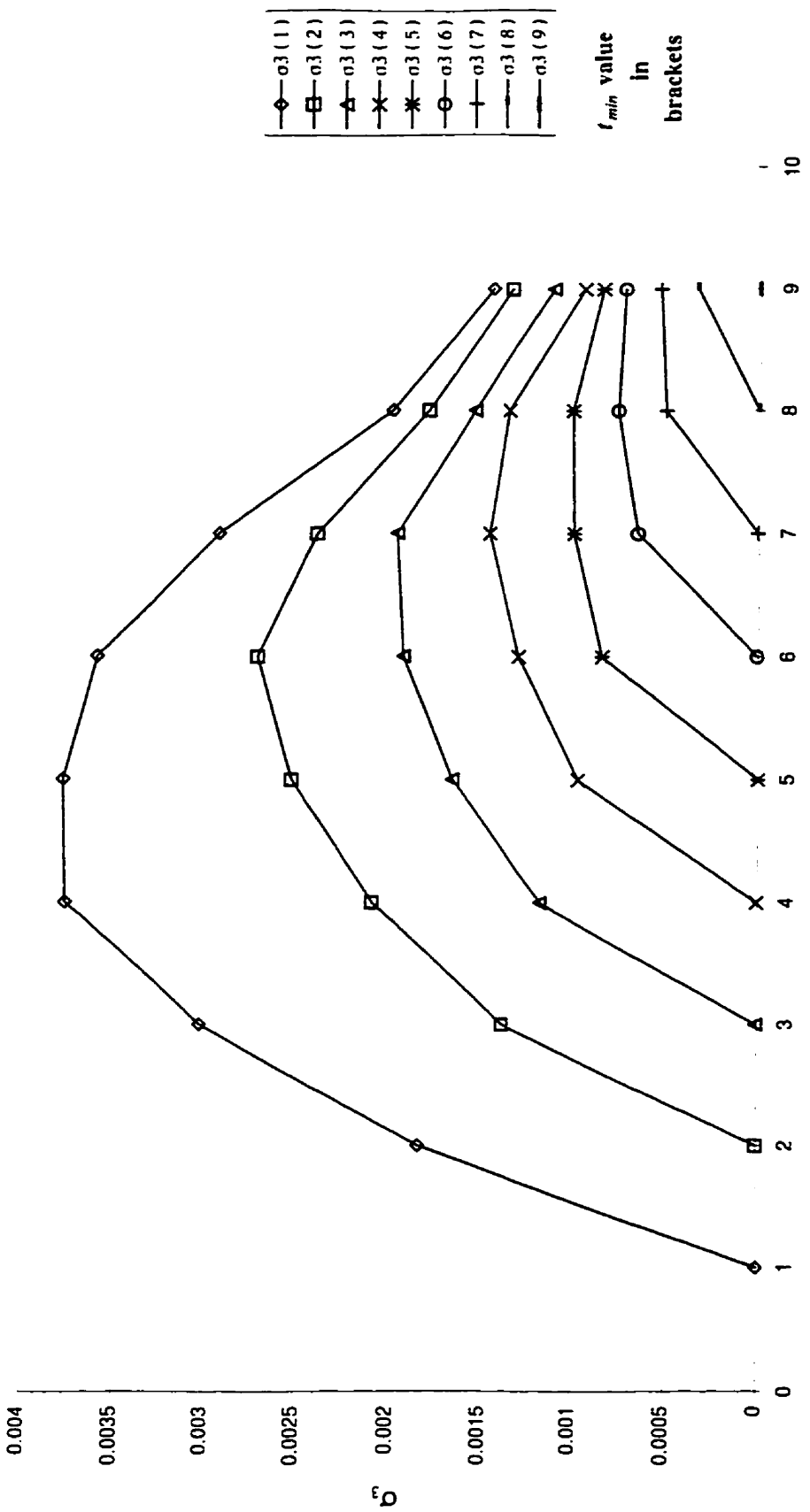

Figure 3.18 Standard deviation of mean, σ_3 of S/S_o versus average wall thickness

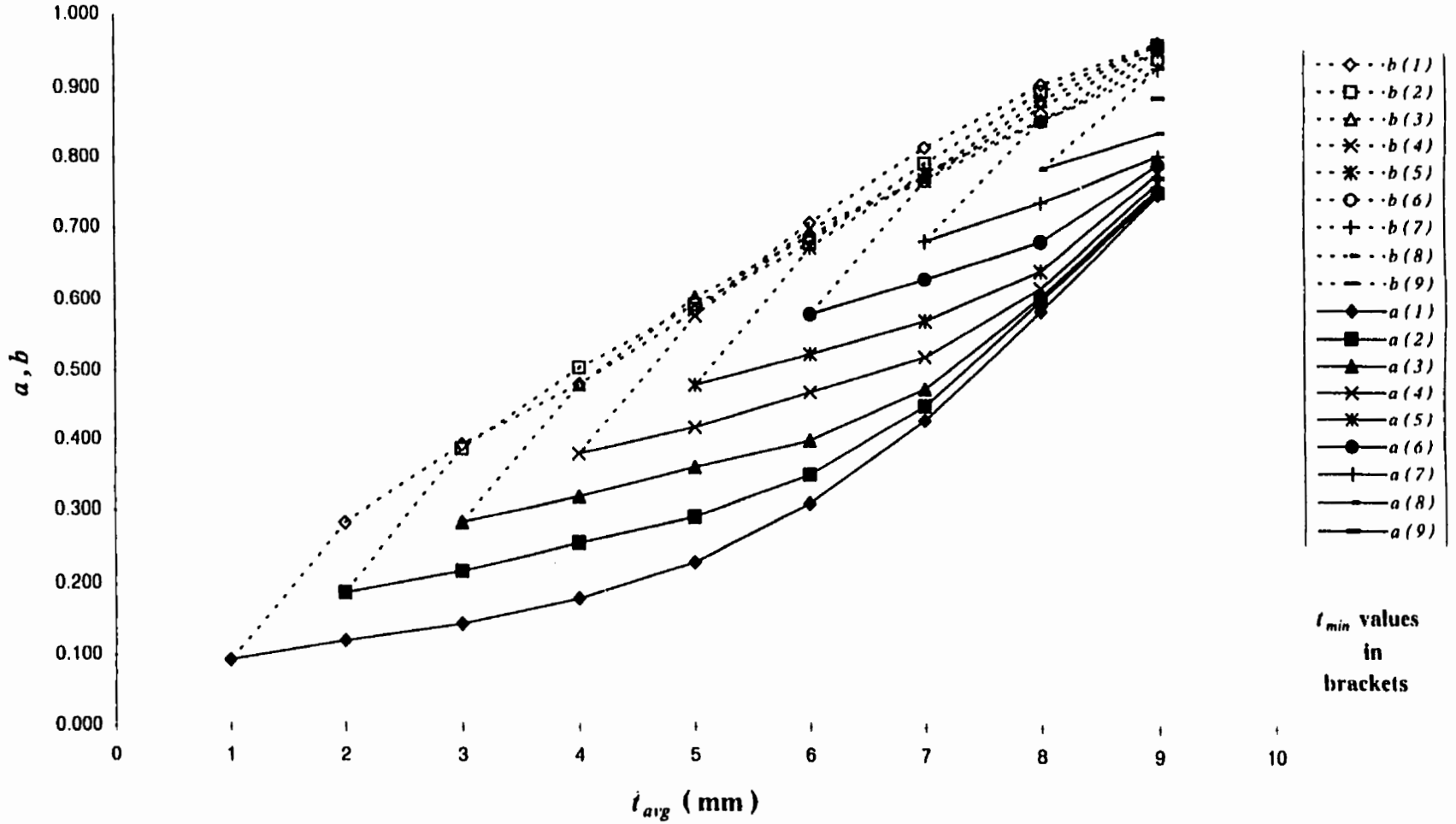

Figure 3.19 Minimum and maximum values of S/S_o versus average wall thickness

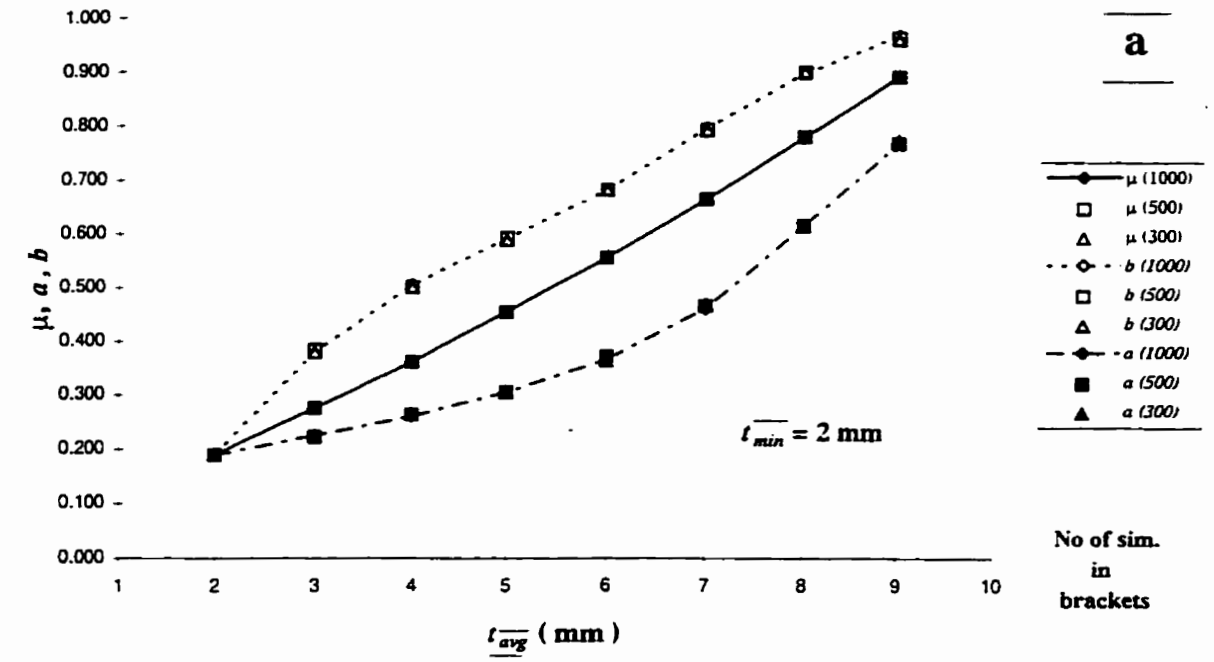

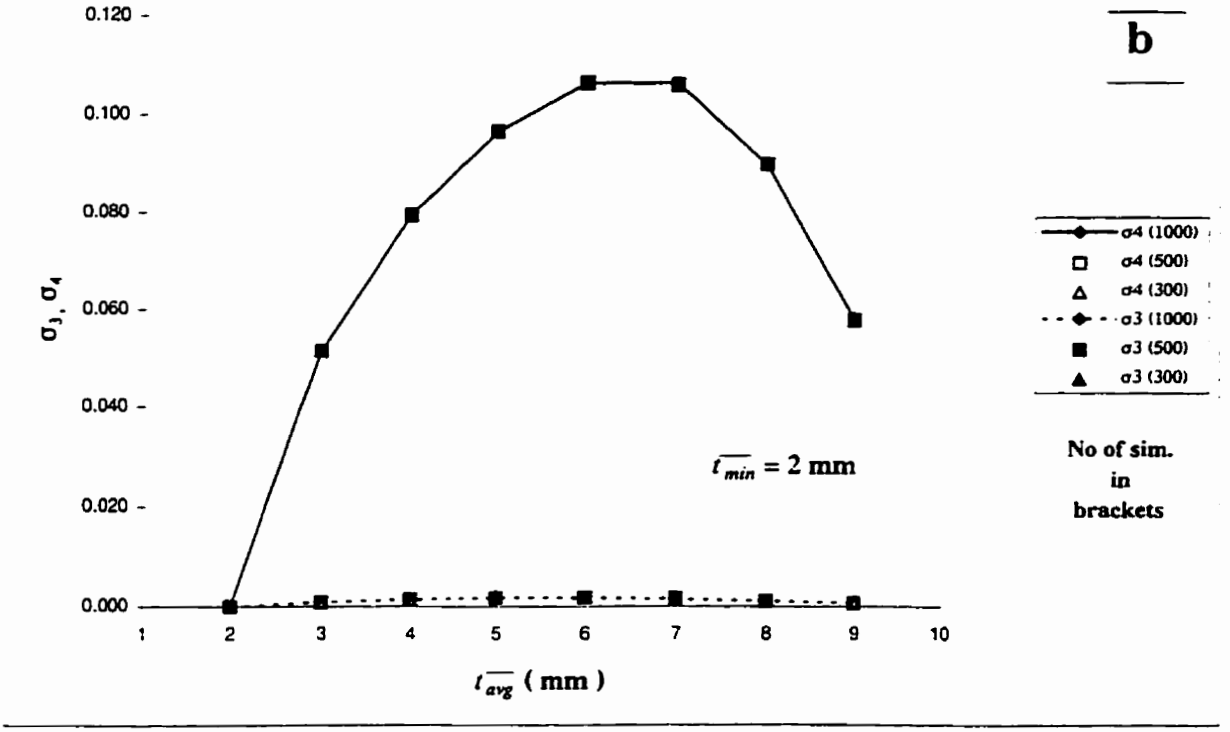

Figure 3.20 Variation of parameters of S/S_o distribution with the number of simulations

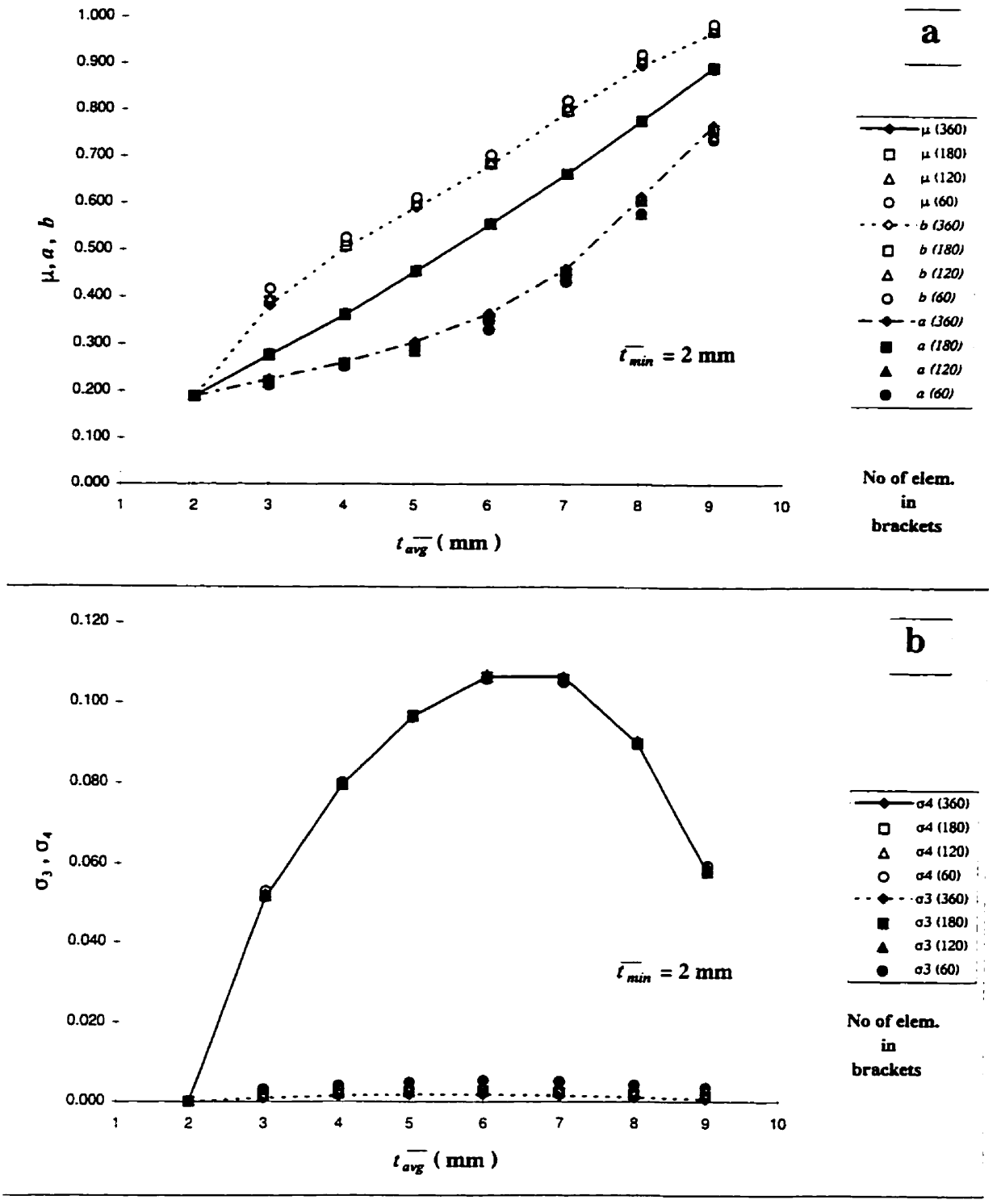

Figure 3.21 Variation of parameters of S/S_o distribution with the number of elements

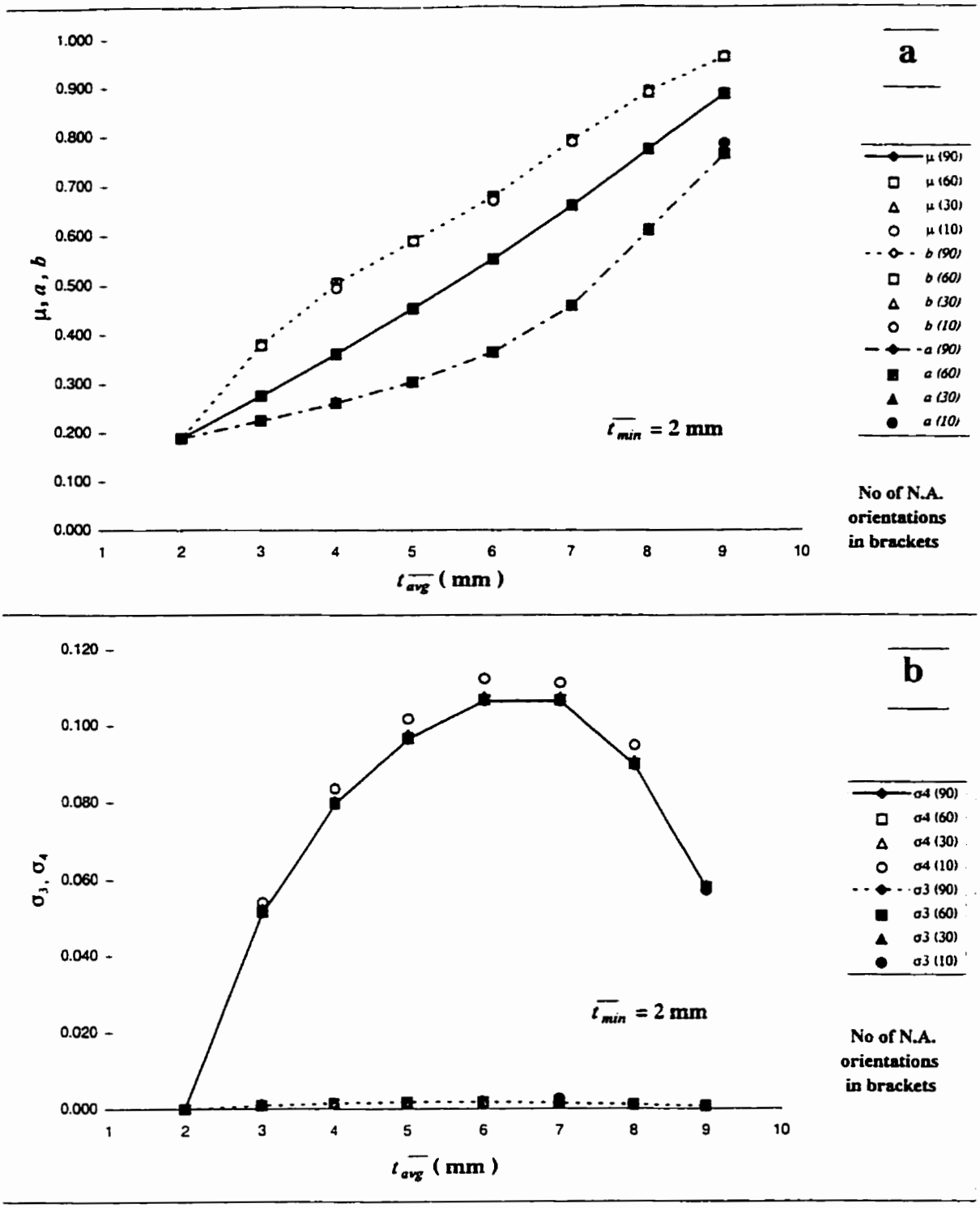

Figure 3.22 Variation of parameters of S/S_o distribution with the number of orientations of bending moment vector

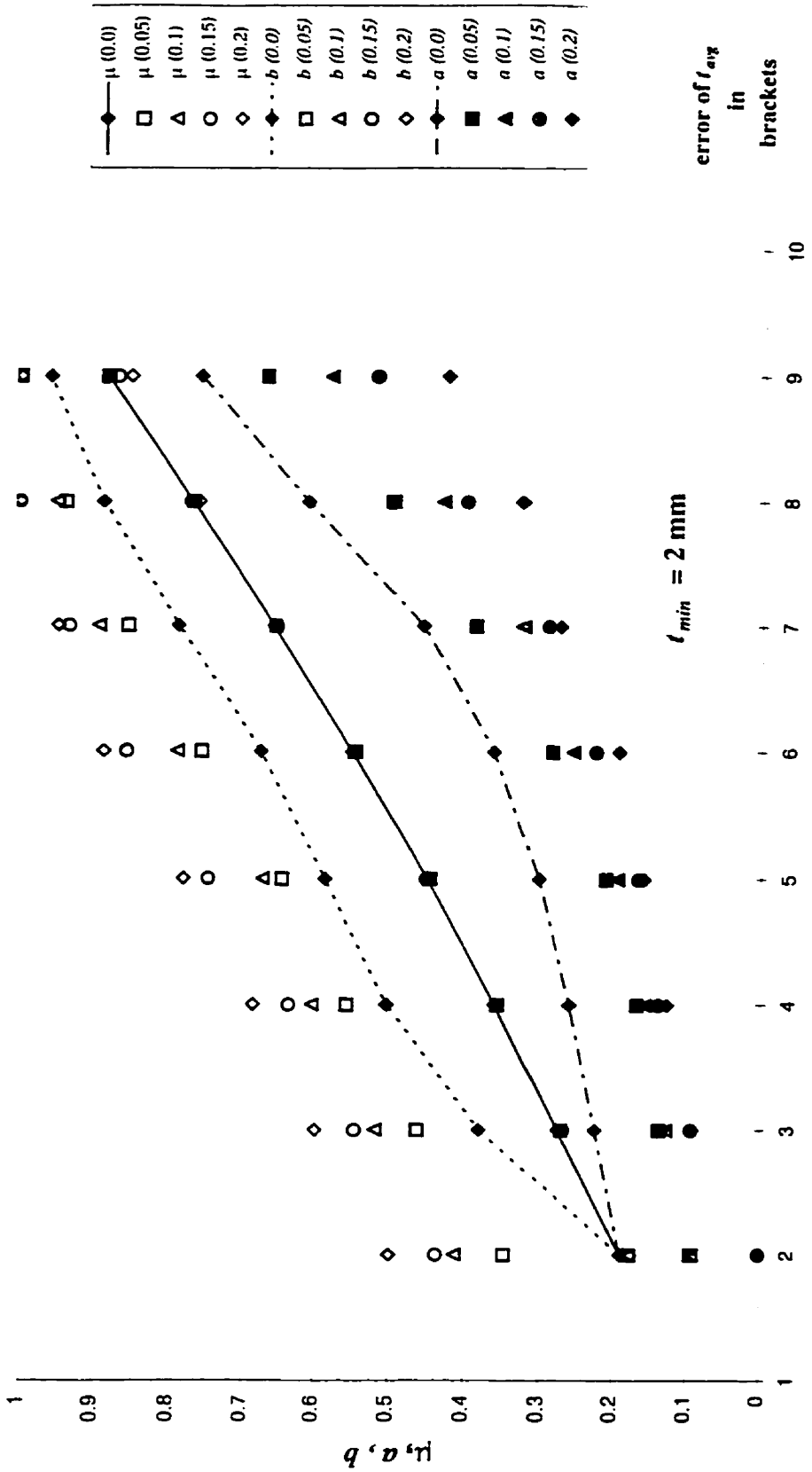

Figure 3.23 Variation of μ, a and b with measurement errors

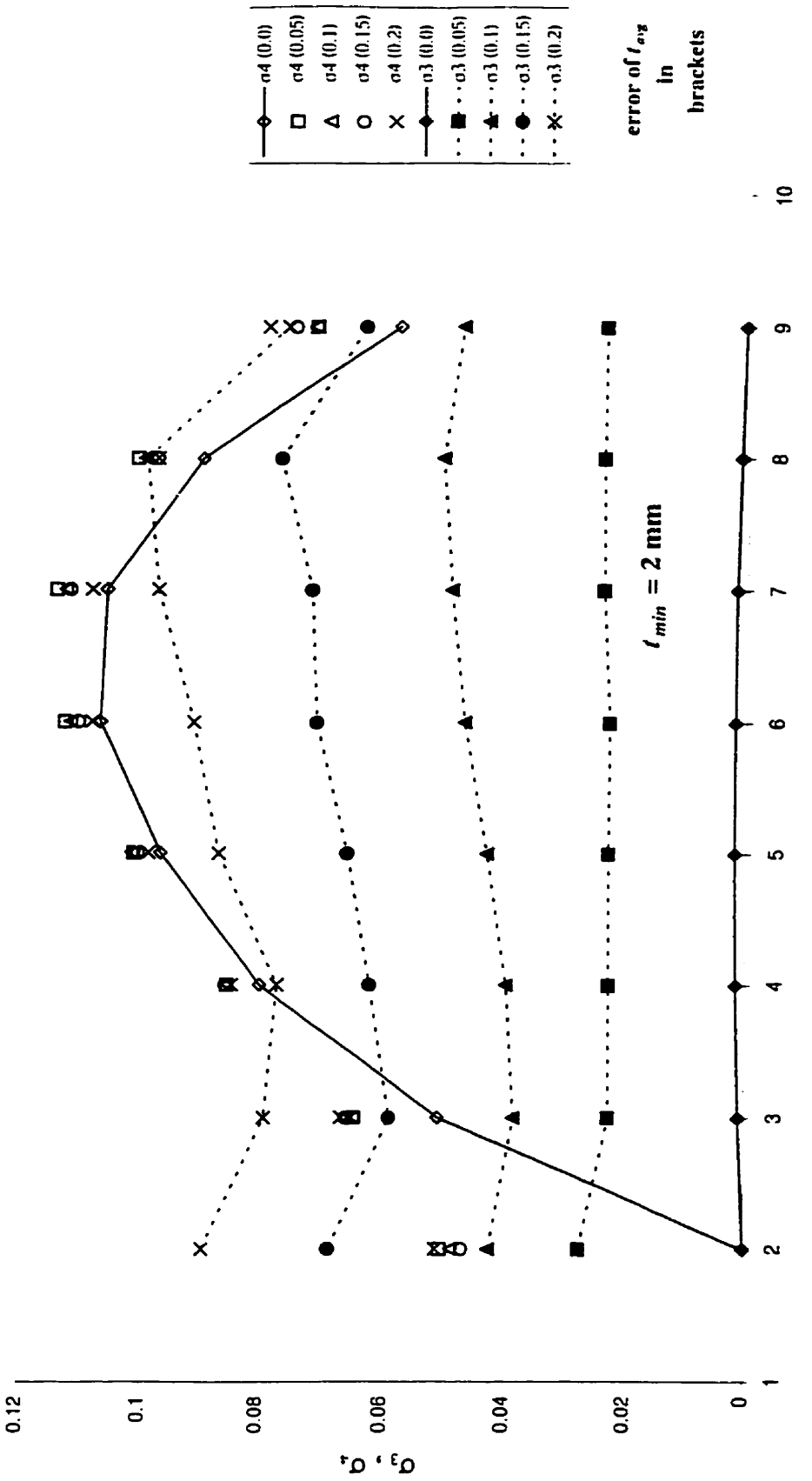

Figure 3.24 Variation of σ_3 and σ_4 with measurement errors

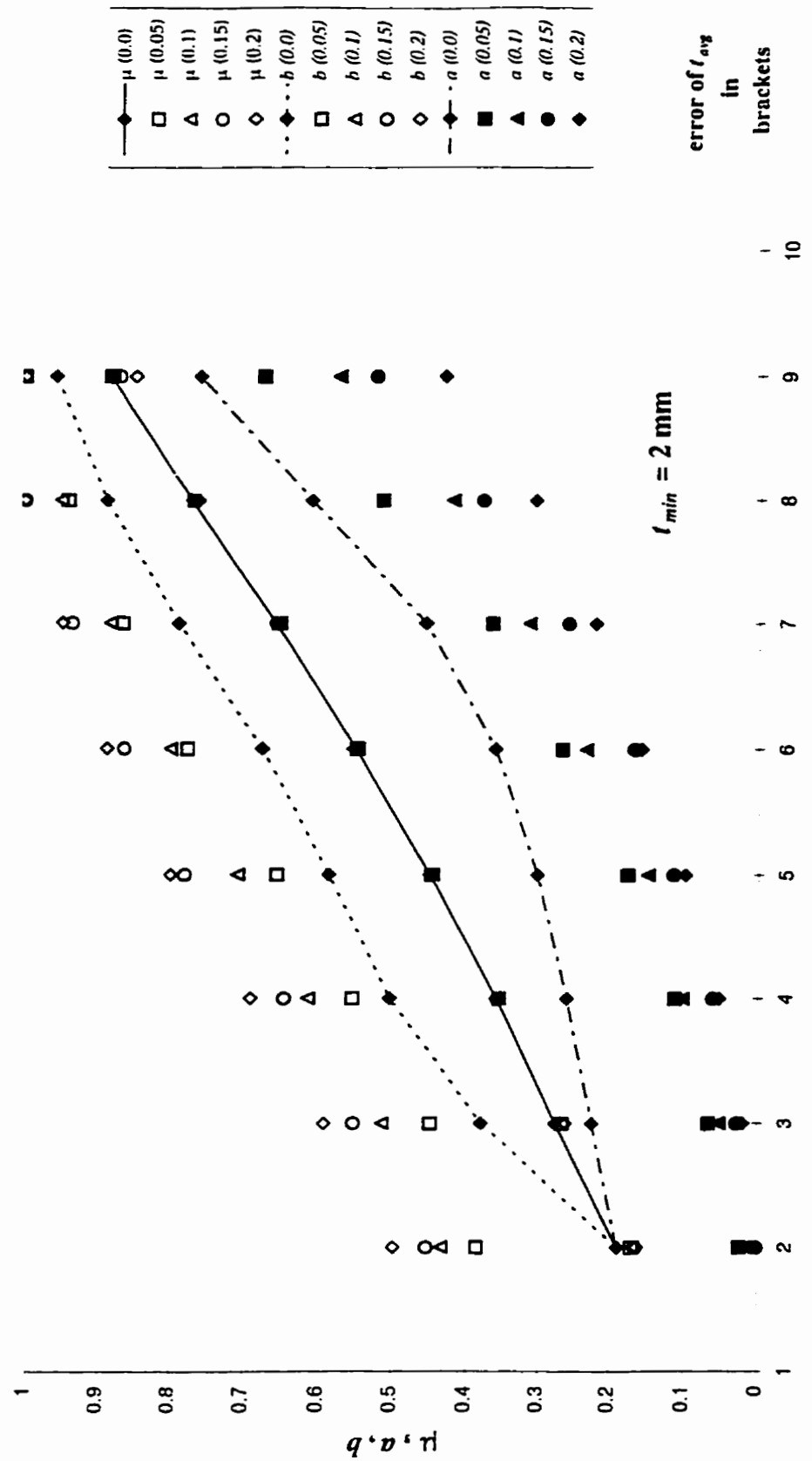

Figure 3.25 Variation of μ, a and b with measurement errors

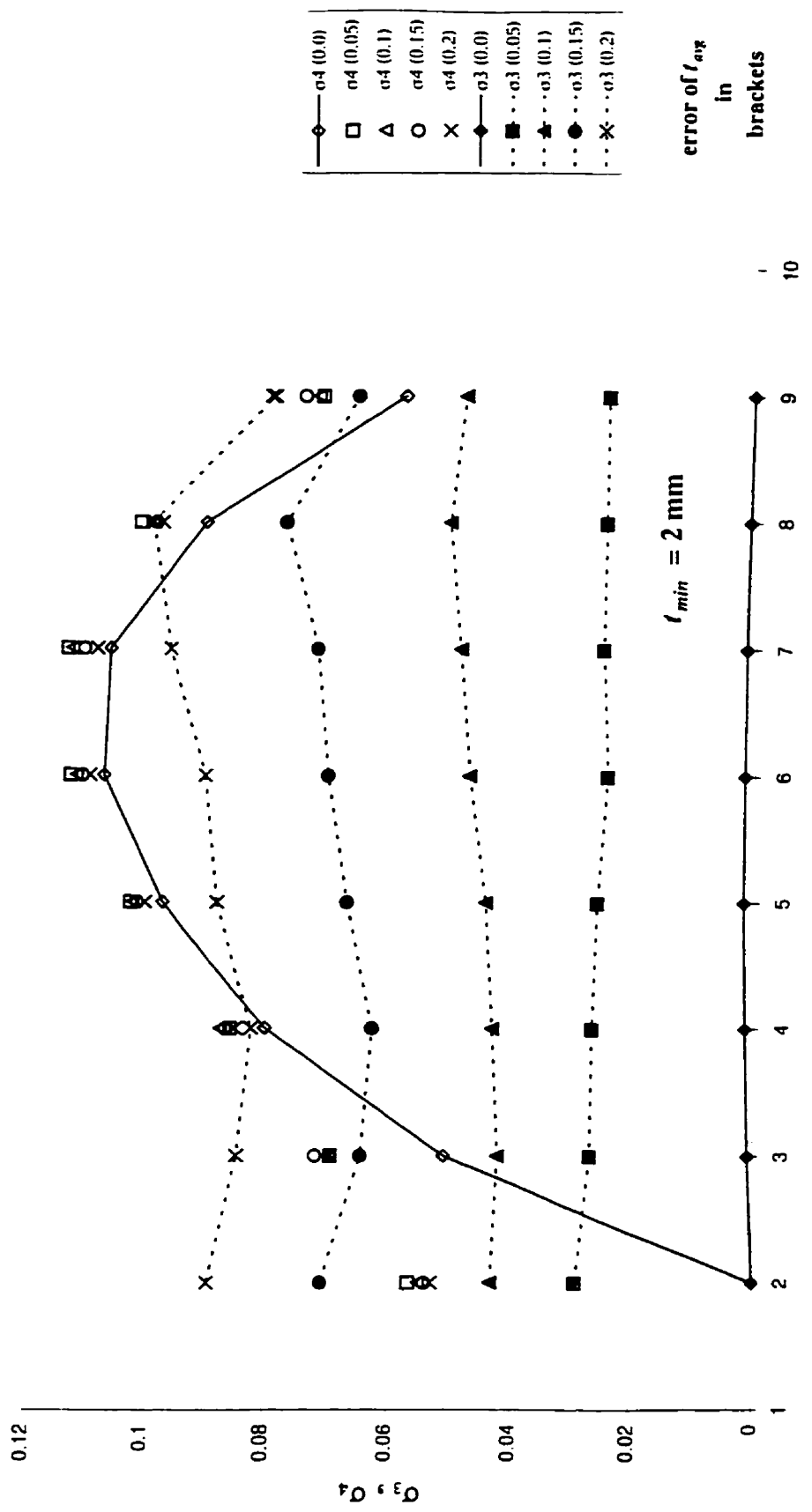

Figure 3.26 Variation of σ_3 and σ_4 with measurement errors

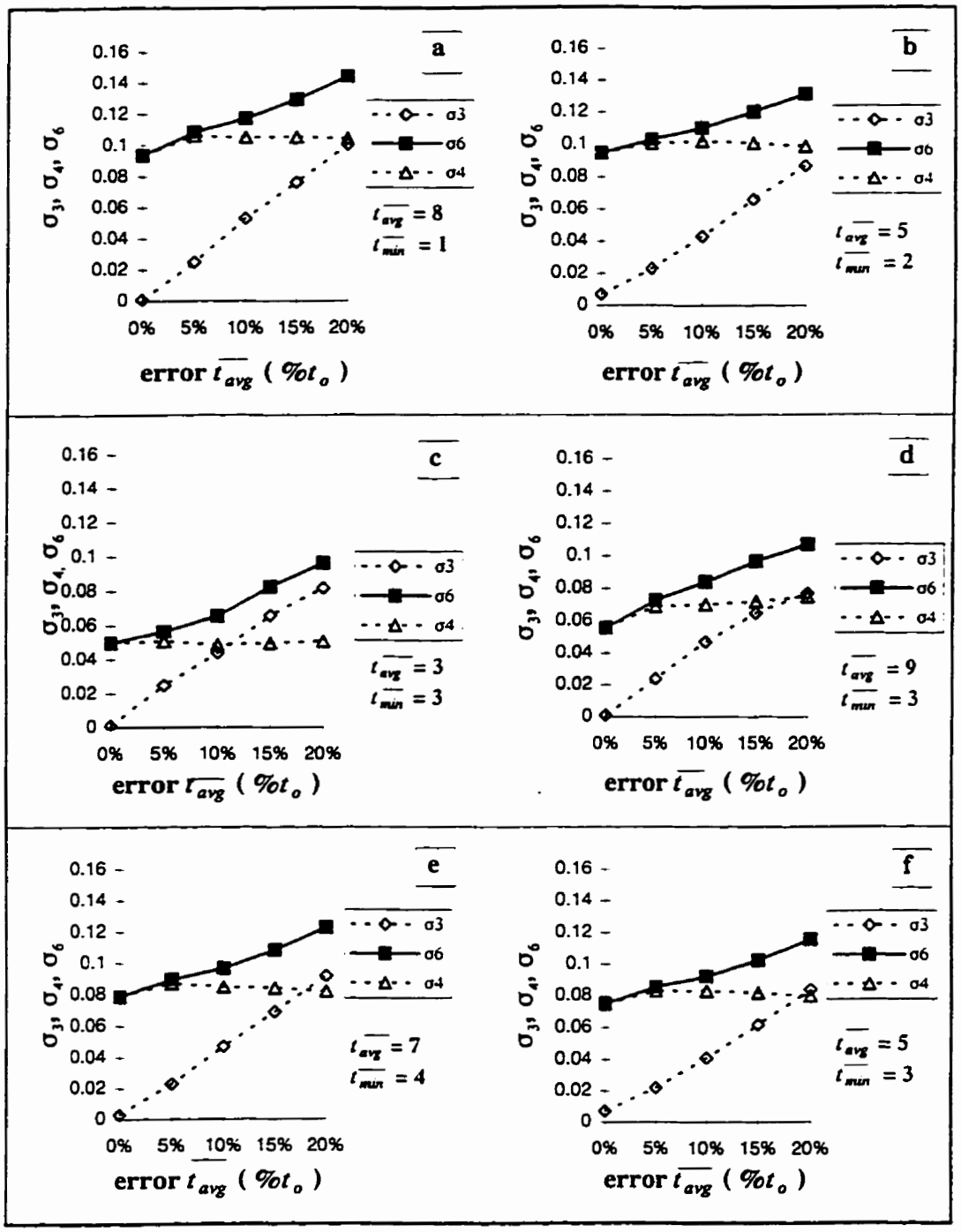

Figure 3.27 Graphs of the overall standard deviation for different wall thickness measurements

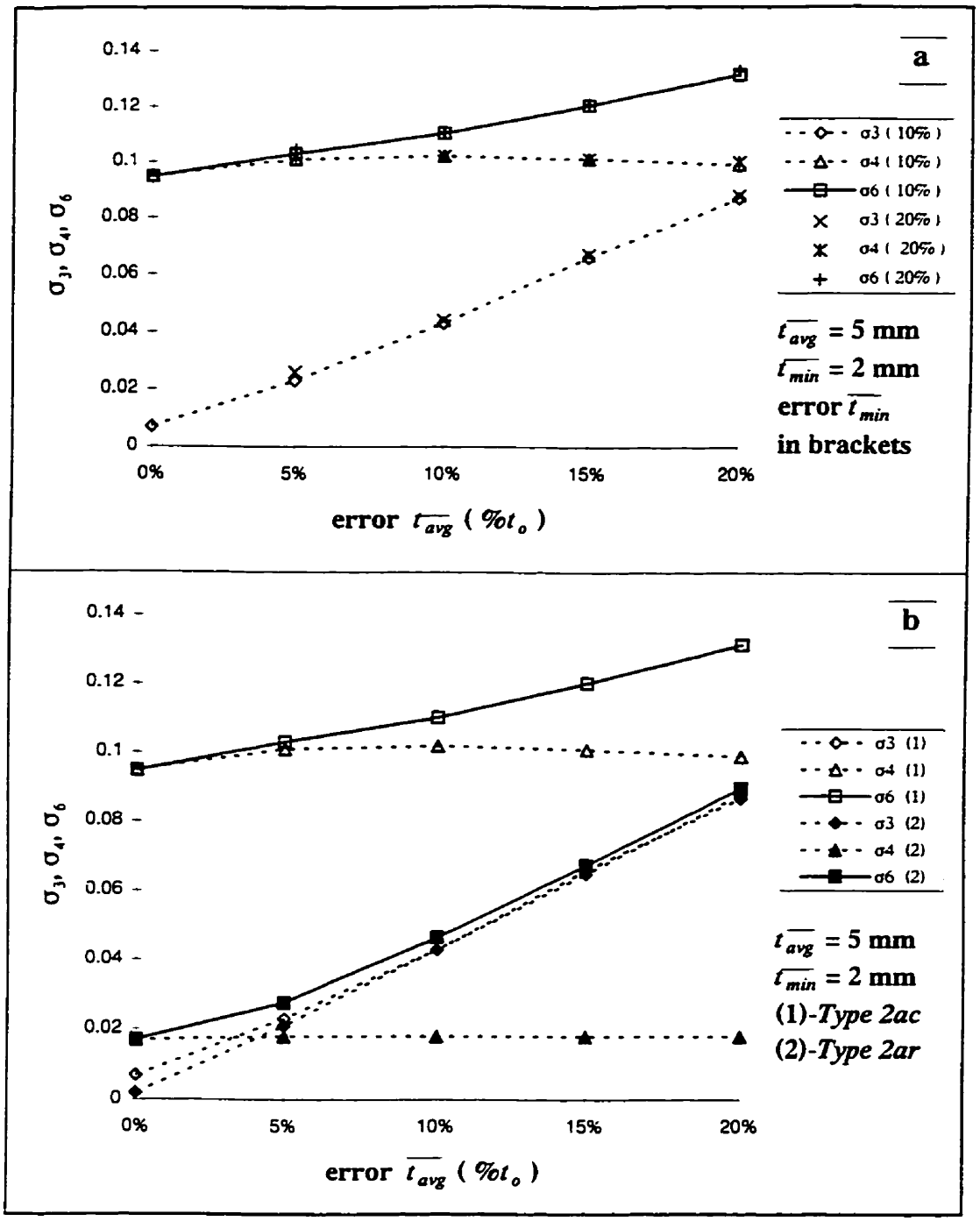

Figure 3.28 Graphs of the overall standard deviation for different models and wall thickness measurements

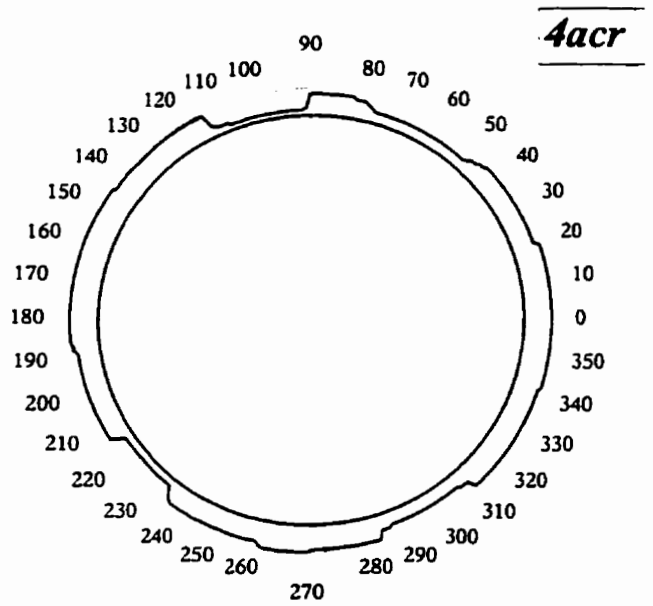

Figure 3.29 Simulated *Type 4a* section with ordered arrangement of elements and random positions of pits within quadrants

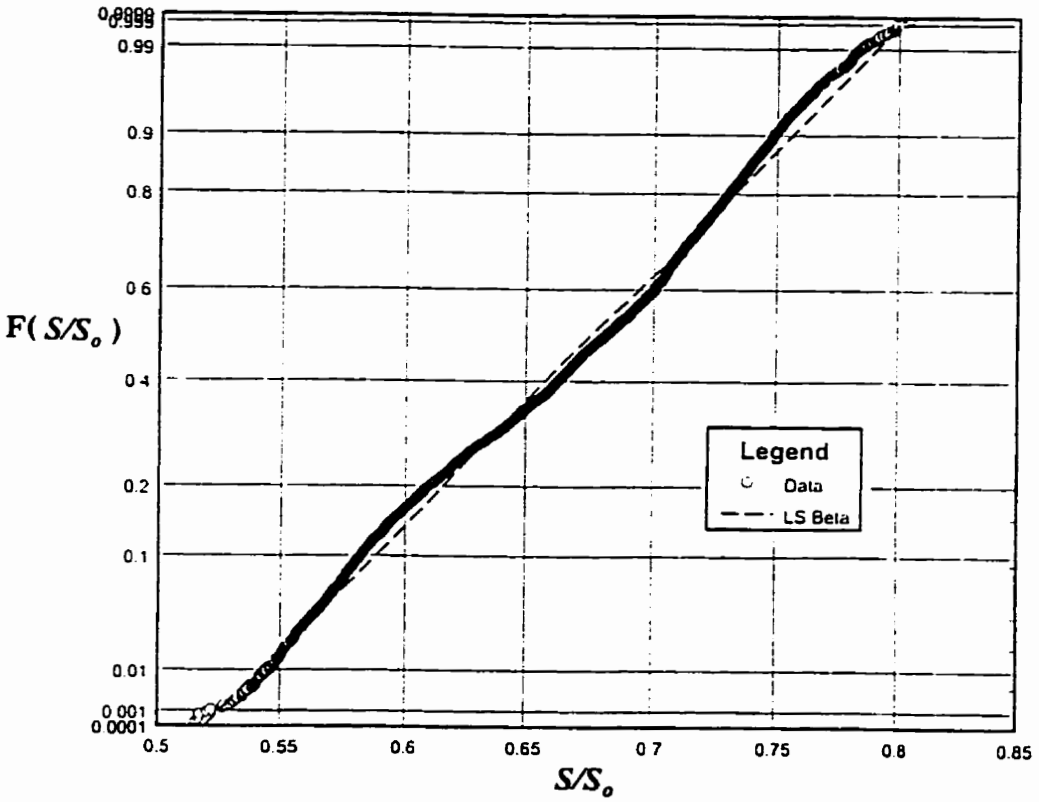

Figure 3.30 S/S_o distribution plotted on Beta probability paper (cross-section *4acr*, $\overline{t_{avg}}$ = 7.0 mm, $\overline{t_{min(1)}}$ = 3.0 mm, $\overline{t_{min(2)}}$ = 6.0 mm, $\overline{t_{min(3)}}$ = 7.0 mm, $\overline{t_{min(4)}}$ = 6.0 mm, no measurement errors)

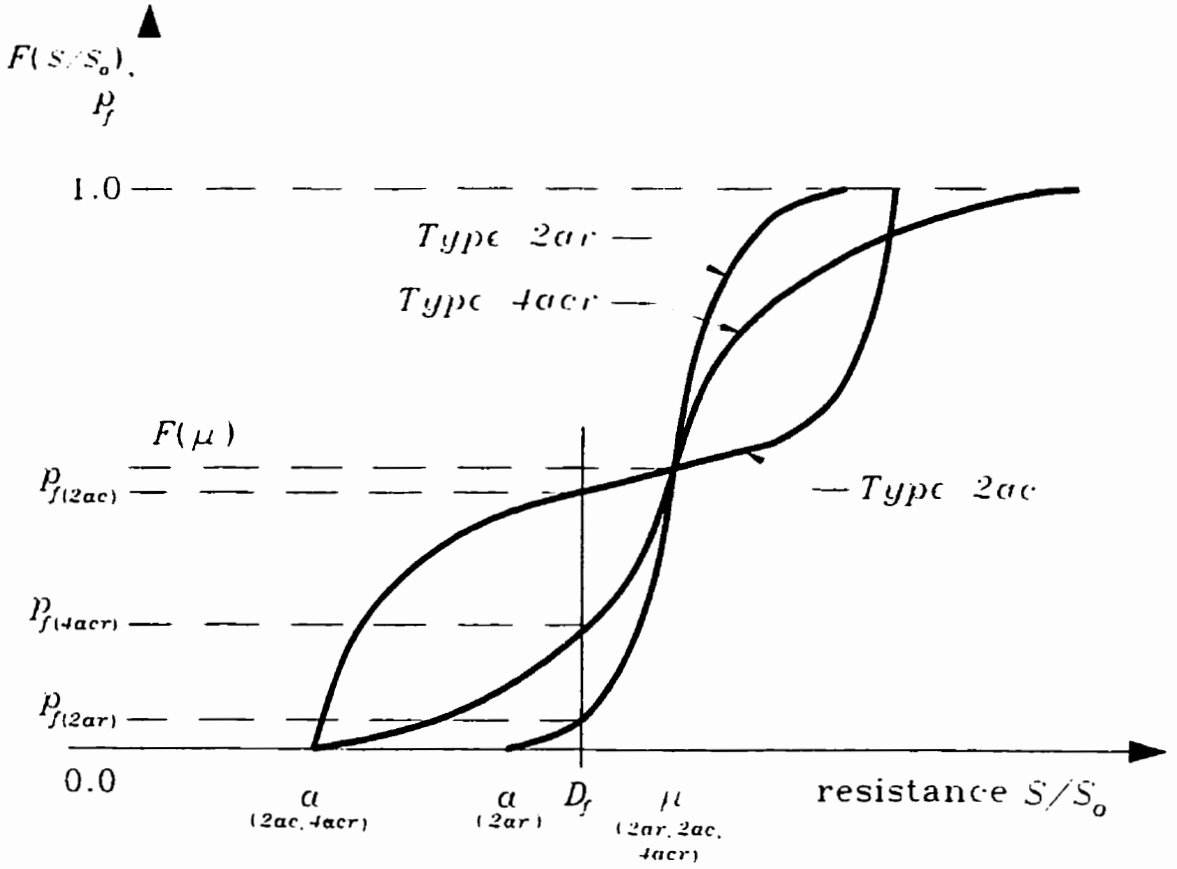

Figure 3.31 Approximate probabilities of flexural failure for *Type 2ac*, *Type 2ar* and *Type 4acr* models

Chapter 4 Literature review on underground corrosion

4.1 Introduction

Chapter 4 presents a literature review on corrosion of underground cast and ductile iron pipes. The rate and extent of corrosion of buried structures such as water mains depends on many environmental factors. Corrosion rate models for cast and ductile iron, based on extensive experimental studies done in the USA, which were published between the late 1950's and 1960's, are reviewed. The current composition and age of American and Canadian water distribution infrastructure makes these results still relevant to the problem of deterioration of water mains. The theoretical studies corroborating the experimental findings are also discussed in this chapter.

4.2. Experimental studies of corrosion rates for ferrous materials

In 1922, the National Bureau of Standards (now the National Institute of Standards and Technology) initiated a very comprehensive study of the effect of soils on the corrosion of commonly used pipe materials (Romanoff, 1957). Specimens of various ferrous and non-ferrous materials were buried in wide trenches at 47 sites, and were exposed to underground corrosion for different periods of time. Specimens were removed from the soil for examination in 1924, 1926, 1928, 1930, 1932, and 1934, and some samples were left in the ground until 1939. In 1924, 1928, 1937, 1939 and 1941, new specimens were

buried to extend the scope of the investigation. The study ended in 1952 with the removal of the last specimen. During the thirty year duration of the study, over 37,000 specimens made from 333 different materials were investigated in 128 test sites throughout the United States.

4.2.1 Test sites

The 128 test sites represent 95 different types of soils. The chemical and physical properties of the soils were documented to investigate their effect on both the initiation and the progress of the corrosion process. Generally, the following properties were determined and recorded:

- resistivity
- pH
- internal drainage
- aeration
- composition of water extract (total acidity, Na + K, Ca, Mg, CO_2, Cl, SO_4)
- moisture content
- apparent specific gravity
- volumetric shrinkage

The sites were selected to be representative of a wide range of environmental conditions. The selected sites had pH ranging from 2.6 to 10.2, soil resistivity from 51 ohm-cm to

54400 ohm-cm. and soil aeration ranging from poor to very good. Recent discussion of the relationship of environmental factors to the corrosive nature of soil (Robinson, 1993; Fitzgerald, 1993), shown in Figure 4.1, have corroborated the significant physical and chemical properties that were originally recognized over 70 years earlier in the NBS study.

4.2.2 Cast iron specimens

The cast iron specimens used in the NBS program were short segments of pipes and small plates. The diameter of the pipe specimens varied from 1.25 to 6 inches (31.7 to 152.4 mm), and the length varied between 6 and 13.5 inches (152.4 to 342.9 mm). The cast iron specimens also had different chemical compositions, and were cast using different methods.

Three chemical compositions were investigated: plain cast iron, low alloy cast iron, and high alloy cast iron. The alloys investigated included copper (Cu), manganese (Mn), nickel (Ni), chromium (Cr) and silicon (Si), with the content of each alloy varying as follows:

- plain cast iron: 0.91% Mn, 2.19% Si, and traces of Cu, Ni, and Cr not specified
- low alloy cast iron: 0.15% -3.32% Ni, 0.70%-0.83% Mn, 2.09%-2.50% Si, 0.32%-1.10% Cu, 0.30% Cr

- high alloy cast iron: 15% Ni, 1.0% Mn, 6.58% Cu, 2.61% Cr, and 13.44% Si for high-silicon cast iron

The total number of cast iron specimens was 4207, comprising 3539 specimens of plain or low alloy cast iron, and 668 specimens of high alloy cast iron.

Pit-cast and spun-cast products were investigated in the NBS corrosion studies to assess the difference in corrosion resistance for the two production methods. The pit, or vertical, casting method, where the molten metal is poured inside sand molds, was the only method of producing cast iron pipes prior to 1922. Figure 4.2 shows a typical microstructure of pit-cast iron. Long graphite flakes in the matrix of perlite are mainly responsible for the brittle behaviour of cast iron. The graphite flakes, which appear as discontinuous solid lines in the figure, facilitate both the initiation and the propagation of cracks. They also act as the cathode of galvanic microcells in the graphitic corrosion process. The spin, or centrifugal, casting process was introduced in 1922. It improved considerably the mechanical properties of cast iron, by reducing the size of graphite flakes and making their distribution more uniform. The effect of the new technology on the corrosion resistance of cast iron was intended to be determined by the field tests.

4.2.3 Results of the field experiments for cast iron test specimens

After two years initial exposure in the soil environments, two specimens of the same material were removed for testing from each site at two year time intervals. All specimens were transported to the NBS laboratory and the corrosion products were removed by mechanical and chemical treatments. A series of measurements was conducted to obtain the maximum pit depth and the weight loss for each sample. Based on the data collected over 30 years of experiments the following conclusions were drawn (Romanoff, 1964):

1. The rate of corrosion is controlled by the characteristics and properties of the soils and varies widely for different soils. Figure 4.3 shows the specimens of the same plain cast iron pipe, exposed to underground corrosion for 14 years, from 14 different test sites. The corrosion damage varies widely, for example between specimens 51, which is severely corroded and 53, which is in excellent condition. This indicates that the environmental factors affect significantly both the extent and the rate of corrosion.
2. Commonly-used cast iron pipe materials corrode at nearly the same rate in the same soil environment.
3. Low alloy cast iron pipes corrode at approximately the same rate as plain cast iron pipes in the same soil environment. For example, Figure 4.4 shows average weight loss and maximum pit depth versus time for plain cast iron (denoted as A, F and G), low alloy cast iron (denoted as I, J, and C) and high alloy cast iron (E). For each

pipe material, the plotted values are the average obtained from the samples collected at 14 different test sites. The weight loss and maximum penetration for high alloy cast iron is markedly less than that of other materials.

4. High alloy cast iron is considerably more corrosion-resistant than plain cast iron. This is really a consequence of the previous conclusion, and is clearly shown in Figure 4.4.
5. Cast iron in the advanced stage of graphitic corrosion may retain sufficient strength to withstand water main pressures up to 500 psi.
6. There is no appreciable difference in the corrosion of cast irons manufactured by pit casting or spin casting methods.

Besides these general conclusions, very interesting results were obtained from the quantitative analysis of data for a particular test site. An approximately linear relationship was obtained by plotting the logarithm of the average maximum pit depth against the logarithm of time. This suggested that pit depth can be modeled using general equations of the form:

$$P = KT^n \qquad [4.1]$$

where is P the average maximum pit depth; T is the exposure time; and K and n are constants. Similar results were obtained for the average weight loss, with the governing equation in the form

$$W = kT^u \qquad [4.2]$$

where W is the average weight loss; and k and u are constants.

Further examination of the results for pitting corrosion of all specimens buried in different soils revealed that the time constant n was dependent largely on the degree of aeration of the soil. To obtain quantitative results for n, the test sites were arranged in four groups according to the degree of aeration, which was classified as good, fair, poor, and very poor. The aeration of different soils was based primarily upon physical characteristics such as the apparent specific gravity, the particle size and particle-size distribution. Special consideration were also given to drainage, indicated by the topographic features, the average height of the water table and the texture of the soil. For each group, statistical analyses were performed and the results are shown in the Table 4.1.

Table 4.1 Calculated values of time constant n according to soil aeration (Romanoff, 1957)

Soil aeration	Mean n	St.deviation σ_n
very poor	0.68	0.10
poor	0.47	0.04
fair	0.35	0.03
good	0.19	0.03

In the case of the average weight loss the same tendency of the corrosion rate, namely a lower time constant u for better aerated soils, was observed. However, the mean values of u were often somewhat higher than corresponding values of n, with larger coefficients of

variation. Ultimately the summary results listing u and σ_u for different classifications of soil aeration, were deemed to be inconclusive, and were not reported in the NBS studies.

4.3 Supplementary experimental corrosion studies of ductile cast iron pipes

Ductile cast iron was introduced in 1948. The investigation of its performance in the soil environment was initiated by the Cast Iron Pipe Research Association (CIPRA) in 1952 (Sears, 1968). The NBS independently undertook a series of field tests of ductile cast iron pipes in 1957 to supplement its previous studies of the underground corrosion of cast iron.

4.3.1 Ductile cast iron material

The chemical composition of ductile iron is very similar to that of cast iron, with the graphite particles in both cases accounting for about 10% of the volume. The major differences between ductile and cast iron are the size and shape of graphite particles in the microstructure. Figure 4.5 shows a magnified view of the microstructure of ductile cast iron. The manufacturing process converts the graphite flake to nodules that are more or less uniformly distributed throughout the metal matrix. This spheroidal shape of the graphite particles reduces the surface area of the graphite, improving both the strength and ductility of the material (LaQue, 1964).

4.3.2 Experimental studies done by CIPRA (Sears, 1968)

CIPRA began its soil corrosion field tests of ductile cast iron pipes in 1952. Only test sites which were known to be very corrosive were selected for the accelerated underground corrosion studies. The soil resistivity in the sites selected varied between 200 and 400 ohm-cm. Specimens of both ductile and cast iron pipe, 6 inches in diameter and 5 ft. in length, were buried at each site for up to 14 years. They were gradually removed for inspection at 2 or 3 year time intervals over a period of 14 years. Based on the results of CIPRA tests. Sears concluded that the corrosion resistance of buried ductile iron pipe is equal to or somewhat better than that of gray cast iron pipe.

4.3.3 The NBS experimental studies (Romanoff, 1964 and 1967; Gerhold, 1976)

The NBS tests of ductile cast iron pipe commenced in 1958, but the extent of the research was not as broad as it had been for cast iron pipes. Six sites were selected for the tests, with widely varying environmental factors known to affect the underground corrosion rate. The soil resistivity varied between 55 and 30000 ohm-cm, the pH ranged 4.0 to 8.8, and the aeration was either poor or good. Only one test site was involved in some of previous tests of cast iron pipes, and this site served as a reference site in the correlation of data obtained for specimens buried in five new locations. The ductile cast iron pipe samples investigated were 2 inches (50 mm) in diameter and 12 inches (300 mm) long. Unlike the CIPRA tests, cast iron pipes were not used in the NBS studies. To provide another means of comparing the data for cast and ductile iron, carbon steel specimens that

had been used in earlier tests of cast iron, were used. The following conclusions of the investigation were presented by Romanoff:

1. ductile and cast iron corrode at nearly the same rate in the same soil environment
2. the pattern of corrosion and the nature of the corrosion products are similar in the same soil environments

4.4 Theoretical derivation of corrosion rates (Rossum, 1969)

The electrochemical theory of corrosion was used by Rossum as a basis to derive corrosion rate equations. In his derivation Rossum considered the degree of aeration of the soil as the primary factor that defined which of four different corrosion processes would occur. Similarly to the NBS approach, the soil aeration was classified as good, fair, poor and very poor. The theoretical pitting corrosion equations developed were identical in form to Eq.[4.1] as proposed by Romanoff. The remarkable agreement of the theoretical and experimental values is shown in Table 4.2

Table 4.2 Theoretical and experimental values of time constant *n* according to soil aeration (Rossum, 1969)

Soil aeration	NBS mean *n* (Romanoff, 1957)	Theoretical *n* (Rossum, 1969)
very poor	0.68	0.67
poor	0.47	0.50
fair	0.35	0.33
good	0.19	0.17

Rossum also presented an interesting reasoning that the time constant u in the equation governing the weight loss due to corrosion, Eq.[4.2], should approach with time the exponent n in the pit depth equation, Eq.[4.1]. Assuming that at the beginning corrosion process the material is covered with separated hemispherical pits, the weight loss time exponent u will be equal to $3n$ due to the fact that the volume of a pit is proportional to the cube of its depth. As the corrosion proceeds smaller pits will be enveloped by the larger ones, and the rate of "disappearance" of smaller pits will be proportional to the growth rate of the area large pit. The area of the large pit is proportional to the square of pit depth, and therefore the total weight loss will become with time proportional to the pit depth. The proportionality between the pit depth and the weight loss established over time means that the time exponent u in the weight loss equation will approach n.

4.5 Corrosion rates assumed for subsequent analysis of a pipeline

Based on the literature review the corrosion models assumed for the simplified reliability analysis of a pipeline in Chapters 5 and 6 will be of the form:

- corrosion rate for pitting - $P = KT^n$ [4.1]
- corrosion rate for weight loss - $W = kT^n$ [4.3]

where the weight loss is equivalent to the loss of the average thickness of pipe wall. The assumed models can be used irrespective of the pipe manufacturing process or the type, i.e., ductile or cast iron, and chemical composition of the pipe material except for high

alloy cast iron. However, the soil environment that the pipe is subjected to should be free of stray currents (Romanoff, 1957). It is also assumed that pipe joints are connected using rubber gaskets, hence the rise of a significant long line currents due to varying soil conditions along the line can be neglected. A similar model of corrosion rate was adopted by Ahammed and Melchers for the reliability analysis of underground pipelines subjected to corrosion (Ahammed and Melchers, 1994).

Based on the prevalent failure modes for cast and ductile iron pipes, discussed in Chapter 1, the assumed pitting corrosion model will govern the rate of failure for ductile cast iron pipes, while the weight loss or the average wall thickness corrosion model will apply predominantly to the cast iron pipes. The time exponent n, assumed the same in both corrosion models, stipulates applicability of Eq.[4.3] to fairly old pipes only. Considering the average age of cast iron pipes, as described in Chapter 1, this condition will be satisfied.

In the absence of detailed information characterizing the corrosive nature of the soil environment, the use of the NBS values of mean exponent n and the standard deviation σ_n is proposed. The degree of aeration of the soil will be used to select the most suitable value of n. The degree of soil aeration can be established from the measurements of the oxidation reduction, or "redox", potential, but it will also require a great deal of engineering judgment. Table 4.3 shows the correlation between the measured redox

potential and the classification of the soil aeration based on two different sources (Doleac *et al*, 1980; Sears, 1968)

Table 4.3 Soil aeration classifications based on measured redox potential

Soil aeration	Reduction oxidation potential in milivolts	
	(Doleac *et al*. 1980)	(Sears. 1968)
very poor	< 50	< 0
poor	50 - 150	0 - 50
fair	150 - 250	50 - 100
good	> 250	> 100

The determination of the remaining parameters of corrosion rate, K and k, which can be established using the Hydroscope data will be discussed in the Chapter 5.

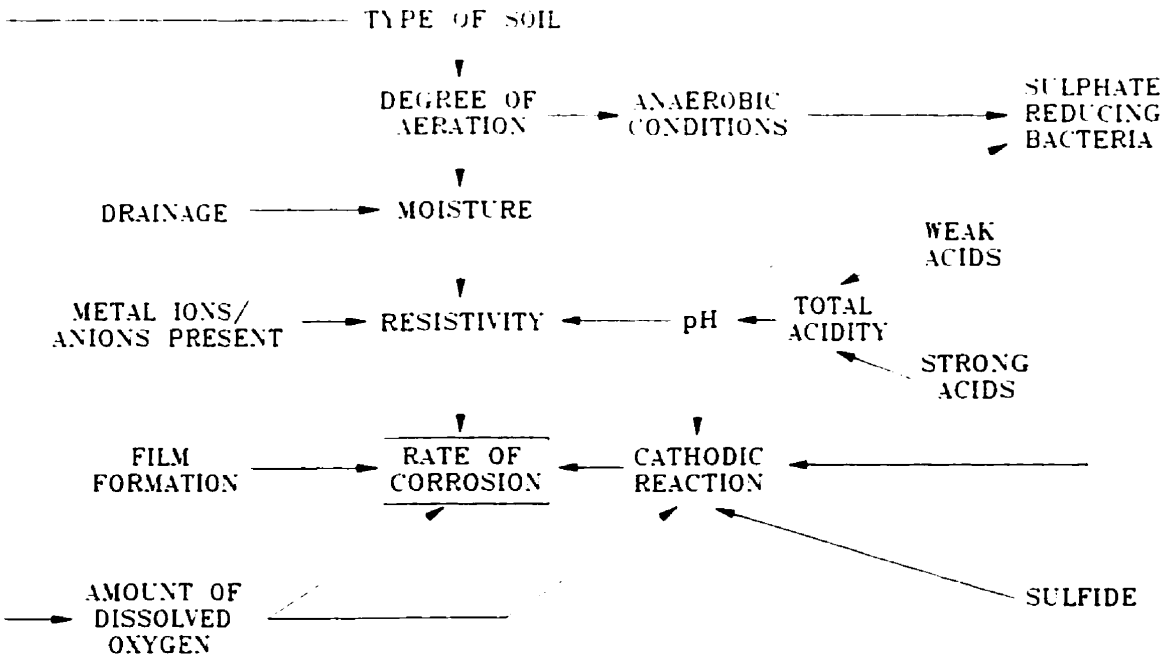

Figure 4.1 Relationship of environmental factors to the corrosive nature of soil (Robinson, 1993)

Figure 4.2 Grey cast iron - microstructure (×300) (Gedge, 1993)

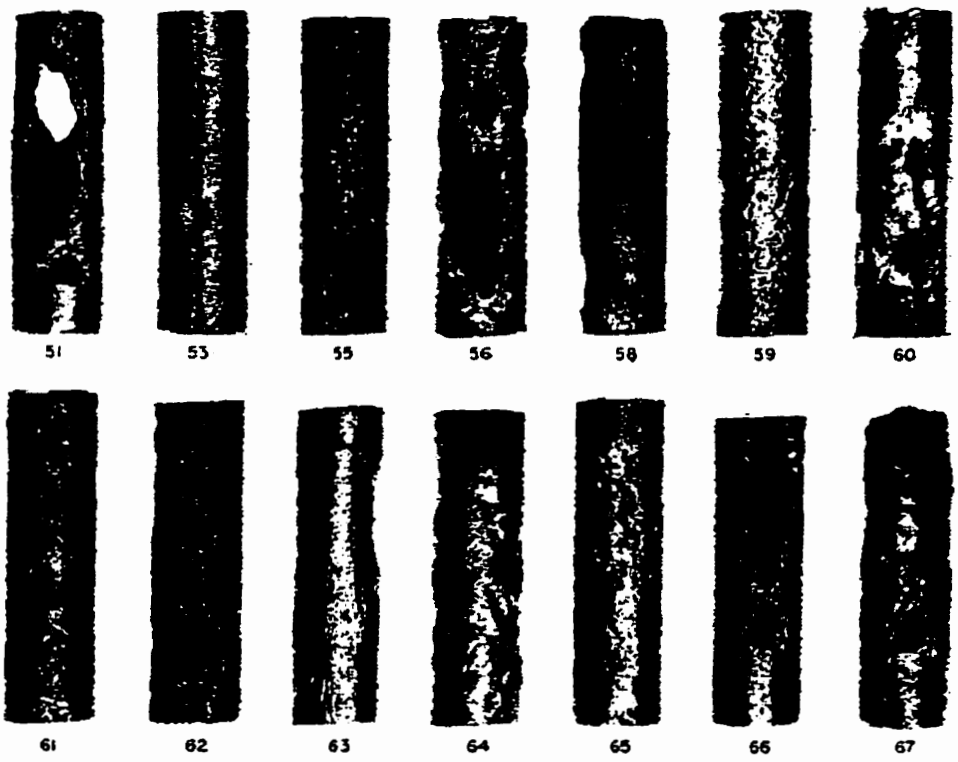

Figure 4.3 Corrosion of plain cast iron exposed 14 years at 14 test sites (Romanoff, 1957)

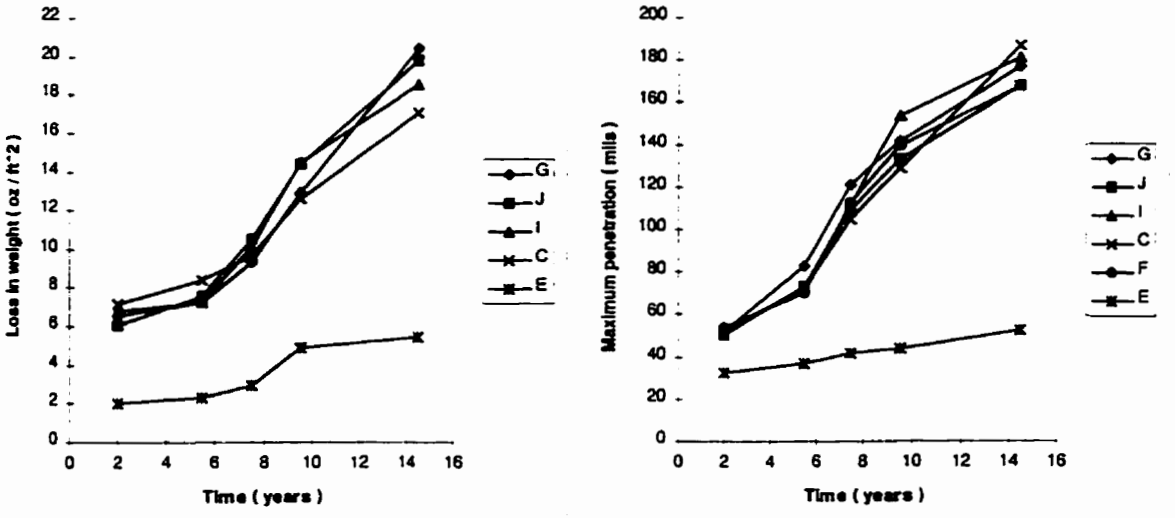

Figure 4.4 Average loss in weight and maximum pit depth of cast iron pipe specimens exposed in 14 soils (Romanoff, 1957)

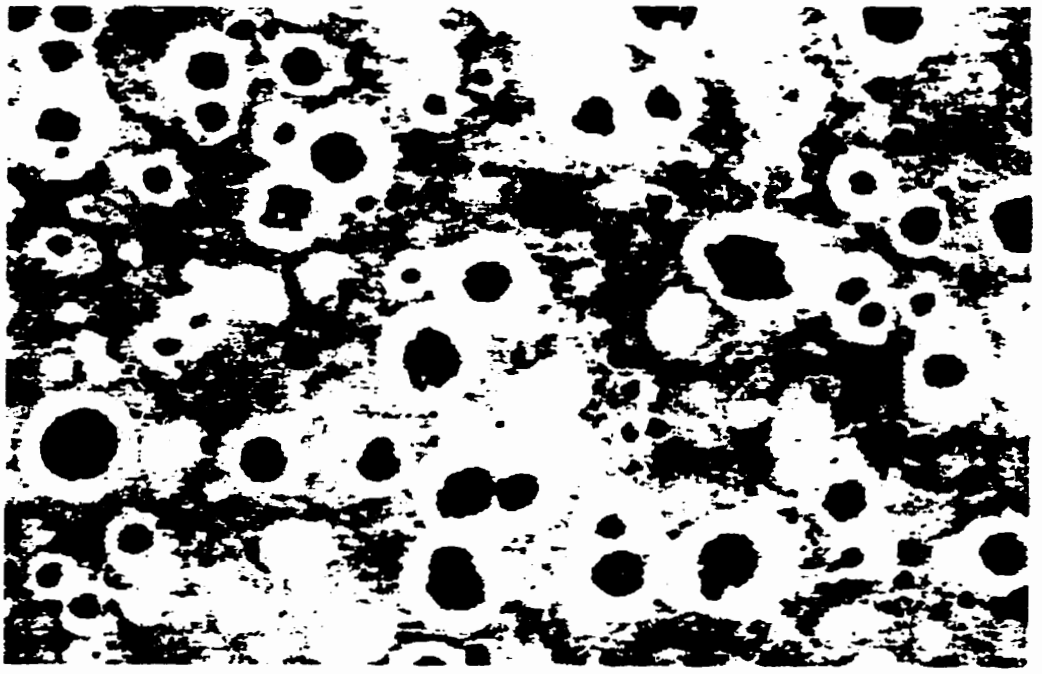

Figure 4.5 Ductile cast iron - microstructure (× 100) (Gedge, 1993)

Chapter 5 Reliability analysis of a pipeline

5.1 Introduction

The objective of this chapter is to present the simplified time-dependent reliability analysis of a deteriorating pipeline incorporated in the program PIPEREL.EXE. The program accounts for either one or both of the two most common failure modes of cast iron pipes: the flexural failure, which is the predominant failure mode for the gray cast iron; and, the corrosion failure, which is the predominant failure mode for the ductile cast iron

The analysis of flexural failures of a pipeline will show the practical application of statistical information obtained from simulations of deteriorated pipe cross-section described in Chapters 2&3. The analysis of the flexural or the corrosion failure of a pipeline will allow the use of the historic data regarding the past frequency of failures experienced by the pipeline. Some examples of such data for 21 Canadian cities are shown in Figures 1.2 and 1.3.

The analysis is based on the assumption that the reliability of the pipeline can be calculated from the probability density functions for the state of the sampled cross-sections defined in Chapter 2. The current Hydroscope tool samples 4 or 5 sections per pipe joint, which gives a very good description of the pipe joint condition. However, it is

possible that a cross-section exists which is weaker in bending than the ones reported by the tool, or a cross-section has a pit deeper than any of those reported. This uncertainty is due to the tool resolution as represented by the minimum observable pit volume, V_{min}, and the uncertainty of the reported mean and minimum wall thicknesses. Also, the reported local average thickness, $\overline{t_{avg}}$, correspond to the cross-sections with the deepest pits identified, $\overline{t_{min}}$. Other assumptions that simplify the reliability analysis, which are failure mode specific, are explained in the subsequent sections of this chapter.

If a cast iron pipeline fails, several responses are possible to restore the line to service. The two common responses to cast iron pipeline failures are joints replacement and installation of clamps. The program allows consideration of both repair methods for the analyzed pipeline. Hence, the examination of the effect of joint replacement or the installation of clamps on the estimated future rate of a pipeline failures can also be performed.

In the subsequent sections of this chapter the reliability analysis of flexural failures is discussed, followed by the presentation of the methodology for the analysis of corrosion failures. The implication of repair options, which apply to the analysis of both failure modes, and associated present worth cost analysis of a pipeline are discussed in the two last sections of this chapter.

5.2 Reliability analysis of flexural failures

For the reliability analysis of flexural failure of a pipeline, the distribution of the flexural resistance and the distribution of the flexural demand must be defined prior to the analysis. Figure 5.1 shows the probability density functions for the resistance and the demand plotted on a common horizontal axis. The flexural resistance, or capacity, is characterized by the distribution of the normalized section modulus S/S_o. The demand D_f, is expressed as the dimensionless ratio $M / f_t S_o$, where M is the applied bending moment, f_t is the tensile strength, and S_o is the section modulus of the undeteriorated cross-section. Failure occurs when the demand exceeds the resistance. Combinations of demand and resistance that can cause failure occur only when the two curves overlap, in the region that is shown shaded. The probability of failure is not simply the area of the shaded region, but is given by the following equation:

$$p_f = \int_{-\infty}^{\infty} F_r(r) \cdot f_D(r) dr \qquad [5.1]$$

where $F_r(r)$ is the cumulative distribution function of the resistance and $f_D(r)$ is the probability density function of the applied load effect.

The Hydroscope tool provides information that allows the resistance distribution to be defined, but provides no information whatsoever concerning the distribution of the demand. Hence it was necessary to simplify the problem for analysis as shown in Figure

5.2. The demand is treated as a deterministic quantity, that is, a quantity with no uncertainty, with magnitude D_f. The probability of failure is calculated for this case as

$$p_f = \int_{-\infty}^{D_f} f_R(r)dr = F_R(D_f) \qquad [5.2]$$

The magnitude of the demand D_f, will be determined analytically such that the predicted failure rate at the time of the Hydroscope tool inspection equals the actual failure rate based on historic records for the line.

Once the magnitude of the demand D_f is determined, the user-defined corrosion rates will be used to extrapolate the state of deterioration of pipe cross-sections, characterized by the minimum and the average wall thickness measurements, into the future. The extrapolated minimum and average wall thicknesses corresponding to some particular time in the future will allow the prediction of the future frequency of failures.

5.2.1 Calculation of probability of flexural failure

The user of the program PIPEREL.EXE must select a method for of calculation of the probability of flexural failure p_f, of some cross-section of deteriorated pipe, from the two alternative methods available. One alternative is to do an exact analysis, and the other alternative, which is much more computationally efficient, is to do an approximate analysis. In this section the bases of both methods are described in detail.

For each method, the following data regarding the pipe cross-section must be available:

- $\overline{t_{min}}$ - the measured minimum wall thickness
- $\overline{t_{avg}}$ - the measured average wall thickness
- errors of the $\overline{t_{avg}}$ and $\overline{t_{min}}$ measurements, defined in terms of standard deviations σ_a and σ_m, respectively
- D_f - flexural demand, which will be assumed known. The method for determining the demand from historic failure rate data will be presented in Section 5.2.2.2.

Using these input data, the flexural capacity of each cross-section of deteriorated pipe is defined using a Beta distribution of the normalized section modulus S/S_o.

5.2.1.1 Beta distribution

This section describes how a Beta distribution can be fit to describe the distribution of S/S_o if the average value, standard deviation, minimum and maximum value of the S/S_o distribution are known. Some examples of the goodness of fit of a Beta distribution for different sets of data of the normalized section modulus S/S_o were presented in Chapter 3. The probability density function, $f_Y(y)$, of Beta distribution for a random variable y, where $a \le y \le b$, is defined by the following equation (Benjamin and Cornell, 1970):

$$f_Y(y) = \frac{1}{B(b-a)^{r-1}}(y-a)^{r-1}(b-y)^{t-r-1} \qquad [5.3]$$

where t and r are parameters of the distribution, and B is a normalizing constant given by the equation:

$$B = \frac{\Gamma(r)\Gamma(t-r)}{\Gamma(t)} \qquad [5.4]$$

The symbol Γ represents the Gamma function, which will be defined in detailed below. The mean value of y, m_Y , is:

$$m_Y = a + \frac{r}{t}(b-a) \qquad [5.5]$$

The variance of y, σ_Y^2 , is:

$$\sigma_Y^2 = (b-a)^2 \frac{r(t-r)}{t^2(t+1)} \qquad [5.6]$$

The Gamma function, $\Gamma(x)$, is evaluated for $1 \le x < 2$ using the approximation (personal comunication F.M. Bartlett):

$$\begin{aligned}\Gamma(x) \approx\ & 1 - 0.57710166(x-1) + 0.98585399(x-1)^2 - 0.87642182(x-1)^3 \\ & +0.83282120(x-1)^4 - 0.56847290(x-1)^5 + 0.25482049(x-1)^6 \\ & -0.05149930(x-1)^7\end{aligned} \qquad [5.7]$$

If x is a positive value that lies outside of this interval, the function can be transformed to a value within this interval using the general recurrence relationship:

$$\Gamma(x+1) = x\Gamma(x) \qquad [5.8]$$

Rearranging Eqs.[5.5] and [5.6], parameters (r , t) of the Beta distribution can be expressed in terms of the mean, standard deviation, maximum and minimum value of y as:

$$t = \left(\frac{m_Y - a}{\sigma_Y}\right)\left(\frac{b - m_Y}{\sigma_Y}\right) - 1 \qquad [5.9]$$

$$r = \left(\frac{m_Y - a}{b - a}\right)\left[\left(\frac{m_Y - a}{\sigma_Y}\right)\left(\frac{b - m_Y}{\sigma_Y}\right) - 1\right] \qquad [5.10]$$

From Eqs.[5.3] to [5.10], it is clear that the Beta distribution of random variable y is completely defined if the parameters m_Y, σ_Y, a and b are known. For the pipe cross-section analysis, these parameters correspond to the mean value, standard deviation, minimum and maximum value of the S/S_o distribution, respectively, which have been determined for values of $\overline{t_{avg}}$ and $\overline{t_{min}}$ reported by the Hydroscope tool using simulation technique described in Chapter 2.

5.2.1.2 Exact calculation of probability of failure of cross-section

For this calculation, the parameters of the S/S_o distribution are directly interpolated from the tables generated by the program PIPEXSC.EXE using the methodology described in Chapter 2. The tables must be appropriate given the specific type of the pipe cross-section model and the corrosion pattern. The measurement errors for which tables were derived

should exactly match those for the analyzed pipe cross-section. The Beta distribution of S/S_o is then represented by Beta probability density function, using the fitting procedure described in the previous section. The probability of failure is calculated using Eq.[5.2], corresponding to the representation shown in Figure 5.2:

$$p_f = \int_a^{D_f} f\left(S/S_o\right) d\left(S/S_o\right) \qquad [5.11]$$

The integral in the Eq.[5.11] can be evaluated using any standard numerical methods. In the program PIPEREL.EXE the Simpson's 1/3 rule is used (Gerald and Wheatley, 1994).

5.2.1.3 Approximation of probability of failure of cross-section

The major advantage of the approximation method presented is that, while the actual measurement errors of each individual cross-section are accounted for, only the single set of tables generated for the "no measurement errors" case is required for the analysis. This simplification allows rapid computation without appreciable loss of accuracy.

For the case where there are no measurement errors in the values of minimum and average thicknesses reported by the Hydroscope tool, the tabulated parameters for the normalized section modulus reflect variability due to two sources. First, the orientation of the neutral axis of bending is unknown. Second, the variation of element thicknesses, and their ordering around the perimeter of cross-section is also unknown.

In the approximate method, measurement errors of the minimum and average wall thicknesses are assumed to be normally distributed as stated previously in Chapter 2. However, errors are not modelled as continuous distributions but instead as a number of discrete thickness values with assigned weights as shown in Figure 5.3. Thus the discretization of the error distribution requires that the centroid and weight associated with each interval of the continuous normal distribution be determined.

The first step is to divide the standard normal distribution, shown in Figure 5.3(a), into N_e equal intervals. The distribution has the mean value $m_z = 0.0$ and the standard deviation $\sigma_z = 1.0$, ant it is assumed to be defined for the range $\pm 3.4\sigma_z$, which represents over 99.9% of all possible values. The width of each interval is therefore $(2 \cdot 3.4\sigma_z / N_e =) 6.8\sigma_z / N_e$, or $6.8/N_e$.

The second step is to determine the area under the curve, w_k, and its centroid Z_k, for each interval k, where $k = 1, N_e$. The area under the standard normal probability density function, w_k, is evaluated by numerical integration from:

$$w_k = \frac{1}{\sqrt{2\pi}} \int_{z_k}^{z_{k+1}} e^{-z^2/2} dz \qquad [5.12]$$

where z_k and z_{k+1} define the boundaries of the interval k. Numerically, $z_k = -3.4 + (k-1)/N_c$. The first moment of area under the probability density function curve with respect to the line $z = 0$, S_k, is evaluated numerically as:

$$S_k = \frac{1}{\sqrt{2\pi}} \int_{z_k}^{z_{k+1}} z e^{-z^2/2} dz \qquad [5.13]$$

The value of normal variate defining the centre of gravity of the k^{th} interval with respect to the line $z = 0$, Z_k, is calculated as:

$$Z_k = \frac{S_k}{w_k} \qquad [5.14]$$

Thus the standard normal distribution is discretized as a set of Z_k values representing the centres of gravity of k intervals. This discretization can be scaled to represent the normal distributions of the average and the minimum wall thicknesses. Generally both can be approximated by the same number of discrete intervals, unless the standard deviations of the minimum and average thicknesses, σ_m and σ_a respectively, differ markedly. The distribution of the minimum wall thickness, shown in Figure 5.3(b) is defined over the interval $\pm 3.4\sigma_m$. The discrete value of the minimum thickness for the k^{th} interval, t_{mk}, is given by the equation:

$$t_{mk} = \overline{t_{min}} + Z_k \sigma_m \qquad 0 \le t_{mk} \le t_o \qquad [5.15]$$

Similarly, the distribution of the average wall thickness, shown in Figure 5.3(c), is defined over the interval $\pm 3.4\sigma_a$. The discrete value of the average thickness for the k^{th} interval, t_{ak}, is given by the equation:

$$t_{ak} = \overline{t_{avg}} + Z_k \sigma_a \qquad 0 \le t_{ak} \le t_o \qquad [5.16]$$

Figure 5.4(a) shows the discretized normal distributions of the minimum and average thicknesses for the case of N_e=7 intervals for each distribution. As suggested by the figure, a matrix can be developed that contains in each cell a unique pair (t_{aj}, t_{mi}), where $i, j \in$ (1, N_e). For the case illustrated, the matrix has 7 rows and 7 columns and in general it will have dimensions N_e by N_e. Each pair has an associated probability of occurrence p_{ij}, which is calculated as:

$$p_{ij} = \frac{C_{ij} \cdot w_i \cdot w_j}{W} \qquad [5.17]$$

In this equation, w_i and w_j are the weights calculated using Eq.[5.12] for the j^{th} discrete value of the average and i^{th} discrete value of the minimum wall thicknesses, respectively. The C_{ij} value represents the condition that the average thickness must be greater or equal to the minimum wall thickness and, as shown in Figure 5.4(b), equals 1 if $t_{aj} \ge t_{mi}$ and 0 if $t_{aj} < t_{mi}$. The weighting factor W, is calculated as:

$$W = \sum_i \sum_j C_{ij} \cdot w_i \cdot w_j \qquad [5.18]$$

and is necessary to ensure that the set of p_{ij} values satisfies

$$\sum_i \sum_j p_{ij} = 1.0 \qquad [5.19]$$

The probability of failure of the cross-section can be computed as a sum of probabilities of failure calculated for each valid pair, $p_{f_{ij}}$, weighted by the probability of occurrence of each pair p_{ij}:

$$p_f = \sum_i \sum_j \left(p_{f_{ij}} \cdot p_{ij}\right) \qquad [5.20]$$

Thus the calculations of the probability of failure, $p_{f_{ij}}$, follow the procedure outlined for the exact method. The only difference is that the parameters of the Beta distribution representing S/S_o are interpolated from the single set of tables for "no measurement errors" case.

The probability of flexural failure of a cross-section, calculated based on [5.20], depends on the number of discrete points used to approximate the normal distributions of the average and the minimum wall thicknesses. To examine the sensitivity of the probability p_f to the assumed number of points N_e, and also to assess the rate of convergence of the approximate method, the subroutine calculating the probability of failure was tested for a number different of pipe cross-sections. Figure 5.5(a) shows typical results obtained for

for one particular cross-section of 152 mm diameter pipe with t_o=10 mm, $\overline{t_{avg}}$ = 7.1 mm, $\overline{t_{min}}$ = 4.2 mm, and measurement errors equal to ±10% of t_o for both $\overline{t_{avg}}$ and $\overline{t_{min}}$. Five different levels of demand, between 0.4 and 0.8, were considered. The results indicate that the calculated probability of failure is relatively insensitive to the number of points when the demand is close to the mean resistance, and is more sensitive to the number of points when the demand is much larger or much smaller than the mean resistance. In this case the calculated probability of failure is not sensitive to the number of points for $N_e \geq 6$. Figure 5.5(b) shows the enlarged plot of the probability of failure for the demand equal to 0.5, illustrating the rate of convergence of p_f with the increasing number of points.

5.2.2 Reliability analysis of a pipeline

The Hydroscope tool provides measurements of the minimum and the average wall thicknesses at a number of cross-sections for each pipe joint. To efficiently manage these data in the program PIPEREL.EXE, each cross-section is identified by the indices (l, m), where l is the joint number, and m is the sampled cross-section (point) within the joint. Thus $\overline{t_{min}}(l,m)$ is the measured minimum wall thickness, $\overline{t_{avg}}(l,m)$ is the measured average wall thickness, and $D_f(l,m)$ is the flexural demand. The index l varies between 1 and N_J, where N_J is the number of inspected joints. Similarly, the index m varies between 1 and N_S, where N_S is the number of sampled cross-section within each joint.

The reliability analysis presented in this section will required idealization of the flexural demand prior to the analysis. The use of historic failure records will allow scaling of the idealized demand, and finally assumed corrosion rates experienced by the cross-sections of the pipeline will be used to predict frequency of future failures.

5.2.2.1 Idealization of flexural demand D_f

As noted previously the applied flexural demand is idealized in a simple manner for analysis of the pipeline reliability. In reality, the demand is random at each particular cross-section, and also varies to an unknown extent along the axis of the pipeline. As noted earlier, the demand at a given section will be modelled as a deterministic reference value that allows the actual failure rate data to be simulated. To address the spatial variability of the demand, a relative demand factor, *rd*, is introduced that represents the ratio of the real demand at any cross-section to the reference demand. Thus the real demand at any point, $D_f(l,m)$, can be estimated as the product of the reference demand, D_r, which is characteristic for a particular pipeline, and the relative demand *rd*(*l*, *m*). The relative demand has to be defined for each cross-section (*l*, *m*) of a pipeline, because the reliability analysis of the line is performed considering reliability analysis of individual cross-sections (*l*, *m*).

Figure 5.6 shows four joints of a pipeline with the relative demand defined to be constant for all critical cross-sections of any particular joint. Specifically, the relative demand is

shown assumed to 1.0 for joint l, 1.10 for joint l+1, and 1.05 for joints l+2 and l+3. To assess the variation of the relative demand along the line, the following factors should be considered:

- surface live load
- pipe depth
- soil type
- maximum tensile stress of pipe material, if unique for a particular section of the line
- joint length
- historical break records
- position of the sampled cross-section within the joint

Once the relative demand is defined, the magnitude of the reference demand may be obtained by scaling as described in the next section, such that the calculated number of failures equals the expected number of failures, ν_e, extrapolated from historic failure records.

5.2.2.2 Calculation of the reference demand by scaling

The reference demand is obtained by scaling, so that predictions of the frequency of future line failures can be made. The scaling procedure requires that the data concerning the past frequency of the pipeline failures, expressed as a number of joint failures per kilometre of line per year, is available. The reference demand is chosen such that the

expected number of failures, ν_e , equals to the number predicted using the PIPREL.EXE program, ν_c. The predicted number of failures for a line, ν_c, is determined from the probabilities of failure of the m^{th} cross-sections in the l^{th} joint, $p_f(l,m)$, obtained using the exact or approximate methods described previously. The probability of no failure at cross-section (l,m) is [1 - $p_f(l,m)$]. Assuming that failures of cross-sections within a joint are statistically independent, the probability of no failures in a joint, $P_f'(l)$, is:

$$P_f'(l) = \prod_{m=1}^{N_s} \left(1 - p_f(l,m)\right) \qquad [5.21]$$

Thus the probability of at least one failure in joint l , $P_f(l)$, is:

$$P_f(l) = 1 - P_f'(l) = 1 - \prod_{m=1}^{N_s} \left(1 - p_f(l,m)\right) \qquad [5.22]$$

Assuming that failures of joints are also statistically independent, the expected number of joint failures in a line is:

$$\nu_c = \sum_{l=1}^{N_j} P_f(l) \qquad [5.23]$$

The reference demand value that matches the predicted number of failures, as obtained using Eq.[5.23], with the expected number is determined using the bisection method in an iterative procedure requiring the following four steps:

1. Two values of the reference demand, which bound the value that represents the solution to the problem, are assumed (D_{r1}, D_{r2}). As shown in Figure 5.6, it is usually appropriate to assume that $D_{r1} = 1.0$ and $D_{r2} = 0.0$. If the relative demand values are set improperly, it is possible that the solution will lie out of this range.

2. The probabilities of failure are calculated for each cross-section and joint using Eqs.[5.11] or [5.20] and [5.22] for values of the reference demand equal to D_{r1}, D_{r2} and $D_{r3} = 0.5(D_{r1} + D_{r2})$. The predicted number of failures of the line is also calculated using Eq.[5.23], for the three reference demand values.

3. The predicted number of failures is compared with the expected number ν_e . A new range bounding the solution is selected - either the range from D_{r1} to D_{r3}, or the range from D_{r3} to D_{r2}.

4. If the range determined in Step 3 is greater than the desired accuracy of the solution, Step 2 and 3 are repeated with the new limits of the range. Otherwise the reference demand D_r is assumed to be equal to the average value of the interval.

Once the reference demand is determined, the frequency of future joint failures can be predicted by assuming that the current demand imposed at each sampled cross-section, is:

$$D_f(l,m) = rd(l,m) \cdot D_r \qquad [5.24]$$

It would be relatively easy to modify this equation to account for a change in demand over time.

5.2.2.3 Corrosion rates for analysis of the frequency of future joint failures

The previous sections have presented the method for calculation of the predicted frequency of present joint failures, which is done without any consideration of corrosion rates experienced by the pipeline. However, for estimation of the frequency of future failures, the mean and minimum wall thicknesses must be forecast for all sampled pipe cross-section using current data, and so corrosion rates for pitting and for the average section loss are essential.

The program PIPEREL.EXE assumes the following two simple models for the change of wall thicknesses of a pipe cross-section:

$$t_{avg}(T) = t_o - kT^n \qquad [5.25]$$

$$t_{min}(T) = t_o - KT^n \qquad [5.26]$$

where T is the duration of time that the pipe is buried in years, and $t_{min}(T)$ and $t_{avg}(T)$ are the minimum and average wall thicknesses, respectively, of the cross-section at time T, in mm. The corrosion rates, in mm/year, are represented by the variable K for pitting, and by the variable k for average section loss. As described in Chapter 4, n is the

exponent in the corrosion equation that depends on the type of corrosion present, which in turn depends on the degree of aeration of the soil.

Using the two models of corrosion rate, the deterioration of any pipe cross-section over the time period, characterized by the average wall thickness and the minimum wall thickness, can be readily established if only three parameters defining corrosion rates (k, K and n) are known. The exponent n associated with the degree of aeration of the soil is a random variable that is assumed to be normally distributed. The default parameters of the distribution of n assumed in the program, were based on the *National Bureau of Standards Circular 579* (Romanoff, 1957), as described in Section 4.2.3, and are shown in the Table 5.1.

Table 5.1 Default exponents n of corrosion rates

Soil aeration	Corrosion rate	Design.	Mean n	St. deviation σ_n
poor	High	H	0.68	0.10
fair	Medium	M	0.47	0.04
good	Low	L	0.35	0.03
very good	Very Low	VL	0.19	0.03

To provide some flexibility in the modeling of the corrosion rates, the program allows the user to specify H, M, L and VL corrosion rates, that are different from the default values shown in Table 5.1. The program also allows the user to specify more than one corrosion rate for each pipe cross-section, and assign a probability to each corrosion rate specified.

Once the exponent n has been assumed for a particular pipe cross-section, the remaining parameters can be determined using the data $\overline{t_{avg}}$ and $\overline{t_{min}}$ reported by the Hydroscope tool.

5.2.2.4 Calculation of the estimated frequency of future joint failures

The estimation of the frequency of future joint failures at some time T_e, where T_e is an elapsed time from the inspection of the line, requires the prediction of the future condition of the pipeline. The current condition of the pipeline is characterized by the measurements of the average and the minimum wall thicknesses at all sampled cross-sections. Extrapolation of those measurements using the assumed corrosion rates described in the previous section will allow the probabilities of failure of all cross-sections and the predicted number of failures to be calculated for time T_e.

One way of calculating the probability of failure at time T_e for a single cross-section is by simulation of the distribution of S/S_o at time T_e. In this case the procedure outlined in Chapter 2 applies, with only a very small modification necessary to include the effect of corrosion as shown schematically in Figure 5.7. The simulation is carried out using wall thicknesses t_{min} and t_{avg} that correspond to the condition at time T_e. The wall thicknesses t_{min} and t_{avg} are generated randomly from the distributions of measured wall thicknesses and the distribution of assumed corrosion rate exponent n. The random wall thicknesses,

t_{min} and t_{avg}, at the time of inspection by the tool, T_o, where T_o is also the age of a pipe at the time of inspection, are randomly generated as described in Chapter 2. The corrosion exponent n is generated randomly from the normal distribution with mean $\bar{n}$ and standard deviation σ_n. The corrosion rate parameters, K and k, are calculated using Eq.[5.25] and [5.26] as:

$$k = \frac{t_o - t_{avg}}{T_o^{\,n}} \qquad [5.25a]$$

$$K = \frac{t_o - t_{min}}{T_o^{\,n}} \qquad [5.26a]$$

Finally the wall thicknesses t'_{min} and t'_{avg} corresponding to the condition at time T_e are obtained from the following equations:

$$t'_{avg} = t_o - k(T_o + T_e)^n \qquad [5.25b]$$

$$t'_{min} = t_o - K(T_o + T_e)^n \qquad [5.26b]$$

The random wall thicknesses t'_{min} and t'_{avg} can than be used to simulate the random pipe cross-section, and a number of simulations will provided the distribution of the normalized section modulus S/S_o at time T_e. Knowing the distribution of the S/S_o the probability of failure of a single cross-section is calculated according to Eq.[5.11],

followed by the calculation of the frequency of future joint failures using Eqs.[5.22] and [5.23].

This method of calculation of the probability of failure using simulation of the S/S_o distribution at time T_e requires considerable computations. To avoid the simulation of the S/S_o distribution an alternative method was developed, which is very similar to the approximate method for calculating the probability of failure of cross-section described in Section 5.2.1.3.

Figure 5.8 shows all steps involved in the alternative method of calculation of the probability of failure of a cross-section at some time T_e after inspection by the Hydroscope tool. The cross-section is subjected to the corrosion as described by the Eqs.[5.25] and [5.26], with exponent n normally distributed with mean $\bar{n}$ and standard deviation σ_n. The distributions of t_{avg} and t_{min} are discretized as described in Section 5.2.1.3 and shown in Figure 5.3. The normal distribution of the corrosion rate exponent n is also discretized in the same manner as t_{avg} or t_{min}, using the same discretized standard normal distribution. Combinations of discrete values of t_{aj} and n_r, and t_{mi} and n_r, where i, j and $r \in (1, N_e)$, allow the definition of matrices $[k]$ and $[K]$ respectively, using Eqs.[5.25a] and [5.26a]

$$k_{jr} = \frac{t_o - t_{aj}}{T_o^{n_r}} \qquad [5.25c]$$

$$K_{ir} = \frac{t_o - t_{mi}}{T_o^{n_r}} \qquad [5.26c]$$

Once matrices $[k]$ and $[K]$ are defined, they are used to calculate the probability of failure of the cross-section at time T_e. Considering column r of the matrix $[K]$ and $[k]$, the matrix of pairs $[(t'_{mi} \, . t'_{aj})_{ij}]$ is obtained, where t'_{aj} and t'_{mi} are calculated based on [5.25b] and [5.26b] as:

$$t'_{aj} = t_o - k_{jr}(T_o + T_e)^{n_r} \qquad [5.25d]$$

$$t'_{mi} = t_o - K_{ir}(T_o + T_e)^{n_r} \qquad [5.26d]$$

Each pair has an associated probability p_{ij} defined by the Eq.[5.17]. The weight w_r corresponding to the corrosion rate exponent n_r, is assigned to the whole matrix of pairs. The probability of failure for this matrix, p_{fr}, is calculated using Eq.[5.20], following exactly the procedure presented in Section 5.2.1.3. Finally, the probability of failure of the sampled cross-section at time T_e is calculated as:

$$p_f = \sum_{r=1}^{N_r} p_{fr} w_r \qquad [5.28]$$

Once the probabilities of failure at time T_e of all sampled cross-sections are determined, the probabilities of joints failure are calculated using Eq. [5.22], and then the frequency of joint failures is obtained using Eq.[5.23].

5.3 Reliability analysis of corrosion failures

The reliability analysis for corrosion failures is based only on sampled cross-sections and is therefore similar to the reliability analysis of flexural failure of a pipeline presented in the previous section. It is assumed that the set of available data is similar to that for the flexural failure. However, because corrosion failures depend only on the minimum wall thickness at a cross-section, the fundamental analysis method for failure of the cross-section must be modified. The relative demand and the average wall thickness measurement at each sampled cross-section are irrelevant for the corrosion failure analysis.

Subsequent sections outline two methods of calculation of the probability of corrosion failure of a pipe cross-section, followed by the reliability analysis of a pipeline which involves an optional scaling of measurement error of $\overline{t_{min}}$. The method of calculating of the frequency of future corrosion failures, which accounts for assumed corrosion rates, is also presented.

5.3.1 The probability of corrosion failure of a cross-section of deteriorated pipe

The reliability analysis of corrosion failure at some particular pipe cross-section requires the distribution of the minimum wall thickness and the specification of a failure criterion. Generally, a minimum wall thickness equal to zero represents failure. Figure 5.9 shows the distribution of minimum wall thickness for an example cross-section and the thickness of the wall t_f representing failure. The shaded area represents the probability

of corrosion failure p_f in this case. It may seem intuitive that $t_f = 0$ defines the failure criterion. However, for water pipelines, even complete perforation of the pipe wall does not necessarily constitute a failure of a pipe because the by-products of corrosion can effectively plug the hole. Thus the minimum hole area which defines failure will be much larger for gray cast iron than for ductile cast iron due to the formation of the graphite plaque which prevents leakage.

Figure 5.10 shows a cross-section of a pipe wall at some point along the length of a pipeline, with three spherical pits having radii r_{p1}, r_{p2} and r_{p3}. The minimum areas of the perforations caused by these pits, A_{h1}, A_{h2} and A_{h3} are also shown in the figure. The pit with radius r_{p1} equal to the thickness of the wall t_o has $A_{h1} = 0$. The radii of the other pits exceed the wall thickness, and so the areas of the perforations A_{h2} and A_{h3} are greater than zero and can be defined by the radius of the perforation r_{h2} and r_{h3}. The three areas A_{h1}, A_{h2} and A_{h3} represent three potential corrosion failure criteria. Considering these three cases, it can be concluded that the probability of failure p_f is proportional to the minimum area of the perforation. The minimum area of the perforation is:

$$A_h = \pi \cdot r_h^2 \qquad [5.32]$$

where r_h is the minimum radius of the perforation. The associated depth, or radius of the pit, r_p is:

$$r_p = \sqrt{r_h^2 + t_o^2} \qquad [5.33]$$

where t_o is the nominal wall thickness of the pipe. Thus the critical wall thickness. t_f . is

$$t_f = t_o - r_p \qquad [5.34]$$

which using Eqs.[5.32] and [5.33] can be expressed as:

$$t_f = t_o - \sqrt{\frac{A_h}{\pi} + t_o^2} \qquad [5.35]$$

Thus to achieve complete perforation of the pipe wall with some minimum perforation area greater than zero, the critical wall thickness t_f must be less than zero.

There are two methods used in the program PIPEREL.EXE for the calculation of the probability of failure of a sampled cross-section. This is the reason why discretized thicknesses t_{mi} of the t_{min} distribution in both methods of calculation of p_f are not restricted to positive values only.

5.3.1.1 Exact calculation of probability of failure of cross-section

The exact method assumes that the minimum thickness of a pipe cross-section is normally distributed with the mean reported by the Hydroscope tool, $\overline{t_{min}}$, and the standard deviation, σ_m , dependent on the measurement error. Transforming the distribution of the minimum thickness to the standard normal distribution, the standard normal variate z_f corresponding to the critical wall thickness t_f is:

$$z_f = \frac{t_f - \overline{t_{min}}}{\sigma_m} \qquad [5.29]$$

For simplicity, the standard normal distribution is truncated at ±3.4 standard deviations from the mean. Thus for $z_f \leq -3.4$, $p_f = 0.0$, and for $z_f \geq 3.4$, $p_f = 1.0$. The exact values corresponding to these limits are 0.00034 and 0.99966 respectively. For $-3.4 < z_f < 3.4$ the probability of failure is:

$$p_f = \frac{1}{\sqrt{2\pi}} \int_{-3.4}^{z_f} e^{-z^2/2} dz \qquad [5.30]$$

where the integral is evaluated numerically using Simpson's 1/3 rule.

5.3.1.2 Approximation of probability of failure of cross-section

The exact method of calculation of the probability of corrosion failure for a particular pipe cross-section requires a normal distribution of t_{min}. This condition is satisfied if the reliability analysis is conducted for the time frame shortly after the inspection of the pipeline. However, the normal distribution of t_{min} extrapolated into the future will no longer be normal due to corrosion. To address this problem an approximate method was derived.

The approximate method discretizes normal distribution of the minimum wall thickness for the calculation of the probability of failure. The continuous distribution of the

minimum wall thickness is represented by N_e discrete thicknesses t_{mi}, with associated weights w_i, using the procedure that is similar to the one already described in Section 5.2.1.3. However, in this case, t_{mi} is not restricted to positive values only.

Figure 5.11 shows the discretized distribution of the minimum wall thickness for a typical pipe cross-section. In this case, the probability of failure, p_f, is taken to be 0 if $t_f \leq t_{m1}$, and is taken to be 1.0 if $t_f \geq t_{mN_e}$. For the range $t_{m1} < t_f < t_{mN_e}$, the probability of failure is:

$$p_f = \sum_i w_i \qquad [5.31]$$

where the summation applies only to those weights w_i for which $t_{mi} \leq t_f$. The value obtained using this method is equivalent to the shaded area shown in Figure 5.11. The accuracy of the approximate calculation increases as the number of intervals, N_e, is increased.

5.3.2 Reliability analysis of a pipeline

The reliability analysis of a pipeline is based on the set of $\overline{t_{min}}$ measurements collected for various critical sections of each joint by the Hydroscope tool during the inspection of the line. The standard deviation σ_m which reflects the magnitude of the measurement error, is assumed to be a known constant for all cross-sections. The other information necessary for the analysis is the critical failure thickness, t_f, which defines the corrosion

failure, and is used in both methods for calculating the probability of failure described in the previous section.

5.3.2.1 Scaling of the standard deviation of t_{min}

The probability of corrosion failure p_f of a cross-section depends on the error of the minimum wall thickness measurement, σ_m. Figure 5.12. shows a cross-section of a pipe wall with a spherical pit causing a round perforation. The minimum wall thickness for this section reported by the Hydroscope tool, $\overline{t_{min}}$, and its the standard deviation, σ_m, are shown, and the hole area which defines the corrosion failure is assumed equal to A_h. Three other distributions of the minimum wall thickness are also shown, with the same mean value and with standard deviations $\sigma'_m = 0.75\sigma_m$, $\sigma''_m = 1.25\sigma_m$, and $\sigma'''_m = 1.5\sigma_m$. The associated probabilities of failure, p'_f, p''_f and p'''_f, differ significantly from p_f. Thus the measurement error is not only tool dependent but may also be affected by the quality of the inspection performed.

To rectify the measurement error to account for the quality of inspection, the program PIPEREL.EXE includes, as an optional feature, scaling of the standard deviation σ_m if data concerning the historic frequency of corrosion failures, are available. The standard deviation is scaled such that the expected frequency of corrosion failures, ν_e, equals the calculated frequency of failures ν_c. The calculation procedure is similar to that adopted for scaling the reference demand described in Section 5.2.2.2. The program determines

two scaling factors f_1 and $f_2 = f_1 + 1$ which have calculated failure frequencies that bound the expected failure frequency. A bisection method is used to narrow the range of f_1 and f_2. The program displays the value of f ($f_1 < f < f_2$) obtained for the user to accept or reject.

5.3.2.2 Calculation of the frequency of future corrosion failure

Similarly to the flexural failure analysis, the calculation of the estimated frequency of joint corrosion failures at some time T_e in the future, where T_e is an elapsed time from the time of the inspection of the line, T_o, is based on the extrapolation of the discretized distribution of the minimum wall thickness of all cross-sections. For each cross-section the discretized distributions of t_{min} and the corrosion rate exponent n, t_{mi} and n_r, yield the matrices [K] and [p'] as shown in the Figure 5.8. Elements of the matrix [K] are obtained using Eq.[5.26a]. At any particular time T_e in the future, a matrix of minimum wall thicknesses is created. Each element is calculated using Eq.[5.26d] as:

$$t'_{mir} = t_o - K_{ir}\left(T_o + T_e\right)^{n_r}$$

The probability of failure of a sampled cross-section is then:

$$p_f = \sum_i \sum_r p'_{ir} \qquad [5.36]$$

where the summation is carried out for $t'_{mir} \le t_f$.

Once the probability of failure of each cross-section at time T_e is determined, the estimated frequency of future joint failures, ν_c, is calculated using Eqs.[5.22] and [5.23].

5.4 Pipeline repair options

The method of calculation of the frequency of future flexural and corrosion joint failures for a particular pipeline, outlined in Sections 5.2.2.4 and 5.3.3.2, does not account for possible repair of the line. This approach will lead to an overestimated frequency of future joint failures because it ignores possible failures prior to the time frame in consideration. To address this problem an optional feature allowing repairs of a pipeline has been introduced into the program.

Figure 5.13 shows the predicted frequencies of flexural failure, ν_c, versus time for an example pipeline. The frequencies of future failures are calculated at constant time increments ΔT, starting from the observed frequency of failures at the time of the inspection of the line, T_o ($T_e = 0$). The estimated frequency of failures increases with time reflecting the progressive deterioration of the line due to corrosion. Sometimes the number of failures per kilometre of line per year is used by Municipal Engineers as a decision making parameter. When the observed frequency of failures reaches the critical value the whole line is qualified for replacement. Defining this critical frequency of failures as ν_{crit}, the "remaining service life" can be estimated from the plot using the point where the predicted frequency of failures exactly equals this critical value.

The area under the ν_c curve represents the actual number of joint failures, N_{JF}, that occur in an interval of time. For a single time interval ΔT starting at time T_i the number of failures can be calculated approximately as:

$$N_{JF} = \frac{\nu_c(T_{i+1}) + \nu_c(T_i)}{2}\Delta T \qquad \text{where } T_{i+1} = T_i + \Delta T \qquad [5.37]$$

If the number of failures N_{JF} exceeds 1.0, some joint of the line has failed, at least theoretically. In real situation, remedies have to be applied if a pipeline fails to return the line to service. The common responses are either to replace any joint that fails, or to install clamps on any cross-section that has failed. These two repair scenarios are included in the program as an option to allow more realistic analysis of the frequency of future failures.

The program PIPEREL.EXE allows the user to choose either of two modes for the execution of the joints replacement or the installation of clamps. The manual mode allows joints replacement, installation of clamps, or both. It is not restricted by the predicted number of failures, which means that some sort of upgrading of a pipeline can also be considered. The automated mode allows either joint replacement or clamp installation. In either case, the total number of repairs is equal to N_{JF}. If the joint replacement option is selected, N_{JF} pipe joints with the highest probabilities of failure are automatically replaced. If the clamp installation option is selected, N_{JF} cross-sections with the highest probabilities of failure are automatically clamped. In the case of joint

replacement, the new joint is assumed to be uncorroded initially and subjected to the same corrosion rates as those established for the old joint. If a clamp is installed, the probability of failure of the repaired section is set permanently to 0. In either case, no change of assumed corrosion rates or the condition of joints adjacent to the one repaired is considered.

Figure 5.14 shows predicted frequencies of future failures for the pipeline considered in Figure 5.13, but considering repair options in this case. The automated mode was used to replace joints at the end of each time interval ΔT, which the cumulative number of failures N_{JF}, calculated for the elapsed time from the last repairs applied to the pipeline, was greater than 1.0. Thus sudden drops of the estimated failure frequency shown in the figure at the end of some time intervals are the result of the repair activity. Figure 5.14 also shows that if repairs are considered in analysis of the pipeline the estimated "remaining service life" will be considerably greater than if no repairs are considered.

5.5 Cost analysis option

For the analysis of a pipeline considering various repair options, the user can specify that the program performs a present worth cost (PWC). The data required for the simplified cost analysis are the present cost of joint replacement or clamping, c_J or c_{CL} respectively, the present cost of the replacement of the whole line, c_L, and the interest rate, IR, which is applied on the time interval, ΔT, basis. The cost of repairs and the cost

of replacement are assumed to be constant over time. Neither inflation nor the cost associated with the failure of the pipeline are considered.

For each time interval, the user can specify that the program determine: the present worth cost of the line replacement, PW(LRC); the present worth cost of repairs, PW(MC); and, the total present worth cost, PW(LRC+MC). The present worth cost calculation is done using standard present worth cost formulae (e.g., Dergamo *et al*, 1993). For the elapsed time $T_i = i \cdot \Delta T$ shown in Figure 5.14, where $i = 0,1...N_{\Delta T}$ and $N_{\Delta T}$ is the number of time intervals considered in analysis, the present worth cost of the line replacement is calculated as:

$$\mathrm{PW(LRC)}_i = c_L \cdot \frac{1}{(1+IR)^i} \qquad [5.38]$$

Similarly, the present worth cost of repairs is calculated as:

$$\mathrm{PW(MC)}_i = \mathrm{PW(MC)}_{i-1} + \left(c_J \cdot N_{JF} + c_{CL} \cdot N_{SF}\right) \cdot \frac{1}{(1+IR)^i} \qquad [5.39]$$

where N_{SF} and N_{JF} are the number of replaced joints and the number of installed clamps, respectively, which were calculated for time T_i, and $\mathrm{PW(MC)}_{i-1}$ is the present worth cost of repairs calculated at the end of the previous time interval. The total present worth cost is calculated using Eqs.[5.38] and [5.39] as:

$$\mathrm{PW(LRC+MC)}_i = \mathrm{PW(LRC)}_i + \mathrm{PW(MC)}_i \qquad [5.40]$$

The present worth total cost for various maintenance strategies can be also used as a decision-making parameter which can be minimized to determine the optimal remaining service life of a pipeline.

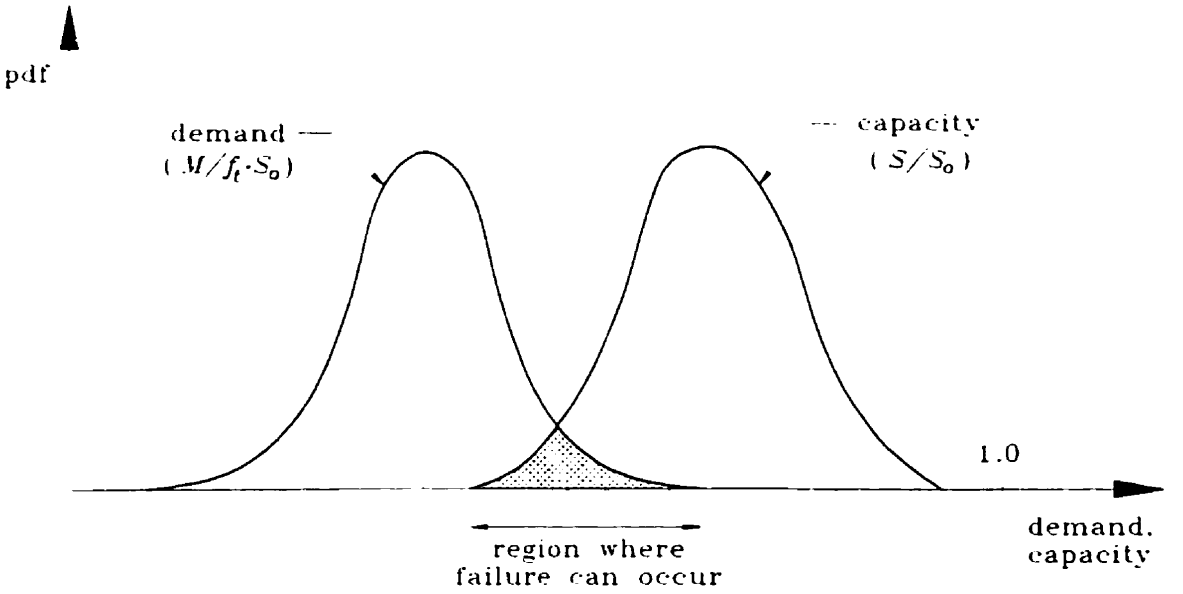

Figure 5.1 General reliability problem of a sampled cross-section subjected to the bending moment

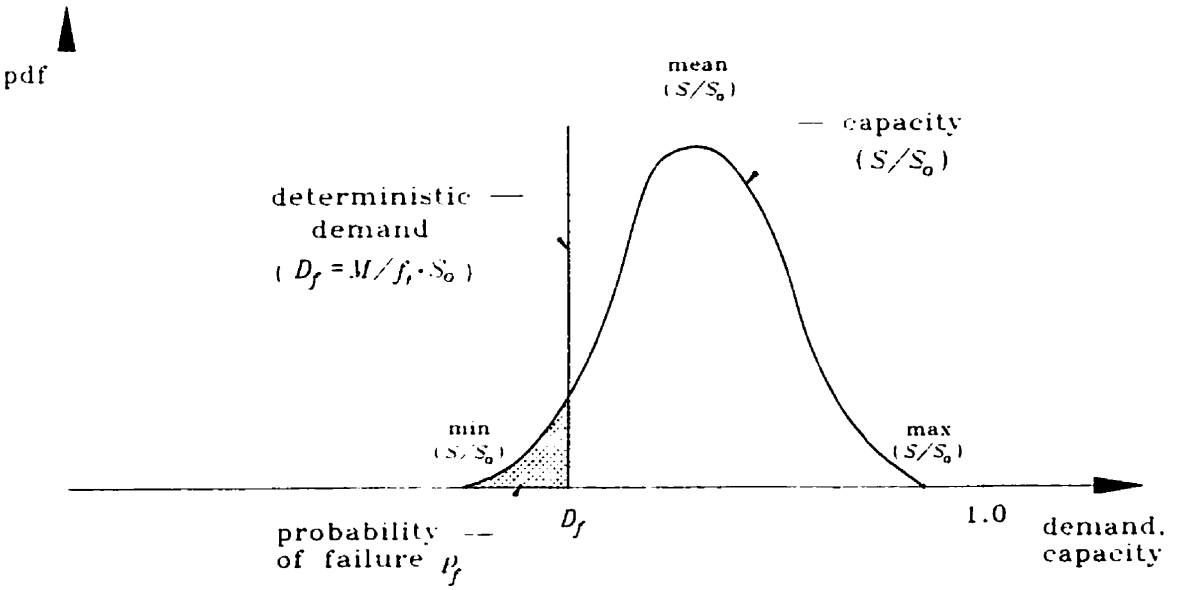

Figure 5.2 Simplified reliability problem of a sampled cross-section subjected to the bending moment

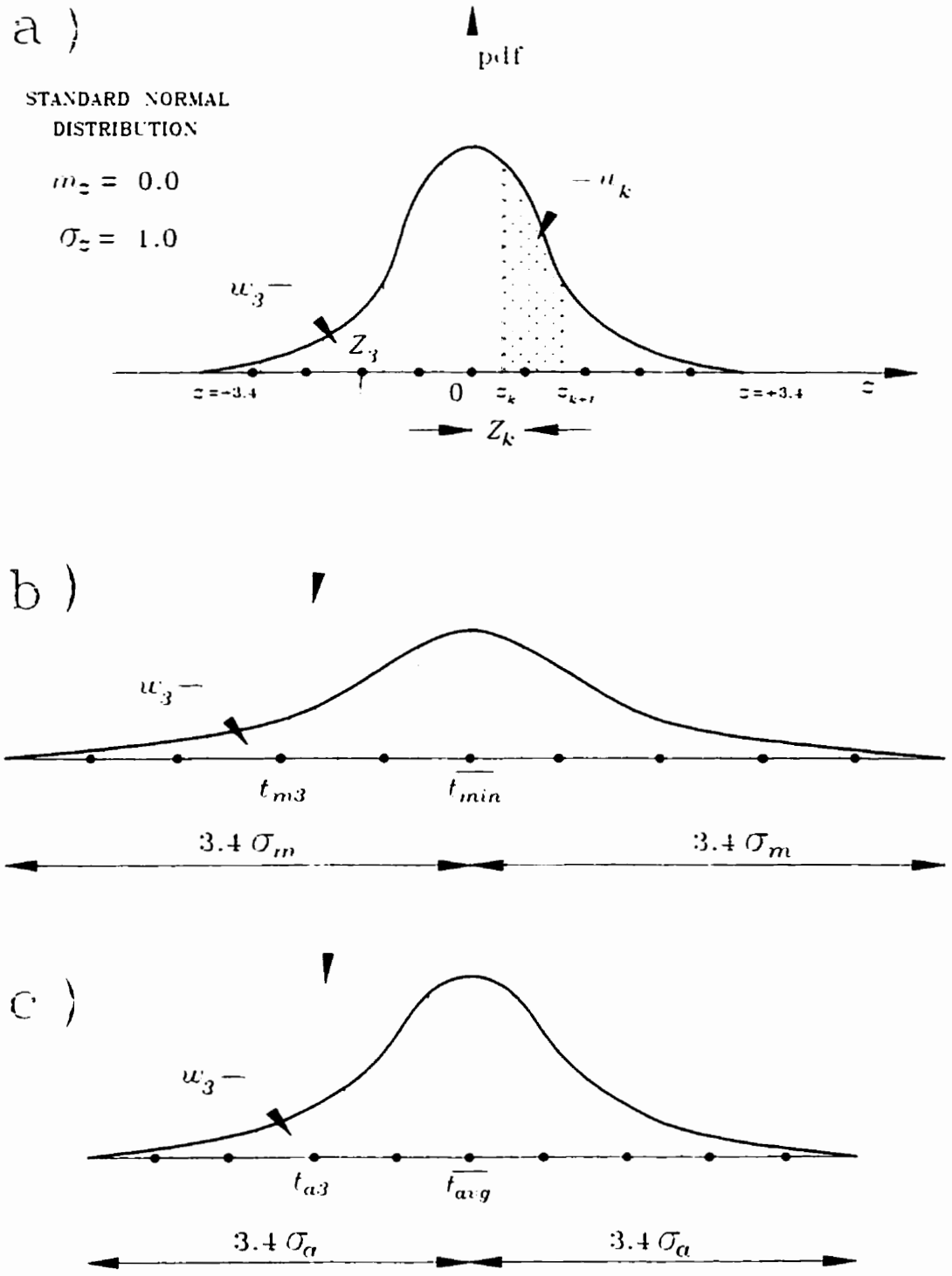

Figure 5.3 Discretization of the minimum and the average thickness distributions, based on the standard normal distribution

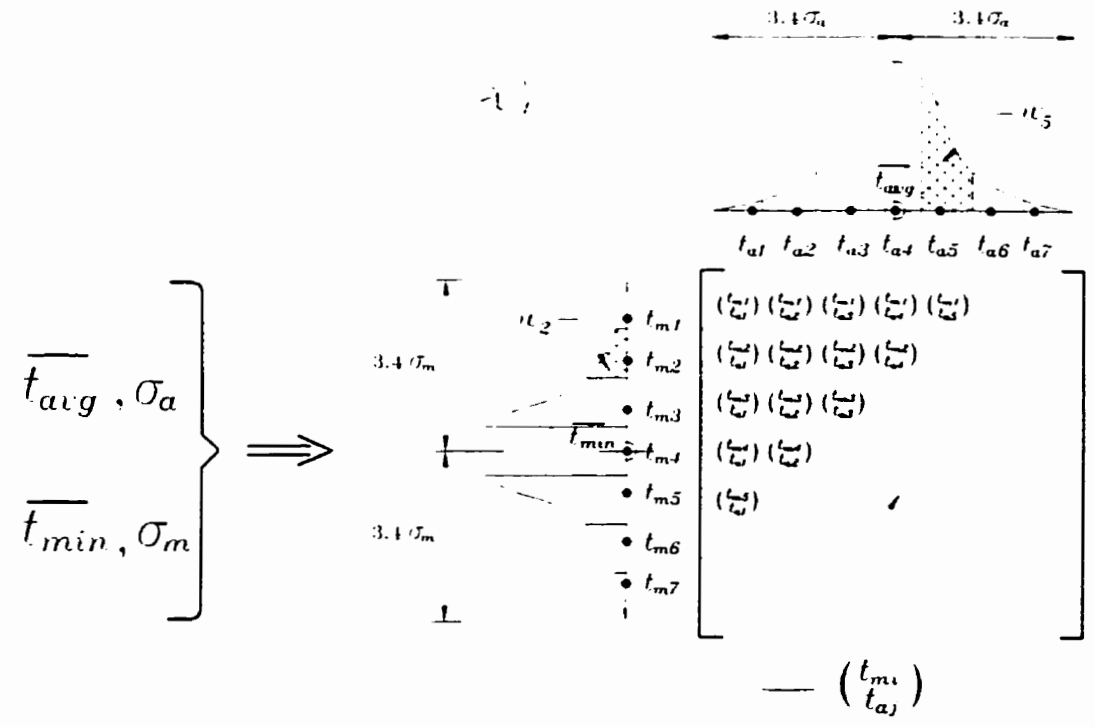

b)

	t_{a1}	t_{a2}	t_{a3}	t_{a4}	t_{a5}	t_{a6}	t_{a7}
t_{m1}	1	1	1	1	1	1	
t_{m2}	1	1	1	1	1		
t_{m3}	1	1	1	1			
t_{m4}	1	1	1				
t_{m5}	1	1					0
t_{m6}	1					0	0
t_{m7}					0	0	0

$\rightarrow C_{ij}$

1 if $t_{aj} \geq t_{mi}$

0 otherwise

c)

	t_{a1}	t_{a2}	t_{a3}	t_{a4}	t_{a5}	t_{a6}	t_{a7}
t_{m1}	p_{11}	p_{12}	p_{13}	p_{14}	p_{15}		
t_{m2}	p_{21}	p_{22}	p_{23}	p_{24}			
t_{m3}	p_{31}	p_{32}	p_{33}				
t_{m4}	p_{41}	p_{42}					
t_{m5}	p_{51}						
t_{m6}							
t_{m7}							

$\rightarrow p_{ij} = C_{ij} \cdot w_i \cdot w_j / W$

$\sum_i \sum_j p_{ij} = 1.0$

Figure 5.4 Approximate method of calculation of the probability of failure for a sampled cross-section

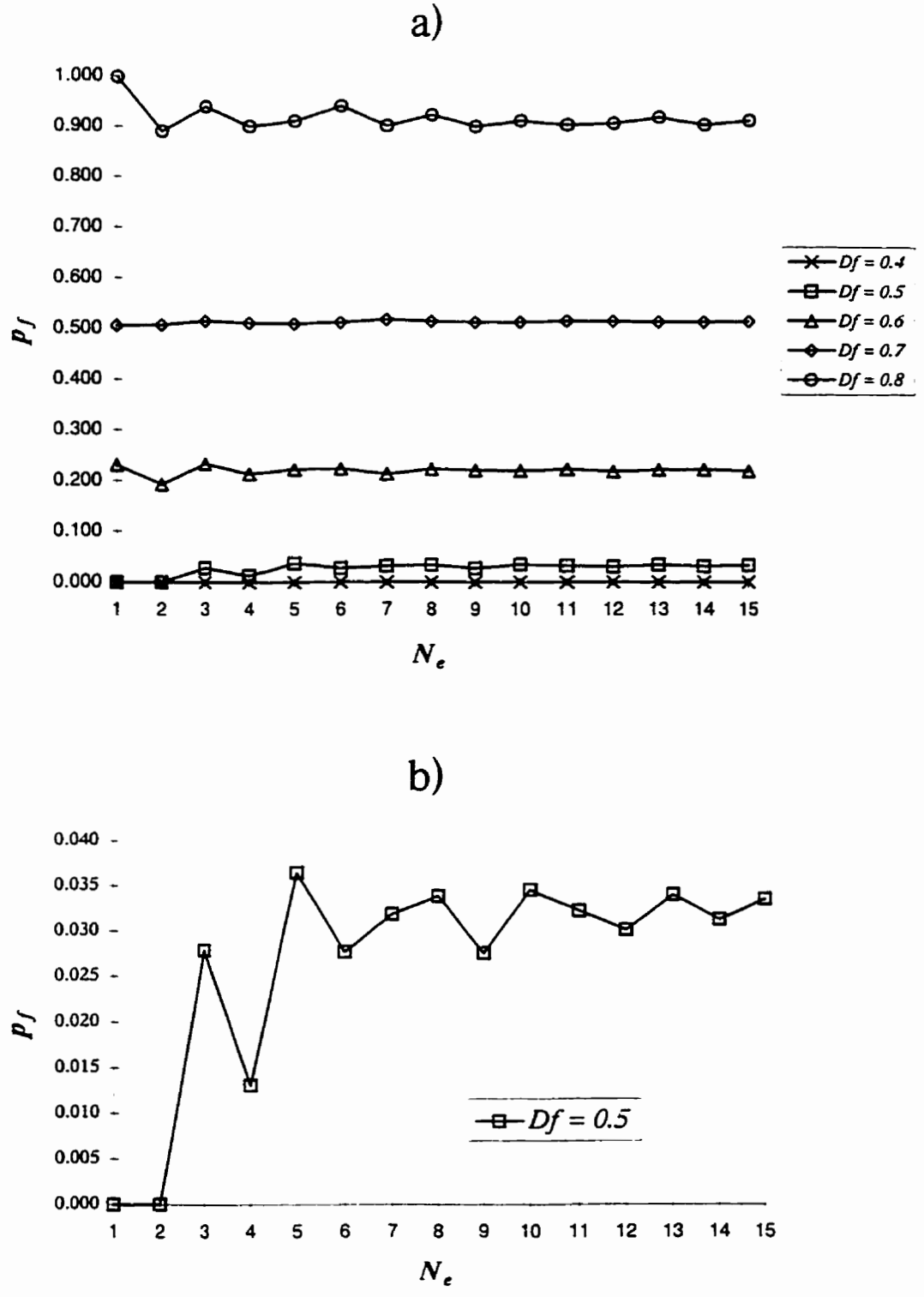

Figure 5.5 Results of calculation of the probability of flexular failure using approximate method

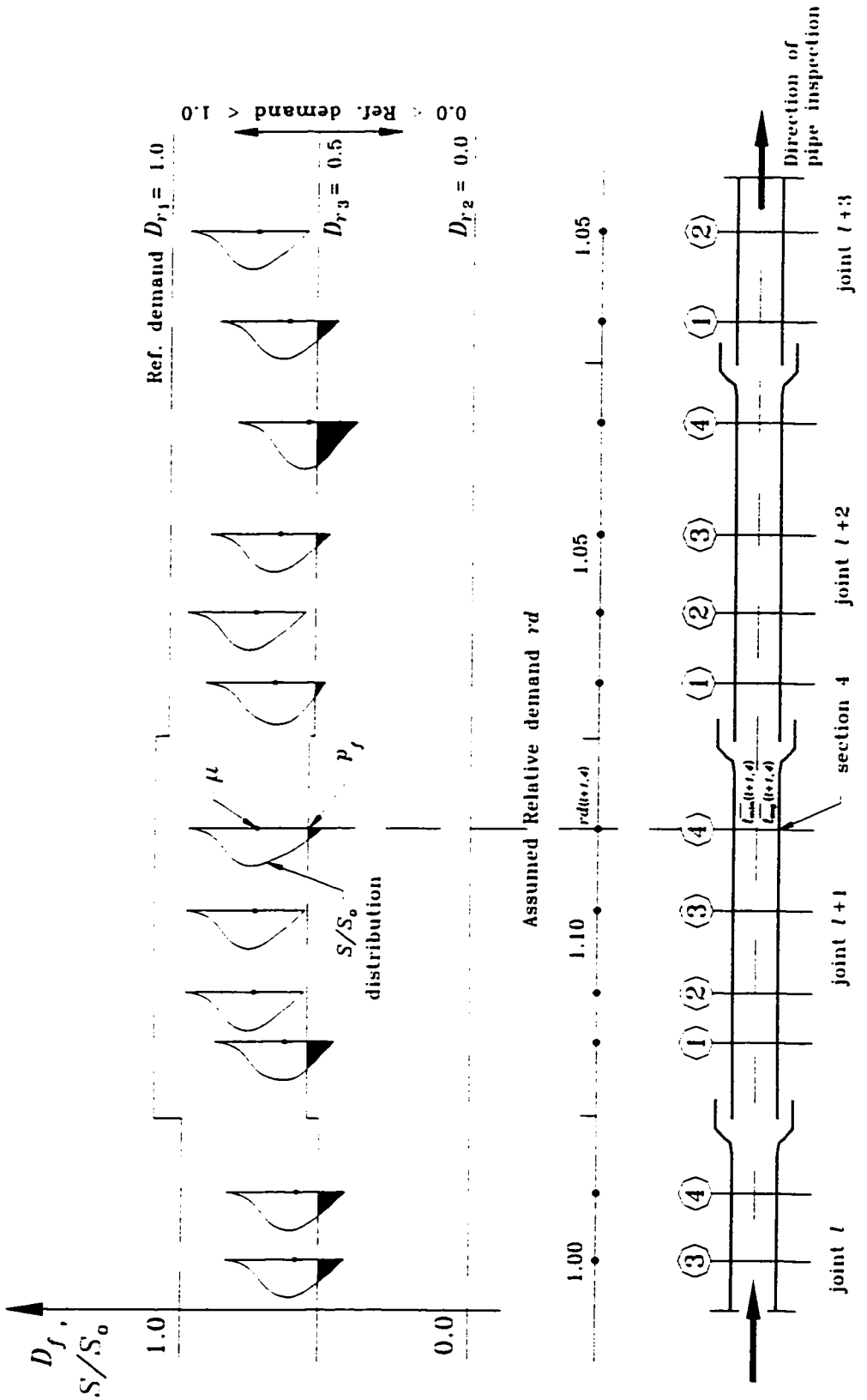

Figure 5.6 Scaling of the reference demand

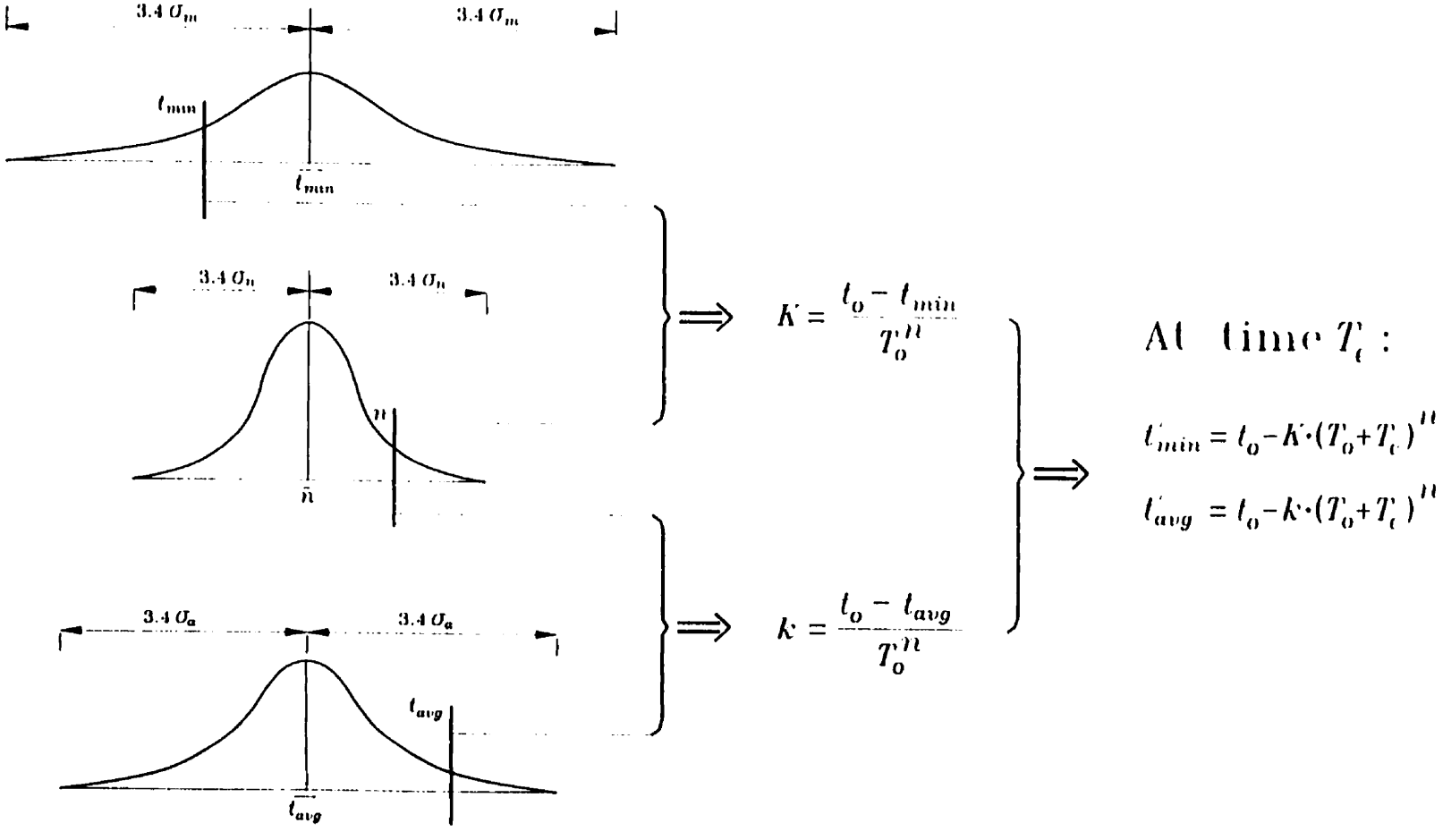

Figure 5.7 Simulation of random wall thicknesses at time T_e

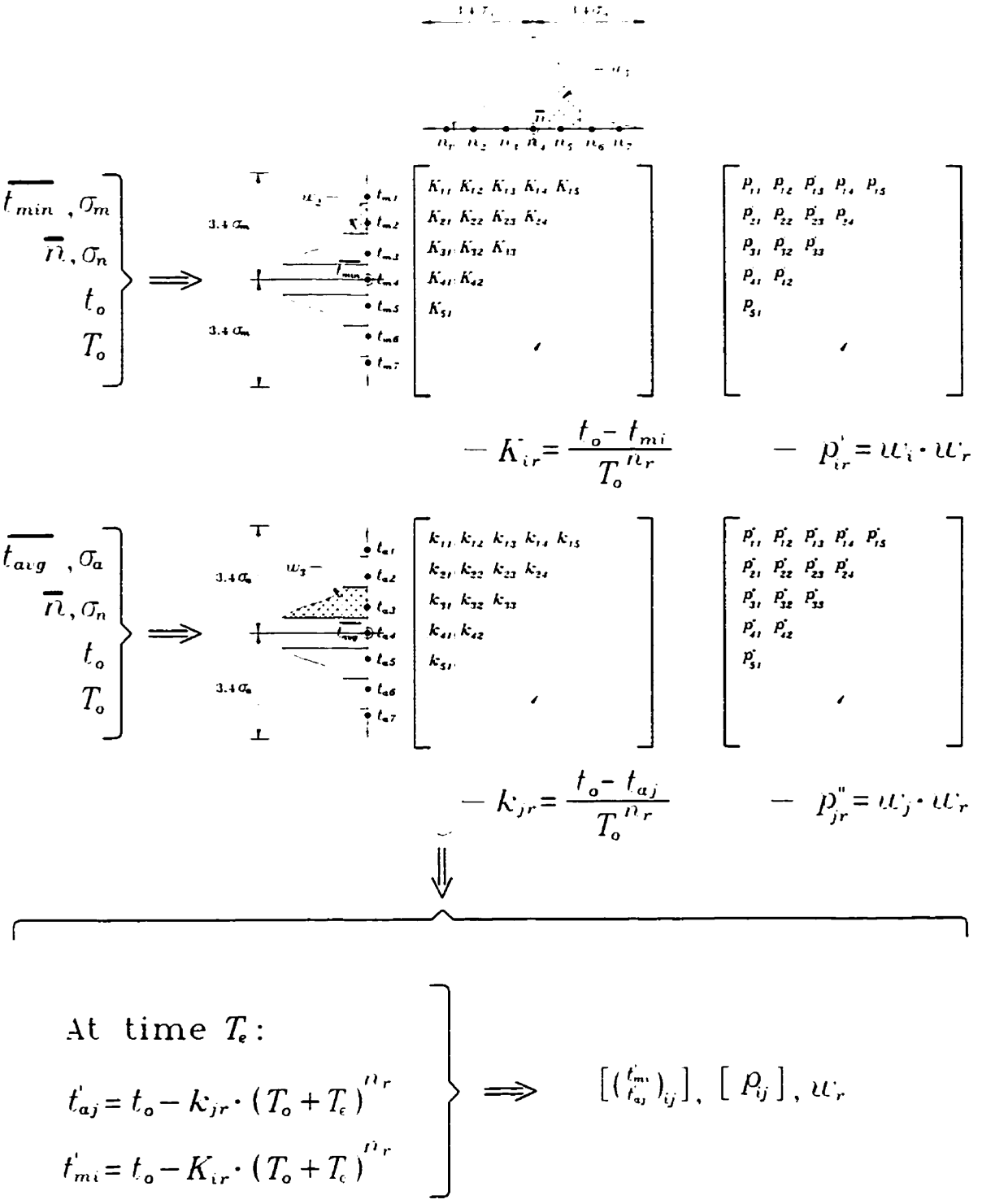

Figure 5.8 Calculation of the probability of failure for a sampled cross-section at time T_e

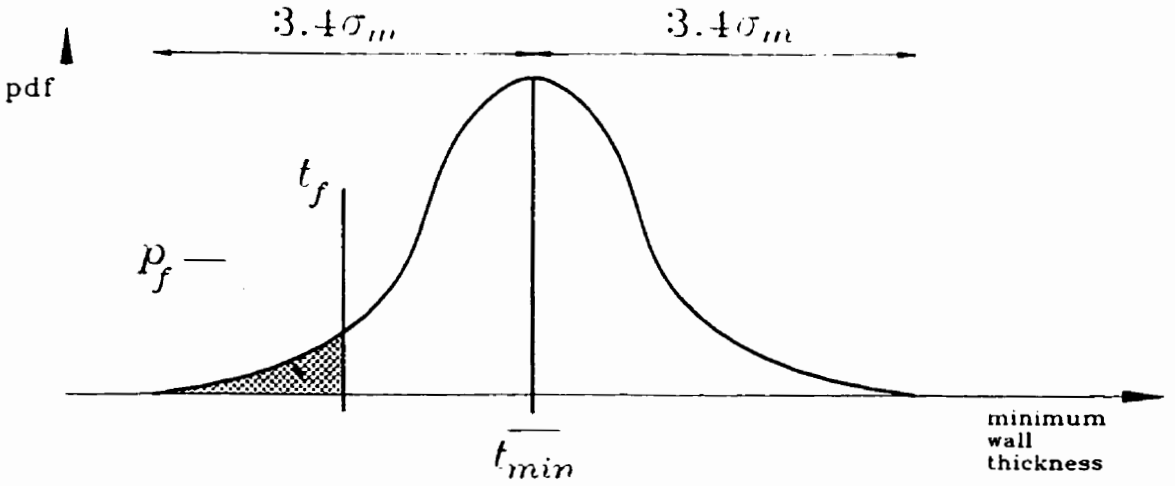

Figure 5.9 Exact calculation of the probability of corrosion failure of a sampled cross-section

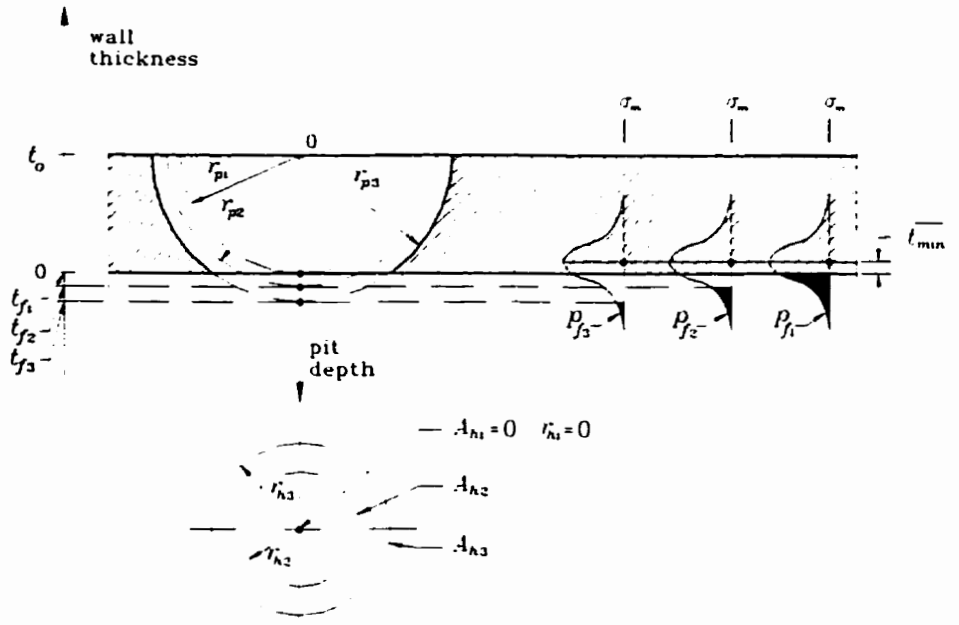

Figure 5.10 Variation of the calculated probability of corrosion failure due to the minimum thickness of the pipe wall considered as failure

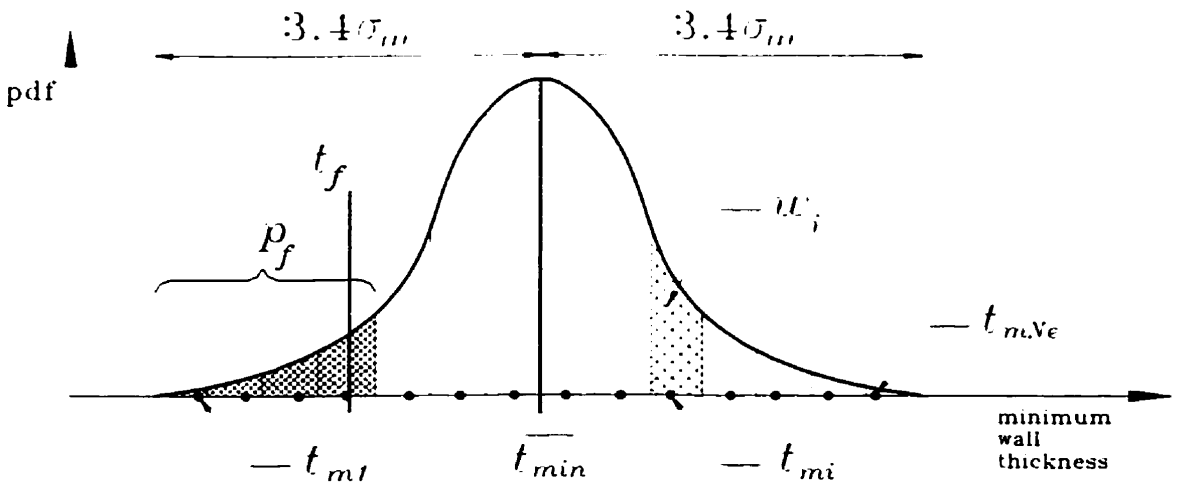

Figure 5.11 Approximate calculation of the probability of corrosion failure of a sampled cross-section

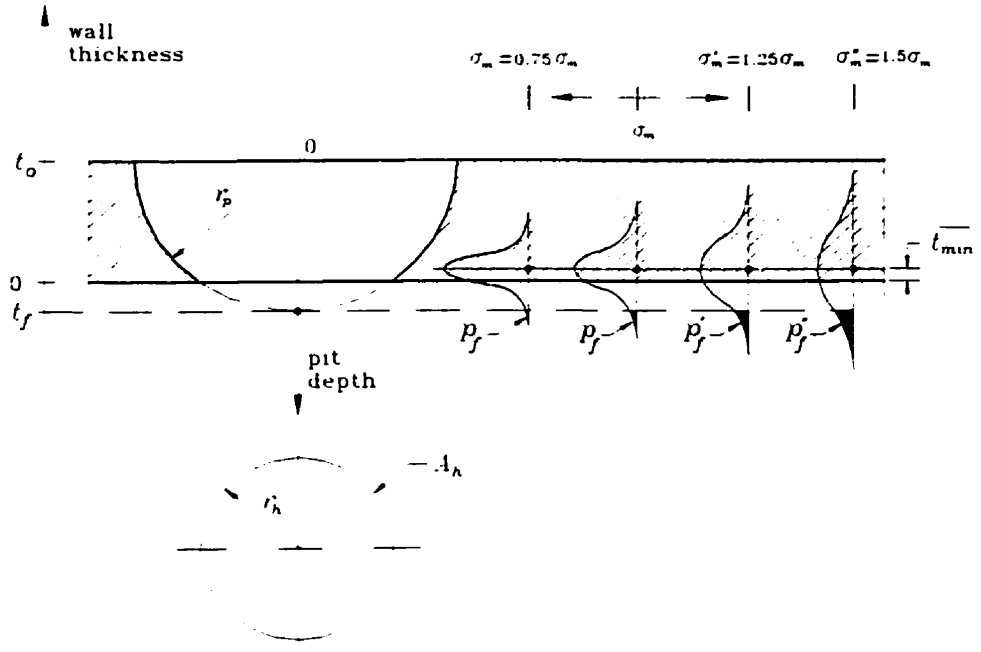

Figure 5.12 Variation of the calculated probability of corrosion failure due to the standard deviation of the minimum thickness distribution

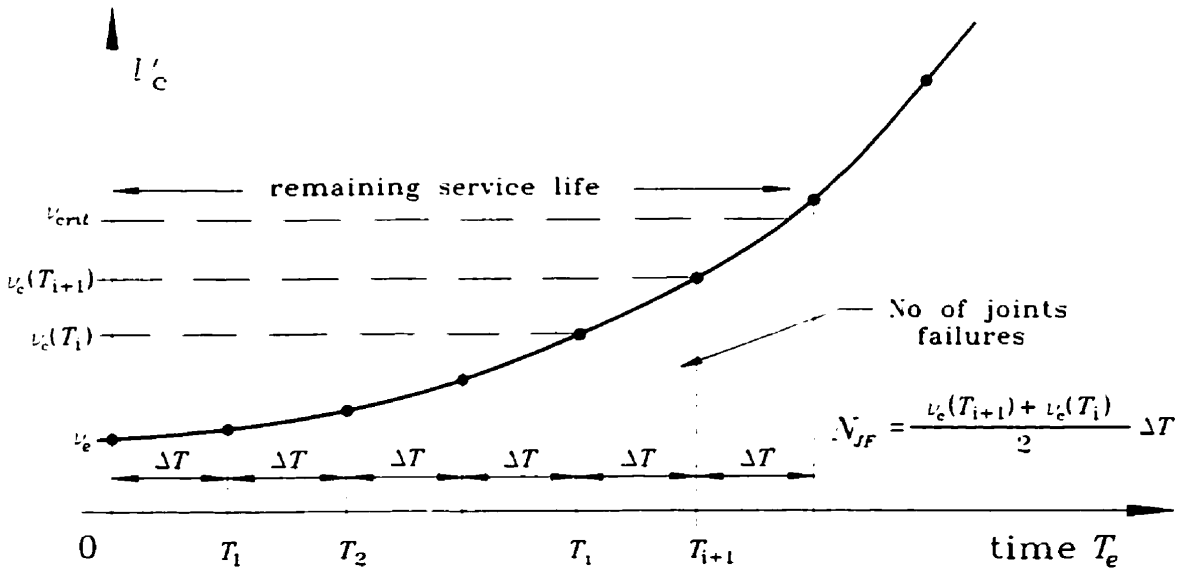

Figure 5.13 Predicted frequencies of joint failures without considering repairs

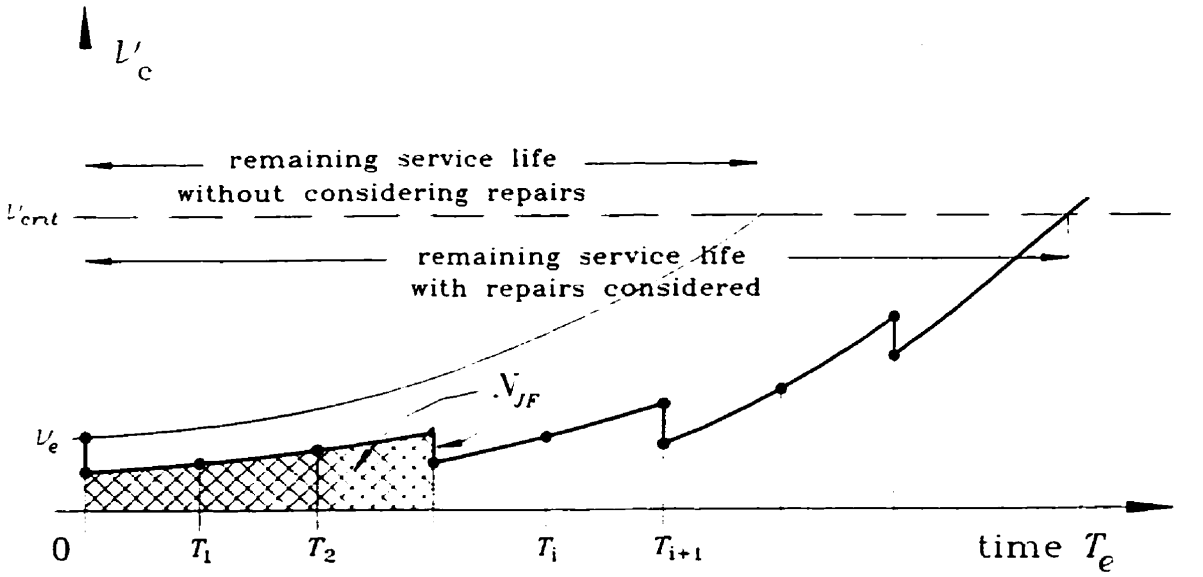

Figure 5.14 Predicted frequencies of joint failure with repairs considered in calculations

Chapter 6 Results of reliability analysis of a pipeline

6.1. Introduction

Chapter 6 presents the analytical results from the program PIPEREL.EXE for a typical deteriorated pipeline. A file containing simulated field measurements collected by the Hydroscope tool during the line inspection is the basis for all analyses. The two predominant failure modes are investigated by the program, and the effects of the adopted calculation procedures, the measurement errors associated with the data from the field inspection, and other parameters affecting the real pipeline performance such as the corrosion rates or the maintenance strategy are investigated. The pipeline performance is characterized by the "remaining service life", discussed in Section 5.4, which is the elapsed time from the line inspection when the pipeline reaches the critical failure rate and it is qualified for replacement.

Although the program allows analysis of both flexural and the corrosion failure modes simultaneously, the results presented in this chapter consider the flexural and the corrosion failure modes separately. Decoupling the two failure modes allows qualitative assessment of whether the effect of a given parameter on the remaining service life of a pipeline is failure mode sensitive. The first part of Chapter 6 presents the results of parametric studies that consider only flexural failures of a cast iron pipeline, while the

second part presents the results of studies that consider only corrosion failures of a ductile cast iron pipeline.

6.2. Analysis of flexural failures of a cast iron pipeline

As shown in Chapter 1, over 60% of cast iron pipelines failures in Canada, on average, are attributed to flexure. In this section, analysis results from the program PIPEREL.EXE are presented for a simulated cast iron pipeline considering flexural failures only. The analysis considers either the "no repairs" option or the repair by joint replacement option, as described in Section 5.4. The results for the "no repairs" case will be used in the next section as the basis for a qualitative assessment of the effect of various parameters on the predicted flexural failure frequency and the remaining service life of the pipeline. These quantities were discussed in Sections 5.2.2.4 and 5.4.

6.2.1 Data for analyses of flexural failures

In this example, a 60 year old cast iron pipeline consisting of 50 pipe joints, numbered from 1 to 50, was analyzed. Each pipe joint was assumed to have an outside diameter, D, equal to 152 mm (6"), a nominal wall thickness, t_0, equal to 10 mm, and a length varying between 5.3 m and 5.4 m. In this section, the input data are summarized. A detailed discussion of the type and the format of data files and the user-specified input options required by the program PIPEREL.EXE to conduct the reliability analysis is presented in Appendix B.

The Hydroscope tool was assumed to provide measurements of the minimum and the average wall thickness at four cross-sections within each joint. Measurement errors of both the average and the minimum wall thicknesses were assumed equal to $\pm 10\%$ of t_o. The *Type 2a* model of the pipe cross-section was chosen for the analysis because it is consistent with two wall thickness measurements at each cross-section. A *Type 2ac* model, which has the elements ordered from least to largest thickness across the depth of the cross-section as described in Chapter 3, was used.

The relative demand, discussed in Section 5.2.2.1, was assumed constant within each joint, and the reference demand was assumed constant over the time period investigated.

The probabilities, or weighting factors, for the four possible corrosion rates, discussed in Section 5.2.2.3, were also assumed constant for each joint. The default values of the corrosion rates, presented in Table 5.1, were used for analysis.

The reference demand was scaled using the method described in Section 5.2.2.2 for an assumed failure frequency of 2 joint failures per kilometre of line per year. The critical frequency of joint failures, ν_{crit} , qualifying the whole line for replacement, was assumed to be 5.0 joint failures per kilometre of line per year. Prior to the analysis, the observed and critical failure frequencies are scaled based on the actual length of the line, as obtained by the summation of the lengths of all pipe joints.

The input data used for the reliability analysis of the cast iron pipeline is presented in Figure 6.1. The data which are not shown on the figure are: the number of points, N_c, for the approximation of distributions of t_{min}, t_{avg}, and n, which was equal to 7; and, the number of integration panels for the various numerical integrations, which was equal to 100.

6.2.2 Results of reliability analyses of flexural failures

The reliability analysis of the pipeline was conducted for the time period of 15 years, with the calculations of the frequencies of future joint failures performed for 1 year time intervals. The detailed results for each time interval, which include calculated probabilities of failures of each cross-section and each joint, increase the size of the output file substantially and so are not presented in this chapter. Instead, the results are presented as plots of the predicted failure frequencies versus elapsed time from the inspection of the pipeline.

Scaling of the reference demand, D_r, was performed according to the method described in Section 5.2.2.2, using approximate method described in Section 5.2.1.3. The scaled reference demand equalled 0.219, which corresponds to a predicted frequency of failures 1.986 per kilometre of line per year, and closely matches the input value of 2.0 joint failures per kilometer of line per year.

Figure 6.2 shows plots of the predicted failure frequencies obtained for the two cases considered in the analysis. The first case, denoted as "No-action", represents analysis of the pipeline without repairs being considered. The second case, denoted as "Repair", represents the analysis which accounts for the specified repair option. The critical joint failure frequency for this particular length of pipeline is shown as a horizontal line denoted as "Failure". Based on the "No-action" and the "Failure" graphs, the estimated remaining service life of the pipeline for the "No-action" case, or the time at which the "No-action" and "Failure" lines intersect, is 9.2 years. This idealized case is very conservative with respect to the "Repair" case for which the remaining service life is much greater than 15 years.

Table 6.1 summarizes all pipeline repairs for the "Repair" case, where joints considered by the program as failed had been automatically replaced with the new ones, as described in Section 5.4. The record of repairs is included in the primary output file, shown in Appendix B, but is not a part of the secondary output file used for the graphic presentation of final results, which are the predicted failure frequencies only. Table 6.1 shows that the first failure predicted by the program occurred one year after the inspection. At this time, joint No 42 had the highest probability of failure, so the program assumed that this joint failed and was replaced with a new one. Similarly, six years after the inspection, another failure was predicted. In this case joint No 1 was assumed to have failed and was replaced, because it was the joint with the largest probability of failure. The summary of predicted repairs, as shown in Table 6.1, provides more details regarding

the predicted future performance of the pipeline, and identifies potential joints which are the most prone to failure at a specific time in the future.

Table 6.1 Summary of joints replaced over the analyzed time period of 15 years

Time T_e (years)	Designation of replaced joint	Time T_e (years)	Designation of replaced joint
0	-	8	-
1	42	9	26
2	-	10	-
3	-	11	-
4	-	12	45
5	-	13	-
6	1	14	5
7	-	15	-

The sudden drops of the predicted failure frequencies shown for the "Repair" case in Figure 6.2 reflect replacement of particular pipe joints listed in Table 6.1 at the end of analyzed time interval. Replacing joint No 42 one year after the inspection is particularly beneficial because several of the cross-sections of that joint contribute considerably to the predicted number of failures per year. Replacement of other joints is less beneficial. However, the increase of the predicted failure rate, which is the slope of the failure frequency curve, is not affected markedly by these isolated repairs performed to maintain serviceability of the line. The increase of failure rate is instead largely due to progressive deterioration of the line due to corrosion. In the case of an upgrading of the line, which goes beyond the necessary maintenance, the change of the slope of the failure frequency

curve would be more apparent. An upgrading would also further increase the remaining service life of the pipeline.

This single example shows the effect of considering repairs in the reliability analysis of a pipeline. However, the results of the "No-action" case can still be used for a qualitative investigation of the effect of various parameters on the estimated remaining service life of a pipeline. Thus the limited parametric study of flexural failures presented in the next section is based on the results for analysis of the "No-action".

6.3 Sensitivity analysis and parametric studies for flexural failures

The reliability analysis of a pipeline conducted using the PIPEREL.EXE program depends on user-specified parameters, that include, for example: the measurement errors of the average and minimum wall thicknesses; the corrosion rates; the number of failures used to scale the reference demand; and, the variation of the reference demand with time. The results may also depend on parameters for the various numerical approximations, such as the number of integration panels used for numerical integrations, and the number of points used to approximate the t_{avg}, t_{min}, and n distributions. In this section, a parametric study is presented that investigates the overall effect of each of these parameters on the estimated remaining service life. The results of the study are obtained for the "No-action" case, with the "No-action" results presented in Figure 6.2 used as the reference.

6.3.1 Average wall thickness measurement error

The results of analysis presented in Section 6.2.2 were obtained for the measurement errors of the average and the minimum wall thicknesses equal to ±10% of t_o. The analysis of the effect of measurement errors on the parameters of the S/S_o distribution, conducted in Chapter 3, concluded that the range of the S/S_o distribution increases if the measurement error of $\overline{t_{avg}}$ increases, and that all parameters of the S/S_o distribution are fairly insensitive to the measurement error of $\overline{t_{min}}$. The implication of the first conclusion is that, if the error $\overline{t_{avg}}$ increases, the failure frequency would also increase, perhaps even if the flexural demand was reduced. The second conclusion allows the analysis presented in this section to be limited to consider only measurement error of the average wall thickness. Thus all input data used were the same as described in Section 6.2.1, with two different cases of the measurement error of $\overline{t_{avg}}$, ±15% and ±20% of t_o.

Figure 6.3 shows results of the two reliability analysis conducted for the increased errors of $\overline{t_{avg}}$, with the reference results for the measurement error ±10% of t_o. The remaining service life for the line with the error of the mean wall thickness equal to ±10% of t_o is 9.2 years. The remaining service life reduces slightly to 8.6 years if the error of $\overline{t_{avg}}$ equals ±15% of t_o, and increases slightly to 10.1 years if the error of $\overline{t_{avg}}$ equals ±20% of t_o. This apparent inconsistency of the results for different measurement errors can be attributed to different values of the reference demand resulting from the scaling

procedure. For an increase of the error of $\overline{t_{avg}}$, it is to be expected that the resulting reference demand will decrease slightly so that the user-specified failure rate at the time of inspection is maintained. For the error of $\overline{t_{avg}}$ equal to ±10% of t_o, the scaled reference demand was 0.219. For the errors of $\overline{t_{avg}}$ equal to ±15% of t_o and ±20% of t_o the scaled reference demands were 0.211 and 0.191, respectively. These results are only roughly proportional to the errors $\overline{t_{avg}}$ because the accuracy of the scaling of the reference demand was set to ±0.01. The difference in the remaining service life for these three cases is due to a very high sensitivity of predicted frequencies of failure to the reference demand value, which will be investigated further in Section 6.3.5.

Based on the results of this limited investigation, it can be concluded that measurement error of the average wall thickness is not a major factor affecting the predicted remaining service life of this particular pipeline.

6.3.2 Corrosion rates

Corrosion causes the flexural resistance to deteriorate in all cross-sections of the pipeline, and so might be expected to have a very significant effect on the predicted failure frequency, and the remaining service life. For the example analysis presented in Section 6.2, various probabilities of the four distinct corrosion rates were assumed at each cross-section as shown in Figure 6.1. The range of possible remaining service life values is bounded by the results obtained for High (H) and Very Low (VL) corrosion rates applied

to the whole pipeline. The solutions for the intermediate corrosion rates, Medium (M) and Low (L), would further divide the range of possible solution into three intervals.

Figure 6.4 shows the predicted failure frequencies obtained when only one of the four possible corrosion rates is applied to the whole line. The line denoted as H+M+V+VL is the reference result, discussed in Section 6.2.2, which assumes that a combination of corrosion rates occurs for each cross-section. The following values of the remaining service life of the analyzed pipeline can be estimated based on plots for the "No-action" case: for the High corrosion rate, 5.9 years; for the Medium corrosion rate, 8.8 years; for the Low corrosion rate, 12.2 years; and for the Very Low corrosion rate, much greater than 15 years. Thus, the assumed corrosion rates are clearly critical parameters affecting the outcome of the reliability analysis for this particular pipeline.

6.3.3 Number of failures used to determined the reference demand

The idealized demand imposed on the pipeline, D_f, discussed in Section 5.2.2.1, has two components: the relative demand and the reference demand. Scaling of the reference demand, D_r, which is a characteristic quantity for a given pipeline, is based on the user-specified failure frequency, that is extrapolated from failure records. This value will certainly have some associated error even if the simplification associated with the concept of relative demand is ignored. Disregarding entirely the uncertainty associated with the specified relative demand, the effect of the error of the specified failure frequency on the

remaining service life can be investigated. All required data are the same as were presented in Section 6.2.1, and the user-specified historic failure frequency values considered will be from 1.6 to 2.4 failures per kilometre of line per year. Similar to previous analyses, the results presented in Section 6.2.2 for a historic failure rate of 2.0 failures per kilometre of line per year will be used as the reference.

Figure 6.5 shows the effect of the observed failure frequency on the predicted frequency of future failures. The remaining service life increases from 7.6 years to 11.6 years as the observed failure frequency reduces from 2.4 failures per kilometre of line per year to 1.6 failures per kilometre of line per year.

Thus, for this particular pipeline, it can be concluded that the results of the reliability analysis are sensitive to the user-specified historic failure frequency.

6.3.4 Parameters of numerical approximation

The reliability analysis of a pipeline, described in Chapter 5, involves numerical techniques which also can affect the results. Numerical integration using Simpson's 1/3 rule is used for discretization of the standard normal distribution as described by Eqs.[5.12] and [5.16]. It is also used for the calculation of the cross-section probability of flexural failure based on Eq.[5.11], with parameters of the S/S_o distribution interpolated from the appropriate tables. The error of approximation using numerical integration

depends on the width of the integration panel, which is determined as the domain of the function to be integrated divided by the assumed number of panels. The effect of the number of points used to approximate the distributions of t_{avg} and t_{min} on the probability of failure of a cross-section was discussed in Section 5.2.1.3. However, the effect of the number of points approximating distributions of t_{avg} , t_{min} and n for the reliability analysis of a pipeline, where a large number of single cross-sections is considered, must be investigated.

Figure 6.6 shows the results of two analysis. In one, 8 points are used to approximate the t_{avg} and t_{min} distributions instead of 7, and 100 integration panels are considered. In the other, 7 point approximation are used with 300 integration panels, with all remaining data exactly the same as described in Section 6.2.1. Comparing these results with the reference it is clear that the effect of the parameters used in the numerical investigation is not significant.

6.3.5 Variation of demand with time

The analysis presented in Section 6.2 assumed that the reference demand remains constant over the period of time analyzed. It is also possible that the reference demand may increase with time, perhaps due to continuing deterioration of the bedding supporting the pipeline, or some other reason. The effect of steadily increasing demand will be a reduced remaining service life of a pipeline. The program PIPEREL.EXE allows

the user to specify a constant increase of the reference demand with time. The increase of the reference demand with time is linear, and the rate of increase of the reference demand per year is specified as a fraction of the nominal value of reference demand obtained due to scaling.

Figure 6.7 shows the result of analyses obtained if the nominal reference demand is specified to be increased by 0.5% and 1% per year. The remaining service life decreases to 7.5 years and 6.3 years if the reference demand increases by 0.5% and 1% per year, respectively. The results indicate that even a very small annual increase of the demand over a period of time can substantially reduce the remaining service life of a pipeline. In the case of 1% increase per year the reduction of the remaining service life of the particular pipeline investigated is approximately 30%.

The sensitivity of the reliability analysis results to the reference demand indicates the necessity of accurately matching the predicted and observed failure frequencies in the scaling procedure used to determine the reference demand. The program allows the user to specify the desired accuracy in terms of the difference between calculated and specified values. A fairly small number, for example 0.01 or 0.005, should be used to minimize this potential source of error.

6.3.6 Summary

The sensitivity analyses for various parameters affecting the remaining service life of a cast iron pipeline presented in previous sections allows identification of those parameters which have the most significant effect on the predicted performance of the line. The effect of each single parameter can be assessed considering the relative change of the estimated remaining service life with respect to the change of the specific input parameter.

Table 6.2 presents summarized results of the sensitivity analyses conducted in Section 6.3. Based on the sensitivity of the remaining service life to the particular input, the parameters can be ranked in the order of their significance as follow:

1. Corrosion rates - this is the most significant parameter, and the difference between the remaining service life obtained for High and Very Low corrosion rates specified for the whole line exceeds 100% of the reference value obtained for the combination of the four corrosion rates.

2. Increase of the reference demand with time - for the specified increase of 0.5% and 1% per year the decrease of the remaining service life is 18.5% and 31.5%, respectively.

3. Failure frequency for scaling of the reference demand - There is a nearly linear relationship between the input value of the failure frequency and the remaining service life. If the input failure frequency increases by 1%, the remaining service life decreases roughly by 1%. From Table 6.2, the actual values are increases of the remaining service life of 26% and 13% for reductions of the input failure frequency of 20% and 10%, respectively, and reductions of the remaining service life of 9% and 17% for increases of the input failure frequency of 10% and 20%, respectively.

4. Measurement error of $\overline{t_{avg}}$ - for the specified error of ±15% and ±20% the difference in the remaining service life is -6.5% and 9.8%, respectively. This suggests that in this case the measurement error of $\overline{t_{avg}}$ is not a significant factor.

5. Number of points for approximation of wall thickness distributions - no difference was observed for the number of points equal to 7 and 8. This does not mean that the results are not sensitive to the number of points, but rather that they are not sensitive beyond the default value which in this case was 7.

Table 6.2 Summary of the sensitivity analyses of remaining service life T for cast iron pipeline

Parameter	Reference results	Sensitivity analysis	
		results	% [(2)-(3)]/(2)
(1)	(2)	(3)	(4)
Error of $\overline{t_{avg}}$ (Error of t_{min} +/-10% t_o) Section 6.3.1	+/- 10% of t_o T = 9.2 years Section 6.2.2	+/- 15% of t_o T = 8.6 years	- 6.5%
		+/- 20% of t_o T = 10.1 years	9.8%
Corrosion rates Section 6.3.2	H+M+L+VL T = 9.2 years Section 6.2.2	High T = 5.9 years	- 35.8%
		Medium T = 8.8 years	- 4.3%
		Low T = 12.2 years	32.6%
		Very Low T >> 15 years	>> 63%
Frequency of failures for scaling of reference demand D_r Section 6.3.3	2.0/km/year T = 9.2 years Section 6.2.2	1.6/km/year T = 11.6 years	26.1%
		1.8/km/year T = 10.4 years	13%
		2.2/km/year T = 8.4 years	- 8.7%
		2.4/km/year T = 7.6 years	- 17.4%
Number of points for approximation of t_{avg} and t_{min} distribution Section 6.3.4	7 T = 9.2 years Section 6.2.2	8 T = 9.2 years	0%
Increase of reference demand D_r per year Section 6.3.5	0.0% T = 9.2 years Section 6.2.2	0.5% T = 7.5 years	- 18.5%
		1.0% T = 6.3 years	- 31.5%

6.4 Analysis of corrosion failures of a ductile iron pipeline

As shown in Chapter 1, over 80% of ductile iron pipelines failures in Canada, on average, are attributed to corrosion failure, or perforation of the pipe wall. In this section, analysis results from the program PIPEREL.EXE are presented for a simulated ductile iron pipeline considering corrosion failures only. The analysis considers either the "no repairs" option or the repair by joint replacement option, as described in Section 5.4. The results for the "no repairs" case will be used in the next section as the basis for a qualitative assessment of the effect of various parameters on the predicted corrosion failure frequency and the remaining service life of the pipeline. These quantities were discussed in Sections 5.2.2.4 and 5.4.

6.4.1 Data for analyses of corrosion failures

The ductile cast iron pipeline assumed for the analysis consisted of 50 pipe joints numbered from 1 to 50. Each pipe joint was assumed to have an outside diameter, D, equal to 152 mm (6"), a nominal wall thickness, t_o, equal to 10 mm, and a length varying between 5.3 m and 5.4 m. The input data file for the analysis was identical to that shown in Figure 6.1 except that all joints were assumed to be 20 years old. The demand data and tabulated parameters of the S/S_o distribution were irrelevant, because only corrosion failures were analyzed. Similarly, the measurements of the average wall thicknesses collected by the Hydroscope tool are of no use in the case of corrosion failures, because methods of calculation of the probability of corrosion failure of a cross-

section, presented in Sections 5.3.1.1 and 5.3.1.2, use only information pertaining to the measured minimum wall thickness, $\overline{t_{min}}$, with associated measurement error.

The optional scaling of the standard deviation of $\overline{t_{min}}$, described in Section 5.3.2.1, was not used in the analysis, which implies high confidence in the quality of the inspection performed. Because the scaling of the standard deviation of $\overline{t_{min}}$ was not performed, the data regarding the observed frequency of failures were irrelevant. This is quite different from the case of flexural failures only where the data regarding the observed frequency of failures are indispensable for scaling of the reference demand and subsequently for the prediction of the failure frequency for a pipeline.

The corrosion failure analysis requires specification of the failure criterion for a pipe cross-section in terms of the minimum area of the perforation of pipe wall, as described in Section 5.3.1. It was assumed that the failure of a cross-section corresponded to the hole area exceeding 100 mm^2. The line failure criterion, expressed as the critical joint failure frequency, ν_{crit}, was again assumed equal to 5.0 joint failures per kilometre of line per year.

6.4.2 Results of reliability analyses of corrosion failures

Similar to the flexural failures analysis presented in Section 6.2, the analysis of corrosion failures of the ductile cast iron pipeline was conducted for the time period of 15 years,

with the calculations of the frequencies future joint failures performed for 1 year time intervals.

Figure 6.8 shows graphs of the predicted frequencies of future joint failures obtained for two cases considered in the analysis, denoted as "No-action" and "Repair". The "No-action" case represents analysis of a pipeline that is not repaired, and the "Repair" case represents analysis which considers the complete replacement of joints as the repair option. The estimated remaining service life is 12.6 years for the "No-action" case and 13.4 years for the "Repair". This virtually insignificant difference is due to the rapid increase of the predicted failure frequency over the time period from 6 to 15 years after inspection by the Hydroscope tool. In this case there are no failures during the first 5 years and very little warning of the need for line replacement by an increased frequency of repairs.

Table 6.3 shows the summary of repairs effected for the "Repair" case, where joints considered by the program as failed had been automatically replaced with the new ones. Similar to the flexural failure analysis presented in the previous section, the first failure of the pipeline was predicted to occur 11 years from the time of the line inspection. Joint No 42 again had the highest probability of failure, and thus was assumed automatically by the program to have failed and been replaced. The measurements of wall thicknesses for the joint No 42 are the same for both failure modes analyzed, the age of the joint differs

in both cases. and so different corrosion rates are experienced by the joint depending on the failure mode.

Table 6.3 Summary of joints replaced over the analyzed time period of 15 years

Time T_c (years)	Designation of replaced joint	Time T_c (years)	Designation of replaced joint
0	-	8	-
1	-	9	-
2	-	10	-
3	-	11	42
4	-	12	-
5	-	13	34
6	-	14	39
7	-	15	-

In this case, shortly after only the second replacement of a pipe joint, joint No 34 at 13 year after inspection, the line has reached the specified critical frequency of joint failures, qualifying the whole line for replacement.

Comparing the results of the corrosion failures analysis of ductile cast iron pipeline with the results obtained for the flexural failure analysis of cast iron pipeline shown in Figure 6.2. it can be noted that there is virtually no difference between the estimated remaining service life for the "No-action" and the "Repair" cases of the corrosion failures analysis, where for the flexural failures analysis this difference is significant. The rate of change of the slope of the curve for the case of corrosion failure is significantly greater than the corresponding rate for the flexural failure case shown in Figure 6.2. Because the specified

corrosion rates and characteristic measurements for all pipe cross-sections were the same in both cases, it can be concluded that the corrosion is more detrimental to the reliability of ductile cast iron pipelines than cast iron pipelines.

This conclusion can also be verified by a theoretical derivation. The approximate section modulus of an undeteriorated cast iron pipe cross-section, with inside radius of R_o and nominal wall thickness t_o , can be calculated using Eq.[3.2a] as:

$$S_o = \pi \cdot R_{avg}^2 \cdot t_o \qquad [3.2b]$$

where, R_{avg} is an average radius of the pipe equal to $R_o + 0.5t_o$. Eq.[3.2b] is valid if R_{avg} is much greater than t_o, which is the case for the cast iron pipeline discussed in Section 6.2. Similarly, the average section modulus of a corroded pipe cross-section at some particular time T, $S(T)$, is approximately:

$$S(T) = \pi \cdot R_{avg}^2 \cdot t_{avg}(T) \qquad [6.1]$$

where $t_{avg}(T)$ represents the average wall thickness at time T. Using Eq.[5.25] describing the change of the average wall thickness with time, this becomes:

$$S(T) = \pi \cdot R_{avg}^2 \cdot (t_o - kT^n \qquad [6.1b]$$

Thus the deterioration of the average flexural capacity due to corrosion can be expressed as the ratio of the section modulus of a deteriorated cross-section, $S(T)$, given by

Eq.[6.1b] and the initial section modulus of pipe cross-section, S_o, given by Eq.[3.2b], as:

$$\frac{S(T)}{S_o} = 1 - \frac{k}{t_o} T^n \qquad [6.2]$$

Similarly, for the corrosion failure case, the change of the minimum wall thickness with time is described by Eq.[5.26]

$$t_{min}(T) = t_o - KT^n \qquad [5.26]$$

and, the effect of the corrosion can be expressed as the ratio of the minimum wall thickness $t_{min}(T)$ and the nominal wall thickness t_o :

$$\frac{t_{min}(T)}{t_o} = 1 - \frac{K}{t_o} T^n \qquad [6.3]$$

Assuming that the minimum and the average wall thickness defined by Eqs.[5.25] and [5.26] satisfy the condition that $t_{min}(T) \le t_{avg}(T)$, the relationship between corrosion rates K and k can be therefore expressed as $K \ge k$. Applying this relationship of corrosion rates to Eqs.[6.2] and [6.3], the relationship of deteriorating "capacities" of the flexural and corrosion failure can be expressed as:

$$\frac{t_{min}(T)}{t_o} \le \frac{S(T)}{S_o} \qquad [6.4]$$

Eq.[6.4] shows that the development of a perforation with time will generally progress faster than the deterioration of the flexural capacity, and so will cause a higher rate of increase of the frequency of failures with time for the corrosion failure mode. This conclusion is corroborated by the observed failure rate for cast and ductile iron pipes (Jakobs and Hewes, 1987). However, it should be noted that the thickness of a ductile iron pipe wall may be up to a 50% thinner than that for the same diameter cast iron pipe, which certainly plays a role in higher rate of failures for ductile cast iron pipes.

6.5 Sensitivity analysis and parametric studies for corrosion failures

Similar to the reliability analysis of flexural failures, the reliability analysis of corrosion failures depends on user-specified parameters, that include, for example: the measurement error of the minimum wall thickness; the corrosion rates; and, the specified minimum perforation area defining the corrosion failure of a single pipe cross-section. The results may also depend on parameters for the various numerical approximations, such as number of integration panels used for numerical integrations, and the number of points, N_c, used to approximate the $\overline{t_{min}}$ distribution. In this section, a parametric study is presented that investigates the overall effect of each of these parameters on the estimated remaining service life. The results of the study are obtained for the "No-action" case, with the "No-action" results presented in Figure 6.8 used as the reference.

6.5.1. Measurement error of minimum wall thickness

The results shown in Figure 6.8 were obtained for the measurement error of the minimum wall thickness of ±10% of t_o. The effect of this measurement error on the probability of corrosion failure of a single cross-section is discussed in Section 5.3.2.1, and shown in Figure 5.12. In this section the sensitivity of the reliability of an entire line to the measurement error of the minimum wall thickness is examined. Two analyses, with measurement errors of $\overline{t_{min}}$ equal to ±15% and ±20% of t_o, and the remaining input data as shown in Figure 6.1, will be presented.

Figure 6.9 shows the results of the reliability analysis conducted for errors of $\overline{t_{min}}$ of ±10%, ±15% and ±20% of t_o for the "No-action" repair case. The remaining service life of the pipeline analyzed reduces as the error of $\overline{t_{min}}$ increases: for an error of ±10% of t_o the remaining service life is 12.6 years; for an error of ±15% of t_o it is 10.5 years and for an error of ±20% of t_o it is 8.6 years. In this case, the relationship between the remaining service life and the measurement error of $\overline{t_{min}}$ appears to be linear. However, this may be only the case for this particular pipeline, and more analyses would be needed to generalized this observation. It seems clear that measurement error of the minimum wall thickness is a major factor affecting the predicted remaining service life of this particular pipeline.

6.5.2 Corrosion rates

The relationship between the corrosion rate and the corrosion failure of a cross-section is much clearer than it is in the case of flexural failure. The time dependent minimum wall thickness of a cross-section expressed by Eq.[5.26], defines the failure state at time T. The equation involves only the initial wall thickness, t_o, and the depth of corrosion pit defined by the corrosion parameters, K and n. Therefore, the effect of the assumed corrosion rate on the minimum wall thickness, and subsequently on the probability of perforation of a pipe cross-section, is easy to assess. However, the effect of various corrosion rates on the remaining service life of an entire pipeline, accounting for the minimum perforation area and measurement error, is a more complicated problem that will be investigated in this section.

For the reference case described in Section 6.4, various probabilities of the four distinct corrosion rates were assumed at each sampled cross-section as shown in Figure 6.1. In this section, analyses will be presented assuming a single corrosion rate for the entire pipeline length to investigate the effect of a particular corrosion rate on the remaining service life. Similar to the flexural failure case presented in Section 6.3.2, a solution for the combination of corrosion rates will be bounded by appropriate solutions obtained for the four cases of single corrosion rate.

Figure 6.10 shows the predicted failure frequencies when High, Medium, Low and Very Low corrosion rates are applied to the whole line. The curve denoted as H+M+L+VL is

the reference result, discussed in Section 6.4.2, which assumes that a particular combination of corrosion rates occur at each cross-section. The following values of remaining service life of the analyzed pipeline can be estimated based on plots for the "No-action" case: for the High corrosion rate, 10.0 years; for the Medium corrosion rate, approximately 15 years; for the Low corrosion rate, much greater than 15 years; and, for the Very Low corrosion rate, much greater than 15 years. Thus the outcome of the reliability analysis for this particular pipeline is extremely sensitive to the assumed corrosion rates.

Although the specification of exact corrosion rates at each cross-section analyzed is difficult in practice, useful information can still be obtained from the analyses of the four corrosion rates separately, leading to four estimates of the remaining service life. If, for example, the exclusion of the high corrosion rate (H) for all analyzed pipe cross-section can be justified, the estimated remaining service life exceeds 15 years without having to make any assumptions regarding the remaining corrosion rates. In practice, this bound on the remaining service life may be a satisfactory outcome of the analysis.

6.5.3 Perforation areas

The effect of the perforation area used to define the corrosion failure criterion for a cross-section is shown in Figure 5.10, and discussed in detail in Section 5.3.1. The reference case presented in Section 6.4.2 assumes that a perforation area of at least 100 mm^2

constitutes the failure of a cross-section. The specified minimum, or critical, perforation area, which defines the corrosion failure of a single pipe cross-section, is a very subjective parameter.

Figure 6.11 shows the predicted corrosion failure frequencies for the "No-action" repair option and for critical minimum perforation areas equal to: 0 mm^2, 100 mm^2, 200 mm^2 and 300 mm^2. The following remaining service life of the analyzed pipeline can be estimated based on plots of the predicted failure frequencies: for the minimum perforation area equal to 0 mm^2, 6.5 years; for the minimum perforation area equal to 100 mm^2, which is the reference result, 12.6 years; for the minimum perforation are equal to 200 mm^2, much greater than 15 years; and, for the minimum perforation are equal to 300 mm^2, much greater than 15 years. Clearly the remaining service life is more sensitive to the critical minimum perforation area than it is to either the corrosion rate of the measurement error of $\overline{t_{min}}$.

In reality, the hole size used to define the failure criterion and the variation of the corrosion rate with time are not independent, as the analysis summarized in Figure 6.11 assumes. Once even a very small perforation of the pipe wall occurs, additional moisture will be introduced to the environment surrounding the pipe. Depending on the local drainage conditions, this may significantly alter the corrosion rates, and is likely to promote much higher corrosion rates. With the high sensitivity of the remaining service life to the corrosion rates, as shown in the previous section, the substantial differences of

the remaining service life obtained for various critical perforation areas, may in fact be much smaller. This issue will be less significant for the case of corrosion failures of cast iron pipes, where the complete perforation of the pipe wall may not necessarily cause a leak. For the cast iron pipes the characteristic formation of graphite plaques can successfully prevent leaks for perforations of a reasonable size (Romanoff, 1957).

6.5.4 Parameters of numerical approximations

The calculation of the probability of failure of a single cross-section uses a point approximation for the normal distribution of the minimum wall thickness as described in Section 5.3.1.2. The difference between the probability of failure calculated using the exact and the approximate method is shown in Figures 5.9 and 5.11. Although the probability of failure for a single cross-section is quite sensitive to the number of points, N_c, approximating the distribution of t_{min}, it is likely that the predicted corrosion failure frequency for a length of pipeline will be far less sensitive, due to the large number of cross-sections analyzed and the compensating error of the approximation.

Figure 6.12 shows the results of analyses obtained for the number of points, N_c, equal to 7 and 14, where the reference results obtained for $N_c = 10$ are also shown with the solid line on the figure. There is no appreciable difference of the estimated remaining service life of the pipeline for these three analyzed cases.

6.5.5 Summary

The sensitivity analyses of various parameters affecting the remaining service life of a ductile iron pipeline presented in previous sections allows identification of those parameters which have the most significant effect on the predicted performance of the line. The effect of each single parameter can be assessed considering the relative change of the estimated remaining service life with respect to the change of the specific input parameter.

Table 6.4 summarizes results of the sensitivity analyses conducted in Section 6.5. Based on the sensitivity of the remaining service life to the particular input, the parameters can be ranked in the order of their significance as follow:

1. Corrosion rates - this is probably the most significant parameter. The remaining service life obtained for High corrosion rate specified for the whole line is 10.0 years. For Very Low corrosion rate specified for the whole line the remaining service life can not be determined precisely, but it exceeds by far the time period of 15 years. This significant difference between the remaining service lives obtained for High and Very Low corrosion rates specified for the whole line suggests great significance of this parameter for the outcome of reliability analysis.

2. Measurement error of $\overline{t_{min}}$ - for specified errors of ±15% and ±20% of t_o the differences in the remaining service life with respect to the reference case with

specified error of ±10% of t_o are -16.6% and -31.8%, respectively. Thus the measurement error of $\overline{t_{min}}$ is a significant factor. The relationship between the increase in measurement error of $\overline{t_{min}}$ and the decrease of the remaining service life is almost linear. For example, for every ±1% increase of the error the decrease of the remaining service life is roughly a little over 3%.

3. Critical area defining perforation failure - this is a very significant parameter. If the critical hole area is reduced to 0 mm^2 from 100 mm^2, the remaining service life is reduced by almost 50%. However, the assumption that the specified corrosion rate remains constant after the initial perforation of the pipe wall is questionable, and for this reason this parameter was not ranked as one of the two most significant for ductile iron pipe.

4. Number of points for approximation of t_{min} distribution - no appreciable difference was observed for the number of points equal to 7, 10 and 14 for the analyzed period of time. Thus the default number of points, which in this case was 10, gives sufficiently accurate results.

Table 6.4 Summary of the sensitivity analyses of remaining service life T for ductile iron pipeline

Parameter	Reference results	Sensitivity analysis	
		results	% [(2)-(3)]/(2)
(1)	(2)	(3)	(4)
Error of $\overline{t_{min}}$ (Error of $\overline{t_{avg}}$ +/-10% t_o) Section 6.5.1	+/- 10% of t_o T = 12.6 years Section 6.4.2	+/- 15% of t_o T = 10.5 years	- 16.6%
		+/- 20% of t_o T = 8.6 years	-31.8%
Corrosion rates Section 6.5.2	H+M+L+VL T = 12.6 years Section 6.4.2	High T = 10.0 years	- 20.6%
		Medium T = 15.0 years	19.1%
		Low T >> 15 years	>>19.1%
		Very Low T >> 15 years	>> 19.1%
Perforation areas Section 6.5.3	100 mm^2 T = 12.6 years Section 6.4.2	0 mm^2 T = 6.5 years	-48.4%
		200 mm^2 T >> 15 years	>>19.1%
		300 mm^2 T >> 15 years	>>19.1%
Number of points for approximation of t_{min} distribution Section 6.5.4	10 T = 12.6 years Section 6.4.2	7 T = 12.6 years	0%
		14 T = 12.6 years	0%

```
**********************************************************
*          DATA FOR ANALYSIS OF THE PIPELINE             *
**********************************************************

LINE No   1

TYPE OF ANALYSIS - FLEXURAL FAILURES

TYPE OF THE CROSS SECTION MODEL - 1a

FAILURE BREAK FREQUENCY = 5.00 /km  year

MEASUREMENT ERRORS:
         Tavg  (- +) error = 0.10tc / 0.10tc
         Tmin  (- +) error = 0.10tc   0.10tc

TOTAL LENGTH OF THE LINE = 0.266 km

CORROSION RATES:
                 High    Medium     Low     Very Low
   mean  m      0.680    0.470    0.350     0.190
   stdev m      0.100    0.040    0.030     0.030

THE INCREASE OF REF.DEMAND PER YEAR = 0.000

LINE DATA:
```

JOINT No	L (m)	PT	Tavg (mean)	Tmin (mean)	AGE yrs.	REL. DEM.	CORR. RATE PROB. H	M	L	VL
1	5.4	1	7.50	3.00	60	1.10	0.15	0.35	0.35	0.15
		2	7.50	2.50		1.10				
		3	7.80	3.10		1.10				
		4	7.60	2.80		1.10				
2	5.4	1	7.30	3.00	60	1.05	0.20	0.30	0.30	0.20
		2	7.00	3.10		1.05				
		3	7.10	3.50		1.05				
		4	7.20	3.30		1.05				
3	5.4	1	6.50	3.00	60	1.05	0.10	0.30	0.30	0.30
		2	6.20	2.80		1.05				
		3	6.40	2.50		1.05				
		4	6.00	2.70		1.05				
4	5.3	1	5.80	3.00	60	1.00	0.20	0.30	0.30	0.20
		2	5.70	2.80		1.00				
		3	5.50	2.90		1.00				
		4	5.60	2.50		1.00				
5	5.3	1	5.60	3.00	60	1.20	0.10	0.30	0.30	0.30
		2	4.50	2.50		1.20				
		3	5.90	4.00		1.20				
		4	6.00	3.50		1.20				
6	5.3	1	6.60	3.00	60	1.20	0.15	0.35	0.35	0.15
		2	4.50	2.00		1.20				
		3	5.30	4.50		1.20				
		4	6.00	4.00		1.20				

Figure 6.1 Input of joints data, relative demand and corrosion rates weighting factors

JOINT No	L (m)	PT	Tavg (mean)	Tmin (mean)	AGE yrs.	REL. DEM.	CORR. RATE PROB. H	M	L	VL
7	5.4	1	8.00	6.00	60	1.00	0.20	0.30	0.30	0.20
		2	7.50	6.00		1.00				
		3	7.50	5.50		1.00				
		4	6.00	4.50		1.00				
8	5.3	1	7.50	5.00	60	1.00	0.10	0.30	0.30	0.30
		2	7.50	4.50		1.00				
		3	7.10	5.00		1.00				
		4	6.80	4.50		1.00				
9	5.3	1	6.50	4.80	60	1.00	0.20	0.30	0.30	0.20
		2	6.30	3.00		1.00				
		3	6.50	2.50		1.00				
		4	7.00	3.10		1.00				
10	5.4	1	5.50	4.60	60	0.90	0.10	0.30	0.30	0.30
		2	6.00	2.80		0.90				
		3	5.80	3.50		0.90				
		4	6.30	4.20		0.90				
11	5.4	1	7.00	3.00	60	1.05	0.10	0.40	0.40	0.10
		2	6.50	2.50		1.05				
		3	7.30	3.10		1.05				
		4	7.20	2.80		1.05				
12	5.3	1	8.30	3.00	60	1.05	0.25	0.25	0.30	0.20
		2	6.60	3.10		1.05				
		3	7.40	3.50		1.05				
		4	7.00	3.30		1.05				
13	5.3	1	6.50	3.00	60	1.05	0.10	0.30	0.40	0.20
		2	6.20	3.80		1.05				
		3	6.40	4.50		1.05				
		4	6.50	2.70		1.05				
14	5.3	1	5.80	3.00	60	1.00	0.25	0.30	0.30	0.15
		2	5.70	3.80		1.00				
		3	6.50	2.90		1.00				
		4	5.60	2.50		1.00				
15	5.3	1	5.60	3.00	60	1.15	0.10	0.10	0.30	0.50
		2	6.50	2.50		1.15				
		3	5.90	4.00		1.15				
		4	7.00	3.50		1.15				
16	5.3	1	5.60	3.00	60	1.10	0.15	0.30	0.40	0.15
		2	5.50	2.60		1.10				
		3	5.80	4.60		1.10				
		4	6.00	4.00		1.10				
17	5.3	1	7.00	6.00	60	1.10	0.20	0.20	0.40	0.20
		2	7.50	6.00		1.10				
		3	7.00	5.50		1.10				
		4	6.00	4.50		1.10				

Figure 6.1 (contd) Input of joints data, relative demand and corrosion rates weighting factors

JOINT No	L (m)	PT	Tavg (mean)	Tmin (mean)	AGE yrs.	REL. DEM.	CORR. RATE PROB. H	M	L	VL
18	5.3	1	7.00	5.00	60	1.10	0.40	0.30	0.20	0.20
		2	7.50	4.50		1.10				
		3	6.90	4.80		1.10				
		4	6.80	4.50		1.10				
19	5.3	1	7.50	4.80	60	1.05	0.20	0.50	0.10	0.20
		2	6.80	3.00		1.05				
		3	7.50	2.50		1.05				
		4	7.10	3.10		1.05				
20	5.3	1	5.50	3.60	60	0.95	0.10	0.30	0.10	0.50
		2	6.00	2.80		0.95				
		3	7.80	3.50		0.95				
		4	6.50	4.50		0.95				
21	5.3	1	7.10	3.30	60	1.10	0.25	0.35	0.30	0.10
		2	7.00	2.80		1.10				
		3	7.80	3.10		1.10				
		4	7.80	2.80		1.10				
22	5.4	1	7.30	3.00	60	1.05	0.50	0.30	0.10	0.10
		2	7.40	3.50		1.05				
		3	6.70	2.50		1.05				
		4	7.80	3.80		1.05				
23	5.3	1	6.20	3.10	60	1.00	0.10	0.20	0.50	0.20
		2	6.00	2.80		1.00				
		3	6.30	2.70		1.00				
		4	6.00	2.70		1.00				
24	5.3	1	6.80	3.00	60	1.05	0.20	0.30	0.30	0.20
		2	5.90	2.50		1.05				
		3	6.50	2.90		1.05				
		4	5.70	2.80		1.05				
25	5.3	1	6.60	3.00	60	1.20	0.10	0.30	0.30	0.30
		2	4.50	2.50		1.20				
		3	5.70	3.00		1.20				
		4	6.00	3.60		1.20				
26	5.3	1	5.60	3.00	60	1.15	0.15	0.30	0.35	0.20
		2	4.50	2.30		1.15				
		3	5.80	4.20		1.15				
		4	6.60	4.10		1.15				
27	5.3	1	8.00	6.00	60	1.05	0.20	0.40	0.20	0.20
		2	7.70	6.10		1.05				
		3	7.30	5.30		1.05				
		4	6.30	4.20		1.05				
28	5.3	1	7.20	5.30	60	1.00	0.15	0.30	0.30	0.25
		2	6.50	4.20		1.00				
		3	7.10	5.80		1.00				
		4	6.20	3.50		1.00				

Figure 6.1 (contd) Input of joints data, relative demand and corrosion rates weighting factors

JOINT No	L (m)	PT	Tavg (mean)	Tmin (mean)	AGE yrs.	REL. DEM.	CORR. RATE PROB. H	M	L	VL
29	5.3	1	6.30	4.50	60	1.05	0.25	0.25	0.30	0.20
		2	7.30	4.00		1.05				
		3	6.00	2.50		1.05				
		4	7.30	4.10		1.05				
30	5.3	1	5.90	4.60	60	0.95	0.15	0.25	0.30	0.30
		2	5.40	2.80		0.95				
		3	5.80	4.50		0.95				
		4	5.30	3.20		0.95				
31	5.3	1	7.20	3.30	60	1.10	0.30	0.35	0.35	0.00
		2	4.50	2.60		1.10				
		3	7.90	5.10		1.10				
		4	8.60	4.80		1.10				
32	5.4	1	7.30	3.00	60	1.05	0.00	0.50	0.50	0.00
		2	8.00	3.10		1.05				
		3	7.40	4.50		1.05				
		4	7.90	3.00		1.05				
33	5.3	1	6.70	3.00	60	0.95	0.00	0.10	0.10	0.80
		2	5.20	3.80		0.95				
		3	6.80	2.30		0.95				
		4	6.10	2.90		0.95				
34	5.3	1	6.80	3.00	60	1.05	1.00	0.00	0.00	0.00
		2	6.70	3.80		1.05				
		3	6.50	3.90		1.05				
		4	6.60	2.50		1.05				
35	5.3	1	5.60	3.00	60	1.10	0.00	1.00	0.00	0.00
		2	7.50	2.50		1.10				
		3	6.90	4.00		1.10				
		4	6.50	3.60		1.10				
36	5.3	1	8.60	3.00	60	1.15	0.00	0.00	1.00	0.00
		2	6.50	4.00		1.15				
		3	7.30	3.50		1.15				
		4	6.80	4.40		1.15				
37	5.3	1	8.00	6.00	60	1.05	0.00	0.00	0.00	1.00
		2	7.90	5.00		1.05				
		3	7.60	4.50		1.05				
		4	6.40	4.00		1.05				
38	5.4	1	7.50	5.50	60	1.00	0.10	0.20	0.50	0.20
		2	7.00	4.50		1.00				
		3	8.10	5.50		1.00				
		4	7.80	4.50		1.00				
39	5.4	1	6.50	4.80	60	0.90	0.70	0.30	0.00	0.00
		2	6.30	3.00		0.90				
		3	6.50	2.50		0.90				
		4	7.00	3.10		0.90				

Figure 6.1 (contd) Input of joints data, relative demand and corrosion rates weighting factors

JOINT No	L (m)	PT	Tavg (mean)	Tmin (mean)	AGE yrs.	REL. DEM.	CORR. RATE PROB. H	M	L	VL
40	5.3	1	5.20	4.30	60	0.95	0.00	0.30	0.70	0.00
		2	6.40	3.80		0.95				
		3	6.80	3.50		0.95				
		4	6.30	3.20		0.95				
41	5.3	1	7.50	4.00	60	1.05	0.00	0.50	0.35	0.15
		2	7.70	2.50		1.05				
		3	6.20	4.10		1.05				
		4	7.80	2.80		1.05				
42	5.3	1	5.30	3.00	60	1.15	0.50	0.00	0.30	0.20
		2	7.30	4.10		1.15				
		3	7.10	2.50		1.15				
		4	8.20	1.30		1.15				
43	5.3	1	6.50	2.00	60	1.00	0.10	0.90	0.00	0.00
		2	8.20	2.80		1.00				
		3	7.40	3.50		1.00				
		4	6.30	2.70		1.00				
44	5.3	1	6.50	3.30	60	1.00	0.20	0.30	0.50	0.00
		2	5.80	2.90		1.00				
		3	6.50	3.90		1.00				
		4	5.60	2.50		1.00				
45	5.3	1	5.60	3.00	60	1.20	0.30	0.35	0.35	0.00
		2	4.70	2.50		1.20				
		3	5.20	4.00		1.20				
		4	6.60	3.20		1.20				
46	5.3	1	5.80	3.20	60	1.15	0.15	0.35	0.35	0.15
		2	4.50	3.00		1.15				
		3	6.30	4.50		1.15				
		4	6.80	4.00		1.15				
47	5.3	1	7.00	6.00	60	1.05	0.00	0.20	0.80	0.00
		2	6.50	6.00		1.05				
		3	6.50	5.00		1.05				
		4	6.30	4.50		1.05				
48	5.3	1	6.50	4.80	60	1.00	0.05	0.15	0.30	0.50
		2	7.50	4.50		1.00				
		3	7.50	5.20		1.00				
		4	6.90	4.70		1.00				
49	5.3	1	6.30	4.90	60	0.95	0.25	0.25	0.30	0.20
		2	7.30	3.10		0.95				
		3	6.50	2.50		0.95				
		4	6.00	3.10		0.95				
50	5.3	1	6.50	4.60	60	0.95	0.00	0.20	0.60	0.20
		2	7.00	3.80		0.95				
		3	6.90	3.20		0.95				
		4	7.30	4.20		0.95				

Figure 6.1 (contd) Input of joints data, relative demand and corrosion rates weighting factors

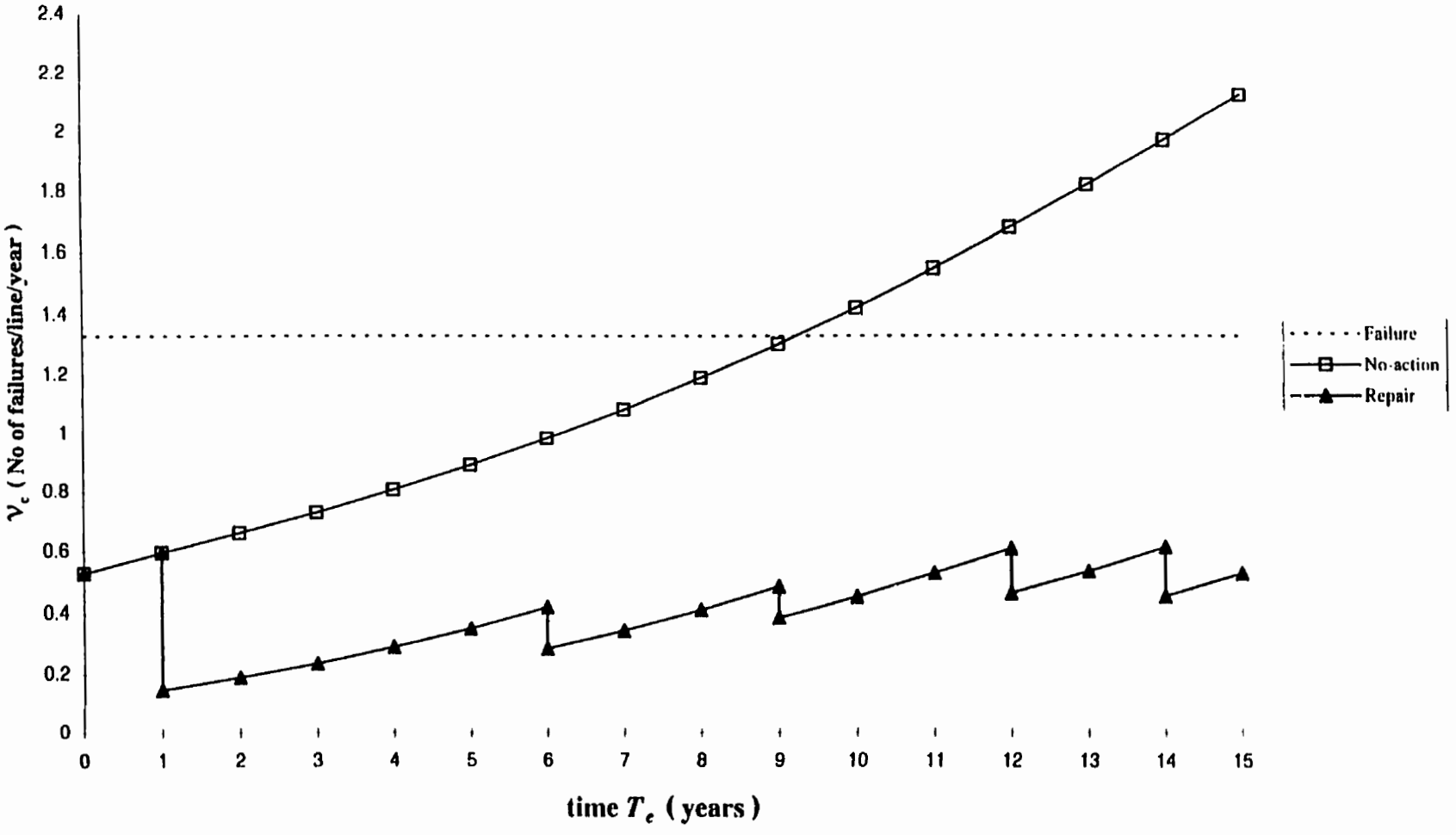

Figure 6.2 Predicted flexural failure frequencies with and without repairs of the line

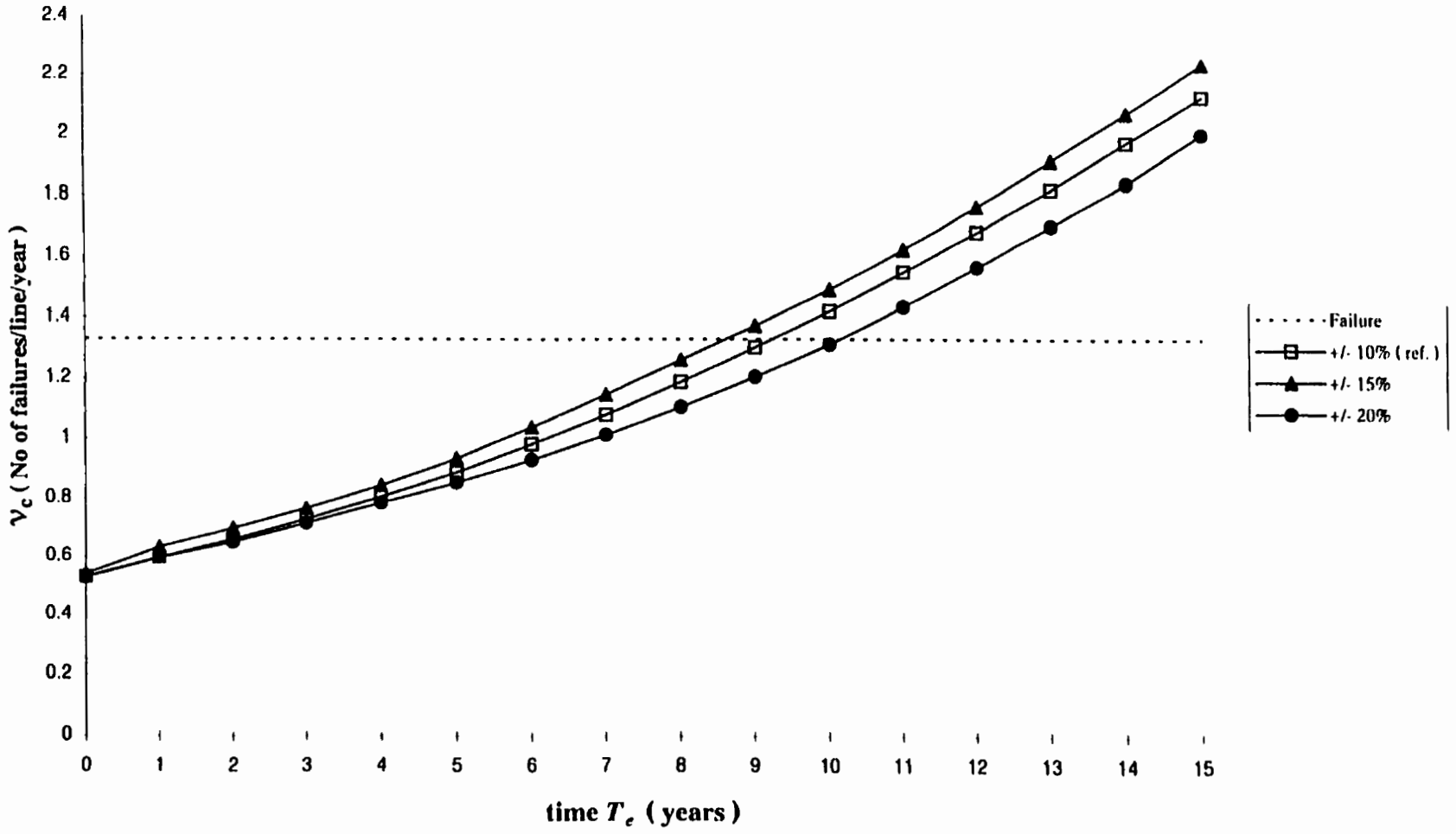

Figure 6.3 Effect of error of $\overline{t_{avg}}$ on predicted flexural failure frequencies

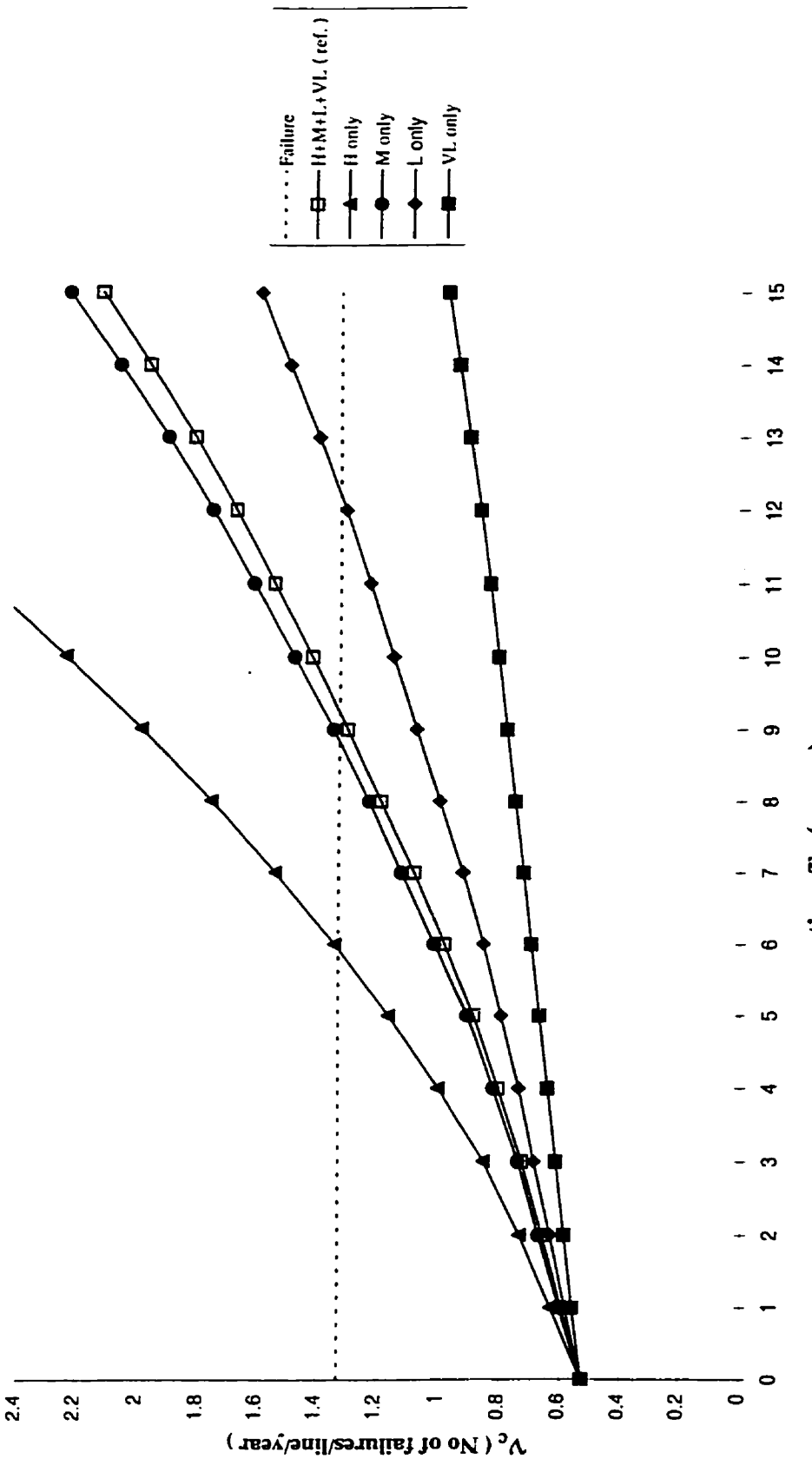

Figure 6.4 Effect of corrosion rates on predicted flexural failure frequencies

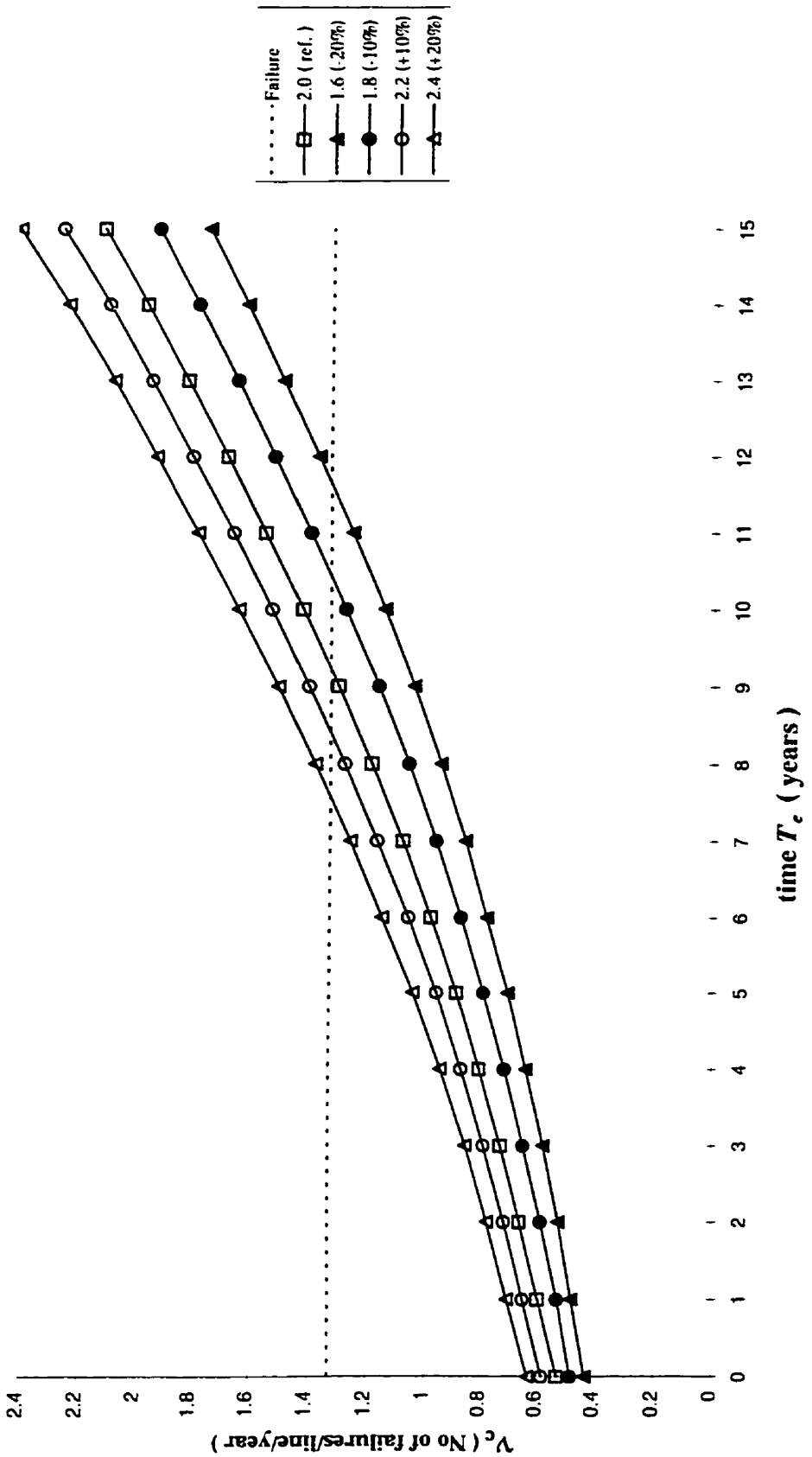

Figure 6.5 Effect of observed failure frequency , ν_c, on predicted flexural failure frequencies

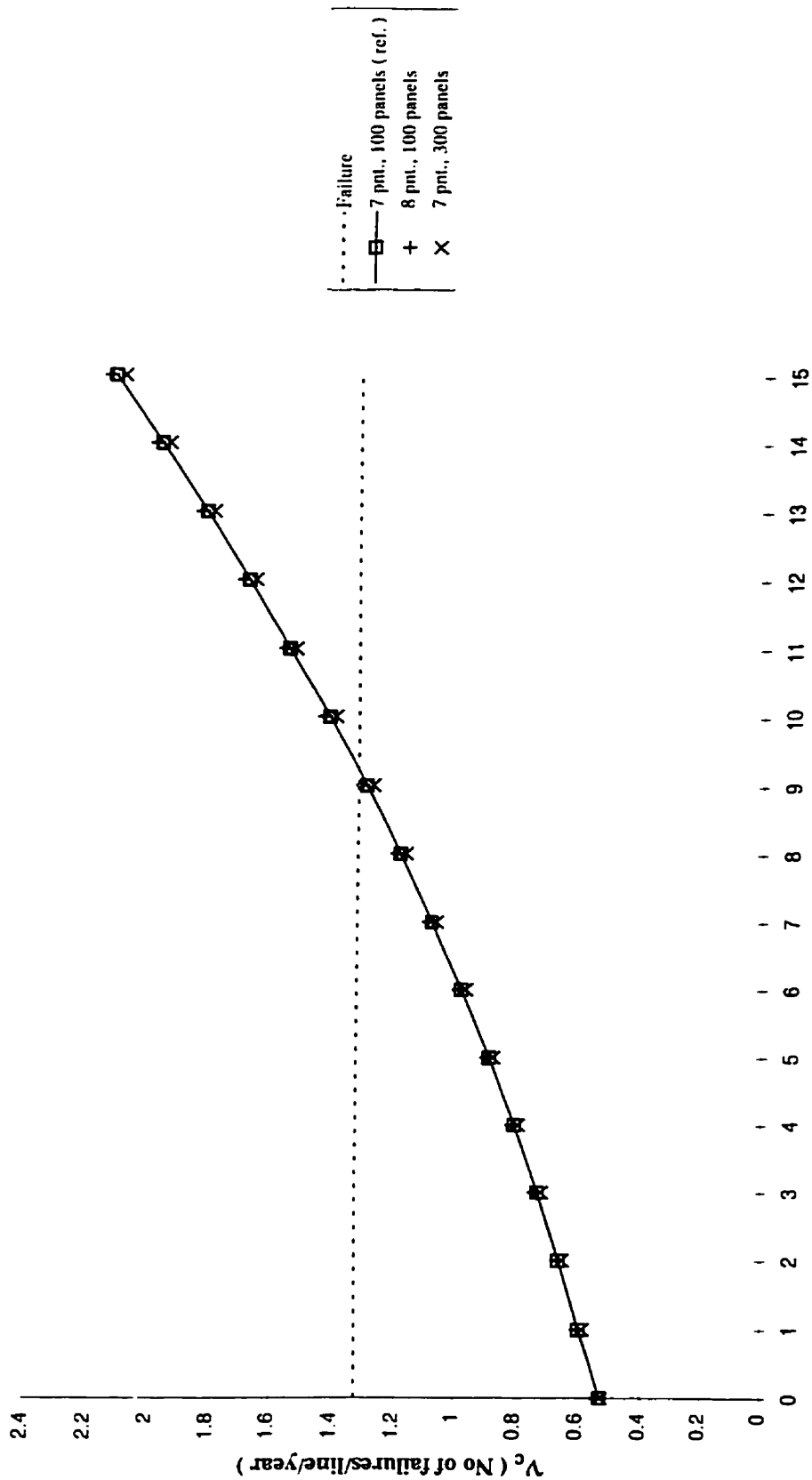

Figure 6.6 Effect of numerical approximation parameters on predicted flexural failure frequencies

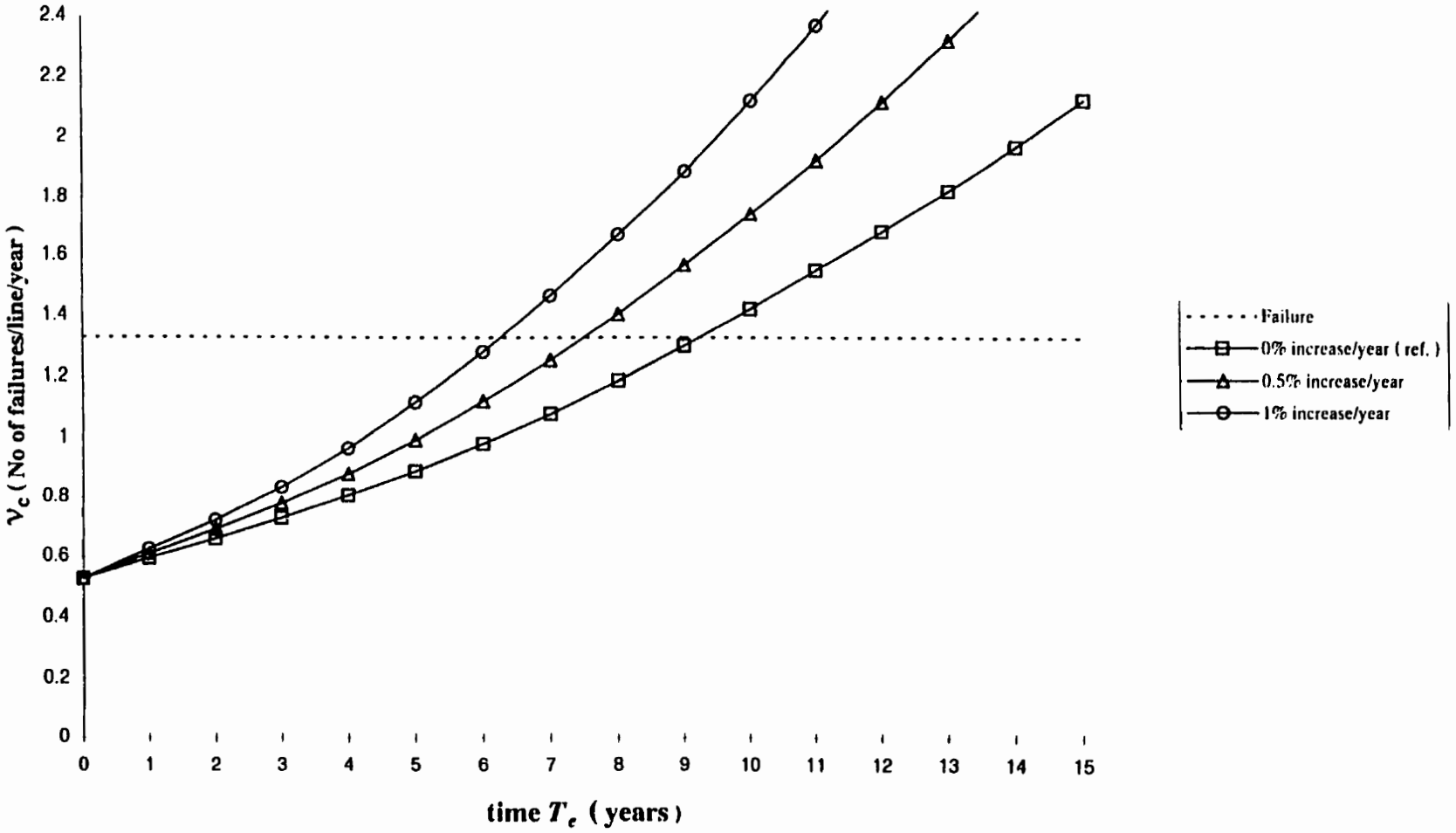

Figure 6.7 Effect of increase of the reference demand, D_r, on predicted flexural failure frequencies

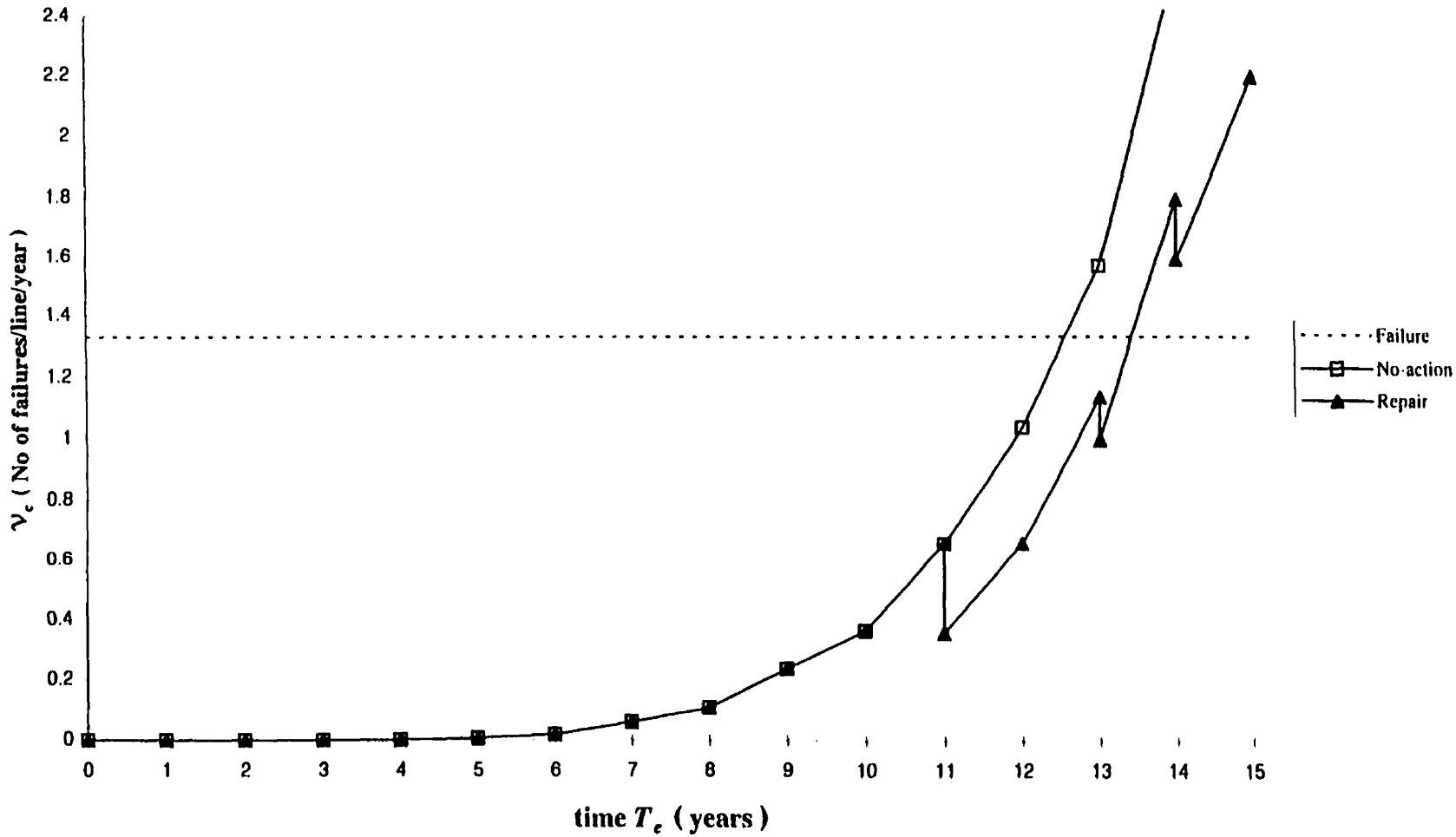

Figure 6.8 Predicted corrosion failure frequencies with and without repairs of the line

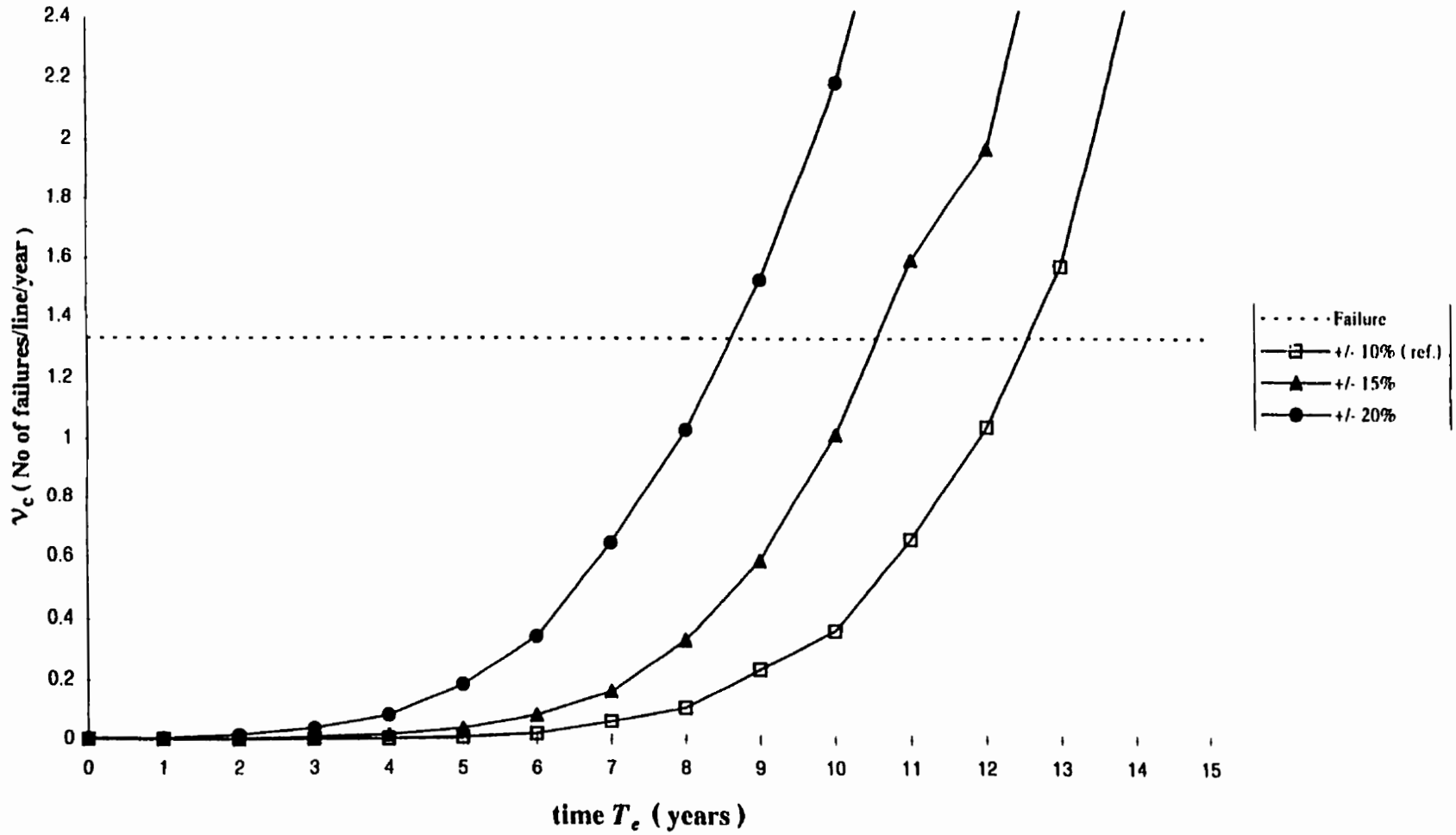

Figure 6.9 Effect of error of $\overline{t_{min}}$ on predicted corrosion failure frequencies

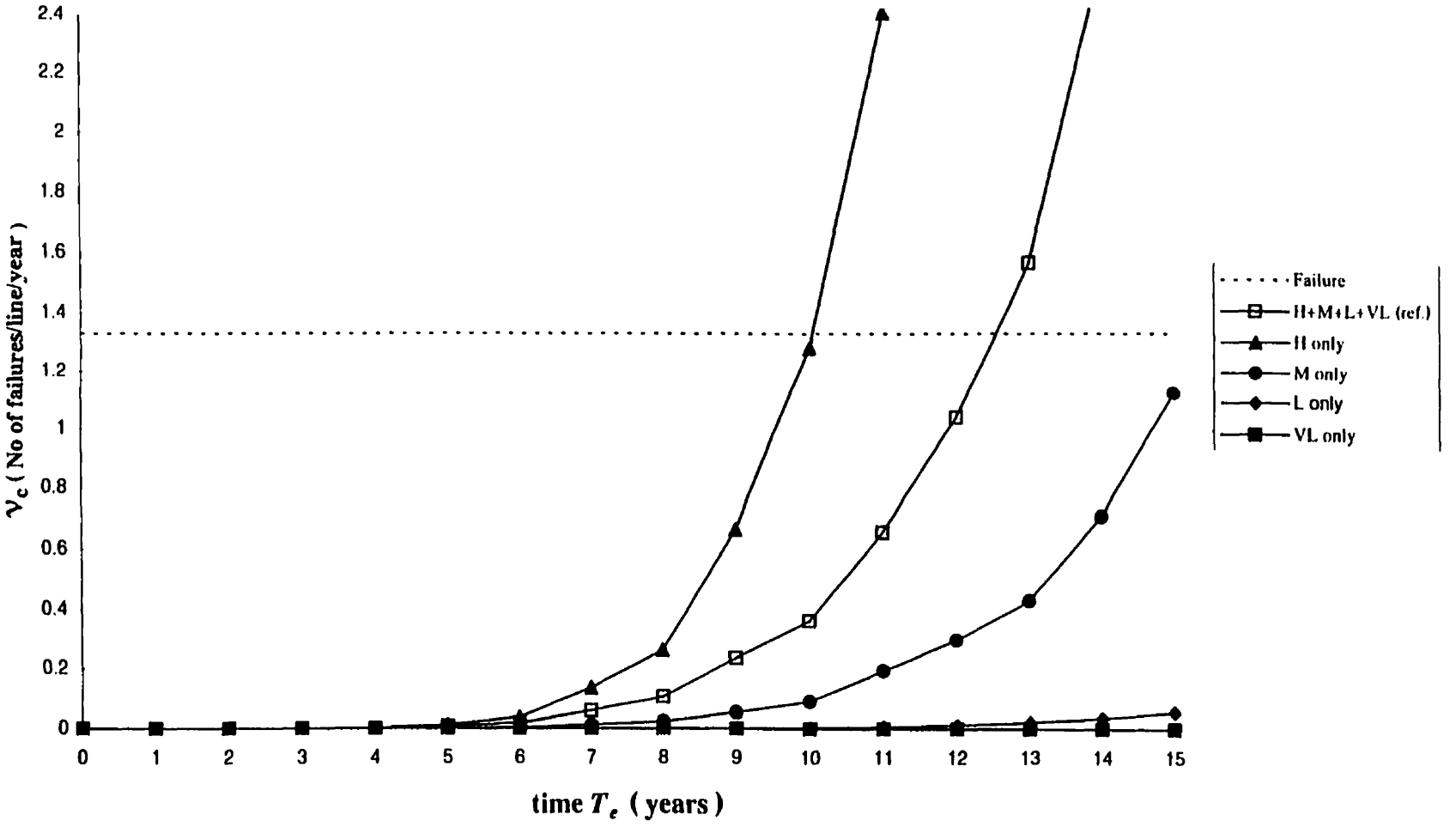

Figure 6.10 Effect of corrosion rates on predicted corrosion failure frequencies

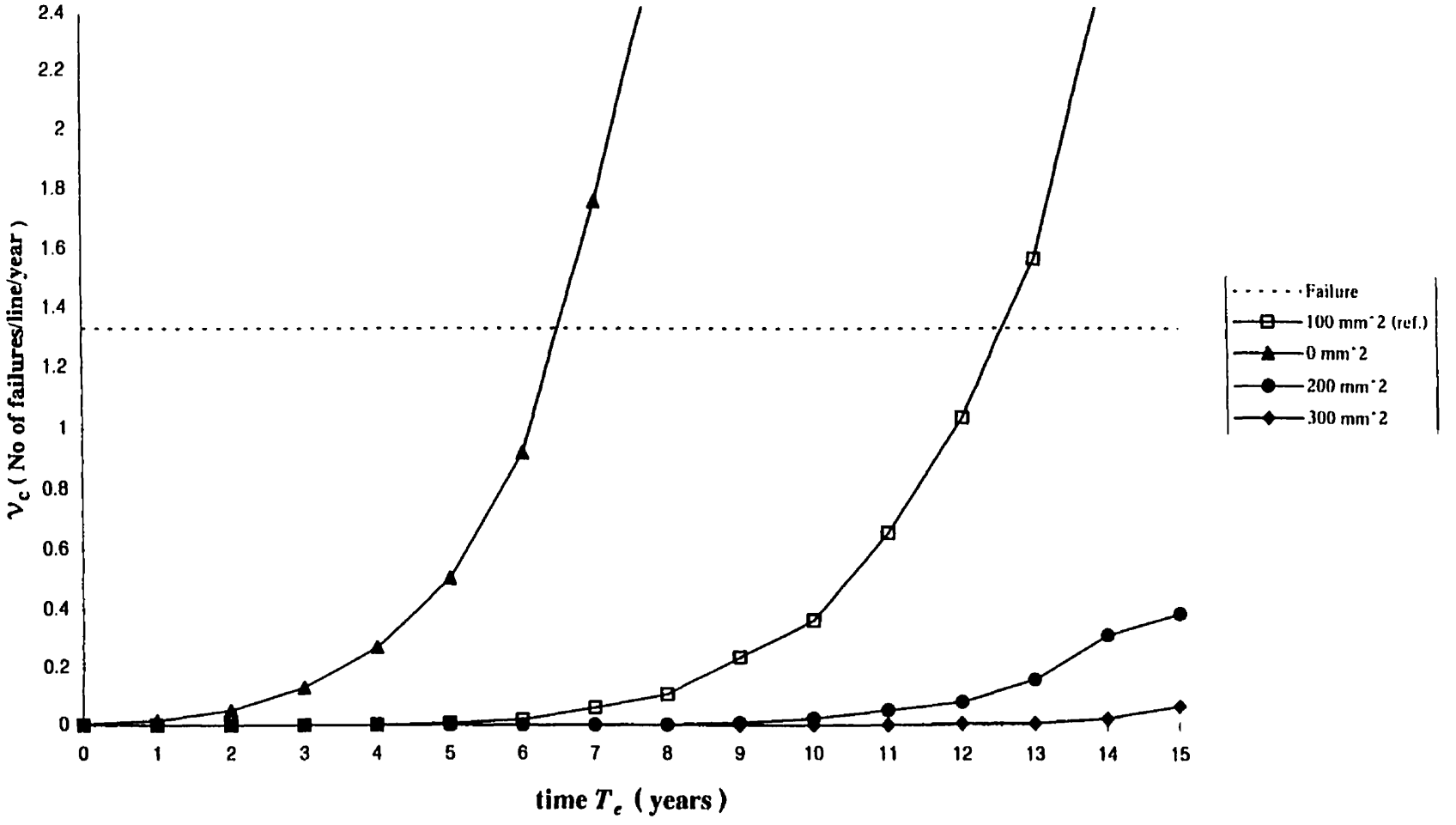

Figure 6.11 Effect of critical perforation area on predicted corrosion failure frequencies

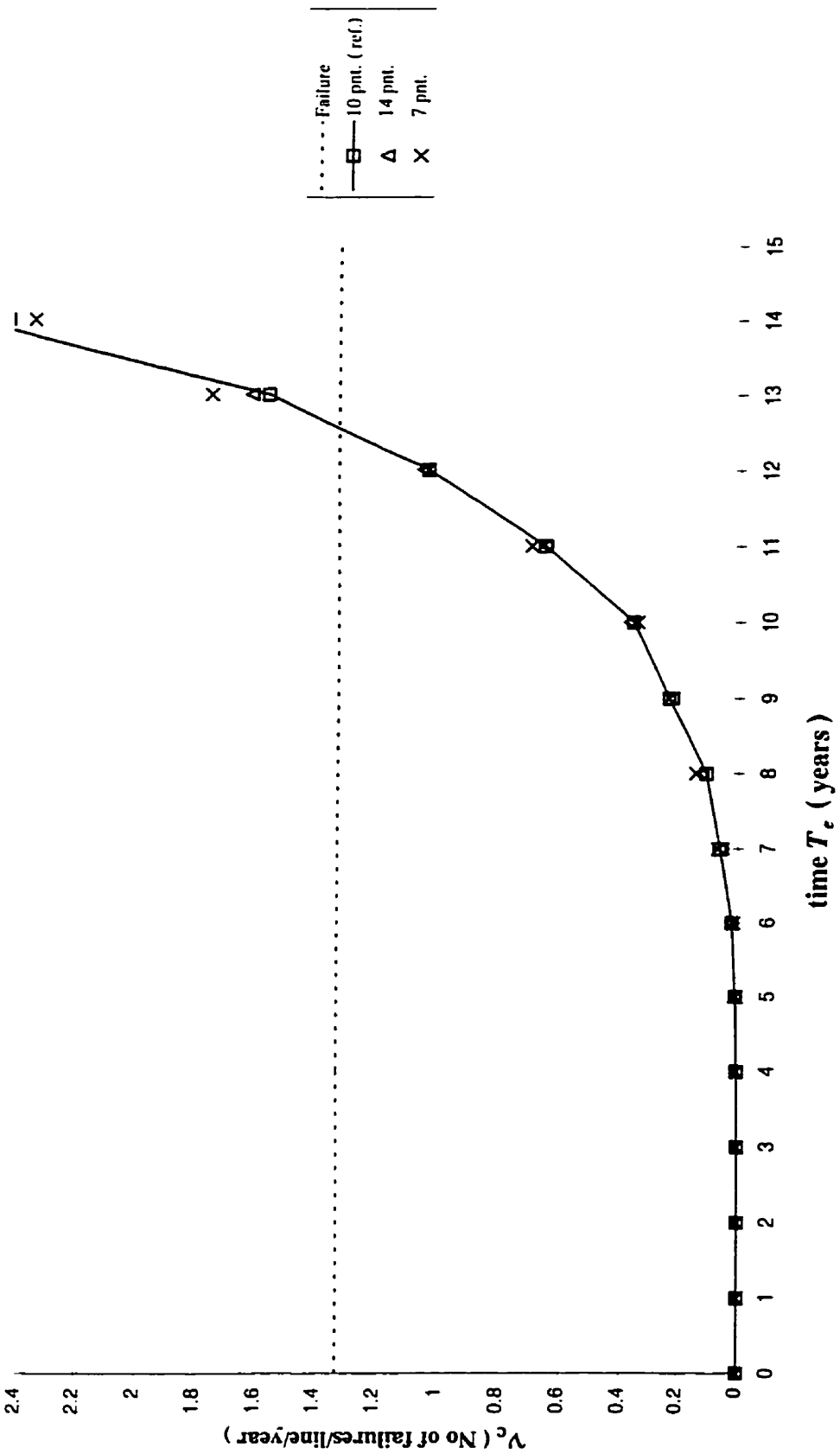

Figure 6.12 Effect of numerical approximation parameters on predicted corrosion failure frequencies

Chapter 7 Summary and Conclusions

7.1 Summary

The accelerating deterioration of water mains and the escalating cost of maintaining existing infrastructure have stimulated the development of the Hydroscope tool for non-destructive evaluation of cast and ductile iron pipes. The tool is able to sample the pipe wall thickness at a particular cross-section of a pipeline and so detect losses of cross-section and local defects (pits). The data from the tool are reported as a pipe wall thickness profile, which lists both the average and the minimum wall thicknesses measured at specific locations along the line.

There are two predominant failure modes for cast and ductile iron pipes: corrosion failures, which occur when the pipe wall is perforated; and, flexural failures, which occur when pipe breaks transversely due to either an applied load or an imposed curvature. From the 1995 NRC (Rajani *et al*, 1995) survey of water main failures in Canadian cities, corrosion failures accounted for over 80% of recorded ductile cast iron pipe failures, and flexural failures accounted for over 60% of recorded cast iron pipes failures. Together, corrosion and flexural failures account for over 80% of failures of cast iron pipes, and over 90% of ductile iron pipes.

The first objective of this thesis was to develop a method for determining the flexural strength of a corroded pipe cross-section using the wall thickness measurements provided by the Hydroscope tool. The second objective was to develop a method of predicting the remaining service life of a pipeline based on the pipe wall thickness profile provided by the Hydroscope tool, the assumed corrosion rates, and the historic failure records. The remaining service life of a pipeline, which is defined as the interval from the time of line inspection to the time when pipeline failure rate reaches a critical value, is an index characterizing the future performance of a pipeline. This index can be used to assess various scenarios of maintaining and upgrading existing water mains.

The first objective was achieved by development of the computer program, called PIPEXSC.EXE, which generates deteriorated pipe cross-sections that have specified average and minimum wall thicknesses by simulation, and determines statistical parameters to describe probability distribution of the remaining simulated flexural strengths. The remaining flexural strength is expressed as the ratio of S/S_o, where S is the section modulus for the extreme tensile fibre of a deteriorated cross-section, and S_o is the section modulus for undeteriorated pipe. The uncertainty associated with the unknown orientation of the neutral axis of bending is addressed by simulating the full range of possible orientations of the applied bending moment vector.

Ten basic models were developed for the analysis using PIPEXSC.EXE, which are distinguished by various user-specified input parameters. Three corrosion patterns are

considered: outside corrosion only, inside corrosion only, or both inside and outside corrosion. Three types of variation of the cross-section wall thickness around the perimeter are consider: semi-constant, random, or ordered. The cross-section models are either based on the set of measurements of wall thicknesses currently provided by the Hydroscope tool, namely the average and minimum wall thicknesses at each pipe cross-section, or based on the minimum wall thicknesses measured at each quadrant of the investigated cross-section, which is consistent with a tool enhancement anticipated in the near future.

The program PIPEXSC.EXE determines the probability distribution of the normalized section modulus, S/S_o, which is proportional to the flexural strength, for pipe cross-sections in various stages of deterioration. The results are presented in a number of tables, each table defining one parameter of the simulated S/S_o distribution for all possible integer combinations of the minimum and average wall thickness measurements. Unique tables can be developed for each type of the pipe and cross-section models, accounting for the corrosion pattern and the variation of the wall thickness around the perimeter of the cross-section. The user can also specify the tolerances on the measured values of minimum and average wall thicknesses reported by the Hydroscope tool.

The program PIPEXSC.EXE allows the effect of possible enhancements of the tool to be evaluated. A sensitivity analysis was performed to assess the effectiveness of tool enhancements which would increase the accuracy of the wall thickness measurements.

An analysis was also conducted to compare the results obtained for the present tool with those for an enhanced tool that collects and records minimum wall thickness measurements for each quadrant of the sampled cross-section.

The second objective was achieved by the development of time-dependent analyses of the flexural strength of corroding pipe cross-sections and time-dependent analyses of the propagation of pits leading to the perforation of the pipe wall. Both analyses require that corrosion rates experienced by the pipe cross-section be assumed. A literature review provided corrosion models which are based on the landmark study by NBS of long time field tests of various pipe materials (Romanoff,1957). The validity of the experimental results was corroborated by theoretical derivations based on the electrochemical theory of underground corrosion (Rossum, 1969).

A method of analysis was developed to predict the remaining service life of a pipeline, which subsequently was incorporated into the computer program PIPEREL.EXE. The program is able to conduct reliability analyses of pipelines considering flexural failures, corrosion failures, or both failure modes simultaneously. The input required for either failure mode includes the pipe wall thickness profile obtained from the Hydroscope tool investigation and the assumed corrosion rates. The analysis is conducted on the basis of the probabilities of failure of the individual pipe joints, with the assumption that the capacities of all joints within the line are statistically independent. The probability of

failure of a single pipe joint is obtained from the probabilities of failure of sampled cross-sections within the joint, which are also assumed to be statistically independent.

The reliability analysis method adopted uses historic failure rate data to calibrate the relative demand and capacity levels for flexural and perforation failures. For the analysis of flexural failures, the flexural demand was idealized as a deterministic quantity, with known relative variation along the line. The actual magnitude of the demand is obtained by scaling so that the predicted number of failures matches the value extrapolated from historic failure records. Historic failure records can also be considered in the analysis of corrosion failures to rectify the measurement error of the minimum wall thicknesses.

The analysis results are presented as predicted failure frequencies for particular times in the future. If a critical failure rate associated with the decision to replace the line is specified, the remaining service life of the pipeline can be estimated. The analysis can also consider various repair scenarios along with the associated costs.

In the last part of this thesis, parametric studies considering the flexural and corrosion failure modes were conducted using the program PIPEREL.EXE. An artificial pipeline data file, containing measurements of the minimum and the average wall thicknesses for 200 sampled pipe cross-sections, was used in the analyses. These limited studies allowed identification of those parameters which have a very significant effect on the outcome of

a reliability analysis, or specifically the estimate of the remaining service life. However, the limited scope of the parametric studies does not permit generalization of its findings.

7.2 Conclusions

1. Although the strength of a corroded cross-section can be assessed using various pipe cross-section models, the Beta distribution was found to best fit the simulated data of the normalized section modulus S/S_o, for all model types.

2. The flexural failure of a cross-section is considerably more sensitive to the average wall thickness than it is to the minimum wall thickness. The average wall thickness determines the mean value of the S/S_o distribution, which is not very sensitive to the minimum wall thickness. Similarly, the upper bound of the S/S_o distribution is not very sensitive to the minimum wall thickness. The minimum wall thickness does affect the lower bound and the overall variance of the S/S_o distribution, and its effect is the greatest if the average wall thickness is equal to the mean value of the minimum wall thickness and the thickness of uncorroded wall.

3. If the flexural demand at cross-section is less than the mean resistance, the probability of flexural failure of a cross-section reduces if the measurement error of the average wall thickness reduces. The error of the average wall thickness has virtually no effect on the mean value of the S/S_o distribution, but is roughly proportional to the range of

the distribution and the overall standard deviation. However, constants of proportionality are model sensitive and depend on whether the variation of the wall thickness is random or the wall thickness changes from thickest to thinnest across the height of the cross-section. The error of the minimum wall thickness does not significantly impact the probability of flexural failure of a cross-section. Thus tool enhancements that reduce the measurement error of the average wall thickness would be very effective in predicting the likelihood of flexural failure.

4. The possible tool enhancement which records the minimum wall thickness for each quadrant of a sampled cross-section is beneficial for the outcome of the flexural failure analysis, because it would permit the use of more refined models that minimize the effect of the unknown arrangement of elements with different wall thicknesses around the perimeter of the cross-section. This would minimize the uncertainty due to the unknown orientation of the neutral axis, and would result in a smaller overall standard deviation of the S/S_o distribution.

5. For the corrosion failure of a cross-section, the minimum wall thickness measurement and its associated measurement error are the most significant parameters. The average wall thickness measurement and corresponding measurement error are irrelevant for this failure mode.

6. The probability of corrosion failure of a cross-section is significantly affected by the measurement error of the minimum wall thickness, which defines the standard deviation of the normal distribution assumed for the minimum wall thickness. Reduction of the measurement error reduces the range of the minimum wall thickness distribution, and so results in lower probability of corrosion failure of a cross-section. Thus, tool enhancements that reduce the measurement error of the minimum wall thickness would be very effective in predicting the likelihood of corrosion failure.

7. The definition of corrosion failure in terms of the area of perforation of the pipe wall is extremely important in calculation of the probability corrosion failure. As the area of perforation deemed to cause failure reduces, the probability of failure increases markedly. The perforation area, as a failure criterion, is more important for ductile iron pipes for two reasons: first, the corrosion failure is the predominant failure mode in this case; and the second, there is no graphite plaque formation to prevent the leak like it is in the case of cast iron pipes.

8. A number of conclusions concerning corrosion rate models can be stated after review of the literature. The experimental investigation by NBS (Romanoff, 1957 and 1968) concluded that the same corrosion rates can be assumed for ductile and cast iron pipes of all common chemical compositions and manufacturing processes, except that for high alloy cast iron rates of corrosion are markedly lower. According to Rossum (Rossum, 1969), whose theoretical derivation corroborated the experimental findings

published by NBS, the same exponent for average thickness loss and for pitting can be assumed for older pipes, with the exponent value being determined based on the degree of aeration of the soil.

9. If the corrosion rate exponent is known, the two corrosion rate constants for average section loss and for pitting can be determined from the Hydroscope tool measurements. Defining these corrosion rates allows the projection of the change of wall thicknesses over time, which is necessary to estimate the future line condition and remaining service life.

10. For the analysis of flexural failures of a pipeline, a simplified definition of demand incorporating the historic failure records can be used in the absence of the more precise data. The relative variation of the demand is assumed and the magnitude of the actual demand is derived using historic failure records. The flexural demand is a key element of the flexural reliability problem, and without the demand being defined the problem is intractable.

11. For the analysis of flexural failures the most important factors affecting the remaining service life of a pipeline are corrosion rates, the repair scenarios, and the possible increase of the demand with time.

12. For the analysis of corrosion failures of a pipeline the major factors affecting the remaining service life of the pipeline are the corrosion rates, the error of the minimum wall thickness measurements, and the definition of corrosion failure in terms of a critical perforation area.

13. For the corrosion failure, a method was developed for using historic failure records to rectify the measurement error of the minimum wall thicknesses collected during the line inspection.

14. Corrosion impacts the corrosion failure rate more significantly than the flexural failure rate. For ductile and cast iron pipelines with identical initial wall thicknesses that are subjected to the same corrosive environment a shorter service life of a ductile cast iron pipeline would be expected.

15. An estimate of the remaining service life of a pipeline, which is an index characterizing the future pipe performance, has a practical value as a decision-making parameter. The most important factors affecting the index are the corrosion rates, the repair scenarios, the measurement errors, a critical perforation area, and the possible increase of the demand with time.

7.3 Suggestions for future work

Future research regarding the modelling and the distribution of the S/S_o for a deteriorated pipe cross-section may consider the following issues:

1. Field studies of real pipes should be initiated to assess the type of thickness variation around the perimeter of the pipe and the distribution of wall thickness of a corroded pipe cross-section. Figure 7.1 shows two real examples of the wall thickness measurements of deteriorated cross-sections of 8" pipe, investigated by the author of this thesis, plotted on the Beta probability paper. The fitted Beta distribution provides good approximation of the distribution of wall thickness for both samples of the pipe cross-section. The routine incorporated in the program PIPEXSC.EXE results in a uniform distribution of wall thickness on both sides of the average wall thickness value. This routine can be modified if more real pipe cross-sections are investigated and more realistic distribution of the wall thickness is established. Similarly, the variation of the pipe wall thickness around the perimeter of a cross-section was found to be neither completely ordered nor completely random. This should also be further investigated, and the findings incorporated to the program.

2. The effect of the assumed deterministic section modulus of undeteriorated pipe, S_o can be investigated. In the calculation of the S/S_o for a simulated cross-section, the section modulus S_o was assumed to be a deterministic quantity. It should rather be treated as a random variable defined by randomly selected values of t_o and D which

distributions can be assumed normal with COV's defined by the manufacturer tolerances.

3. The range of applicability of the generated tables containing parameters of the S/S_o distribution should be investigated. The applicability of generated tables for a range of different types of pipes characterized by similar D / t_o ratio can be further investigated using program PIPEXSC.EXE. Similar corrosion patterns investigation with respect to D / t_o ratio can be conducted to determined whether the corrosion pattern becomes an insignificant parameter of the modelling of pipe cross-section for a certain magnitude of D / t_o.

Future research regarding the reliability analysis and the prediction of the remaining service life of the pipeline may consider the following issues:

1. Studies should be initiated to improve the definition of the flexural demand imposed on the pipeline. In the research reported in this thesis, the idealization of the flexural demand was greatly simplified. The research regarding the flexural demand may consider different mechanical models for buried pipe and the effect of different loads or imposed curvatures. Mechanical models would allow investigation, for example, of: the type of support of a pipe joint, the effect of the connection between pipe joints, or the effect of the joint length. Consideration of different loads acting on the pipe or

imposed curvature would allow investigation, for example, of: surface live load, dead load, or the differential settlement and the frost heave.

2. The method of addressing the problem of corrosion rates experienced by individual cross-sections of the pipeline requires further research. The results of analysis of either the corrosion or the flexural failure are very sensitive to the specified corrosion rates. One possible direction for further research would be to define the scope and method of the soil investigation necessary to determine the variation of corrosion rates along the pipeline. An alternate approach can also be investigated which, instead of determining the actual corrosion rates, would exclude the possibility of the High or perhaps High and Medium corrosion rates occurring for a particular pipeline. The estimate of the minimum remaining service life in this case would be based on the analysis for Medium or Low corrosion rate assumed for the whole line, respectively, as shown in Figures 6.4 and 6.10. Estimated minimum remaining service life may have sufficient practical value as a decision-making parameter.

3. The calculation of the probability of failure of a pipe joint can be improved. Current calculations for a single pipe joint are performed on the basis of a number of sampled cross-sections, with the number of multiple failures allowed to occur equal to the number of cross-sections within the joint. It would be more appropriate to specify the maximum number of multiple failures for the calculation of the probability of failure of the joint, where the number of multiple failures would be less than or equal to the

number of cross-sections, independent of the number of analyzed cross-sections within the joint. The assumption of the statistical independence of joints should also be reconsidered. The results of limited studies conducted in the City of Winnipeg (Goulter and Kazemi, 1988) suggest that joint failures may not be statistically independent.

4. Methods should be developed for updating the initial prediction of the remaining service life using subsequent failure data as they become available. The analysis of a pipeline provides an estimate of the future performance of the line. The results of analysis for the assumed period of time can be further revised using the records of the actual failures occurring after a number of time intervals. For example, assumed corrosion rates can be modified to provide a better fit of the predicted failure frequency curve to the observed failure frequency data.

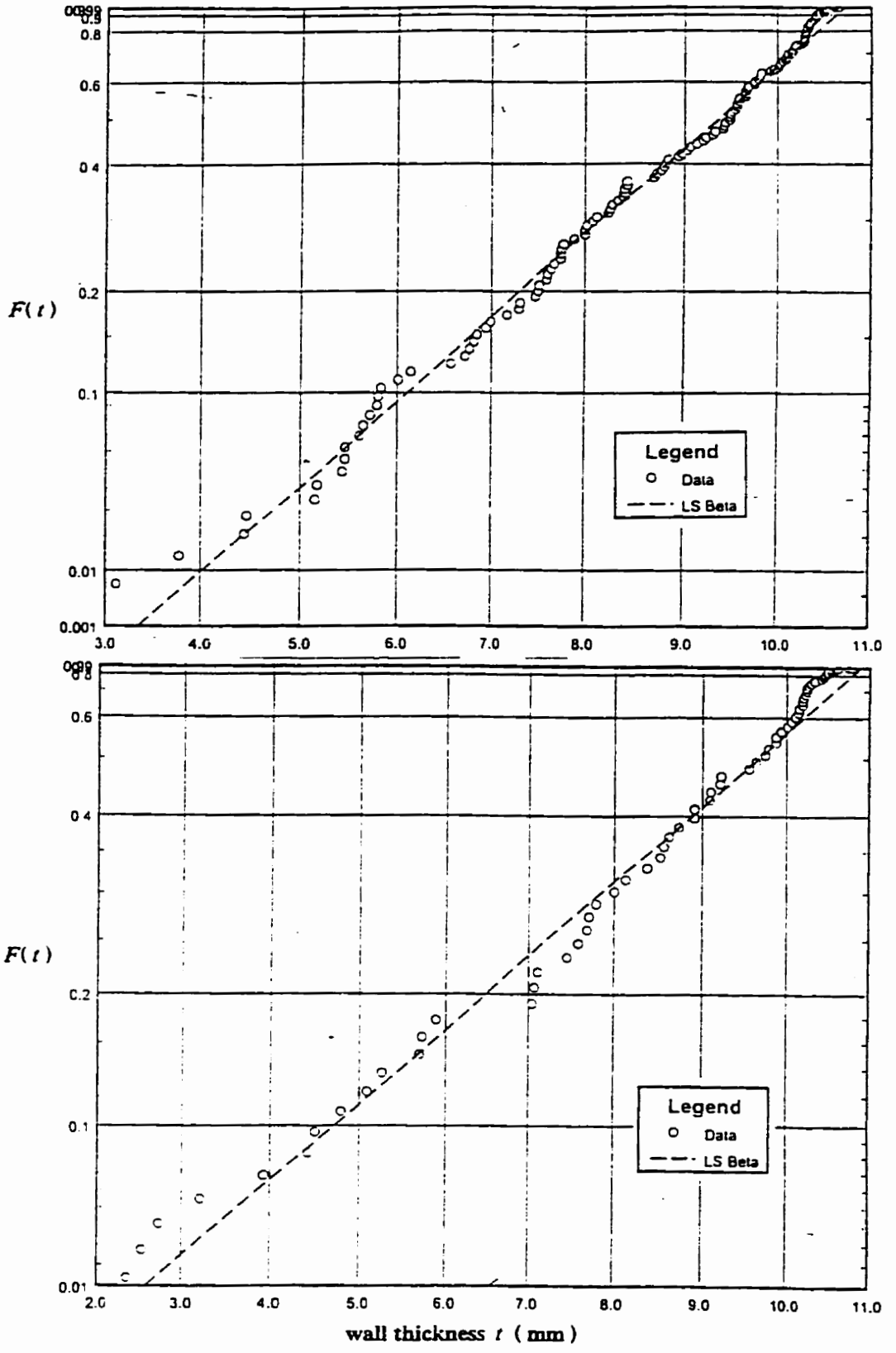

Figure 7.1 Distribution of wall thickness for two cross-sections of 8" pipe

Appendix A PIPEXSC.EXE users guide

A.1 Introduction

Appendix A is a users guide for the program PIPEXSC.EXE, which determines the probabilistic descriptions of deteriorating pipe cross-section using the method described in Chapter 2. The user interface for entering the data is presented in detail. Examples of the various types of output files which can be created using the program are also presented and discussed.

A.2 Types of analysis performed by the program PIPEXSC.EXE

Figure A.1 shows a simplified flowchart of the program PIPEXSC.EXE. There are three types of analysis that can be executed by the program:

- **Type 1: Analysis for single case** - This option performs a number of simulations of a single cross-section, characterized by $\overline{t_{avg}}$, $\overline{t_{min}}$ (or $\overline{t_{min(1)}}$ to $\overline{t_{min(4)}}$) and V_{min}. It includes statistical analysis of the simulated results describing section modulus, recording the mean, standard deviation, COV, skewness coefficient, and the maximum and minimum value of S/S_o encountered during all simulations. For this option Loop 3 shown in Figure A.1 goes through the number of simulations, while Loop 1 & 2 are not active.

- **Type 2: Analysis for multiple cases** - This option creates a number of tables containing statistical measures of S/S_o for a particular type of the pipe. This is essentially the previous option run a number of times to cover all requested combinations of $\overline{t_{avg}}$ and $\overline{t_{min}}$. For this option Loop 1 changes $\overline{t_{avg}}$ from the specified minimum value of $\overline{t_{min}}$ to the specified maximum value of $\overline{t_{avg}}$, Loop 2 changes $\overline{t_{min}}$ from the specified minimum value of $\overline{t_{avg}}$ to the current $\overline{t_{avg}}$ value, and Loop 3 goes through the number of simulations.

- **Type 3: Time dependent analysis of single cross-section** - This option determines the statistical measures of S/S_o with time, based on user-defined deterministic corrosion rates for average section loss and for pitting. The changes of $\overline{t_{avg}}$ and $\overline{t_{min}}$ (or $\overline{t_{min(1)}}$ to $\overline{t_{min(4)}}$) with time are calculated. For every new set of average and minimum wall thicknesses, the analysis for single cross-section is performed. This procedure is repeated until $\overline{t_{min}}$ (or the smallest of $\overline{t_{min(1)}}$ to $\overline{t_{min(4)}}$) reaches 0. For this option, Loop 1 is not active, Loop 2 changes $\overline{t_{min}}$, and Loop 3 goes through the number of simulations.

A.3 Data Input

The data for the analysis of the section modulus of deteriorated pipe cross-sections are entirely supplied through the keyboard input. The input is organized into a number of

screen menus which are related as shown in Figure A.2.

A.3.1 Main menu

Figure A.3 shows the main menu of the program, which organizes the input of data. The program can be only run from the main menu. The selections 1-6 are common for all types of analyses. For simulation of single cross-sections (Type 1), selection item 7 allows specification of the output file as shown in Figure A.3. For time-dependent analysis of a single cross-section (Type 3), item 7 allows input of corrosion rates. For creating tables of statistical data for a number of sections (Type 2), item 7 is not used.

A.3.2 Type of analysis

Figure A.4 shows the selection menu for type of type of analysis. There are three types of analysis, as previously discussed in Section A.2. The current (or default) selection is marked with the asterisk (*).

A.3.3 Type of pipe cross-section model

Figure A.5 shows the selection menu for the model of deteriorated pipe cross-section. All ten models described in Chapter 2 are available for the analysis Type 1 and 3. For the Type 2 analysis, which is the generation of tables containing statistical parameters of the

S/S_o distribution, only models 1 - 5 are available. The current (or default) selection is marked with the asterisk (*).

A.3.4 Simulation and cross-section data entry

Figures A.6 - A.8 show selection menus for the simulation and cross-section data entry. The menu varies depending on the type of analysis and the cross-section model. The submenu for models *Type 1* and *2* is shown in Figure A.6 and the submenu for models *Type 3* and *4* is shown in Figure A.7. These two submenus are not encountered if the tables of statistical analysis results, Analysis Type 2, are specified. The submenu used in this case is shown in Figure A.8. At the top of each menu the currently selected (or default) pipe cross-section model is displayed. For model types 6 through 10 the order of the entries, shown in Figure A.7, for the minimum thickness specified for each quadrant ($\overline{t_{min(1)}}$ to $\overline{t_{min(4)}}$) is counterclockwise. All other prompts in each selection menu are self-explanatory, and the default values shown in brackets indicate the required format of the input data, either integer or real numbers.

A.3.5 Supplementary data

Figure A.9 shows the selection menu allowing the specification of some model-specific data. The menu shown is an example which applies only to the model *Type 4* cross-sections with the analysis carried out on a quadrant-by-quadrant basis. For the model *Type 3* cross-sections the applicable selections are 3 - 6. For the model *Type 2* cross-

sections, the applicable selections are 1 - 4. The supplementary data for the model *Type 1* cross-sections is not shown. The current (or default) selection is marked with the asterisk (*).

A.3.6 Measurement error

Figure A.10 shows the selection menu for the user-defined measurement error of the minimum and average wall thickness. The measurement errors are entered as fractions of the nominal wall thickness t_o. The default is no measurement errors.

A.3.7 Output file destination

Figure A.11 shows the menu which allows optional storage of results to the floppy drive.

A.3.8 Corrosion rates

The time-dependent (Type 3) analysis requires corrosion rates defining both the average wall thickness loss and the pitting rate. Figure A.12 shows the outside corrosion rate specification menu. Two models of corrosion, linear and nonlinear, are allowed by the program. A similar menu is displayed if the model of the cross-section allows both inside and outside corrosion of the pipe wall. The corrosion rates used are deterministic quantities.

A.3.9 Output specification

The output specification is only an option for the analysis of a single cross-section (Type 1). The first menu, shown in Figure A.13, allows the user to limit the size of the output file. Selecting option 3 reduces the output file size because intermediate calculations, which are not essential, are not included.

The output specification menu provides an access to the submenu shown in Figure A.14. This allows the user to specify an optional output, which consists of a detailed record of S/S_o, written to a file named SROT.DAT, and /or the data allowing the plot of simulated cross-sections, written to a file named XSEC.DAT. If either output option (SROT.DAT or XSEC.DAT) is requested, the simulations which are to be included in the optional output are specified using the menu shown in Figure A.15.

A.4 Output files

Figure A.16 shows a flowchart of various output files which can be created by the program. Some of the output files can be used as input data files for further analysis using either the C-fit (CFER, 1996) software or MS Excel. However, in most cases subsequent analyses will require postprocessing of the results obtained from PIPEXSC.EXE using one of the three short postprocessing routines, PROCESS1.EXE, PROCESS2.EXE, or PROCESS3.EXE, as identified in the figure.

A.4.1 Results of the single cross-section (Type 1) analysis

There are four output files which can be created as the result of the single cross-section (Type 1) analysis. Two files, named PIPE.OUT and PIPE.TXT, constitute the basic output. The other two files, named SROT.DAT and XSEC.DAT, are optional as described in Section A.3.9. The simulated pipe cross-section is characterized by a single set of the average and minimum pipe wall thicknesses, and other user-specified features allowed by the program.

A.4.1.1 PIPE.OUT

PIPE.OUT has slightly different format for a part of the output depending on the type of model used for simulations. An example of the PIPE.OUT output file obtained for the model *Type 2a* is shown in Figure A.17. Segment 1 echoes the input data, Segment 2 lists the detailed results of statistical analysis for each simulation, and Segment 3 summarizes statistics for all simulations using equations presented in Section 2.3.5.

For different models of pipe cross-section, Segment 2 will be different. Figure A.17(a) shows Segment 2 of the output for cross-section model *Type 1*, with uniform corrosion along the pipe circumference. The column headings use symbols that are defined in Figure 2.6. Similarly, Figure A.17(b) shows Segment 2 of the output for model *Type 3* cross-section, and A.17(c) shows Segment 2 of the output for a model *Type 4* cross-section. The symbols in the column headings are defined in Figure 2.6.

Segments 1 and 3 are not optional parts of the output for single cross-section (Type 1) analysis. However, the printing of Segment 2 is optional, and it can be either printed in full, or partly, or not at all. The output specification menu shown in Figure A.13 refers to Segment 2, which for the selection 1 is printed in full, for the selection 2 Segment 2 contains intermediate results for a specified range of simulations, and for the selection 3 Segment 2 is not printed at all.

A.4.1.2 PIPE.TXT

PIPE.TXT stores the following results of all simulations:

- mean S/S_o
- standard deviation of S/S_o
- random value of t_{min} (or $t_{min(1)}$ in the case of model *Type 3* and *4*)
- random value of t_{avg}

If PIPE.TXT is processed using the program PROCESS1.EXE, the files PMEAN.TXT, PSTDEV.TXT, PTAVG.TXT, and PTMIN.TXT are created. The format of these files is suitable for import to C-fit (CFER, 1996), a statistical analysis software package. Using C-fit, distributions of the mean and the standard deviations of S/S_o can be investigated. C-fit can also be used to investigate whether the routines used to generate pipe wall thicknesses in PIPEXSC.EXE are performing properly.

A.4.1.3 SROT.DAT

SROT.DAT is an optional output file which stores the variation of S/S_o due to the unknown orientation of the applied bending moment vector. The results can be stored for up to 50 simulations. Once the file is processed using PROCESS2.EXE, the following files are created:

- SROTALL.TXT. This is a text file which contains all calculated S/S_o for up to 50 simulations, where a number of orientations of the applied bending moment is considered for each simulation. SROTALL.TXT has appropriate format to be imported to C-fit.

- ROTS1.TXT - ROTS5.TXT. Up to five files can be created, each containing the detailed results for a single simulation. If detailed results for more than five simulations are needed, SROT.DAT can be processed a number of times, and different simulations can be chosen for the content of files ROTS1.TXT - ROTS5.TXT. The format of ROTS1.TXT - ROTS5.TXT allows analysis using C-fit.

- EXCEL1.TXT. This is a text file containing the same information as SROTALL.DAT. The format of the file is such that plots of the S/S_o variation for each simulation can be easily obtained using MS Excel. This procedure requires only opening of the file EXCEL1.TXT using MS Excel with "comma" specified as the delimiter. Once the file is opened in Excel, the standard plotting functions are used.

A.4.1.4 XSEC.DAT

This optional file allows plotting of the user-specified simulated pipe cross-sections. XSEC.DAT stores information for up to 12 simulations. There are four simple steps involved in obtaining sampled plots of pipe cross-section:

- XSEC.DAT is processed using the program PROCESS3.EXE, and, depending on the number of simulations stored, text files EXCEL21.TXT and EXCEL22.TXT are created. The file EXCEL22.TXT is only created if the number of stored simulations is greater than 6.

- EXCEL21.TXT, or EXCEL22.TXT, is opened in MS Excel using "comma" as the delimiter.
- a specially-prepared MS Excel spreadsheet program, XSEC.XLS, is opened next. It requires that cross-sections are simulated using N = 360 circumferential points or elements.

- the content of EXCEL21.TXT, or EXCEL22.TXT, is copied to the first sheet of XSEC.XLS, and the plots of cross-sections automatically appear on the second sheet of XSEC.XLS

Figures A.18 to A.21 show plots of simulated pipe cross-sections using all ten models, shown in Figure 2.6, for the analysis. The following nomenclature is adopted for designation of plotted pipe cross-sections:

- Model *Type 1* cross-sections - there are only two options as shown in Figure 2.6. model *Type 1a* has outside corrosion only and model *Type 1b* has outside corrosion only.

- Model *Type 2* cross-sections - there are six options. The first letter refers to the specific corrosion pattern with a = outside, b = inside and c = both, as shown in Figure 2.6. The second letter specifies the order of elements with c = in order of increasing thickness, and r = random order.

- Model *Type 3* cross-sections - there are four options. The first letter refers to the specific corrosion pattern, with a = outside and b = inside, as shown in Figure 2.6. The second letter specifies the location of pits within quadrants, with c = pits centered and r = pits randomly placed.

- Model *Type 4* cross-sections - there are 12 options. The first letter refers to the specific corrosion pattern, with a = outside, b = inside and c = both, as shown in Figure 2.6. The second letter specifies the order of elements, with c = in order of increasing thickness and r = random order. The third letter specifies the location of pits within quadrants, with c = pits centered and r = pits randomly placed.

A.4.2 Results of the analysis for Statistical Tables (Type 2)

Output files, PIPETAB.OUT and PIPETAB.TXT, are created for the Type 2 analysis, which involves simulation and analysis of section moduli data for various sets of minimum and the average thicknesses of the deteriorated pipe cross-section. The results of the analysis provide a complete description of the cross-section modulus for the specific type of pipe.

A.4.2.1 PIPETAB.OUT

Output file, PIPETAB.OUT, provides statistical results of a number of simulations performed for a range of the average and the minimum wall thickness values, with each possible combination of $\overline{t_{min}}$ and $\overline{t_{avg}}$ considered in the analysis. An example of the PIPETAB.OUT output file is shown in Figure A.22. The analysis results of are printed out in the form of triangular matrices. The first part of the output echoes the data used in the analysis. The second part, which contains six tables labelled 1-6, lists the statistical parameters. Table 1 gives the mean value of mean S/S_o calculated for a number of simulations (μ) with the standard deviation of mean value (σ_3) shown in brackets. Table 2 shows the square root of the mean variance of S/S_o (σ_4), with the standard deviation of the square root of the mean variance of S/S_o (σ_5) shown in brackets. Table 3 gives the maximum values of S/S_o (b) encountered during simulations for a particular set of $\overline{t_{avg}}$ and $\overline{t_{min}}$, with the minimum value (a) encountered shown in the brackets. Table 4 and 5 give COV and the skewness coefficient respectively. Table 6 lists fractions of

simulated cross-section from the total number of simulations performed for each set of $\overline{t_{avg}}$ and $\overline{t_{min}}$, for which the minimum random pipe wall thickness was equal to 0 (perforation). This last table is meaningful only if the specified error of $\overline{t_{min}}$ is greater than 0.0.

A.4.2.2 PIPETAB.TXT

PIPETAB.TXT is a text file listing all results included in the PIPETAB.OUT output file. One use of PIPETAB.TXT file is to facilitate plotting of results using MS Excel. The file can be opened in Excel using "comma" as the delimiter, and plots of various statistical measures can be obtained using standard plotting routines. The second, very important use of PIPETAB.TXT file is to supply data for the simplified reliability analysis program (discussed in Appendix B). An example of the PIPETAB.TXT file, corresponding to PIPETAB.OUT shown in Figure A.22, is shown in Figure A.23.

A.4.3 Results of the time-dependent analysis of a section (Type 3)

The Type 3 analysis allows the investigation of a particular pipe cross-section subjected to corrosion. The corrosion rates, defined by the user, are assumed to be deterministic. Simulations of pipe cross-sections are conducted in discrete time intervals. At the beginning of each time interval, pitting corrosion is assumed to cause the minimum wall thickness to reduce by 1mm. This type of analysis can be carried out manually using tabulated results from the Type 2 analysis previously discussed. However, for

convenience, Type 3 analysis was included in the program. The Type 3 analysis can also be used as a mean of comparison between models, for example models *Type 2* and *4* can be investigated to assess the effect of having more data describing the pipe cross-section on its deteriorating strength.

A.4.3.1 PIPEVAR.OUT

PIPEVAR.OUT is a primary output of the Type 3 analysis. The first part of the output lists the input data used in the analysis, while the second part provides tabulated results of statistical analysis of simulated pipe cross-sections. An example of the file is shown in Figure A.24.

A.4.3.2 PIPEVAR.TXT

PIPEVAR.TXT is a text file, which echoes the results contained in the file PIPEVAR.OUT. The purpose of the file is to allow plot of the variation of statistical measures with time. PIPEVAR.TXT can be opened in MS Excel using "comma" as the delimiter. Plots of the mean S/S_o, standard deviation of S/S_o etc. versus time can then be obtained using standard plotting routines.

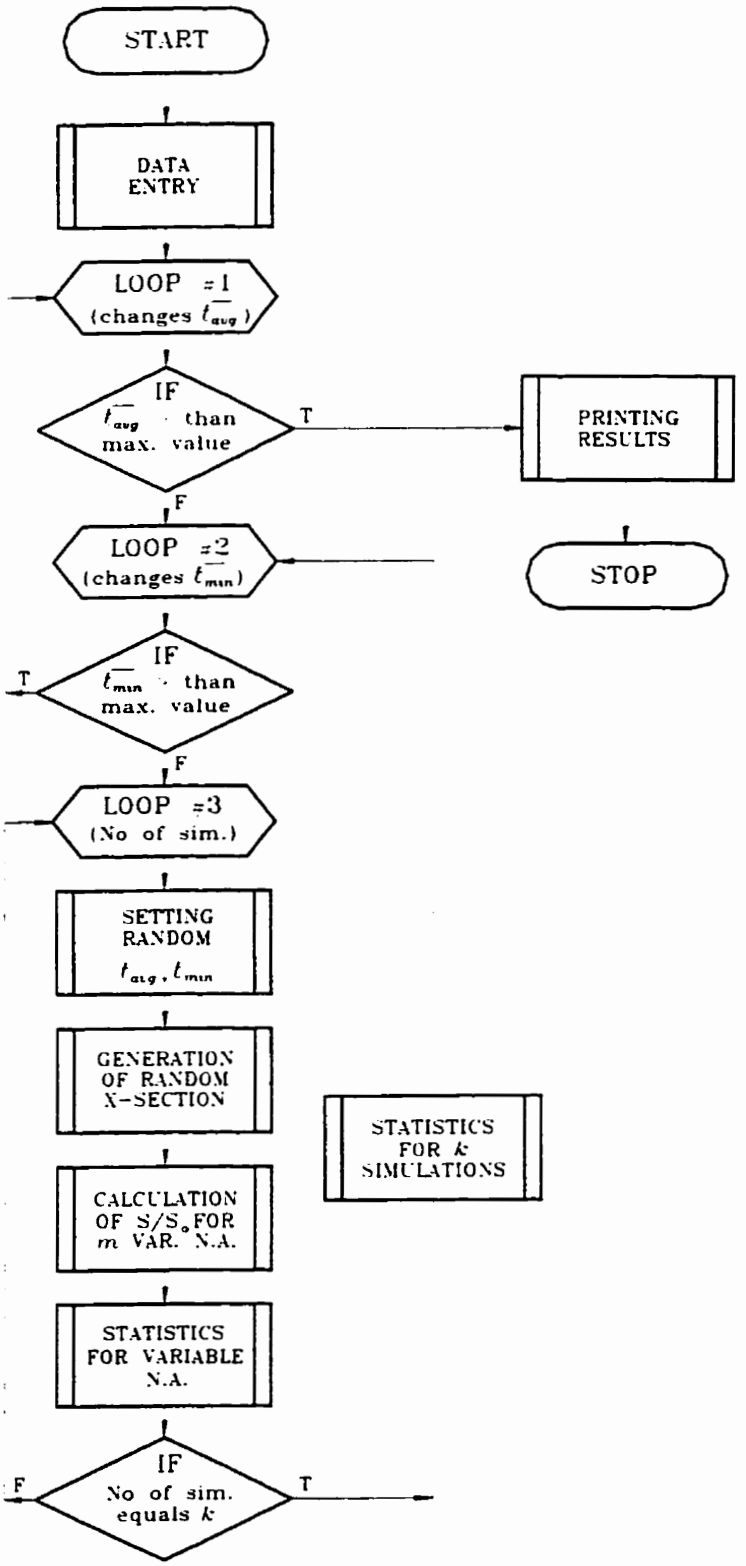

Figure A.1 Simplified flowchart of the program PIPEXSC.EXE

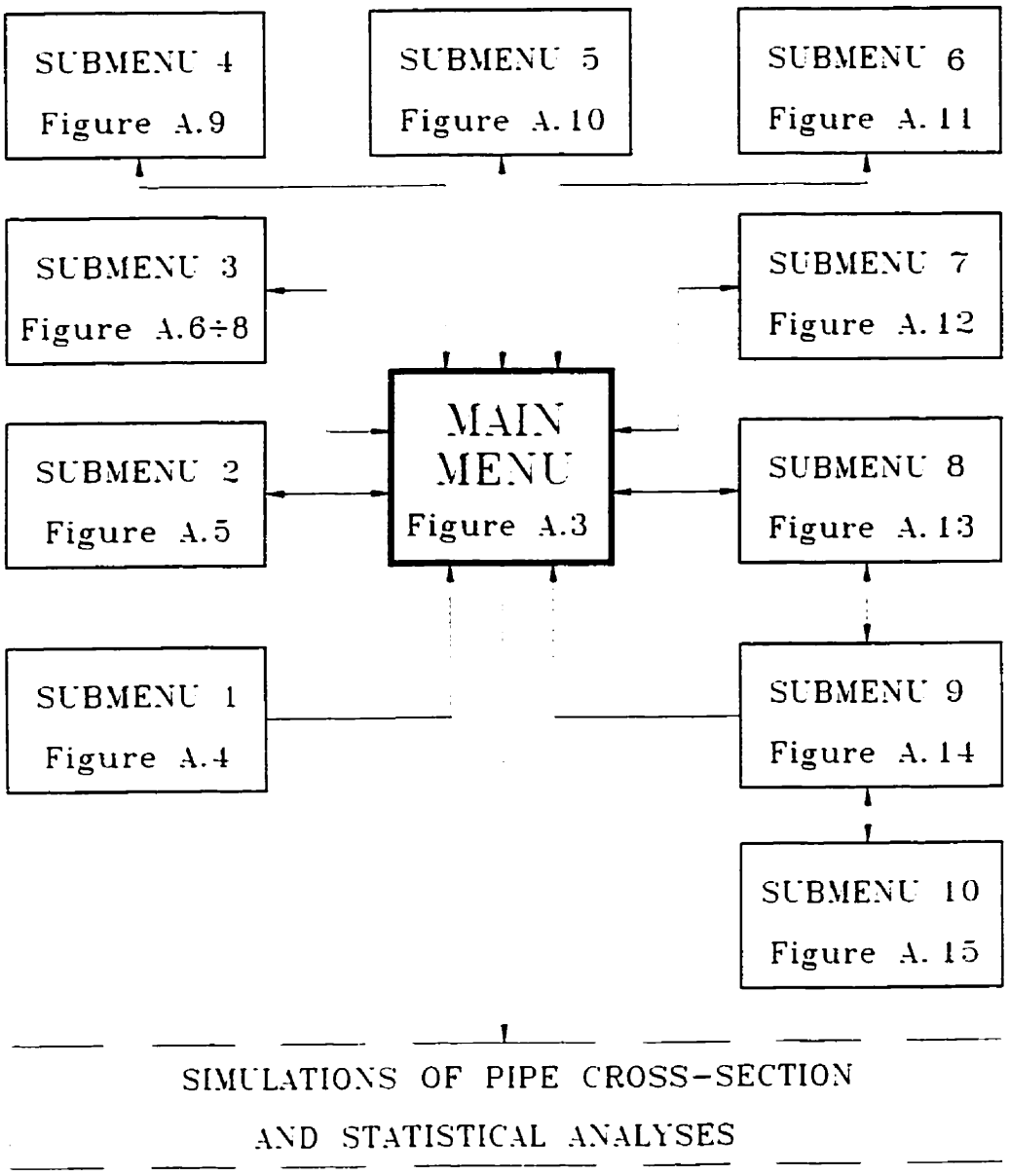

Figure A.2 Organization of data input menus in the program PIPEXSC.EXE

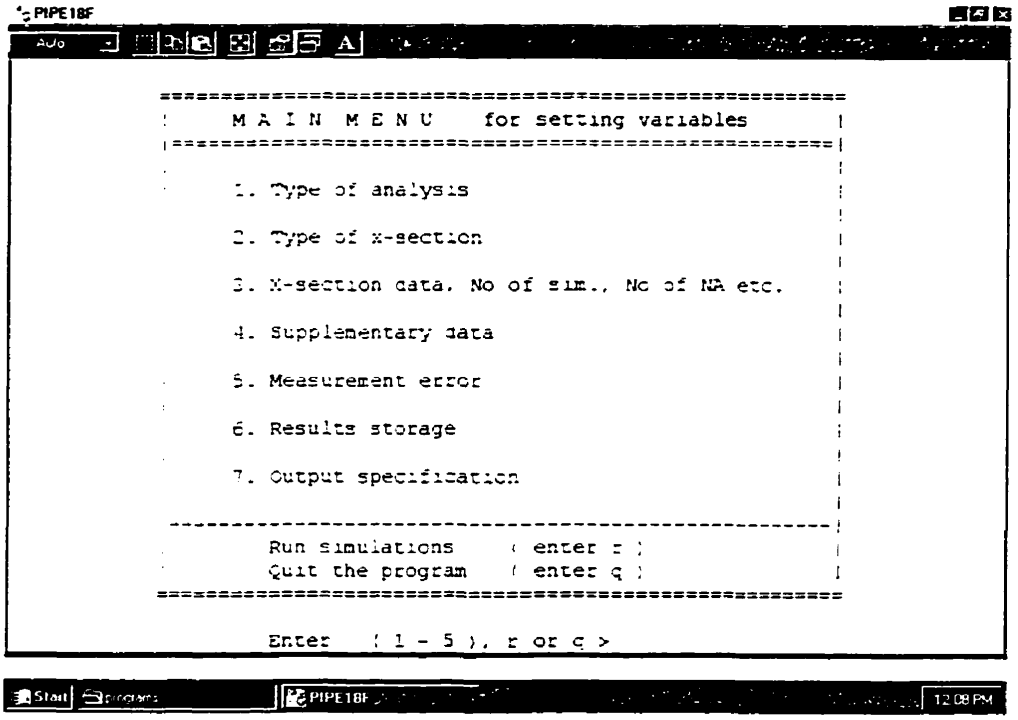

Figure A.3 Main menu - Choice of submenus for specific data entry

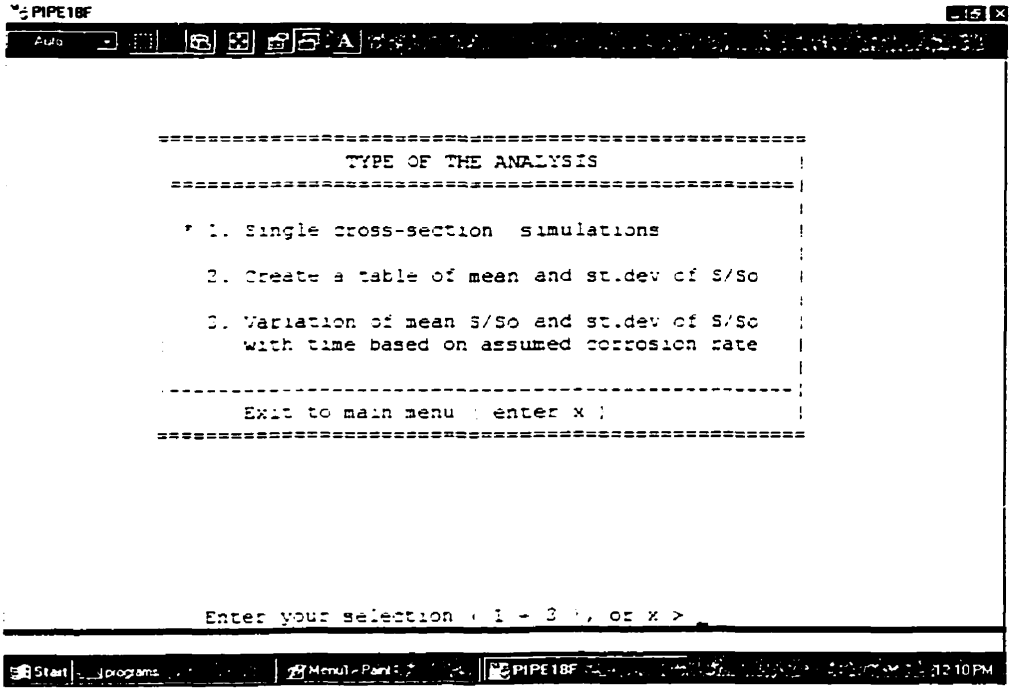

Figure A.4 Submenu 1 - Type of analysis

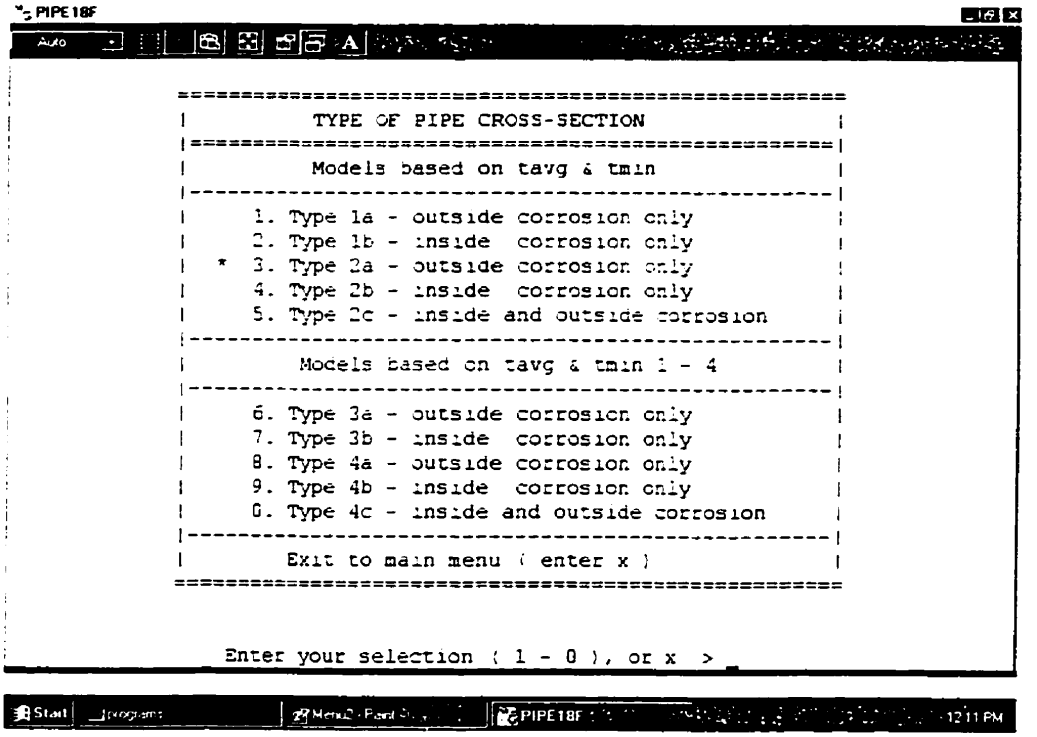

Figure A.5 Submenu 2 - Type of pipe cross-section model

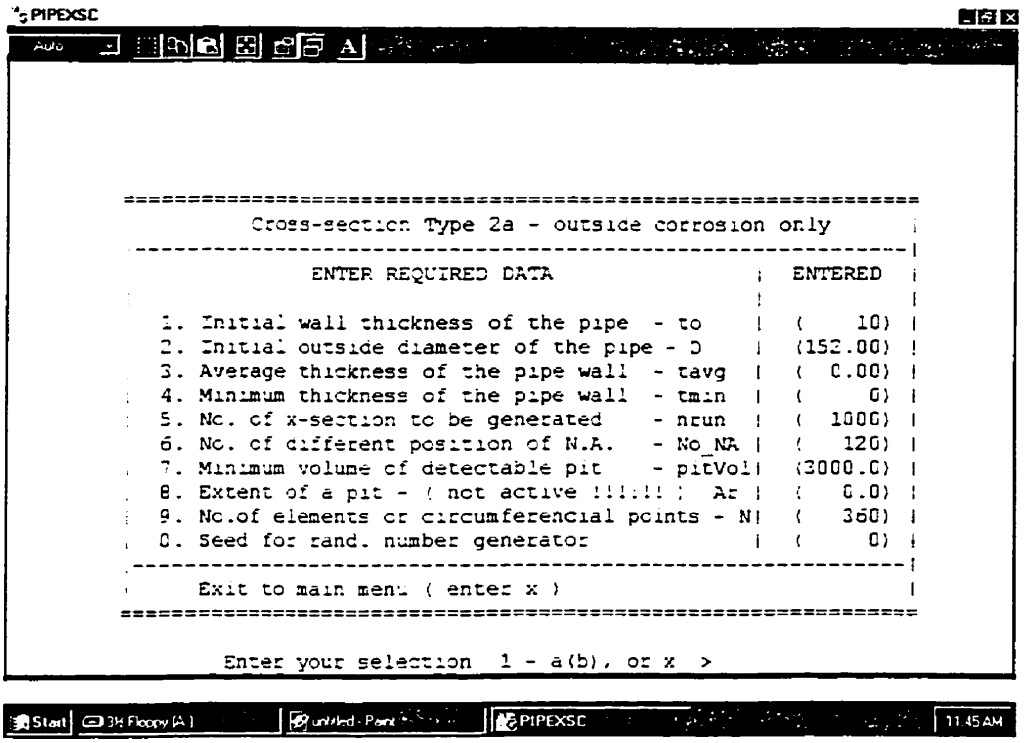

Figure A.6 Submenu 3 - Simulation and cross-section data (models *Type 1* and *2*)

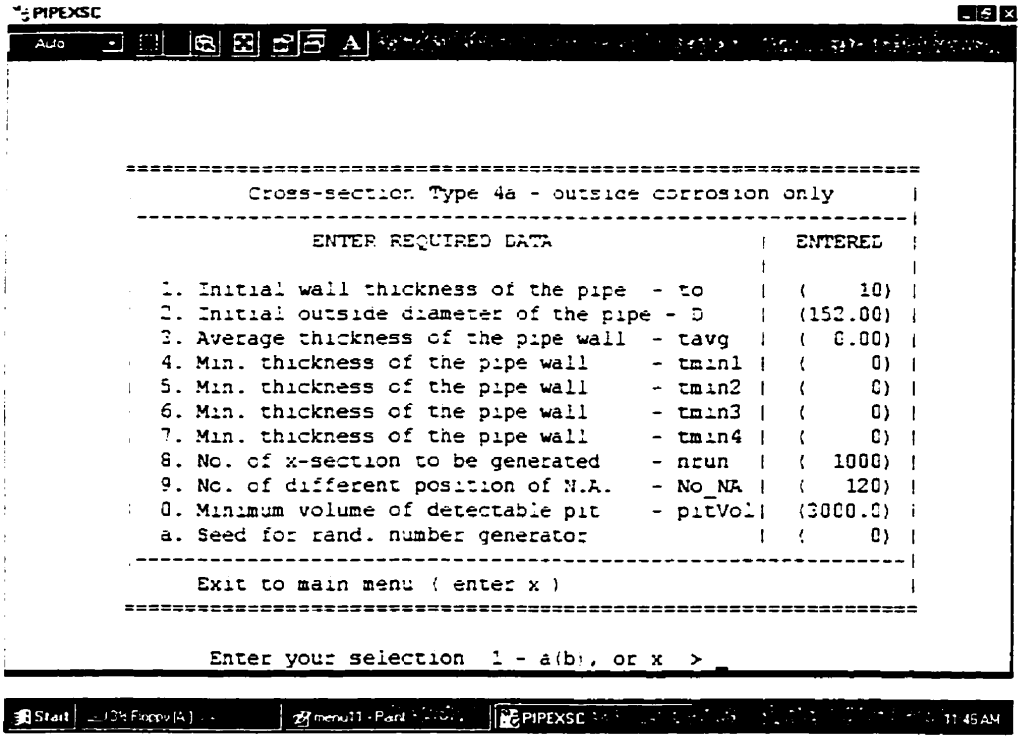

Figure A.7 Submenu 3 - Simulation and cross-section data (models *Type 3* and *4*)

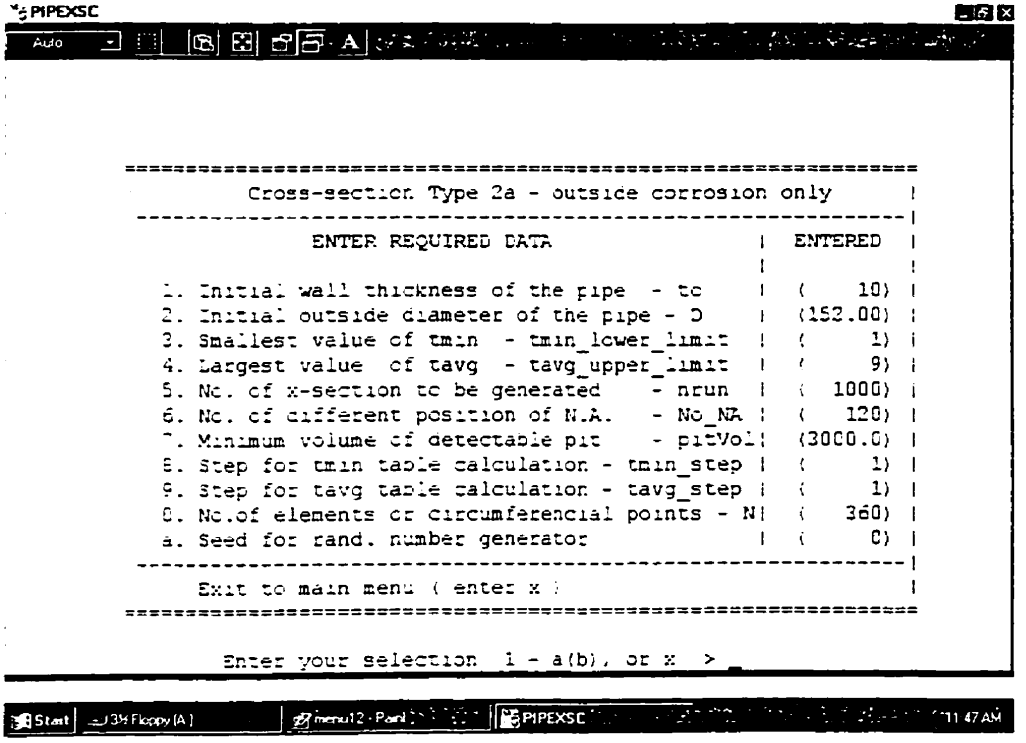

Figure A.8 Submenu 3 - Simulation and cross-section data (generation of tables)

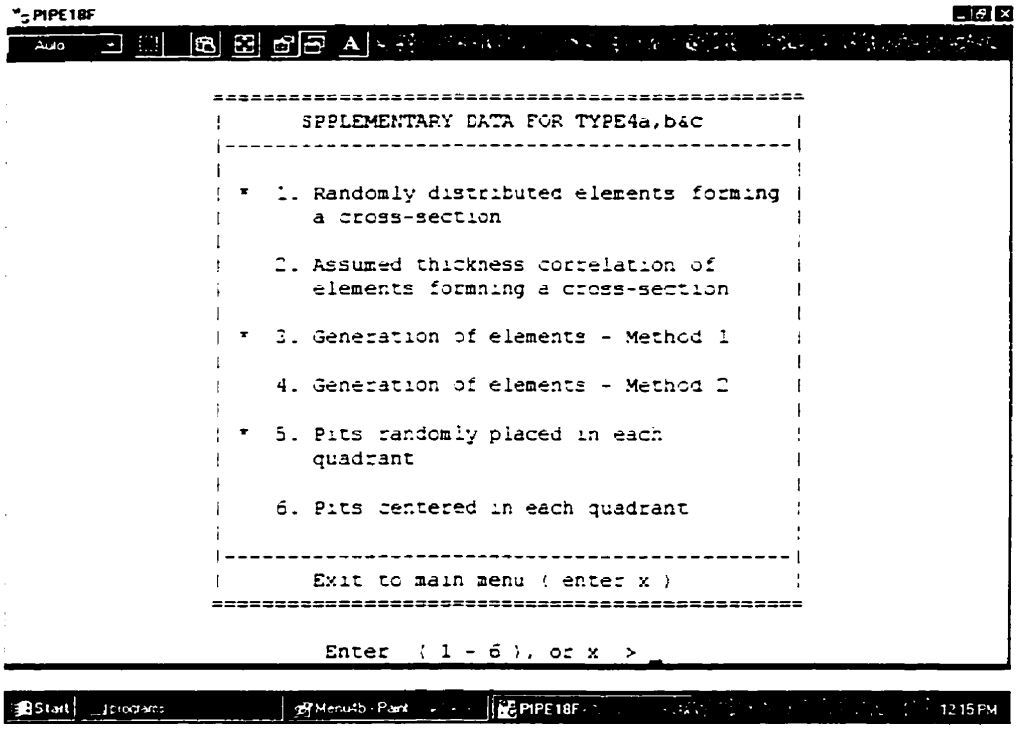

Figure A.9 Submenu 4 - Supplementary model and simulation data

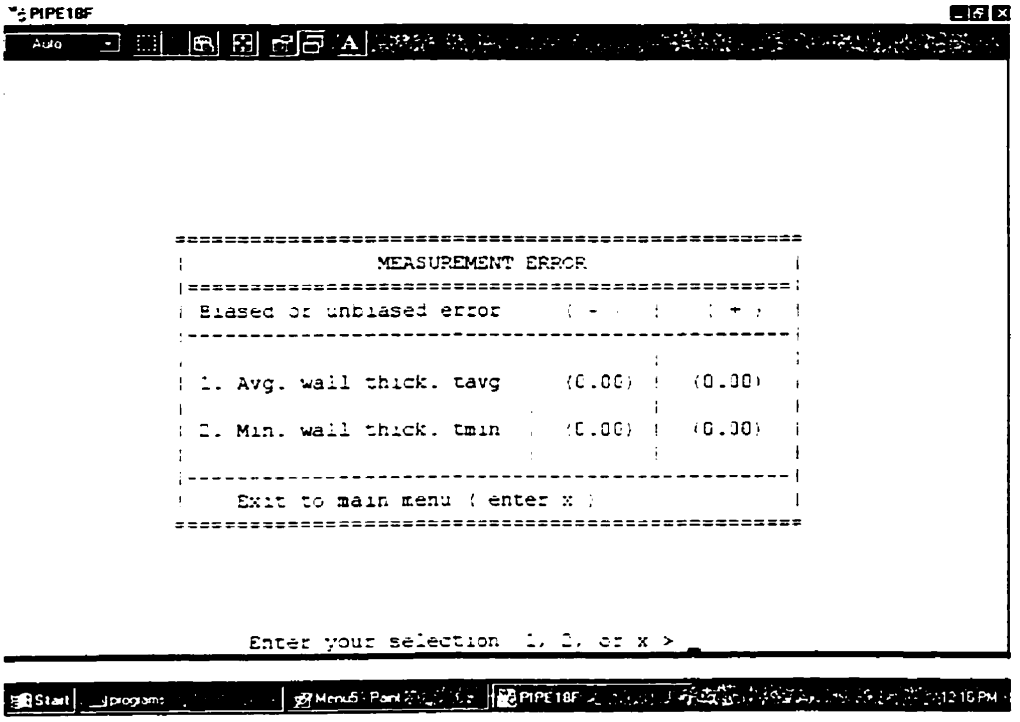

Figure A.10 Submenu 5 - Measurement error

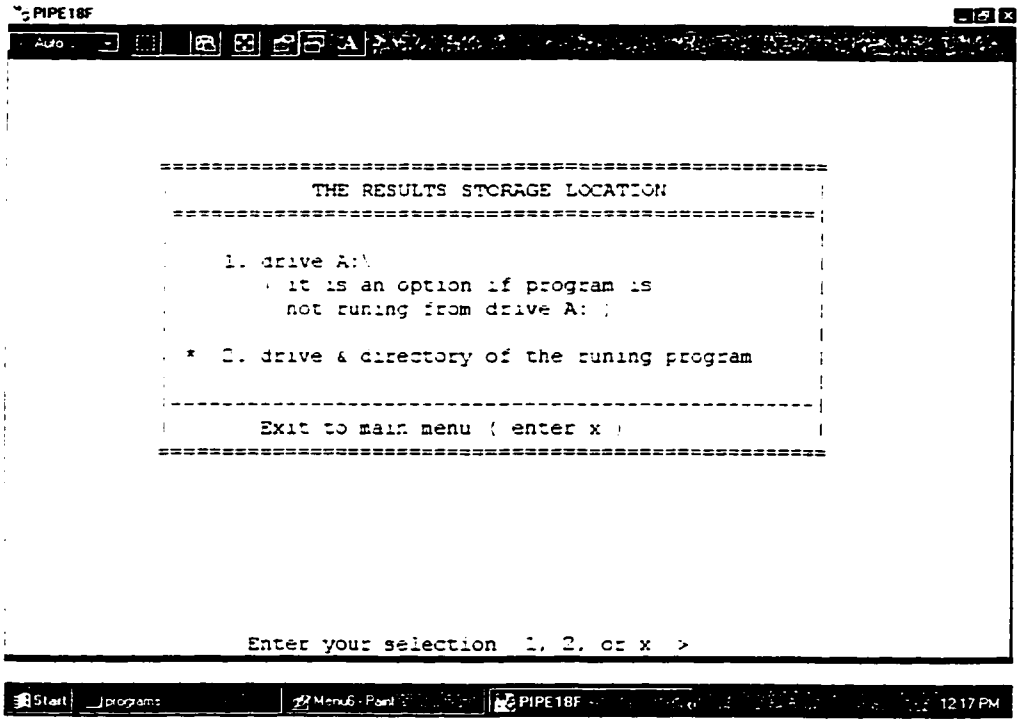

Figure A.11 Submenu 6 - Results storage

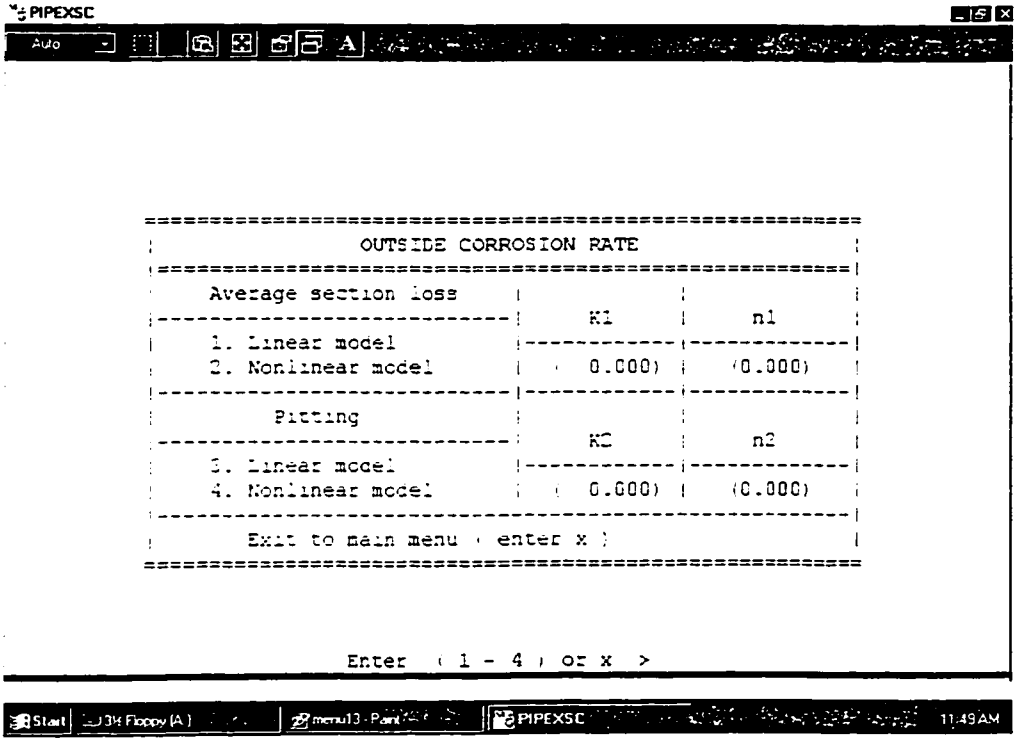

Figure A.12 Submenu 7 - Deterministic corrosion rate models

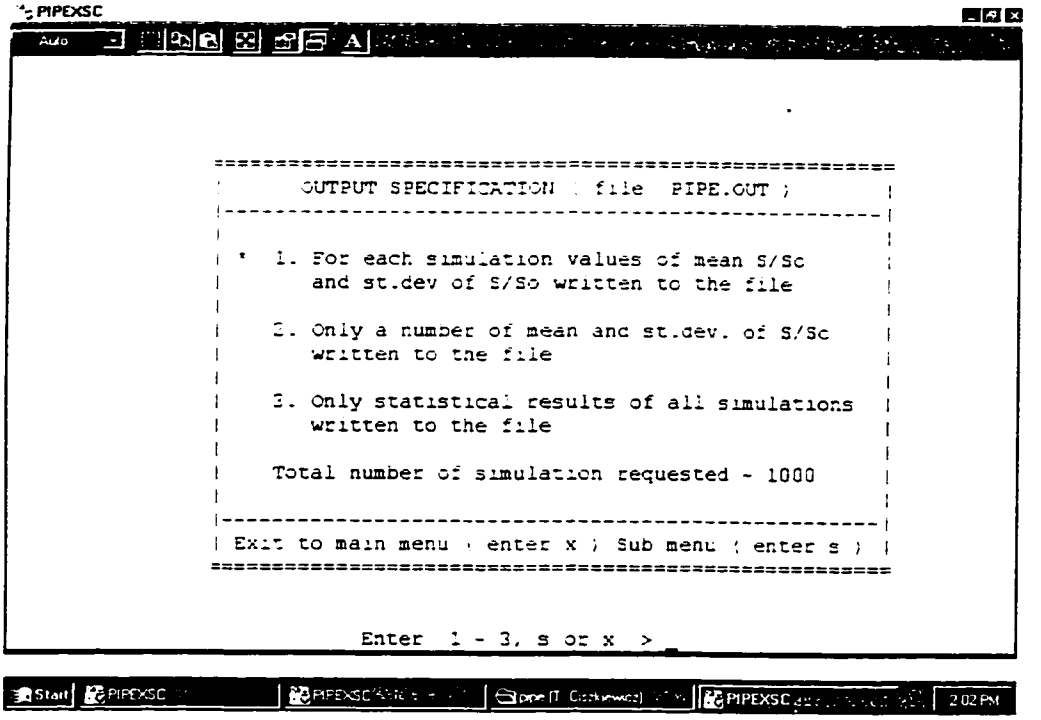

Figure A.13 Submenu 8 - Specification of the results written to the output file (Type 1 analysis only)

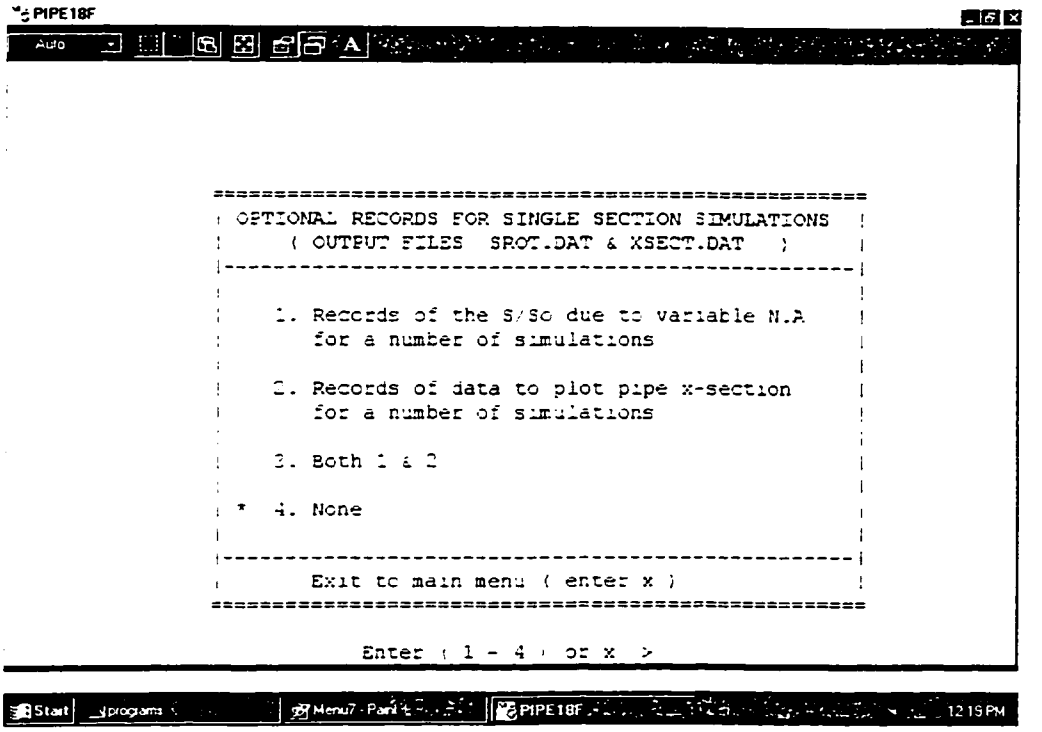

Figure A.14 Submenu 9 - Optional output specification

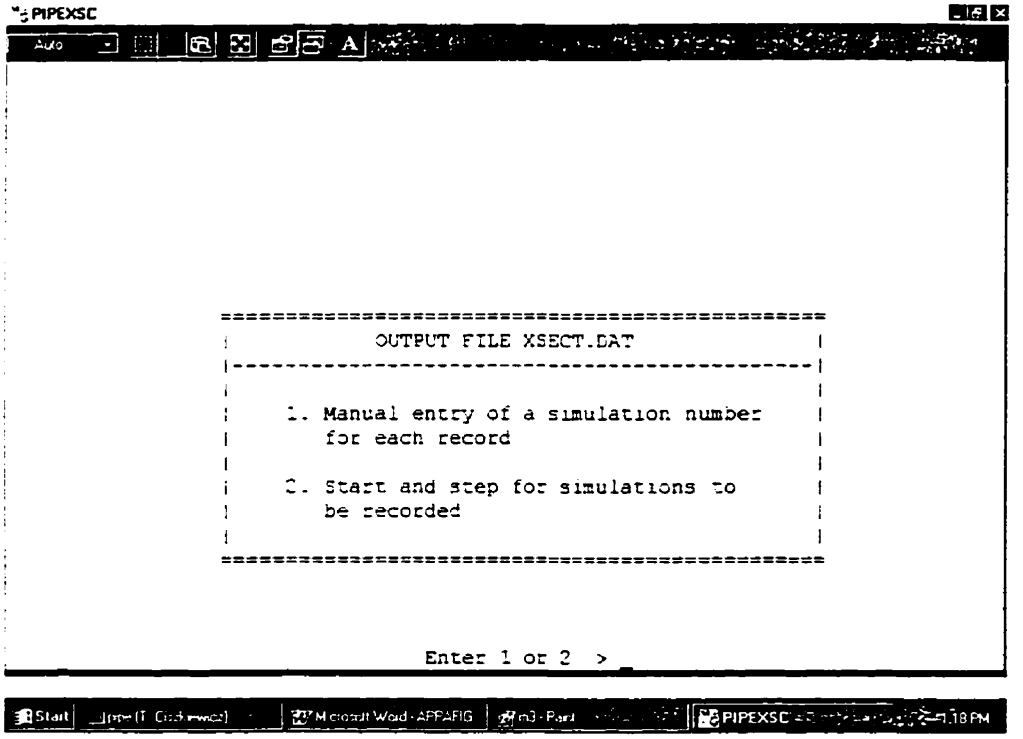

Figure A.15 Submenu 10 - Specification of simulations to be recorded

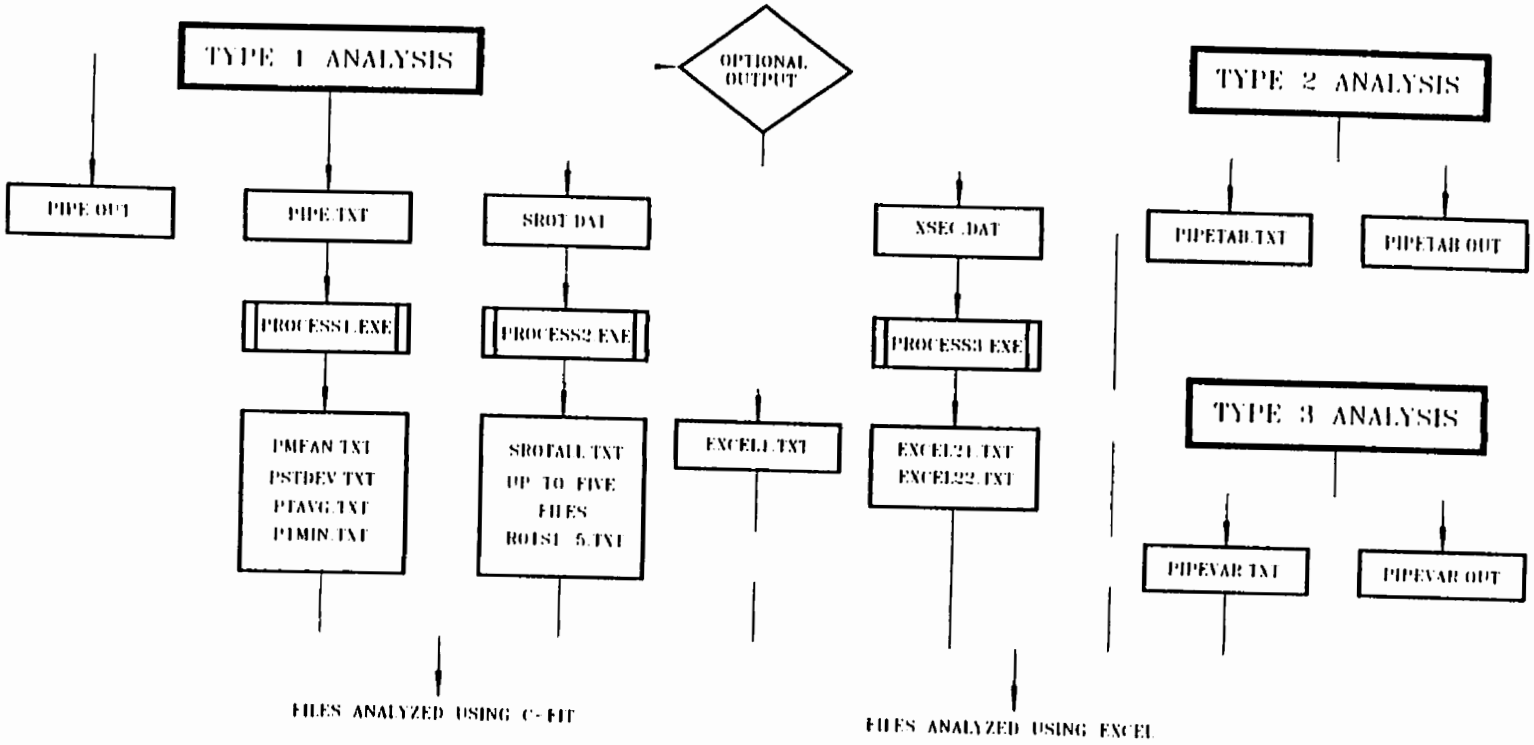

Figure A.16 Output files created by the program PIPEXSC.EXE

Segment 1

```
RESULTS OF CALCULATIONS
**********************************************************

Cross-section Type 1a - outside corrosion only

Data:
  to =  10   mm,       D =  1512.00mm
tavg =  7.50mm,    tmin =   3   mm
assumed exact measurements of tavg
assumed exact measurements of tmin
No. of N.A positions considered =    90
Total number of simulation      =  1000
Number of elements used         =   360
Assumed thickness correlation between elements
distributed along the circumference
Elements chosen using METHOD 1

So =  148682.5mm^3
```

Segment 2

simu. No	mean S/So	st.dev S/So	tavg	tmin	tavg calc.
1	0.715	0.101	7.5	3.0	7.5
2	0.715	0.099	7.5	3.0	7.5
3	0.716	0.097	7.5	3.0	7.5
4	0.717	0.094	7.5	3.0	7.5
1000	0.718	0.096	7.5	3.0	7.5

Segment 3

STATISTICAL MEASURES

TABLE 1	mean S/So	st.dev. of S/So
mean value	0.715	0.101
st. dev.	0.001	0.003
max. value	0.718	0.105
min. value	0.711	0.094

TABLE 2	COV	skew. coeff.
mean value	0.141	-0.516
st. dev.	0.004	0.005
max. value	0.151	-0.497
min. value	0.130	-0.532

Figure A.17 Output file PIPE.OUT for single cross-section simulations

TABLE 3	min. value	max. value
S So	0.528	0.839

Fraction of perforated sections = 0.000

END OF THE OUTPUT FILE

Figure A.17 (contd) Output file PIPE.OUT for single cross-section simulations

simu. No	mean S/So	st.dev S So	X (rad)	tavg	tmin	trem
1	0.733	0.025	0.3	7.5	3.0	7.7
2	0.732	0.044	0.6	7.5	3.0	8.0
3	0.707	0.120	1.8	7.5	3.0	9.3
4	0.723	0.087	1.2	7.5	3.0	8.6
1000	0.721	0.095	1.3	7.5	3.0	8.7

Figure A.17 (a) Example of Segment 2 for model *Type 1* cross-section

sim. No	mean S/So	st.dev S/So	X1	X2	X3	X4	tmin 1	tmin 2	tmin 3	tmin 4	tavg	trem
1	0.678	0.027	0.36	0.69	0.63	0.33	4.0	5.0	3.0	2.0	7.5	9.3
2	0.748	0.045	0.75	0.44	0.33	0.46	4.0	5.0	3.0	2.0	7.5	9.3
3	0.688	0.028	0.77	0.43	0.37	0.45	4.0	5.0	3.0	2.0	7.5	9.4
4	0.799	0.035	0.37	1.01	0.40	0.43	4.0	5.0	3.0	2.0	7.5	9.5
1000	0.716	0.049	0.58	0.40	0.78	0.32	4.0	5.0	3.0	2.0	7.5	9.5

Figure A.17 (b) Example of Segment 2 for model *Type 3* cross-section

sim. No	mean S/So	st.dev S/So	tmin 1	tmin 2	tmin 3	tmin 4	tavg	tavg calc
1	0.681	0.030	3.0	4.0	5.0	3.0	7.0	7.0
2	0.680	0.046	3.0	4.0	5.0	3.0	7.0	7.0
3	0.679	0.048	3.0	4.0	5.0	3.0	7.0	7.0
4	0.679	0.045	3.0	4.0	5.0	3.0	7.0	7.0
1000	0.680	0.045	3.0	4.0	5.0	3.0	7.0	7.0

Figure A.17 (c) Example of Segment 2 for model *Type 4* cross-section

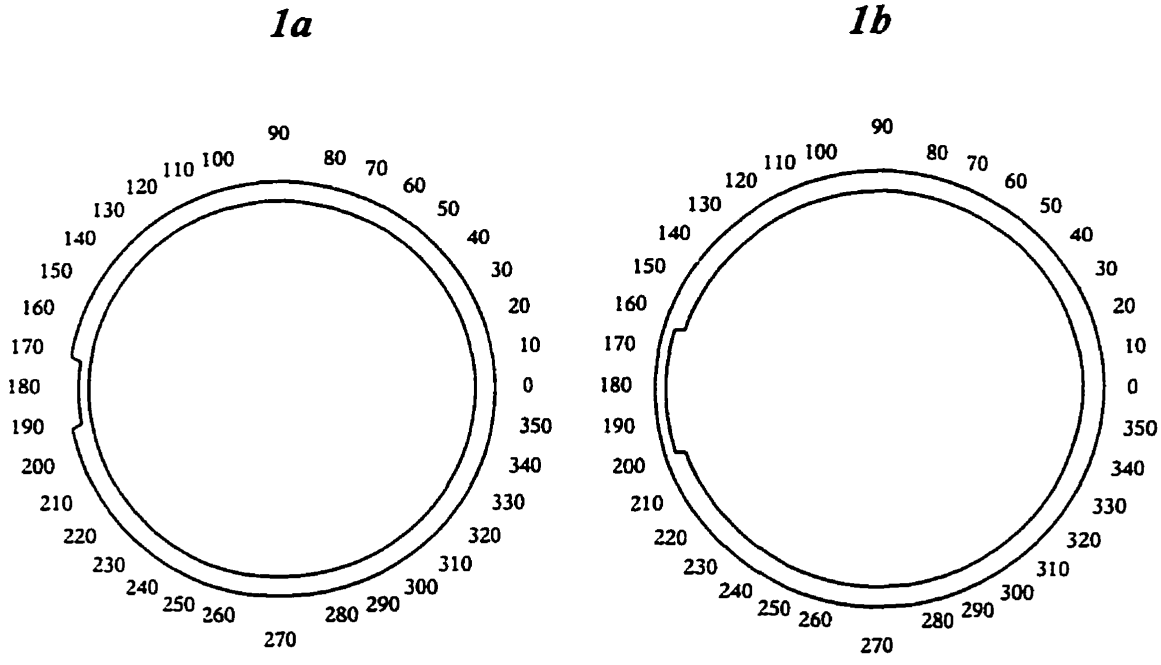

Figure A.18 Simulated pipe cross-sections - *Type 1* models

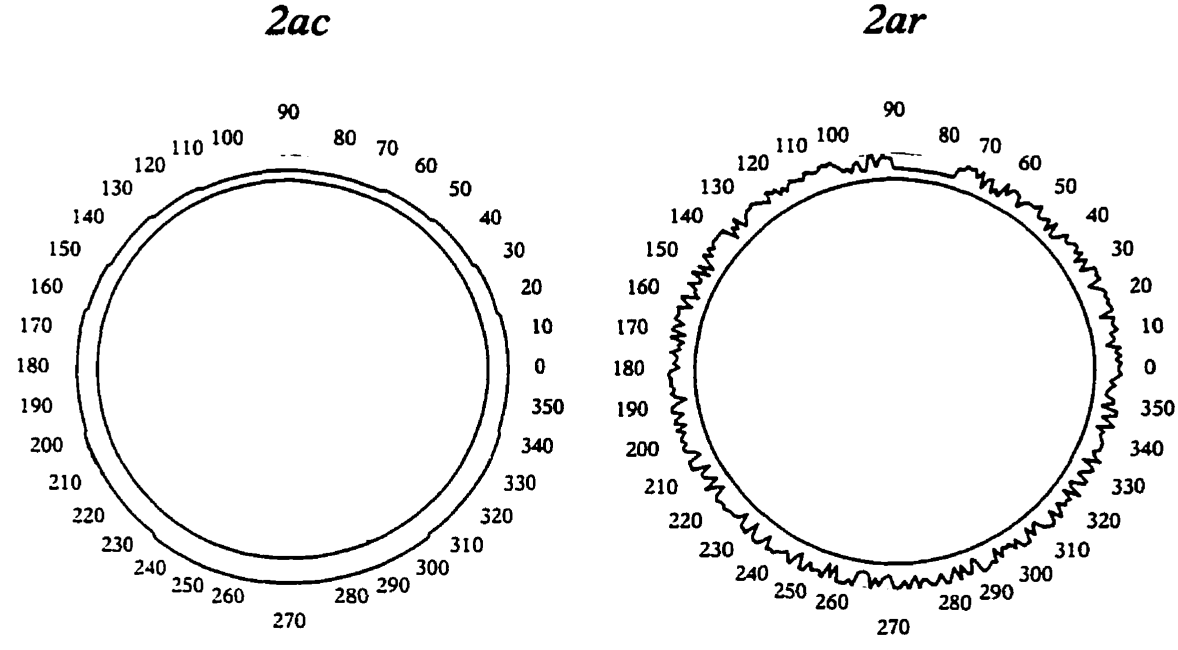

Figure A.19 Simulated pipe cross-sections - *Type 2* models

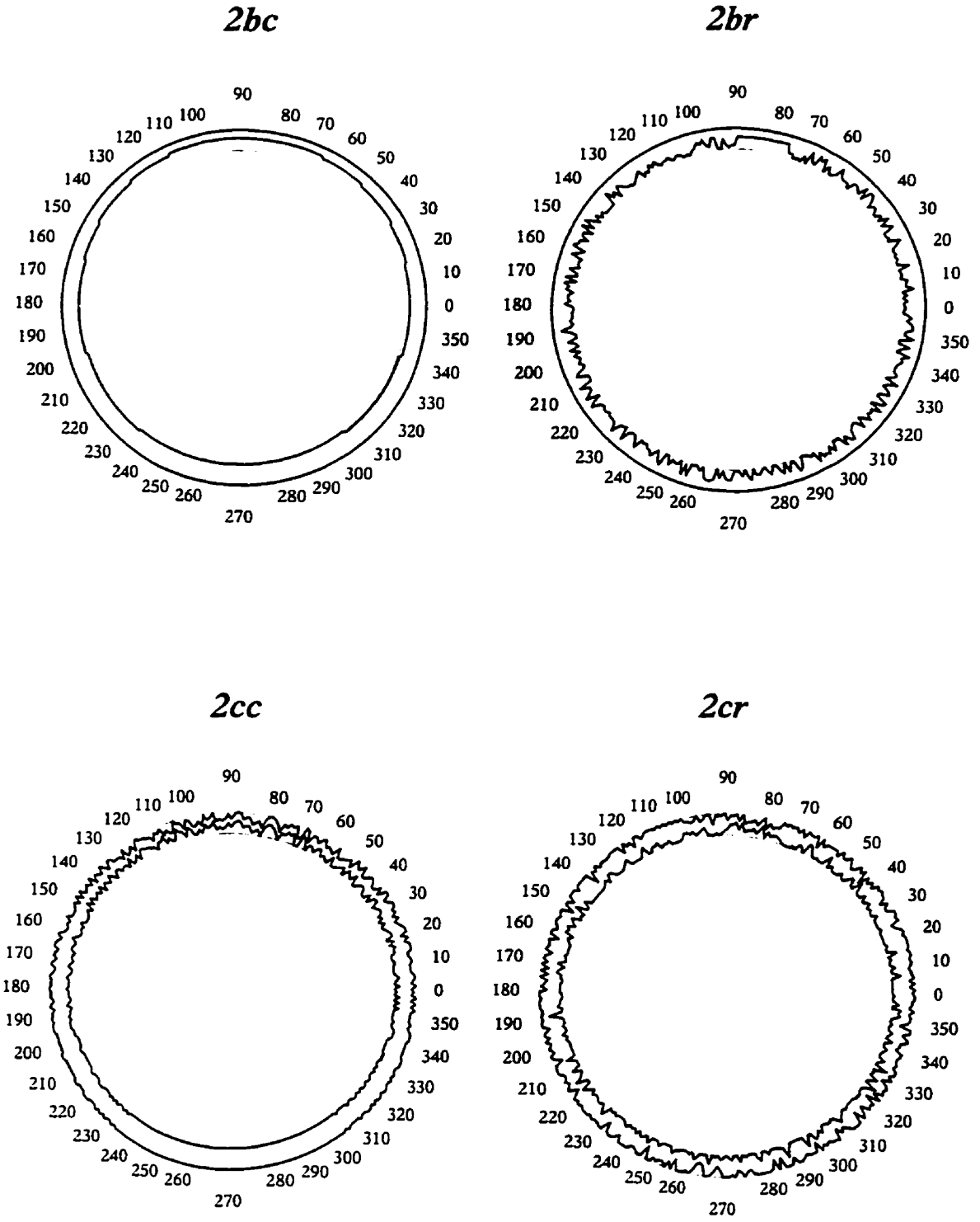

Figure A.19(contd) Simulated pipe cross-sections - *Type 2* models

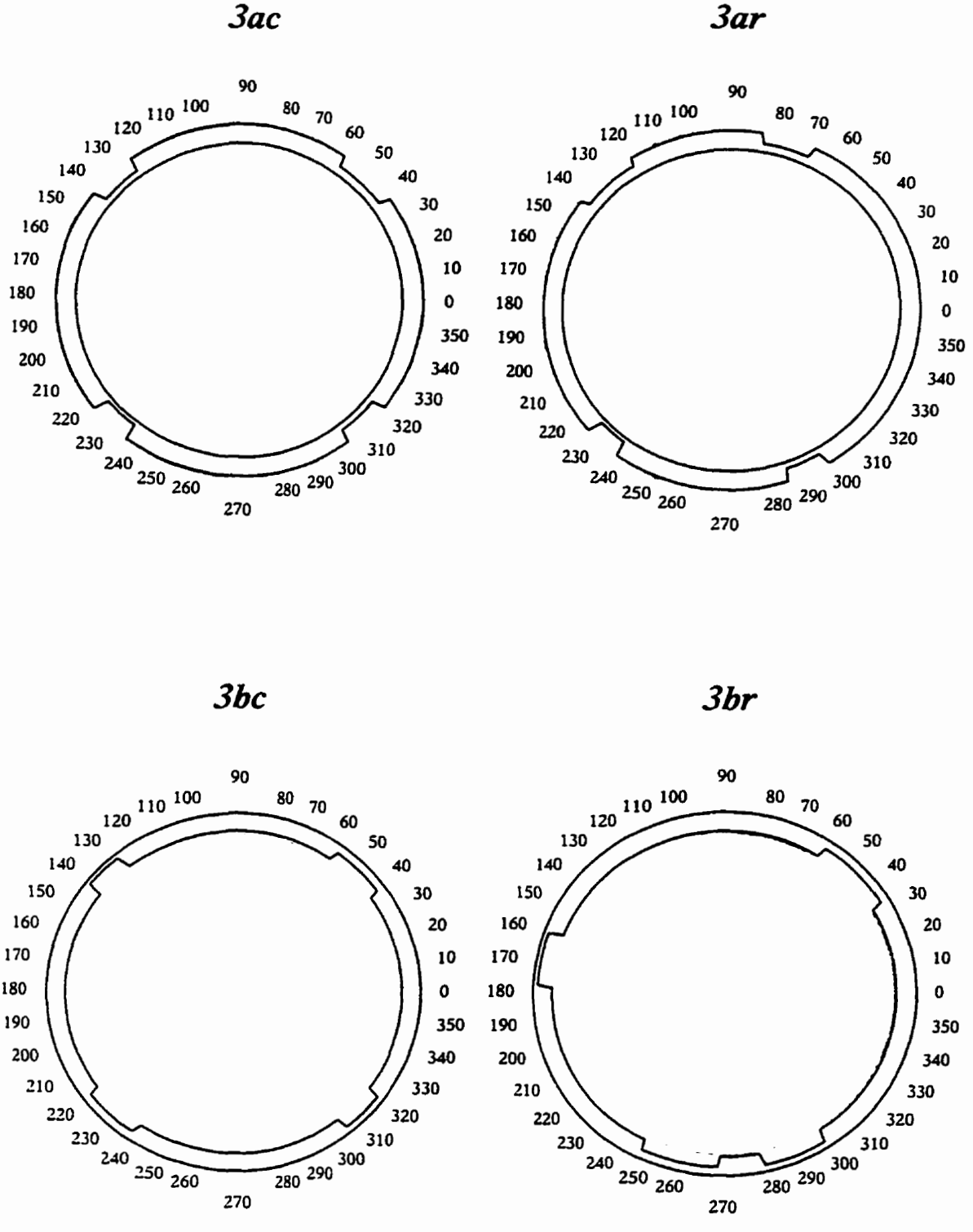

Figure A.20 Simulated pipe cross-sections - *Type 3* models

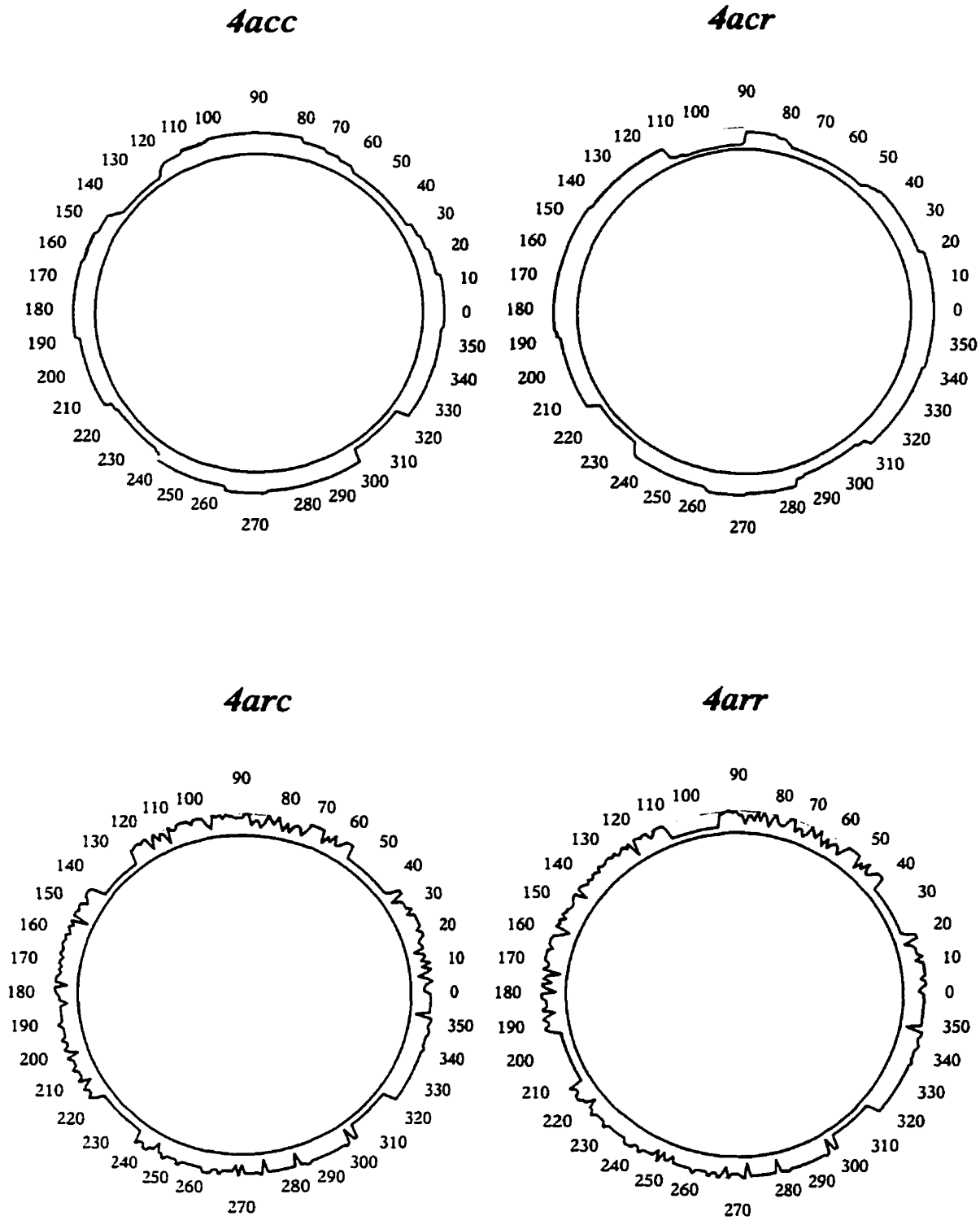

Figure A.21 Simulated pipe cross-sections - *Type 4* models

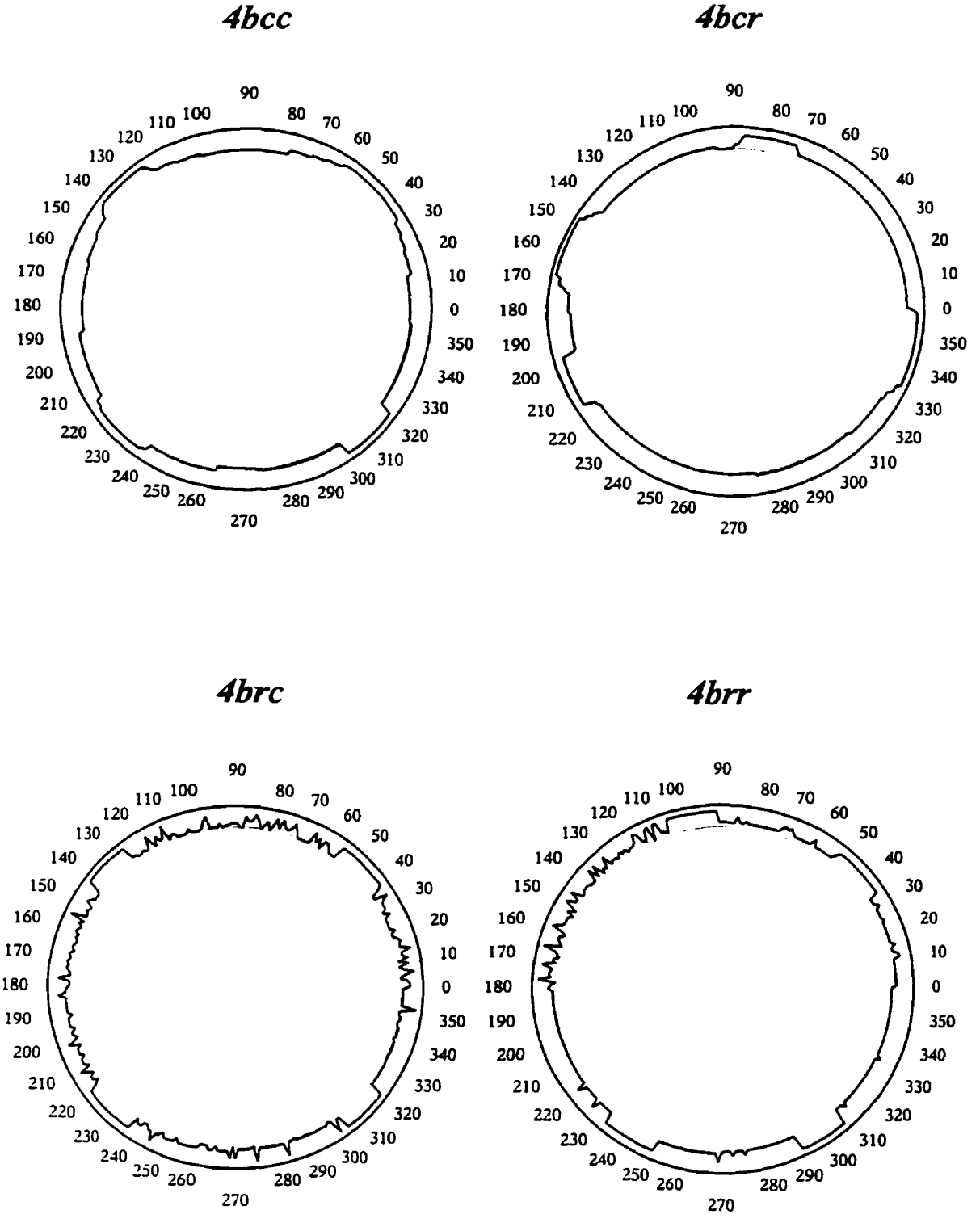

Figure A.21(contd) Simulated pipe cross-sections - *Type 4* models

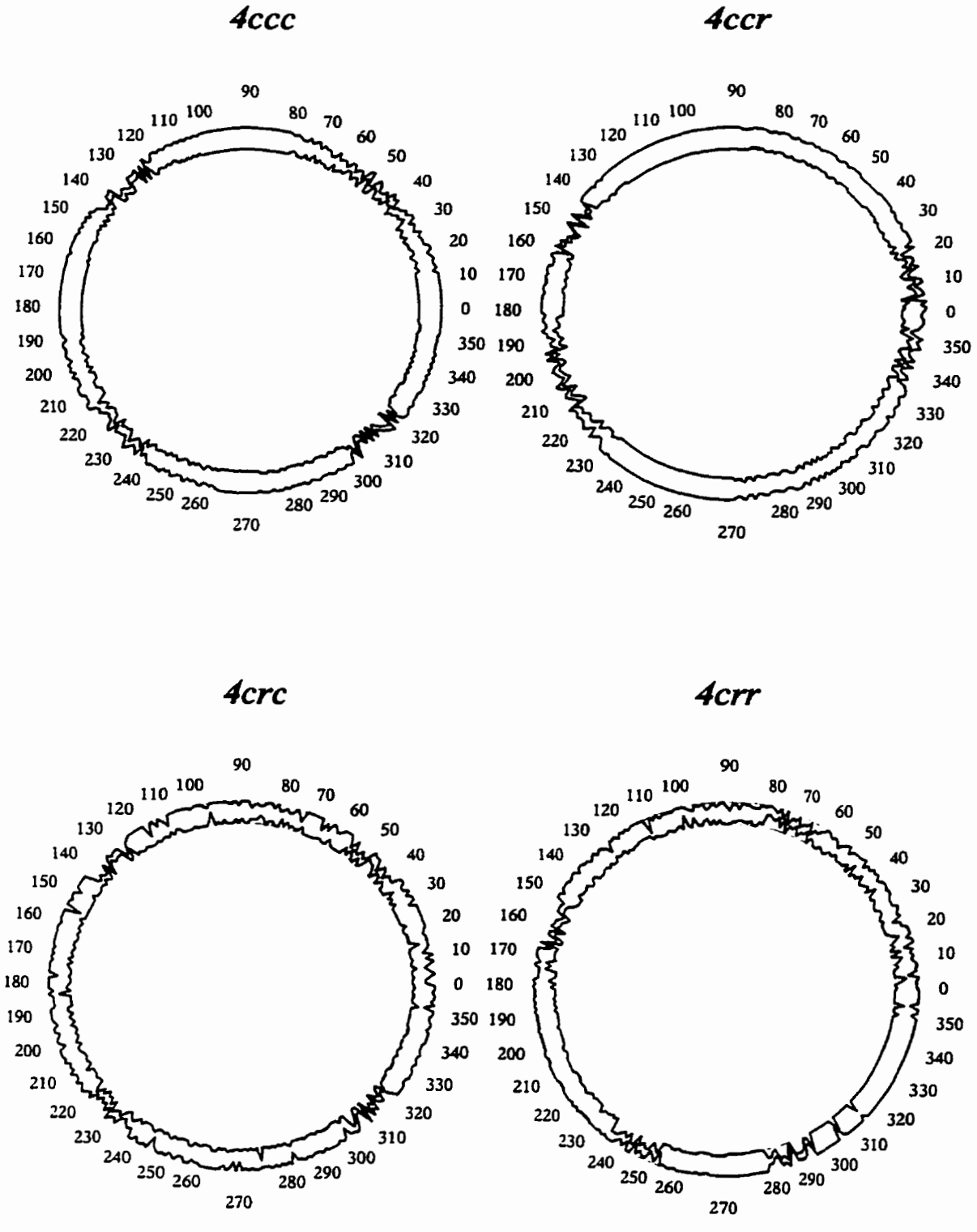

Figure A.21(contd) Simulated pipe cross-sections - *Type 4* models

```
 RESULTS OF CALCULATIONS
 ***********************************************************

 Cross-section Type 2a - outside corrosion only

 Data:
   tc = 10 mm,      D = 152.00 mm
 assumed exact measurements of tavg
 assumed exact measurements of tmin
 No. of N.A positions considered =    90
 Total number of simulation      =  1000
 Number of elements used         =   360
 Assumed thickness correlation between elements
 distributed along the circumference
 Elements chosen using METHOD 1

 Sc =  148682.5mm^3

 ****************************************
 TABLE 1 - MEAN VALUES OF S/Sc
 ****************************************

                      tmin
      ------------------------------------------------------------------
 tavg |  1.0  |  2.0  |  3.0  |  4.0  |  5.0  |  6.0  |  7.0  |  8.0  |  9.0
 -----|-------------------------------------------------------------------
  1.0 | 0.094
 -----|(0.000)
  2.0 | 0.174| 0.189
 -----|(0.001)|(0.000)
  3.0 | 0.254| 0.275| 0.285
 -----|(0.002)|(0.001)|(0.000)
  4.0 | 0.342| 0.360| 0.375| 0.383
 -----|(0.002)|(0.001)|(0.001)|(0.000)
  5.0 | 0.438| 0.452| 0.465| 0.476| 0.48
 -----|(0.003)|(0.002)|(0.001)|(0.001)|0.000
  6.0 | 0.544| 0.552| 0.560| 0.569| 0.577| 0.582
 -----|(0.002)|(0.002)|(0.001)|(0.001)|(0.000)|(0.000)
  7.0 | 0.657| 0.660| 0.664| 0.668| 0.674| 0.679| 0.683
 -----|(0.002)|(0.002)|(0.001)|(0.001)|(0.001)|(0.000)|(0.000)
  8.0 | 0.773| 0.773| 0.774| 0.775| 0.777| 0.780| 0.783| 0.786
 -----|(0.001)|(0.001)|(0.001)|(0.001)|(0.001)|(0.000)|(0.000)|(0.000)
  9.0 | 0.886| 0.886| 0.886| 0.886| 0.886| 0.887| 0.887| 0.889| 0.890
 -----|(0.001)|(0.001)|(0.001)|(0.001)|(0.000)|(0.000)|(0.000)|(0.000)|(0.000)

 ****************************************
 TABLE 2 - MEAN VALUES OF STAND. DEV S/Sc
 ****************************************

                      tmin
      ------------------------------------------------------------------
 tavg |  1.0  |  2.0  |  3.0  |  4.0  |  5.0  |  6.0  |  7.0  |  8.0  |  9.0
 -----|-------------------------------------------------------------------
  1.0 | 0.000
 -----|(0.000)
  2.0 | 0.050| 0.000
 -----|(0.002)|(0.000)

 -----|(0.003)|(0.003)|(0.003)|(0.003)|(0.002)|(0.002)|(0.001)|(0.000)
  9.0 | 0.059| 0.058| 0.056| 0.054| 0.050| 0.046| 0.039| 0.028| 0.000
 -----|(0.003)|(0.003)|(0.003)|(0.002)|(0.002)|(0.002)|(0.001)|(0.001)|(0.000)
```

Figure A.22 Example of output file PIPETAB.OUT

```
**********************************************
 TABLE 3 - MAXIMUM AND MINIMUM VALUES OF S.Sc
**********************************************

                    tmin
      ---------------------------------------------------------------
 tavg|  1.0     2.0     3.0     4.0     5.0  |  6.0  |  7.0  |  8.0  |  9.0
-----|---------------------------------------------------------------
 1.0 |  0.094
-----|(0.094)
 2.0 |  0.278  0.189
-----|  0.123 (0.189)

-----|(0.601)(0.612)(0.614)(0.624)(0.650) 0.688  0.740  0.786
 9.0 |  0.961  0.962  0.957  0.954  0.947  0.940  0.929  0.931 | 0.890
-----|(0.760)(0.762)(0.768)(0.773)(0.784)(0.799) 0.812  0.843|(0.890)


*****************************************
 TABLE 4 - MEAN VALUES OF COV S.Sc
*****************************************

                    tmin
      ---------------------------------------------------------------
 tavg|  1.0     2.0  |  3.0     4.0     5.0     6.0     7.0     8.0  |  9.0
-----|---------------------------------------------------------------
 1.0 | 0.000
-----|(0.000)
 2.0 | 0.286  0.000
-----|(0.014)(0.000)

-----|(0.005)(0.004)(0.004)(0.003)(0.003)(0.002)(0.002)(0.000)
 9.0 |  0.067  0.065  0.064  0.061  0.057  0.050  0.044  0.032 | 0.000
-----|(0.004)(0.003)(0.003)(0.003)(0.003)(0.002)(0.002)(0.001)|(0.000)


***************************************************
 TABLE 5 - MEAN VALUES OF SKEWNESS COEFF. OF S.Sc
***************************************************

                    tmin
      ---------------------------------------------------------------
 tavg|  1.0     2.0     3.0     4.0     5.0     6.0     7.0     8.0  |  9.0
-----|---------------------------------------------------------------
 1.0 |  1.06
-----|  0.00
 2.0 |  0.67  -1.07
-----|  0.07  (0.00)

-----|(0.01)  (0.01)(0.00)  (0.01)(0.02)(0.03)  (0.04)  (0.00)
 9.0 | -0.72  -0.71 -0.70  -0.68  -0.65  -0.60  -0.50  -0.07 | -0.99
-----|  0.01   0.01  0.01   0.01  0.01   0.01   0.02   0.00 |(0.00)
```

Figure A.22(contd) Example of output file PIPETAB.OUT

```
*****************************************************
 TABLE 6 - FRACTIONS OF SECTIONS THAT ARE PERFORATED
*****************************************************

                    tmin
      ---------------------------------------------------------------
 tavg   1.0    2.0    3.0    4.0    5.0    6.0    7.0    8.0    9.0
-----  ---------------------------------------------------------------
 1.0   0.000
-----
 2.0   0.000  0.000
-----

-----
 9.0   0.000  0.000  0.000  0.000  0.000  0.000  0.000  0.000  0.000
-----
*************************************************************

                    END OF THE OUTPUT FILE
```

Figure A.22(contd) Example of output file PIPETAB.OUT

```
3                       - type of the section ( 2a )
152.0 10                - nominal outside diam., nom. wall thickness
0.0 0.0 0.0 0.0 0.0     - measurement errors
1 9 1 1                 - the smallest value of t_min, the largest value of t_avg, step for t_min, step for t_avg
0.093744,               - mean of means S/S_o ( Table 1 )
0.174255,0.188740,
0.254019,0.275789,0.285007,
0.342014,0.360945,0.375647,0.382570,
0.438565,0.452335,0.464946,0.476024,0.481445,
0.543798,0.552221,0.560536,0.569032,0.577105,0.581597,
0.656462,0.659802,0.663703,0.668530,0.673728,0.679356,0.683266,
0.772262,0.772797,0.773672,0.775092,0.777023,0.779728,0.783074,0.786194,
0.885288,0.885124,0.885118,0.885556,0.885976,0.886467,0.887151,0.888484,0.890455,

0.000000,               - standard deviation of mean S/S_o ( Table 1, values in brackets )
0.001838,0.000001,
0.003017,0.001378,0.000003,
0.003754,0.002091,0.001171,0.000003,
0.003770,0.002525,0.001665,0.000966,0.000000,
0.003590,0.002707,0.001930,0.001294,0.000837,0.000008,
0.003219,0.002387,0.001962,0.001457,0.000991,0.000648,0.000037,
0.001988,0.001794,0.001541,0.001348,0.000999,0.000734,0.000503,0.000003,
0.001444,0.001334,0.001109,0.000941,0.000839,0.000730,0.000537,0.000340,0.000004,

0.000000,               - mean standard deviation of S/S_o ( Table 2 )
0.050827,0.000000,
0.079501,0.051668,0.000000,
0.099875,0.079536,0.051093,0.000000,
.....
.....
```

Figure A.23 Example of output file PIPETAB.TXT

```
 RESULTS OF CALCULATIONS
 ***********************************************************

 Cross-section Type 1a - outside corrosion only

 Data:
   to =  10    mm,        D =  152.00mm
 tavg =  7.50mm,    tmin =    3    mm
 assumed exact measurements of tavg
 assumed exact measurements of tmin
 No. of N.A positions considered =     90
 Total number of simulation      =   1000
 Number of elements used         =    360
 External corrosion rates:
 average section loss - K =  0.20000,  n = 0.600
              pitting - K =  0.40000,  n = 0.600
 Elements randomly distributed along the circumference
 Elements chosen using METHOD 1

 So =  148682.5mm^3
```

Time			mean		st. dev	
	tavg	tmin	mean	st.dev	mean	mean
(yrs.)			S/So	S So	m.S/So	st.dev.S/So
0.00	7.50	3.00	0.719	0.029	0.001	0.005
4.61	7.00	2.00	0.666	0.026	0.001	0.007
14.62	6.50	1.00	0.619	0.027	0.001	0.004
28.74	6.00	0.00	0.567	0.029	0.001	0.006

```
 ***********************************************************

                 END OF THE OUTPUT FILE
```

Figure A.24 Example of output file PIPEVAR.OUT

Appendix B PIPEREL.EXE users guide

B.1 Introduction

Appendix B is a users guide for the program PIPEREL.EXE, which carries out time-dependent reliability analysis of a deteriorating pipeline using the methods presented in Chapter 5. The simplified flowchart of the program is shown in Figure B.1. Appendix B presents in detail the user interface for entering data and the necessary format and content of input data files required for analysis. Examples output files are also presented and discussed.

B.2 Data for the analysis of a pipeline

There are two types of input data required for the reliability analysis: the user-specified keyboard input and the data supplied directly from a number of data files.

B.2.1 User-defined keyboard input data

The user-defined keyboard input is organized into a number of screen menus which are related as shown schematically in Figure B.2. Each screen menu is followed by a prompt allowing either the input of values for various variables or access to a submenu. Any input by the user causes an automatic update of variables and/or a change of all appropriate selection menus to display only the applicable options.

B.2.1.1 Main menu

Figure B.3 shows the main menu of the program, which organizes the input of data. The program can be run only from the main menu. The selections 1-6 are common for all types of analysis (corrosion failure, flexural failure, corrosion and flexural failure). The selections 7 and 8 will appear only if "corrosion and flexural failure" was chosen as the type of analysis. In other cases either " Flexural failure - scaling menu" or "Corrosion failure - scaling factor menu" will appear as selection 7 as appropriate. Selection 6, concerning the output file, is the only selection in the main menu which does not lead to a submenu. It functions as a switch between the "limited" and "full" size of the output file REL.OUT, which are described fully in Section B.3.1.

B.2.1.2 Type of reliability analysis

Figure B.4 shows the selection menu for the type of reliability analysis, or more precisely the type of failure mode to be considered in the analysis. There are three options available: the corrosion failure, the flexural failure, and the corrosion and flexural failure. The selected (or default) option is marked with the asterisk (*).

B.2.1.3 Data for reliability analysis of a pipeline

Figure B.4 shows the selection menu for entering the time-dependent reliability analysis data. Selections 1 through 3 are common for all types of analysis. The analysis is carried out for the entered "time period for investigation", with calculations of the failure

frequency performed on the basis of the entered "time interval for analysis". Selection 3 is the frequency of failures assumed as a failure criterion for the whole line, which allows calculation of the remaining service life of the pipeline. The presence of Selections 4 and 5 in the submenu depend on the type of analysis being carried out. Different numbers of discrete values (points) for approximation of distributions, N_e, can be specified for corrosion and flexural failure analysis independently. These define the approximations of the distributions of the minimum wall thickness, t_{min}, the average wall thickness, t_{avg}, and the corrosion rate exponent, n.

B.2.1.4 Choice of the method of scheduling repairs

Figure B.6 shows the menu which allows repairs of the line to be considered in the analysis. The "no action" (or "no repairs") case is the default option. The other two options supported by the program are:

- "repairs" only - where the calculation of the frequencies of future joint failures is performed considering repairs of the line
- "repairs" and "no action" - where the calculation of the frequencies of future joint failures is performed with and without repairs of the line

If repairs of the line are to be considered, the submenu shown in Figure B.7 is invoked. The user must specify one of the following two methods of scheduling repairs:

- user defined repairs at the end of each time interval. This option allows joint replacement or/and installation of clamps to be considered in the analysis. After calculations for the specific time interval are completed, the results for each single joint of the pipeline can be displayed to the screen one at the time, as shown in Figure B.13. with the joints ranked based on their probabilities of failure. Based on the displayed information, the user can decide to replace any joint, install clamps at any location, or do nothing.

- automatic repairs at the end of each time interval. This option allows joint replacement or installation of clamps to be considered in the analysis. If the joint replacement is chosen as the repair option, a number of joints equal to the predicted number of joint failures is automatically replaced at the end of each time interval. The joints selected for replacement are taken from the top of the list of joints that have been ranked based on their probabilities of failure. Similarly, if the installation of clamps is chosen as the repair option, clamps are automatically installed at cross-sections selected from the ranked list which is based of their probabilities of failure. The number of clamps installed at the end of the time interval is equal to the number of failures predicted during the time interval.

B.2.1.5 Cost analysis

The present worth cost analysis can be selected only with the repairs options. Figures B.8

and B.9 show the screen menus for the input cost analysis data. If a cost analysis is specified, the program calculates the present worth cost of the repairs (PW MC), the present worth cost of the replacement of the whole line (PW LRC), and the present worth of the total cost (PW LRC + MC) using the equations presented in Chapter 5. The cost analysis assumes that the cost of repairs for a particular repair option and the cost of the line replacement remain constant over time. Inflation is not included in the cost calculation.

B.2.1.6 Corrosion rates

Figure B.10 shows the selection menu which allows the user to specify the mean and the standard deviation of the normally-distributed corrosion rate exponent n. The default values of four corrosion rates, called High, Medium, Low and Very Low are assumed after the NBS study (Romanoff, 1957). The specification of the user-defined parameters for the n distribution, where the number of corrosion rates to be used for analysis can vary between 1 and 4, is allowed by Selection 2. The active set of corrosion rates chosen for analysis is marked with the asterisk (*).

B.2.1.7 Data for scaling the reference demand

Figure B.11 shows the selection menu for specification of the input parameters required for scaling of the reference demand using the methodology described in Section 5.2.2.2. Selections 2 and 3 allow the specification of two values bracketing the sought reference

demand. The program scales the reference demand so that the predicted number of flexural failures matches the expected (or observed) number of failures as specified by Selection 4. Selection 7 allows the use of either the data file PIPEXSC1.DAT if the value 1 is input, or the data file PIPEXSC2.DAT if the value 0 is input. These two data files are described in Section B.2.2.4.

B.2.1.8 Data for optional scaling of the standard deviation of t_{min}

Figure B.12 shows the selection menu for specification of the input parameters required or scaling the standard deviation of the minimum wall thicknesses measurements, using the methodology described in Section 5.3.2.1. The objective of the scaling procedure is to determine the factor by which the standard deviation of t_{min} distribution should be increased (or decreased) to cause the predicted number of corrosion failures to match the expected (or observed) number specified using Selection 1. The scaling is performed only if the expected number of corrosion failures is set to be greater than 0.0. Otherwise the factor is automatically assigned a default value of 1.0. Selection 2 allows two methods for calculation of the number of corrosion failures using discrete approximation or the numerical integration of the t_{min} distributions as described in Sections 5.3.1.1 and 5.3.1.2. Each options is followed by the prompt for either the number of discrete points or the number of integration panels. The selection 3 allows specification of the corrosion failure of pipe cross-section in terms of the minimum area of a circular perforation of the

pipe wall as described in Section 5.3.1. This failure criterion is also used in subsequent analysis for the prediction of the frequency of future failures.

B.2 2 Input data supplied by data files

The necessary data supplied through data files contain the following information:

- pipeline data required for the flexural and the corrosion failure analysis, are obtained from file LINE.DAT
- corrosion rate data required for the flexural and the corrosion failure analysis, are obtained from file CORR.DAT
- flexural demand data required for the flexural failure analysis only, are obtained from file DEMAND.DAT
- flexural strength of corroded pipe cross-section data required for the flexural failure analysis only, are obtained from files PIPEXSC1.DAT and PIPEXSC2.DAT. The use of the file PIPEXSC1.DAT is optional.

Almost all information contained in files LINE.DAT, CORR.DAT and DEMAND.DAT is organized on the pipe joint basis.

B.2.2.1 Pipeline data file - LINE.DAT

The data file LINE.DAT consists of Hydroscope tool measurements collected during field inspection. The maximum number of sampled cross-sections per pipe joint allowed is

equal to 5. An example of the format and the content of data file LINE.DAT is shown in Figure B.14. The data are shown in large bold type on the left side of the figure, and the descriptions are shown in smaller type on the right side (Note: descriptions do not appear in a real data file). The set of data that is characteristic for a single joint is shown shaded in the figure. Although the joints are numbered from 1 to 50, it is not required that consecutive numbers be used to designate consecutive joints of the pipeline. This allows preservation of the joints numbering system assumed in field inspection. For example, if the pipeline shown in Figure 1.7 is analyzed, the 48 joints would be numbered from 1 to 51 and PVC joints 23,37, and 41 would be excluded from the analysis.

B.2.2.2 Flexural demand data file - DEMAND.DAT

The DEMAND.DAT file supplies the relative demand for the line on either a joint or a sampled sections basis. If the relative demand is constant for each joint, the first line of the data file contains the integer 0. Subsequent lines give the joint number and appropriate relative demand. If the relative demand varies for sampled cross-section within the joint, the integer 1 must appear in the first line, followed by the joint number and specification of the relative demand for all sampled sections along the joint, with each value written on a new line. Figure B.15 shows an example of the relative demand data file where the relative demand is constant for each joint. The shaded area indicates the data used to describe the relative demand for Joint 1. Similarly, as in case of the data

file LINE.DAT, only the data shown in large bold type on the left side of the figure appear in a real data file.

B.2.2.3 Corrosion rates probabilities data file - CORR.DAT

The CORR.DAT file specifies the probability of having the specified High, Medium, Low, and Very Low corrosion rate cases at each particular pipe joint. The specification of probabilities is done for each joint. Figure B.16 shows an example of the CORR.DAT file showing specified probabilities of corrosion rates for each joint. The shaded area indicates the data used to describe the probability of each corrosion rate occurring along Joint 1.

B.2.2.4 Statistical parameters of the pipe section modulus distribution

There are two data files containing statistical parameters of the pipe section modulus:

- PIPEXSC1.DAT, which is a modified form of file PIPETAB.TXT created by the program PIPEXSC.EXE, with consideration of the specific measurement errors of $\overline{t_{avg}}$ and $\overline{t_{min}}$. This file can only be use for scaling of the reference demand using exact method of calculation of the probability of failure of a cross-section described in Section 5.2.1.2. Scaling of the reference demand allows also approximate method, therefore the use of this data file for the analysis is not essential. However, if the file PIPEXSC1.DAT is available, it should be use for the scaling of the reference demand to improve the performance of the program.

- PIPEXSC2.DAT, which is also a modified form of file PIPETAB.TXT created by the program PIPEXSC.EXE, without measurement errors of $\overline{t_{avg}}$ and $\overline{t_{min}}$. PIPEXSC2.DAT is essential for the analysis, because the prediction of frequencies of future joint failures is based on the approximate method of calculation of the probability of failure of a pipe cross-section, described in Section 5.2.1.3. The scaling of the reference demand can also be done using approximate method, therefore availability of PIPEXSC2.DAT data file is sufficient to conduct reliability analysis of a pipeline.

The PIPEXSC1.DAT or PIPEXSC2.DAT can easily be obtained by changing the name and extension of the PIPETAB.TXT (see example of PIPETAB.TXT shown in Figure A.25). However, the PIPETAB.TXT file must include data for the full range (0 to t_o) for the average and the minimum wall thicknesses.

B.3 Output files

The two output files created by the program PIPEREL.EXE are named REL.OUT and EXCEL3.TXT. The output file REL.OUT gives the detailed results of all calculations while the text file EXCEL3.TXT is created to facilitate the plot of the predicted frequencies of future joint failures and the plot of the results of the present worth cost analysis, if this option has been specified.

B.3.1 Main output file - REL.OUT

An example of output file REL.OUT is shown in Figure B.17. It contains the following segments:

1. Segment 1 - the echo of input data used for analysis
2. Segment 2 - the results of the reference demand scaling, or the results of the standard deviation of t_{min} scaling, or both
3. Segment 3 - the results of the analysis for a particular time T, where time T is an elapsed time T_e discussed in Sections 5.2.2.4 and 5.3.2.2, including: detailed results for each pipe joint; the estimated failure frequency; the repairs applied and estimated failure frequency after repairs, if this option is specified; and, the results of the present worth cost analysis, if this option has been specified.

While Segments 1 and 2 appear only once, Segment 3 is repeated for each time T considered in the analysis. There are two options for the size of the output file REL.OUT, which are specified from Selection 6 in the main menu shown in Figure B.3, corresponding to "full" and "limited" output. An example of the "full" size output file, which is the result of the analysis of a pipeline consisting of 50 pipe joints is shown in Figure B.17. The printout of the file is 55 pages long, therefore only part of the file is shown. The "limited" output file does not show the detailed information about each joint in Segment 3, in the table titled "Joints ranked based on the probability of failure". As the result, the size of the output is reduced by almost 90%.

B.3.2 Supplementary output file - EXCEL3.TXT

The output file EXCEL3.TXT is the text file which summarizes both the input and the results of the simplified reliability analysis of a pipeline. However, the main purpose of this file is to facilitate the plot of results using MS EXCEL program. An example of the output file EXCEL3.TXT, opened in MS EXCEL using "comma" as a delimiter is shown in Figure B.18. The results of calculations are shown in columns, where:

- Time - time elapsed since the Hydroscope inspection for which the analysis is conducted
- Failure - critical frequency of failures, used as the failure criterion for the replacement of the whole line. This value is used to estimate the "remaining service life"
- Repair - predicted frequencies of future joint failures for the option considering repairs
- No action - (not shown) predicted frequencies of future joint failures without repairs
- PW LRC - present worth cost of the line replacement, in dollars
- PW MC - present worth cost of repairs, in dollars
- PW LRC+MC - present worth total cost, in dollars

Using the tabulated results of the analysis, the plot of the present worth costs and/or the failure frequencies can be easily obtained as shown in Figure B.19. In this case, only data for Time equals to 0 - 12 years were plotted.

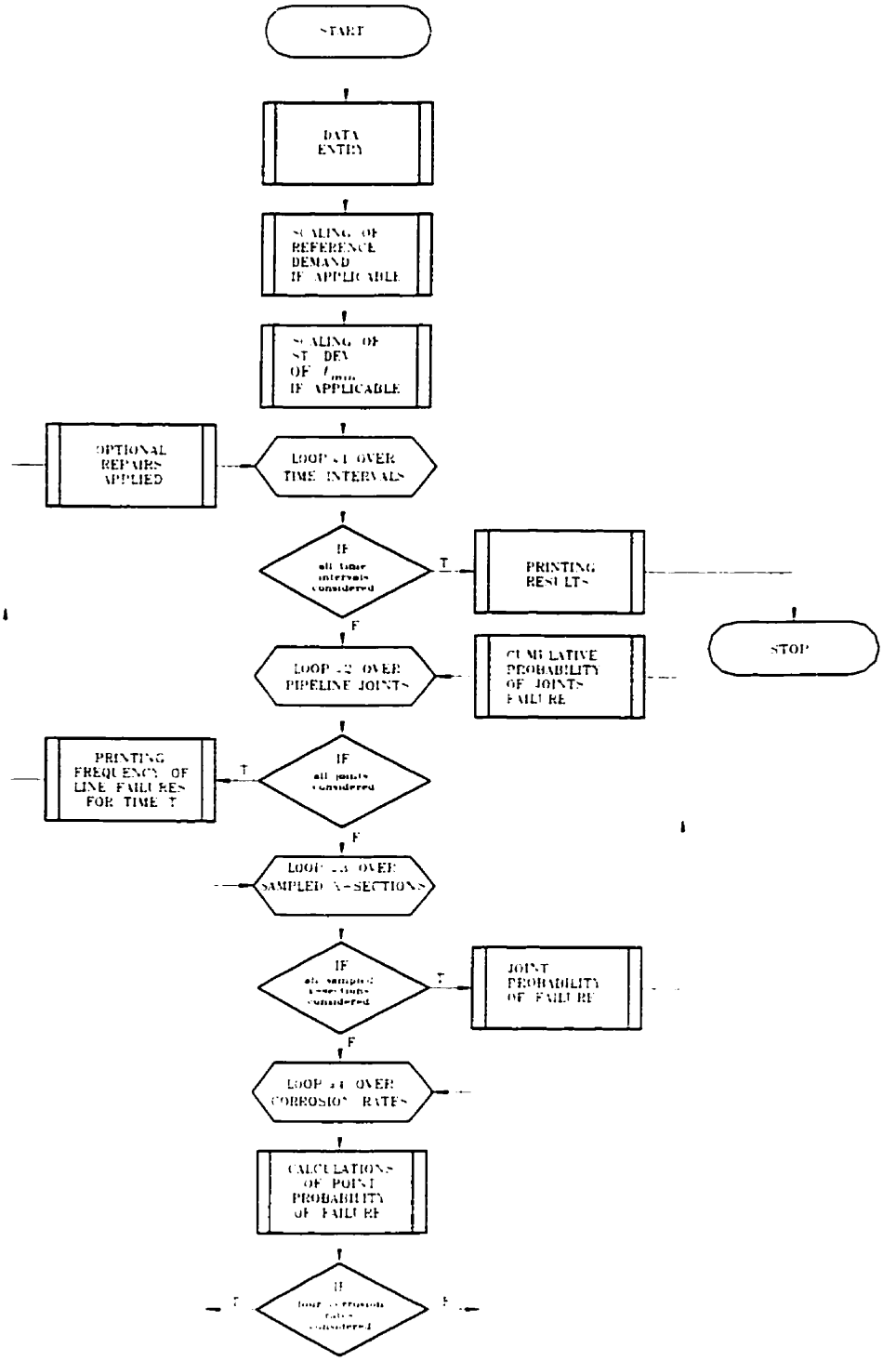

Figure B.1 Simplified flowchart of the program PIPEREL.EXE

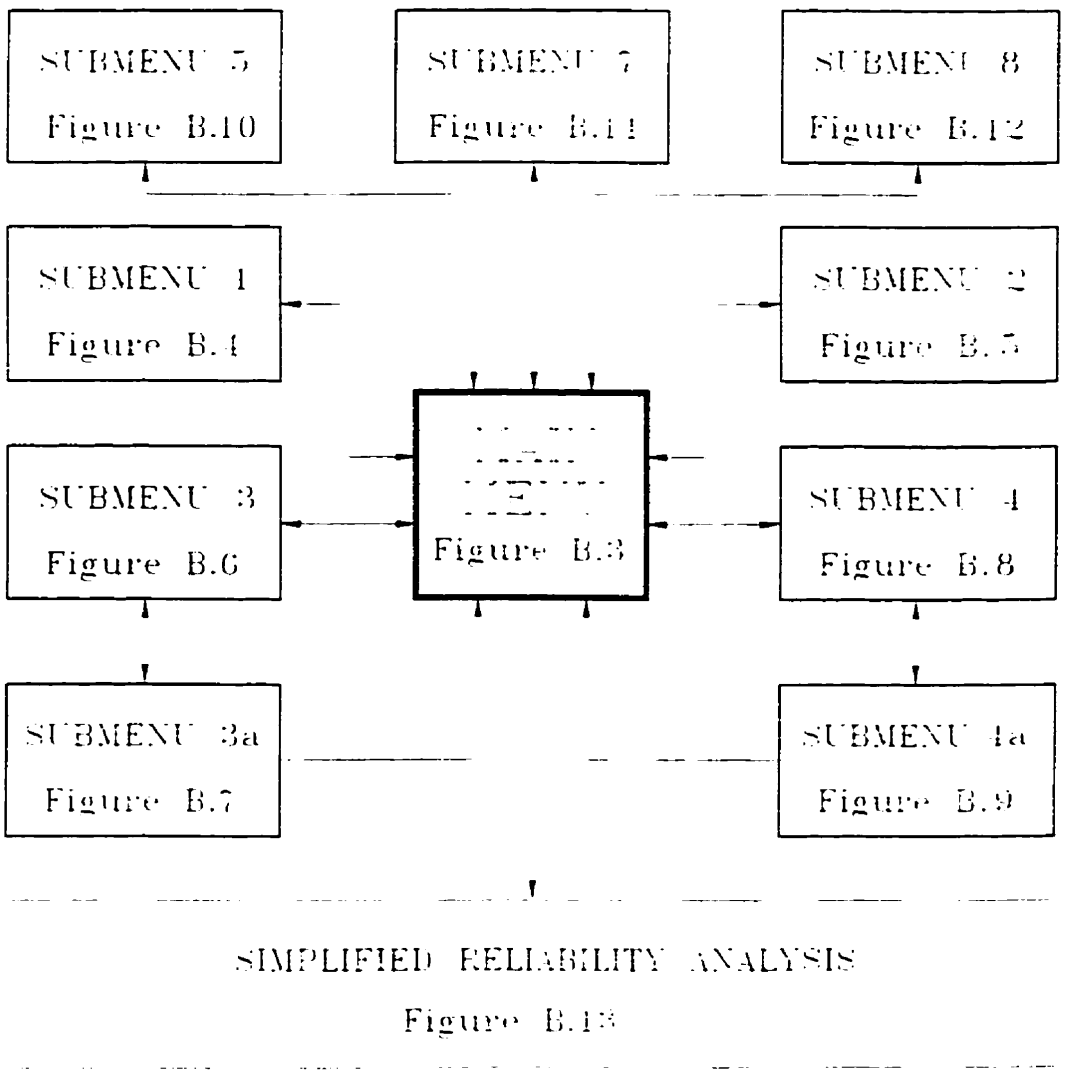

Figure B.2 Organization of data input menus in the program PIPEREL.EXE

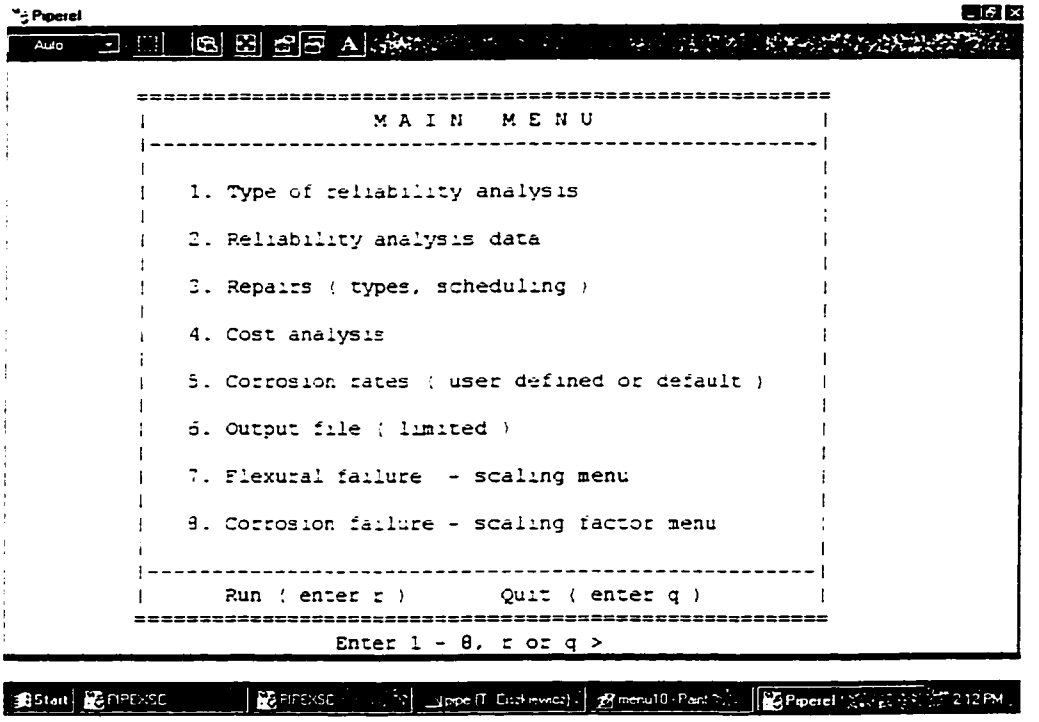

Figure B.3 Main menu - Choice of submenus for specific data entry

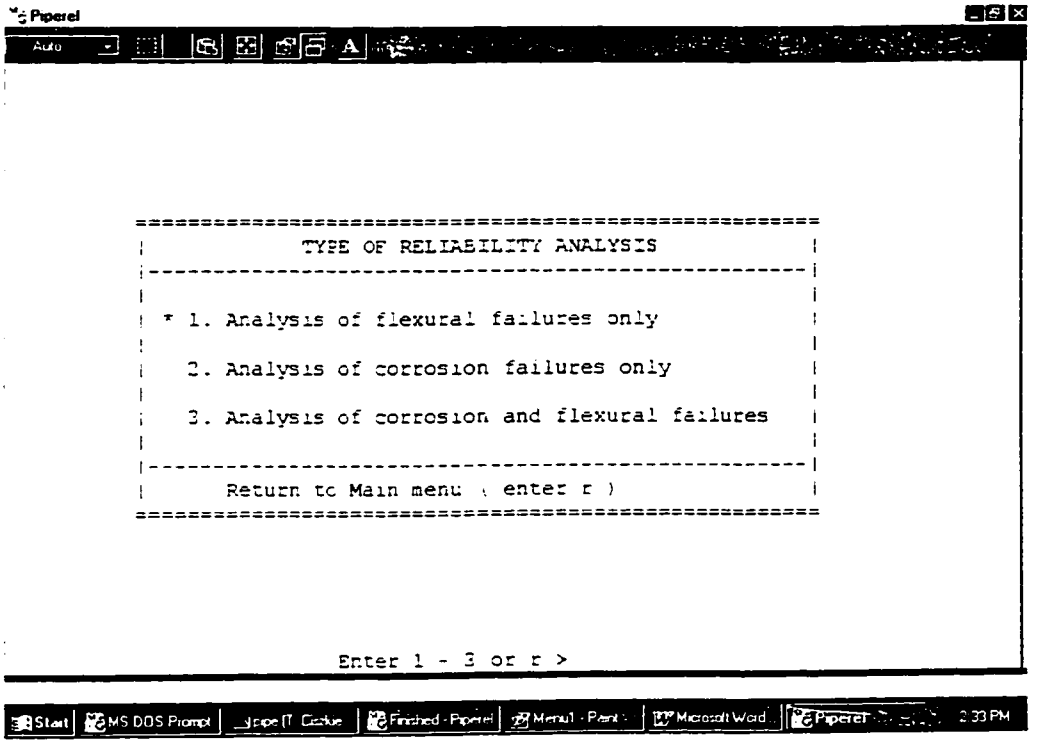

Figure B.4 Submenu 1 - Type of reliability analysis

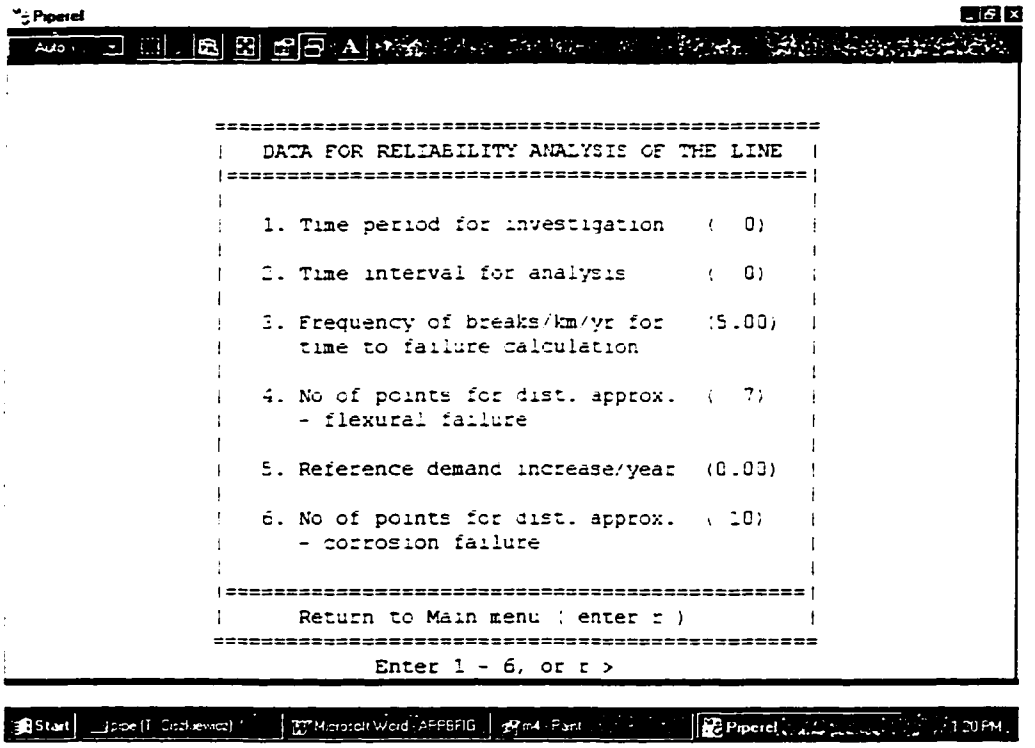

Figure B.5 Submenu 2 - Data for reliability analysis

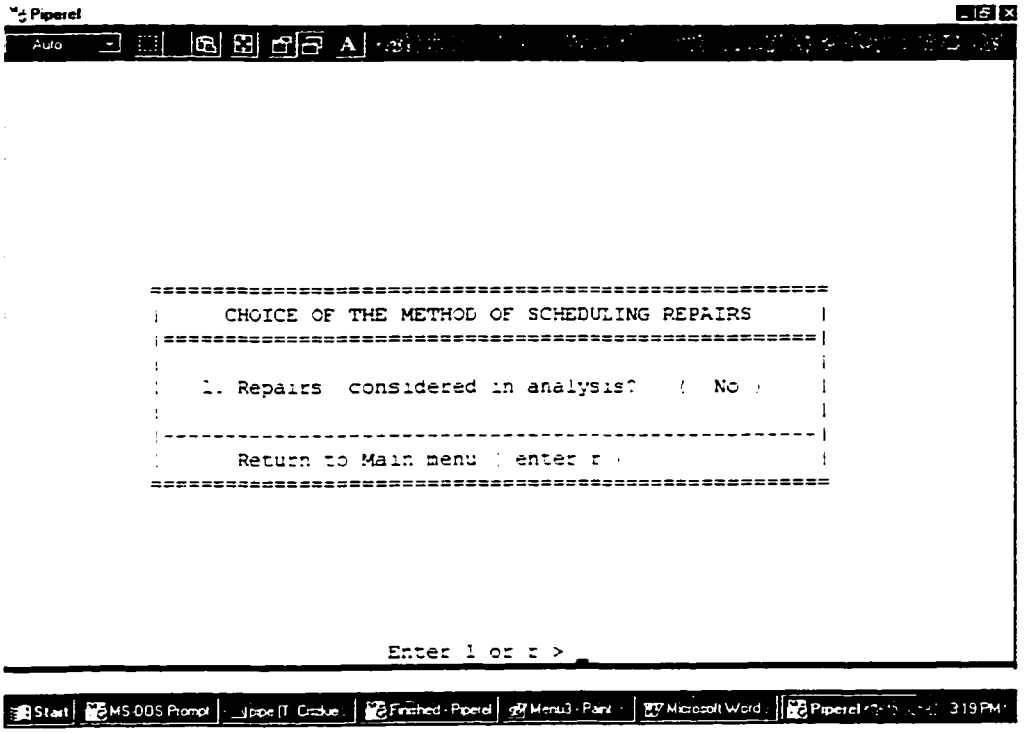

Figure B.6 Submenu 3 - Choice of the method of scheduling repairs

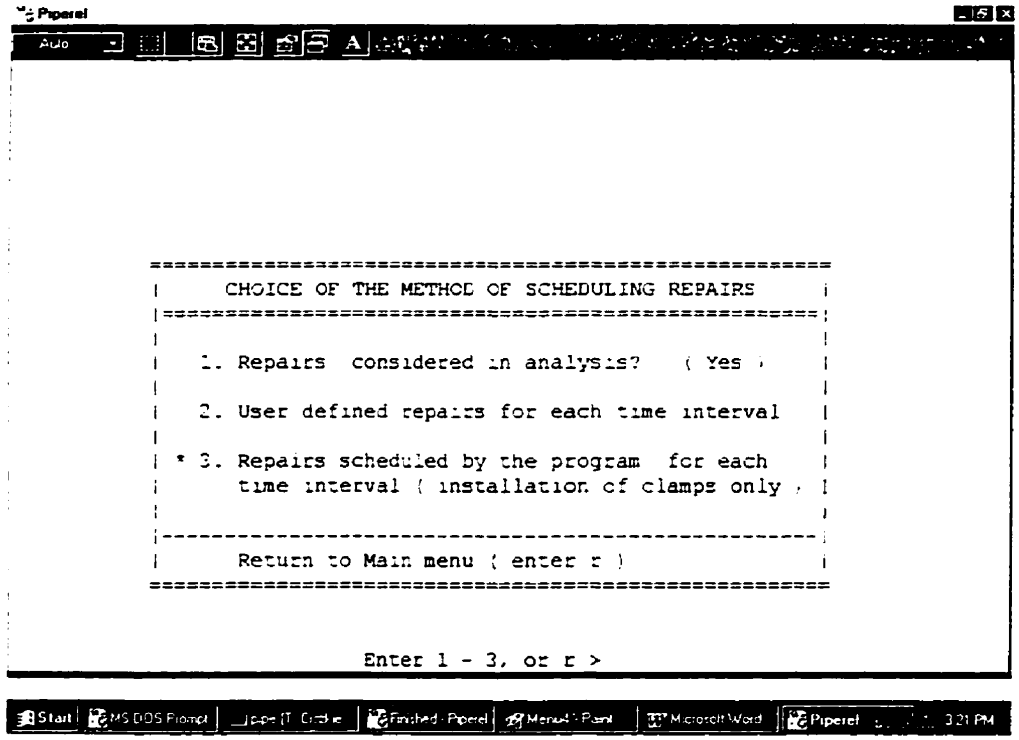

Figure B.7 Submenu 3a - Choice of the method of scheduling repairs

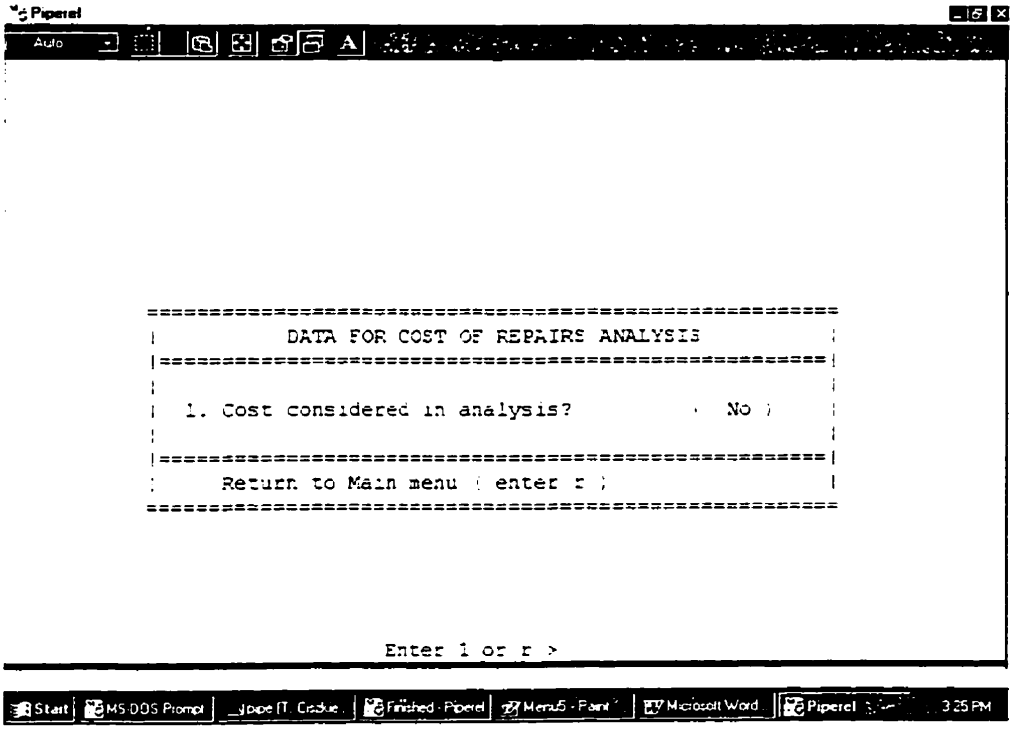

Figure B.8 Submenu 4 - Data for cost of repairs analysis

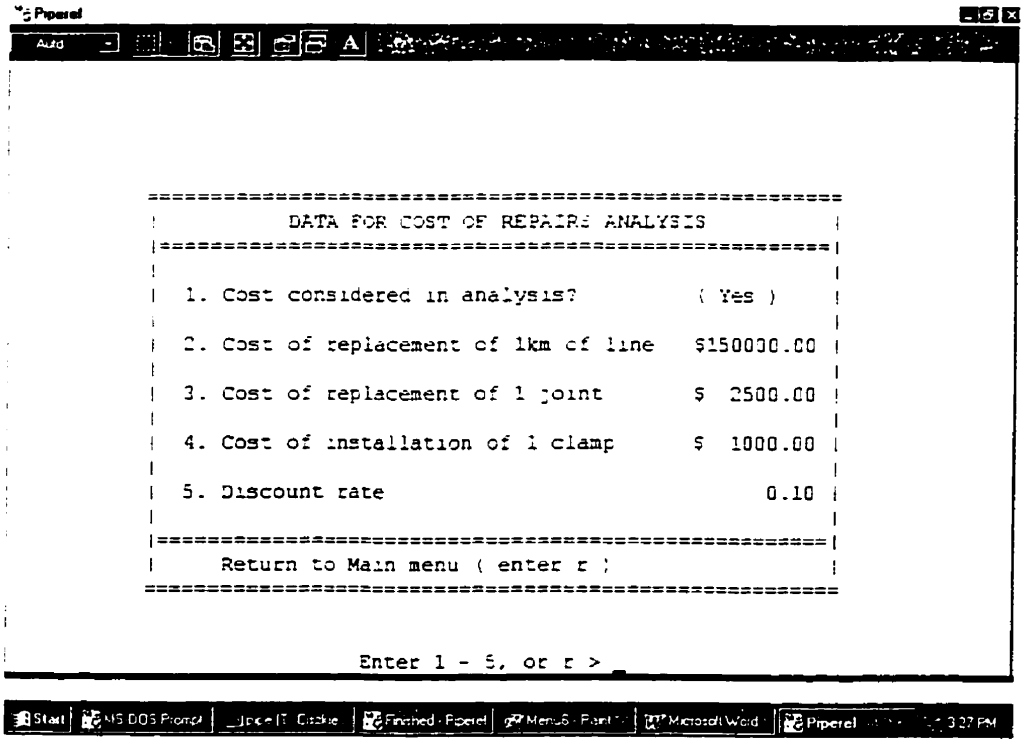

Figure B.9 Submenu 4a - Data for cost of repairs analysis

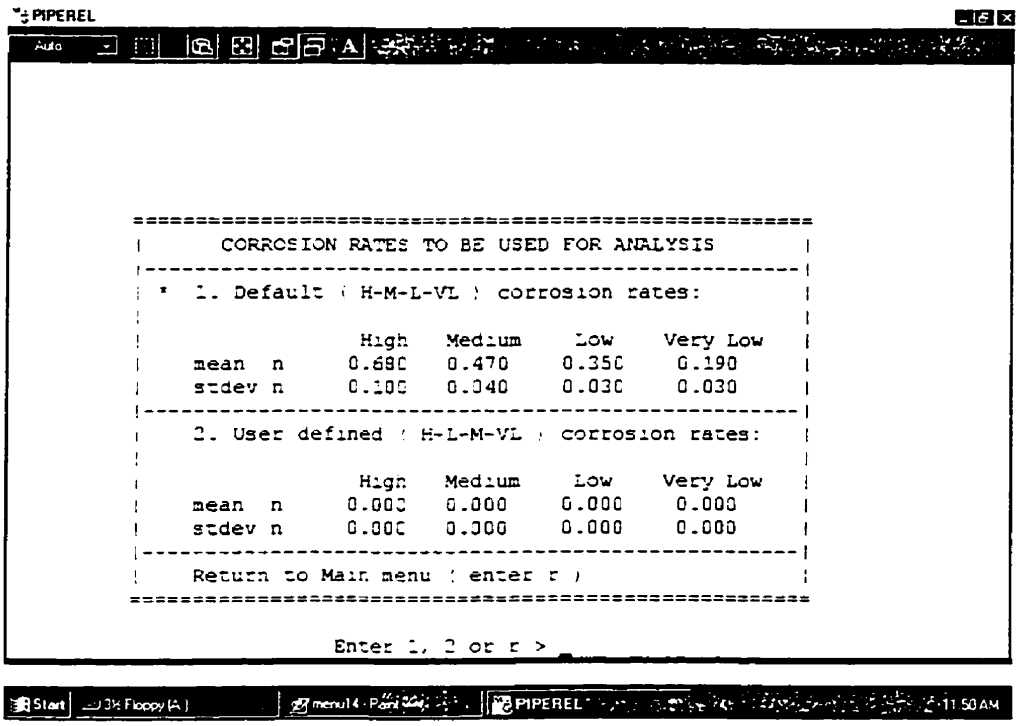

Figure B.10 Submenu 5 - Specification of corrosion rates for analysis

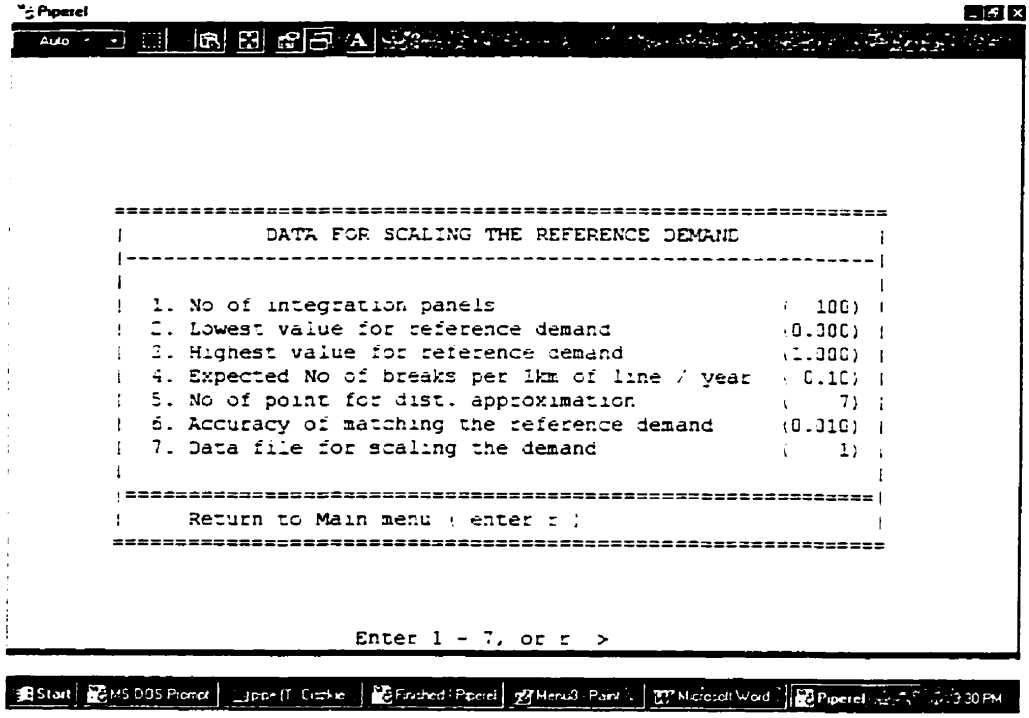

Figure B.11 Submenu 7 - Data for scaling the reference demand

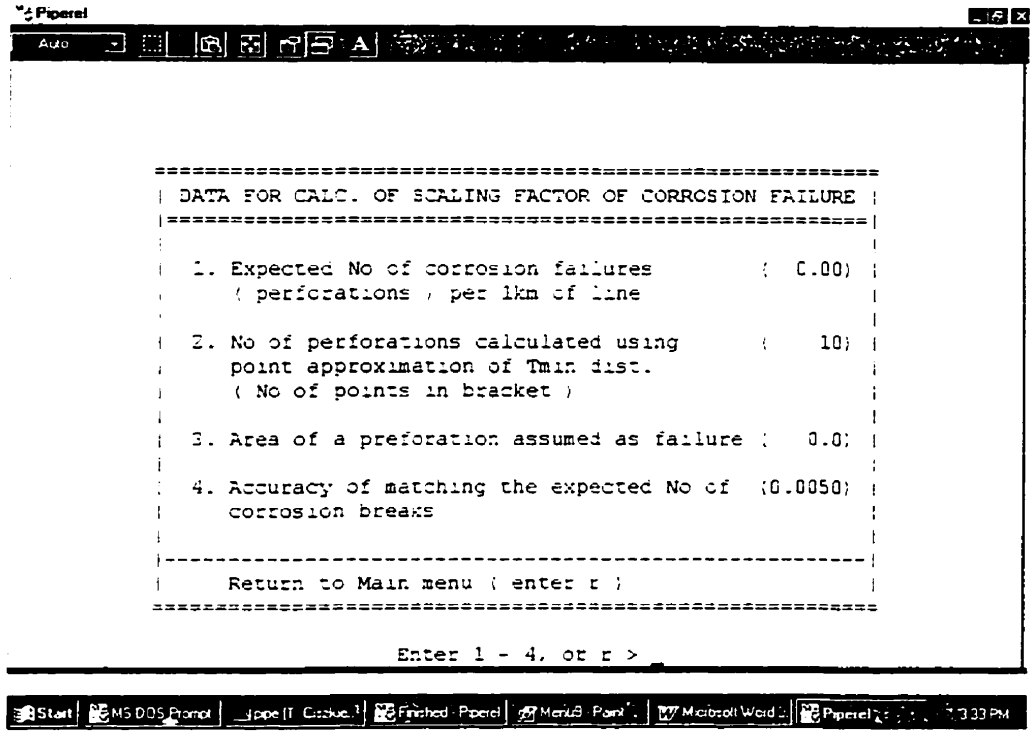

Figure B.12 Submenu 8 - Data for scaling of the measurement error of $\overline{t_{min}}$

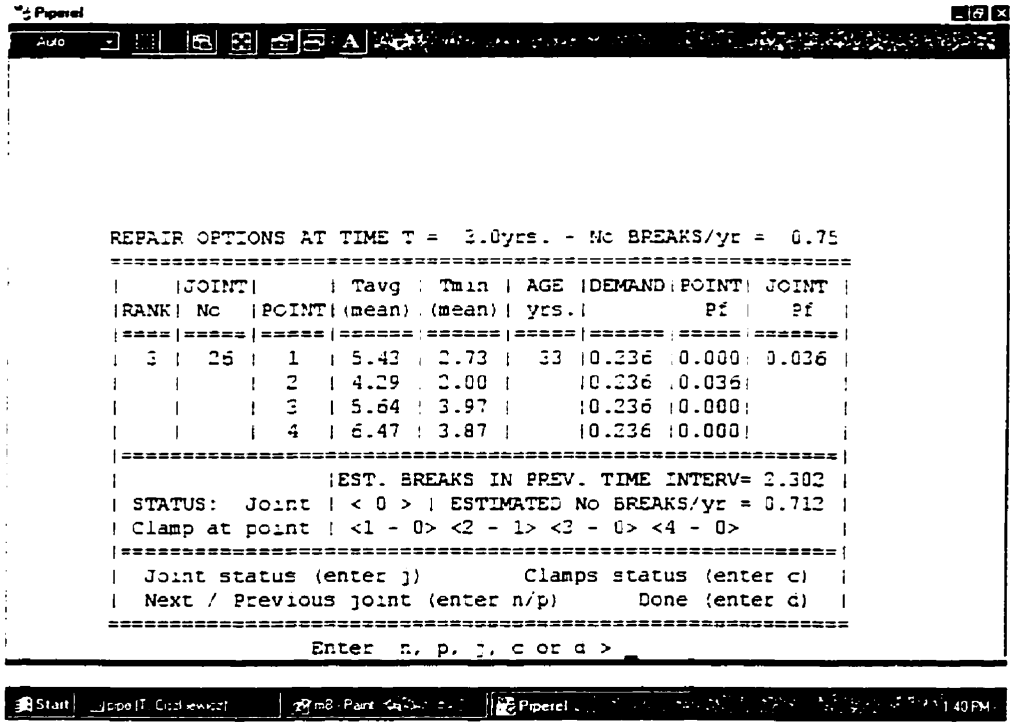

Figure B.13 Example of the joint data for the manual repair option

```
1                          - designation of the analyzed line ( any integer number )
152.0 10                   - outside diameter D and nom. wall thickness. t_o in mm
0.10 0.10 0.10 0.10        - (±) errors of t_avg and t_min ( e.g. for t_min it is ±0.10t_o )
50 4                       - No of pipe joints ( 50 ), No of sampled sections/joint (4 )
1 30 5.4                   - joint No ( 1 ), age ( 30 years ), length ( 5.4 m )
7.5 3.0                    - avg. thickness, min. thickness at sampled section No 1
7.5 2.5                    - avg. thickness, min. thickness at sampled section No 2
7.8 3.1                    - avg. thickness, min. thickness at sampled section No 3
7.6 2.8                    - avg. thickness, min. thickness at sampled section No 4
2 30 5.4                   - joint No ( 2 ), age ( 30 years ), length ( 5.4 m )
7.3 3.0                    - avg. thickness, min. thickness at sampled section No 1
7.0 3.1                    - avg. thickness, min. thickness at sampled section No 2
7.1 3.5                    - avg. thickness, min. thickness at sampled section No 3
7.2 3.3                    - avg. thickness, min. thickness at sampled section No 4
.........
.........
..........
50 30 5.3
5.5 4.6
7.0 3.8
5.9 3.2
7.3 4.2
```

Figure B.14 Example of the format of the data file LINE.DAT

```
0       - relative demand constant for each joint
1       - joint No ( 1 )
1.1     - relative demand for joint No 1 ( 1.1 )
2       - joint No ( 2 )
1.05    - relative demand for joint No 2 ( 1.05 )
.....
.....
.....
50
0.95
```

Figure B.15 Example of the format of the data file DEMAND.DAT

```
1       - joint No ( 1 )
0.15    - probability of specified High corrosion rate
0.35    - probability of specified Medium corrosion rate
0.35    - probability of specified Low corrosion rate
0.15    - probability of specified Very Low corrosion rate
2       - joint No ( 2 )
0.20    - probability of specified High corrosion rate
0.30    - probability of specified Medium corrosion rate
0.30    - probability of specified Low corrosion rate
0.20    - probability of specified Very Low corrosion rate
.....
.....
.....
50
0.00
0.20
0.60
0.20
```

Figure B.16 Example of the format of the data file CORR.DAT

Segment 1

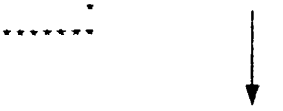

```
**********************************************************
*          DATA FOR ANALYSIS OF THE PIPELINE             *
**********************************************************

LINE No    '

TYPE OF ANALYSIS - FLEXURAL FAILURES

TYPE OF THE CROSS SECTION MODEL - 2a

FAILURE BREAK FREQUENCY = 5.00 /km /year

MEASUREMENT ERRORS:
         Tavg    -/+ error = 0.10to   0.10to
         Tmin    -/+ error = 0.10to   0.10to

TOTAL LENGTH OF THE LINE = 0.166 km

CORROSION RATES:
                 High    Medium     Low     Very Low
   mean  n      0.667    0.500    0.333     0.167
   stdev n      0.100    0.040    0.030     0.030
```

Figure B.17 Example of the output file REL.OUT

```
THE INCREASE OF REF.DEMAND PER YEAR = 0.000

DATA FOR PW COST ANALYSIS:
   cost of replacement of 1km of line = $'50000.00
   cost of replacement of 1 joint     = $  2500.00
   cost of installation of 1 clamp    = $  1000.00
   discount rate                      =       0.10

LINE DATA:
```

JOINT No	L (m)	PT	Tavg (mean)	Tmin (mean)	AGE yrs.	REL. DEM.	CORR. RATE PROB. H	M	L	VL
1	5.4	1	7.50	3.00	30	1.10	0.15	0.35	0.35	0.15
		2	7.50	2.60		1.10				
		3	7.80	3.10		1.10				
		4	7.60	2.80		1.10				
2	5.4	1	7.30	3.00	30	1.05	0.20	0.30	0.30	0.20
		2	7.00	3.10		1.05				
		3	7.10	3.50		1.05				
		4	7.20	3.30		1.05				
50	5.3	1	5.50	4.60	30	0.95	0.00	0.20	0.60	0.20
		2	7.00	3.80		0.95				
		3	5.90	3.20		0.95				
		4	7.30	4.20		0.95				

```
         RESULTS OF THE REFERENCE DEMAND SCALING
**************************************************************

    RATE OF BREAKS DATA:
      Expected No of flexural breaks /km  year =  1.800
     Expected No of flexural breaks /line/year =  0.479

    ESTIMATED RATE OF BREAKS:
     Calculated No of flexural breaks /km  year =  1.774
   Calculated No of flexural breaks /line  year =  0.472

                              Reference demand  =  0.205
```

Segment 2

Figure B.17(contd) Example of the output file REL.OUT

Segment 3

JOINTS RANKED BASED ON THE PROBABILITY OF FAILURE

RANK	JOINT No	POINT	Tavg (mean)	Tmin (mean)	AGE yrs.	DEMAND	POINT Pf	JOINT Pf
1	42	1	5.30	3.00	30	0.236	0.000	0.367
		2	7.30	4.10		0.236	0.000	
		3	7.10	2.50		0.236	0.000	
		4	3.20	1.30		0.236	0.367	
2	6	1	5.60	3.00	30	0.246	0.000	0.051
		2	4.50	2.00		0.246	0.051	
		3	5.30	4.50		0.246	0.000	
		4	6.00	4.00		0.246	0.000	
50	50	1	5.50	4.60	30	0.195	0.000	0.000
		2	7.00	3.80		0.195	0.000	
		3	5.90	3.20		0.195	0.000	
		4	7.30	4.20		0.195	0.000	

NO REPAIR OPTIONS CONSIDERED AT TIME T = 0.0yrs

ESTIMATED RATE OF BREAKS:

Number of breaks per line per year = 0.472
Number of breaks per km per year = 1.774

PRESENT WORTH COST ANALYSIS

OPTION	PW COST
1.Replacement of the line	$ 39900.01
2.Repairs	$ 0.00
3.Total cost 1 & 2	$ 39900.01

Figure B.17(contd) Example of the output file REL.OUT

Segment 3

```
**********************************************************
**********************************************************
*                                                        *
*           ANALYSIS FOR TIME T =  3.0 years             *
*                                                        *
**********************************************************
**********************************************************
```

JOINTS RANKED BASED ON THE PROBABILITY OF FAILURE

RANK	JOINT No	POINT	Tavg (mean)	Tmin (mean)	AGE yrs.	DEMAND	POINT Pf	JOINT Pf
1	42	1	5.09	2.68	33	0.236	0.000	0.505
		2	7.18	3.83		0.236	0.000	
		3	6.97	2.16		0.236	0.000	
		4	2.89	0.90		0.236	0.505	
2	6	1	5.42	2.72	33	0.246	0.000	0.092
		2	4.28	1.68		0.246	0.092	
		3	5.11	4.28		0.246	0.000	
		4	5.84	3.76		0.246	0.000	
50	50	1	5.35	4.43	33	0.195	0.000	0.000
		2	6.90	3.60		0.195	0.000	
		3	5.77	2.98		0.195	0.000	
		4	7.21	4.01		0.195	0.000	

CALCULATED RATE OF BREAKS:

Number of breaks per line per year = 0.748
Number of breaks per 1km of line per year = 2.811

Time to failure is greater than 3.0 yrs.

```
**********************************************************
*            REPAIR OPTIONS AT TIME T =  3.0yrs          *
**********************************************************
```

REPAIR	JOINT No	REPLACED (*)	POINT No	CLAMPED (*)
1	42	*	-	-
2	6	*	-	-

ESTIMATED RATE OF BREAKS:

Number of breaks per line per year = 0.151
Number of breaks per 1km per year = 0.569

Figure B.17(contd) Example of the output file REL.OUT

```
**********************************************************
*              PRESENT WORTH COST ANALYSIS               *
**********************************************************
```

OPTION	PW COST
1.Replacement of the line	$ 29977.47
2.Repairs	$ 3756.57
3.Total cost (1 & 2)	$ 33734.04

Segment 3

```
**********************************************************
**********************************************************
*                                                        *
*           ANALYSIS FOR TIME T =  6.0 years             *
*                                                        *
**********************************************************
**********************************************************

     JOINTS RANKED BASED ON THE PROBABILITY OF FAILURE
**********************************************************
```

RANK	JOINT No	POINT	Tavg (mean)	Tmin (mean)	AGE yrs.	DEMAND	POINT Pf	JOINT Pf
1	26	1	5.27	2.47	36	0.236	0.001	0.099
		2	4.08	1.71		0.236	0.098	
		3	5.48	3.76		0.236	0.000	
		4	6.34	3.65		0.236	0.000	
2	45	1	5.19	2.34	36	0.246	0.004	0.098
		2	4.20	1.79		0.246	0.094	
		3	4.75	3.44		0.246	0.000	
		4	6.28	3.56		0.246	0.000	
50	48	1	6.31	4.51	36	0.205	0.000	0.000
		2	7.36	4.20		0.205	0.000	
		3	7.36	4.94		0.205	0.000	
		4	6.73	4.41		0.205	0.000	

```
     CALCULATED RATE OF BREAKS:

            Number of breaks per line per year =  0.533
       Number of breaks per 1km of line per year =  1.964

       Time to failure is greater than   6.0 yrs.
```

Figure B.17(contd) Example of the output file REL.OUT

```
**********************************************************
*           REPAIR OPTIONS AT TIME T =  6.0yrs           *
**********************************************************

          ==========================================
          |          | JOINT  |REPLACED| POINT  |CLAMPED|
          |  REPAIR  |   No   |  (*)   |   No   |  (*)  |
          |==========|========|========|========|=======|
          |        1 |   26   |   *    |   -    |   -   |
          ==========================================

          ESTIMATED RATE OF BREAKS:

          Number of breaks per line per year =  0.423
          Number of breaks per 1km  per year =  1.590

**********************************************************
*              PRESENT WORTH COST ANALYSIS               *
**********************************************************

          ========================================
          |          OPTION          |  PW COST  |
          |--------------------------|-----------|
          | 1.Replacement of the line| $ 22522.52|
          | 2.Repairs                | $  5167.76|
          | 3.Total cost ( 1 & 2 )   | $ 27690.27|
          ========================================

**********************************************************
**********************************************************
*                                                        *
*           ANALYSIS FOR TIME T =  9.0 years             *
*                                                        *
**********************************************************
**********************************************************

     ( SEGMENT 3 FOR TIME = 9 - 27 YEARS WAS TRUNCATED )
```

Segment 3

Figure B.17(contd) Example of the output file REL.OUT

Segment 3

```
**********************************************************
**********************************************************
*                                                        *
*           ANALYSIS FOR TIME T = 30.0 years             *
*                                                        *
**********************************************************
**********************************************************
```

JOINTS RANKED BASED ON THE PROBABILITY OF FAILURE

RANK	JOINT No	POINT	Tavg (mean)	Tmin (mean)	AGE yrs.	DEMAND	POINT Pf	JOINT Pf
1	42	1	5.52	3.33	27	0.236	0.000	0.198
		2	7.43	4.38		0.236	0.000	
		3	7.24	3.86		0.236	0.000	
		4	3.52	1.72		0.236	0.198	
2	10	1	4.16	2.99	60	0.185	0.042	0.174
		2	4.81	0.66		0.185	0.066	
		3	4.55	1.56		0.185	0.063	
		4	5.20	2.47		0.185	0.014	
50	46	1	6.59	4.49	18	0.236	0.000	0.000
		2	5.54	4.32		0.236	0.000	
		3	7.00	5.54		0.236	0.000	
		4	7.41	5.14		0.236	0.000	

CALCULATED RATE OF BREAKS:

Number of breaks per line per year = 1.588
Number of breaks per 1km of line per year = 5.968

Estimated time to failure corresponding to
failure break frequency (5.00 km/yr) = 11.1 yrs.

```
**********************************************************
```

END OF THE OUTPUT FILE

Figure B.17(contd) Example of the output file REL.OUT

LINE No 1						
TYPE OF ANALYSIS - FLEXURAL FAILURES						
TYPE OF THE CROSS SECTION MODEL - 2a						
FAILURE BREAK FREQUENCY = 5.00 /km /year						
MEASUREMENT ERRORS:						
Tavg (-/+) error = 0.10to / 0.10to						
Tmin (-/+) error = 0.10to / 0.10to						
TOTAL LENGTH OF THE LINE = 0.266 km						
CORROSION RATES:						
	High	Medium	Low	Very Low		
mean n	0.667	0.5	0.333	0.167		
stdev n	0.1	0.04	0.03	0.03		
THE INCREASE OF REF.DEMAND PER YEAR = 0.000						
DATA FOR PW COST ANALYSIS:						
cost of replacement of 1km of line = $150000.00						
cost of replacement of 1 joint = $ 2500.00						
cost of installation of 1 clamp = $ 1000.00						
discount rate = 0.10						
Time	Failure	Repair	PW LRC	PW MC	PW LRC+MC	
0	1.33	0.472	39900.01	0.00	39900.01	
0	1.33	0.472	39900.01	0.00	39900.01	
3	1.33	0.748	29977.47	3756.57	33734.04	
3	1.33	0.151	29977.47	3756.57	33734.04	
6	1.33	0.522	22522.52	5167.76	27690.27	
6	1.33	0.423	22522.52	5167.76	27690.27	
9	1.33	1.094	16921.5	7288.25	24209.75	
9	1.33	0.722	16921.5	7288.25	24209.75	
12	1.33	1.601	12713.37	9677.98	22391.35	
12	1.33	0.932	12713.37	9677.98	22391.35	

(results for the Time = 15 - 24 years truncated)

27	1.33	1.694	3043.48	16999.82	20043.30	
27	1.33	1.043	3043.48	16999.82	20043.30	
30	1.33	1.588				

Figure B.18 Example of the output file EXCEL3.TXT

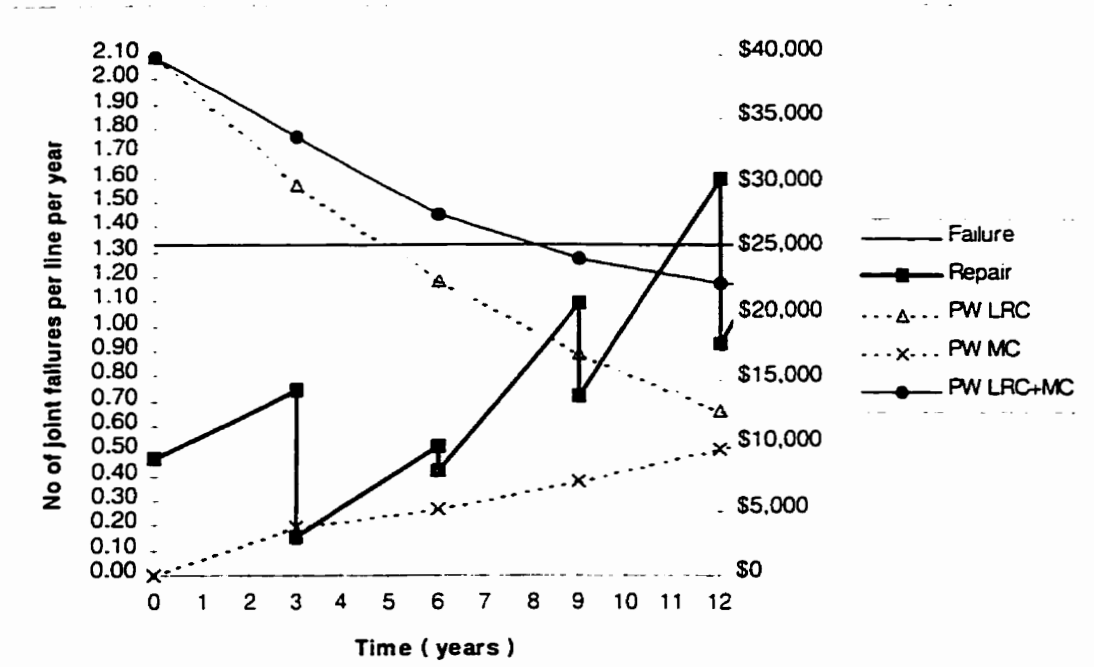

Figure B.19 Example of the graph obtained using output file EXCEL3.TXT

References

Ahammed, M., Melchers, R. E. (1994) "Reliability of underground pipelines subject to corrosion". *Journal of Transportation Engineering*. Vol. 120 , pp. 989-1002.

Beer, F. P., Johnston, R. E. (1972): *Vector Mechanics for Engineers - Statics and Dynamics*. McGraw-Hill Inc. Second edition. pp. 334-358.

Benjamin, J. R., Cornell, C. A. (1970): *Probability, Statistics and Decision for Civil Engineers*. McGraw-Hill Inc., New York, New York, pp. 1-672.

Canadian Institute of Steel Construction (CISC) (1993): *Handbook of Steel Construction*. Fifth edition. p 7-60.

Centre For Engineering Research (CFER) (1996): C-fit computer program, version 1.04. Edmonton, Alberta.

Clarke, N. W. B. (1968): *Buried pipelines (A manual of structural design and installation)*. MacLauren and Sons, London, U.K.

Degarmo, E. P., Sullivan, W. G., Bontadelli, J. A.(1993): *Engineering Economy*. 9th edition, Macmillan Publishing Company, pp. 139-145.

Doleac, M. L., Lackey, S. L., Bratton, G. N. (1980): "Prediction of time-to-failure for buried cast iron pipe". *Proceedings of AWWA Annual Conference*, pp. 31-38.

Fitzgerald, J. H. (1993): " Evaluating Soil Corrosivity-Then and Now". *Material Performance*. October, pp. 17-19.

Gedge, E. (1992): "Corrosion of cast iron in potable water service, Corrosion and related aspects of materials for potable water supplies". *Proceedings of a conference held at the Society of Chemical Industry*. London, UK, 8-9 December, pp.18-28.

Gerald, C. F., Wheatley, P. O.(1994): *Applied Numerical Analysis*. Addison-Wesley Publishing Company Inc. Fifth edition. pp. 210-393.

Gerhold, W. F.(1976): "Corrosion behaviour of ductile cast iron pipe in soil environments". *Journal AWWA*. December 1976, pp. 674-678.

Goulter, I. C., Kazemi, A. (1988):" Spatial and temporal groupings of water main pipe breakage in Winnipeg". *Canadian Journal of Civil Engineering*.Vol.15, pp.91-97

Jakobs, J. A., Hewes, F. W. (1987): "Underground corrosion of water pipes in Calgary, Canada". *Material Performance*. Vol. 26, pp. 42-49.

LaQue, F. L. (1964): "Corrosion characteristics of ductile iron". *Journal AWWA*. Vol. 56. pp. 1433 -1442.

Rajani, B., McDonald, S., Felio, G. (1995): "Water mains break data on different pipe materials for 1992 and 1993". NRC-CNRC Report. Published by Institute for Research in Construction, August 1995, pp 1-10.

Robinson, W. C. (1993): " Testing Soil for Corrosiveness". *Material Performance*. April, pp. 56-58.

Romanoff, M. (1964): "Exterior corrosion of cast iron pipes". *Journal AWWA*. Vol. 56. pp. 1129-1143.

Romanoff, M. (1968): "Performance of ductile iron pipe in soils". *Journal AWWA*. Vol. 60, pp. 645-655.

Romanoff, M.(1957): *Underground corrosion*. National Bureau of Standards Circular 579. US Government Printing Office, Washington, D.C., pp. 1-227.

Rossum, J. R (1969): "Prediction of pitting rates in ferrous metals from soil parameters". *Journal AWWA*. Vol. 61, pp. 305-310.

Sears, E. C. (1968): "Comparison of soil corrosion resistance of ductile iron pipe and gray cast iron pipe". *Material Protection*. Vol. 7, pp. 33-36.

Shamir, U., Howard, C. D. (1979): "An analytical approach to scheduling pipe replacement". *Journal AWWA*. May 1979, pp. 248-258.

Staples, L. B. (1996): "A new tool for condition evaluation of cast and ductile iron pipe". *The NACE International Annual Conference and Exposition*, paper No. 45, pp.2-9.

Wagner, P. (1997): "The 138 Billion Dollar Clean Water Question". *National Undergroud Contractors Association* (*NUCA*). April 1997, pp. 15-16.

IMAGE EVALUATION
TEST TARGET (QA-3)

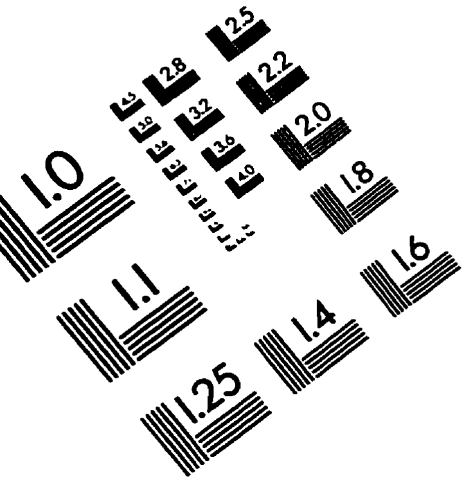

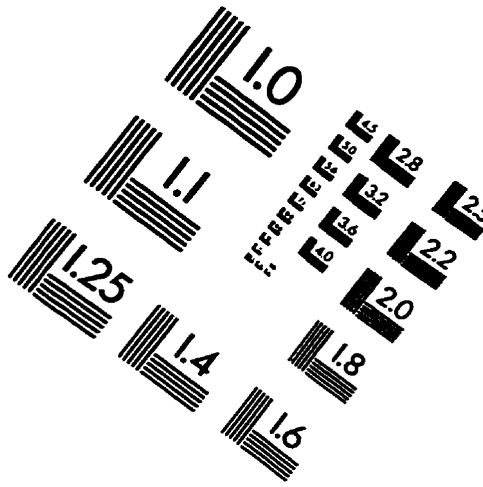

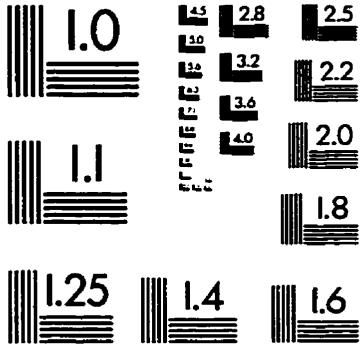

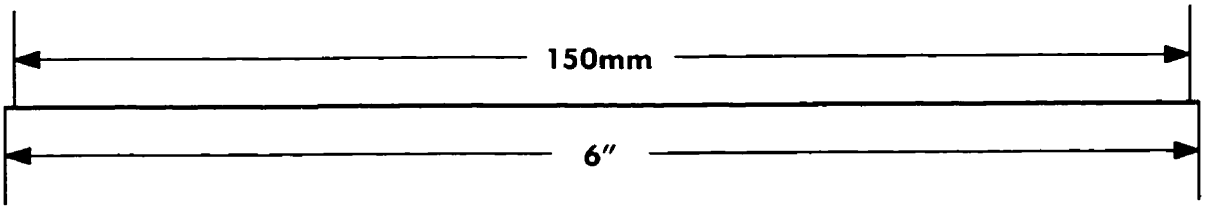

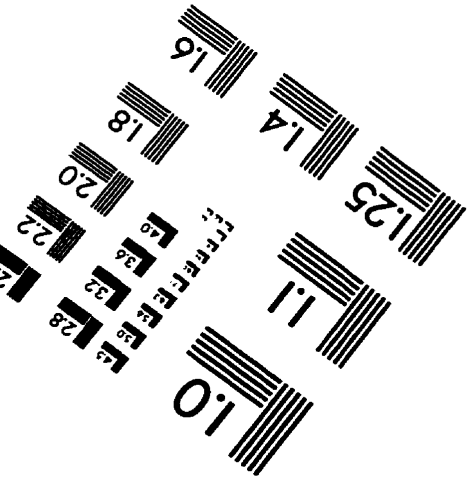

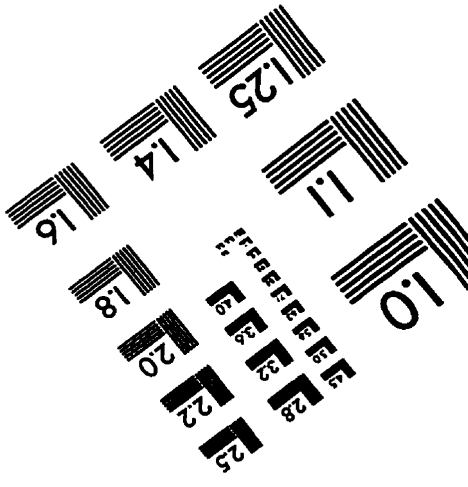

APPLIED IMAGE, Inc
1653 East Main Street
Rochester, NY 14609 USA
Phone: 716/482-0300
Fax: 716/288-5989